

Mechanotherapy of Bone Fracture: Adapted Fixation Conditions

vorgelegt von

Dipl.-Ing.

Mark Heyland

ORCID: 0000-0001-7474-3948

von der Fakultät V – Verkehrs- und Maschinensysteme
der Technischen Universität Berlin
zur Erlangung des akademischen Grades

Doktor der Ingenieurwissenschaften

- Dr.-Ing. -

genehmigte Dissertation

Promotionsausschuss:

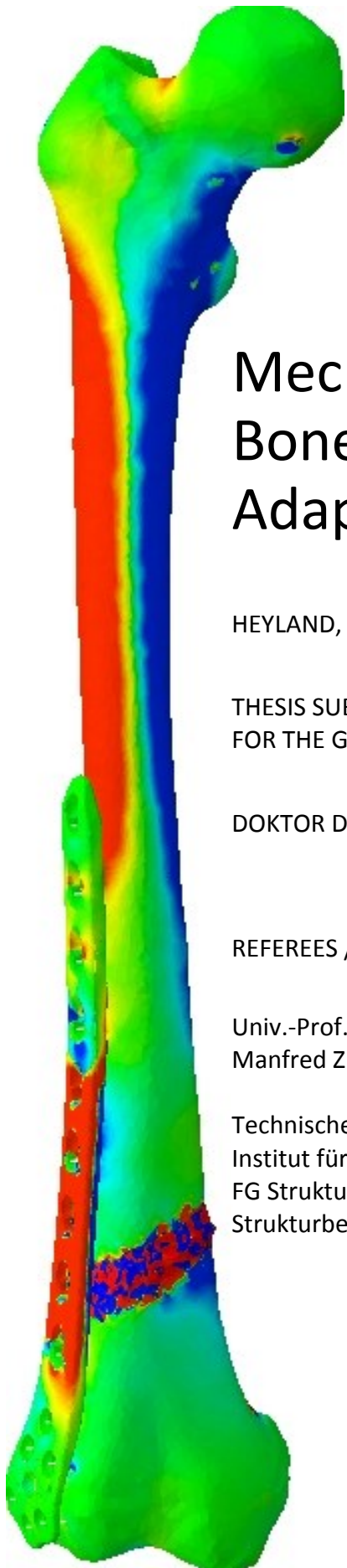
Vorsitzender: Prof. Dr.-Ing. Marc Kraft

Gutachter: Prof. Dr.-Ing. habil. Manfred Zehn

Gutachter: Prof. Dr.-Ing. Georg N. Duda

Tag der wissenschaftlichen Aussprache: 07. August 2019

Berlin 2019



Mechanotherapy of Bone Fracture: Adapted Fixation Conditions

HEYLAND, Mark (Dipl.-Ing.)

THESIS SUBMITTED IN PARTIAL FULFILLMENT OF THE REQUIREMENTS
FOR THE GERMAN ENGINEERING DOCTORATE DEGREE:

DOKTOR DER INGENIEURWISSENSCHAFTEN (DR.-ING.)

REFEREES / GUTACHTER:

Univ.-Prof. Dr.-Ing. habil.
Manfred ZEHN

Univ.- Prof. Dr.-Ing.
Georg N. DUDA

Technische Universität Berlin
Institut für Mechanik
FG Strukturmechanik und
Strukturberechnung

Charité – Universitätsmedizin Berlin
Julius Wolff Institut

Declaration / Erklärung

I, Mark Heyland, declare that this dissertation has been written by me and the used resources and references are listed.

Hiermit versichere ich, Mark Heyland, an Eides statt, daß diese Dissertation selbständig von mir verfasst wurde und die benutzten Hilfsmittel und Quellen aufgeführt wurden.

Table of Contents

DECLARATION / ERKLÄRUNG	2
LIST OF FIGURES	6
CHAPTER 1. BACKGROUND OF FRACTURE HEALING	10
1.0. OVERVIEW	11
1.0.1. <i>General Background</i>	11
1.0.2. <i>Problem</i>	11
1.0.3. <i>Goals</i>	12
1.0.4. <i>Scope</i>	12
1.0.5. <i>Hypotheses</i>	13
1.0.6. <i>Graphical Outline of the Thesis</i>	14
1.1. FRACTURE HEALING.....	15
1.1.1. <i>Overview</i>	15
1.1.2. <i>Basic anatomy of bone</i>	16
1.1.3. <i>Primary fracture healing</i>	18
1.1.4. <i>Secondary fracture healing</i>	18
1.1.5. <i>Complications in fracture healing</i>	21
1.2. TRAUMA PARAMETERS.....	24
1.2.1. <i>Fracture type classification</i>	24
1.2.2. <i>Gap size and interfragmentary movement</i>	25
1.2.3. <i>Injury severity</i>	26
1.2.4. <i>Vascularization and angiogenesis</i>	26
1.3. PATIENT PARAMETERS	26
1.3.1. <i>Demographics (Age and Sex)</i>	27
1.3.2. <i>Comorbidities and clinical parameters</i>	27
1.3.3. <i>Lifestyle</i>	28
1.4. TREATMENT PARAMETERS	30
1.4.1. <i>Overview: Fracture fixation instrumentation (Treatment options using fixation)</i>	31
1.4.2. <i>Conservative fracture management</i>	31
1.4.3. <i>Conventional interfragmentary compression</i>	32
1.4.4. <i>Tension bands</i>	34
1.4.5. <i>Buttress plates</i>	35
1.4.6. <i>External fixators</i>	35
1.4.7. <i>Intramedullary nails</i>	35
1.4.8. <i>Locking fixation</i>	35
1.4.9. <i>Miscellaneous other instrumentation</i>	38
1.4.10. <i>Rehabilitation activities (Loading)</i>	39
1.5. MECHANO-BIOLOGY OF FRACTURE HEALING.....	41
1.5.1. <i>Overview</i>	41
1.5.2. <i>Fracture fixation mechanics</i>	43
1.5.3. <i>Algorithms of fracture healing</i>	53
1.6. TIME RESPONSE OF FRACTURE HEALING	55
1.6.1. <i>Fracture healing cascade interplay with fixation</i>	55
1.6.2. <i>Specific, adapted fracture fixation</i>	60
CHAPTER 2. MODELLING FRACTURE FIXATION	66
2.1. ANALYTICAL MECHANICAL MODELS OF FRACTURE FIXATION	67
2.1.1. <i>Cantilever beam bending</i>	67
2.1.2. <i>Braced cantilever beam bending</i>	69

2.1.3.	<i>Screw stiffness (effective diameter)</i>	72
2.1.4.	<i>System spring stiffness</i>	73
2.2.	FINITE ELEMENT ANALYSIS	79
2.2.1.	<i>Idealization</i>	80
2.2.2.	<i>Parameter identification</i>	81
2.2.3.	<i>General procedure of model creation</i>	82
2.2.4.	<i>Modeling of patient specific geometry</i>	84
2.2.5.	<i>Modelling of patient specific material properties</i>	87
2.2.5.1.	<i>Homogenization of bone tissue</i>	88
2.2.5.2.	<i>Modelling of regenerative tissue</i>	89
2.2.6.	<i>Plate model</i>	90
2.2.7.	<i>Screw model and its interfaces</i>	92
2.2.8.	<i>Physiologically based boundary conditions of the femur</i>	97
2.2.9.	<i>Validation of modelling approaches</i>	100
CHAPTER 3.	MECHANICAL CONSTRAINTS OF THE BIOLOGY OF HEALING	118
3.1.	LITERATURE OVERVIEW	119
3.1.1.	<i>Mechanical parameters that influence fracture healing</i>	119
3.2.	SCREW CONFIGURATION	120
3.2.1.	<i>Screw number</i>	121
3.2.2.	<i>Screw placement</i>	121
3.2.3.	<i>Screw type</i>	123
3.3.	PLATE/NAIL CONFIGURATION & MATERIAL	124
3.3.1.	<i>Plate placement and length</i>	124
3.3.2.	<i>Plate/nail material</i>	126
3.3.3.	<i>Nail / plate design</i>	127
3.4.	FRACTURE CONFIGURATION	129
3.4.1.	<i>Fracture location</i>	129
3.4.2.	<i>Fracture size, reduction and cortical contact</i>	129
3.4.3.	<i>Fracture angle</i>	130
3.5.	LOADING CONDITIONS	131
3.5.1.	<i>Orientation</i>	131
3.5.2.	<i>Magnitude</i>	131
CHAPTER 4.	BIOMECHANICAL EXPLANATIONS AND CLINICAL EXAMPLES	133
4.1.	FIXATION STIFFNESS CONTROL AND LIMITS	134
4.1.1.	<i>Systematic analysis of screw placements and plate working length</i>	135
4.1.2.	<i>Systematic analysis of fracture slope</i>	140
4.1.3.	<i>Hybrid fixation</i>	145
4.1.4.	<i>Further limits of fixation</i>	147
4.2.	SAMPLING OF CLINICAL <i>IN VIVO</i> DATA FOR (MECHANICAL) STIMULATION	148
4.2.1.	<i>Dynamization options</i>	150
4.2.2.	<i>Case reports of delayed healing (with possibly unsuccessful fixation)</i>	151
4.3.	SAMPLING OF CLINICAL <i>IN VIVO</i> DATA FOR IMPLANT FAILURE	153
4.3.1.	<i>Reported failure cases and some possible explanations</i>	153
4.3.2.	<i>Unavoidable failures and revisions</i>	155
CHAPTER 5.	EMPLOYING MECHANO-THERAPY	156
5.1.	CONSEQUENCES: GUIDELINES FOR SURGEONS?	157
5.1.1.	<i>Fracture healing progress prediction and risk assessment</i>	157
5.1.2.	<i>Adapted mechano-therapy for mechano-biologic stimulation</i>	161
5.1.3.	<i>Adapted mechano-therapy for implant survival</i>	162
5.1.4.	<i>Recent evolution of fracture treatment concepts</i>	164

5.1.5.	<i>Requirements for future principles of fracture fixation</i>	165
5.2.	OUTLOOK: POTENTIAL OF OSTEOSYNTHESIS INSTRUMENTATION	166
5.2.1.	<i>Adapted implant choice</i>	166
5.2.2.	<i>Adapted implant designs</i>	166
5.2.3.	<i>Active implants for mechano-biologic stimulation</i>	167
5.3.	CONCEPT: COMPREHENSIVE, COHERENT MECHANO-THERAPY WITH DYNAMIC FIXATION	168
5.3.1.	<i>Preserving the regenerative capacity</i>	168
5.3.2.	<i>Stimulating the healing process</i>	169
5.3.3.	<i>Avoiding implant and bone failure</i>	169
5.3.4.	<i>Achieving and verifying fracture healing results</i>	170
5.2.4.	<i>Standardization of modeling and virtual implant testing</i>	171
SUMMARY		172
ZUSAMMENFASSUNG		173
DANKSAGUNG		175
CURRICULUM VITAE		176
PHD PORTFOLIO		177
REFERENCES		180

List of Figures

FIGURE 1-1: QUALITATIVE ILLUSTRATION OF THE COMPLEX PROCESS OF FRACTURE HEALING. LEFT: SURGICAL INTERVENTION AS ONE FORM OF CLINICAL FRACTURE MANAGEMENT. CENTER: CALLUS CROSS-SECTION AS ASSESSED DURING RESEARCH IN AN ANIMAL MODEL. RIGHT: HEALING RESULT CONTROLLED BY A CLINICAL X-RAY. 15

FIGURE 1-2: LEFT: THE COMPLEX PROCESS OF FRACTURE HEALING IS INFLUENCED BY CONFOUNDING PARAMETERS INVOLVING THE PATIENT (CHARACTERISTICS), TRAUMA AND TREATMENT. RIGHT: SURGEONS DEFINE THE PROPORTIONS HOW MUCH THEY FAVOR BIOLOGY (REGENERATIVE CAPACITY, MINIMIZING IATROGENIC TRAUMA) AT THE EXPENSE OF THE ACHIEVABLE MECHANICAL STIFFNESS AND CLINICAL STABILITY (I.E. ULTIMATE FAILURE STRENGTH AND RETENTION OF ALIGNMENT), (DUDA ET AL., 2001). 22

FIGURE 1-3: FRACTURE EXAMPLE OF AO CLASSIFICATION TYPE 33-A1.2 – SPIRAL FRACTURE AT THE DISTAL METAPHYSEAL FEMUR. 24

FIGURE 1-4: ANALYSIS OF FRACTURE HEALING CONSIDERING THE FRACTURE AS A DYNAMIC SYSTEM AND THE HEALING PROCESS AS A FEEDBACK CONTROL LOOP WITH THE SPECIAL FEATURE THAT BOTH THE PLANT (REGENERATIVE TISSUE) AND THE CONTROLLER SIGNAL ARE BOTH DYNAMICALLY CHANGING. 45

FIGURE 1-5: NEITHER THE FRACTURE BIOLOGY NOR THE LOCAL STIMULATION OR THE MECHANICAL CONDITIONS ALONE CAN EXPLAIN ALL FRACTURE COMPLICATION CASES. THE INTERACTING VARIABLES OF REGENERATIVE POTENTIAL AND EXCITATION DETERMINE THE HEALING RESULT TOGETHER, THUS THE PATIENT-, TRAUMA- AND THERAPY-SPECIFIC RISK FACTORS ARE NOT NECESSARILY ADDITIVE. 46

FIGURE 1-6: SCHEMATIC DIAGRAMS FOR FRACTURE TREATMENT PARAMETERS, LEFT: COMPROMISE OF CREATING HIGH STIFFNESS CONSTRUCT VERSUS PRESERVING HEALING POTENTIAL HAS LED TO THE TWO DIAMETRICALLY OPPOSED PRINCIPLES OF SURGICAL FIXATION: ABSOLUTE STABILITY (BLUE SQUARE) VERSUS RELATIVE STABILITY (BLUE TRIANGLE) ENSURING PARETO OPTIMAL CHOICE OF FIXATION (PARETO FRONTIER DASHED IN BLUE DENOTES GOOD HEALING RESULTS). A HYBRID FIXATION OFTEN LED TO A DECREASE OF STIFFNESS AND HEALING POTENTIAL AND LESS FAVORABLE RESULTS (RED CIRCLE). NOVEL (DYNAMIC) FIXATION (BLUE CIRCLE) MAY PRESERVE HEALING POTENTIAL (REGENERATIVE CAPACITY) MAINTAINING ALIGNMENT AT THE SAME TIME. RIGHT: NOW, THE OSTEOSYNTHESIS STIFFNESS CAN BE CONTROLLED TO ADAPT THE MOVEMENT THAT LEADS TO STIMULATION AND HEALING (EPARI ET AL., 2007) BECAUSE THE HEALING POTENTIAL IS MAINTAINED IN A FIXATION THAT RETAINS THE ALIGNMENT. 48

FIGURE 1-7: SCHEMATIC OF CONSTRUCT ULTIMATE STRENGTH VS. BONE QUALITY AS A FUNCTION OF CONSTRUCT TYPE ADAPTED FROM MEASUREMENTS OF KIM ET AL. (2007) AND THE REVIEW OF MILLER AND GOSWAMI (2007) SUGGESTING HIGHER ULTIMATE STRENGTH FOR NON-LOCKING CONSTRUCTS IN NORMAL BONE QUALITY (DENSITY ABOVE 0.55 G/CM³) AND CONSISTENTLY HIGH ULTIMATE STRENGTH EVEN FOR LOW BONE QUALITY (E.G. OSTEOPOROTIC BONE). 51

FIGURE 1-8: SCHEMATIC TIME PROGRESS OF HEALING SHOWS THAT USING DIFFERENT FIXATION PRINCIPLES LEADS TO DIFFERENT TIME-KINEMATICS OF STIFFNESS INCREASE: INITIALLY LOW RATE OF IMPROVEMENT FOR DYNAMIC FIXATION, BUT IN LATER STAGES MUCH STRONGER INCREASE OF STIFFNESS IN LATER STAGES FOR DYNAMIC FIXATION. 60

FIGURE 2-1: CANTILEVER BEAM WITH SINGLE LOAD AT THE END. 67

FIGURE 2-2: BEAM WITH A LOAD AND A CONFINED CURVATURE AT ONE END AND ONE FIXED END. 69

FIGURE 2-3: TEST SET-UP FOR CANTILEVER BENDING OF A SINGLE SCREW. LOAD WAS APPLIED AS A FORCE AT 50 MM DISTANCE. 72

FIGURE 2-4: SCHEMATIC SPRING SYSTEM 73

FIGURE 2-5: STIFFNESS OF DEFECT BRIDGING FOR VARYING PLATE STIFFNESS (SCREW STIFFNESS CONSTANT) AND VARYING TISSUE COMPLIANCE OVER THE FRACTURE (DEFECT STIFFNESS). 74

FIGURE 2-6: STIFFNESS OF BONY BRIDGING FOR VARYING PLATE STIFFNESS (SCREW STIFFNESS CONSTANT). 75

FIGURE 2-7: TOTAL STIFFNESS OF BONY BRIDGING AND DEFECT BRIDGING FOR VARYING PLATE STIFFNESS (SCREW STIFFNESS CONSTANT). 76

FIGURE 2-8: EXCESS DEFECT STIFFNESS COMPARED TO INTACT BONE STIFFNESS DURING FRACTURE HEALING RELATIVE TO PLATE STIFFNESS FOR THE GIVEN ASSUMPTIONS ABOVE. 77

FIGURE 2-9: SCHEMATIC STEPS OF A BIOMECHANICAL FINITE ELEMENT MODEL CREATION. 83

FIGURE 2-10: LEFT: IMAGING DATA (QCT), HERE FRONTAL PLANE, SERVED AS DATA SOURCE FOR SEGMENTATION, WHICH WAS PERFORMED MANUALLY, PER SLICE DIRECTLY ON THE DATA SET, SEPARATING BONE TISSUE FROM OTHER TISSUES BASED ON IMAGE INTENSITY AND GENERAL SHAPE OF THE BONE. 85

FIGURE 2-11: LEFT (BLUE): REPRESENTATION OF THE FEMUR GEOMETRY WITH SPLINES ALLOWS IMPORT TO PRE-PROCESSING SOFTWARE AND POSITIONING OF OTHER HARDWARE RELATIVE TO BONE (HERE A PLATE). 86

FIGURE 2-12: ALL MESHES HAVE ELEMENT EDGE LENGTHS WELL BELOW 2 MM FOR MOST ELEMENTS. FOR MESH SIZE SENSITIVITY TESTING, DIFFERENT CHARACTERISTIC ELEMENT LENGTHS WERE IMPLEMENTED: 1.67 MM, 240798 DOFS, LEFT, OR 1.37 MM, 459825 DOFS, 1.10 MM, 894900 DOFS, RIGHT. THE REACTION FORCES, SURFACE STRAIN AND DISPLACEMENT WITH FINER MESHES ARE CONSISTENT WITH THE COARSER MESHES, ALLOWING THE USE OF THE MODELS WITH FEWER DOFS AND FASTER COMPUTATION, COMPARE (HEYLAND ET AL., 2015B). 87

FIGURE 2-13: MODELLING RESULT EXAMPLE OF MATERIAL MAPPING APPROACH YIELDING 414 BINS OF 50 MPA SIZE WITH RISING YOUNG'S MODULUS FROM RED TO GREEN, ON THE LEFT FOR THE FEMORAL SURFACE, ON THE RIGHT FOR A CUT OF THE FEMUR. NOTE THE HIGH MATERIAL MODULUS OF THE DIAPHYSEAL CORTEX AND THE LOWER MODULI AT THE META- AND EPIPHYSES WITH SMALL AREAS OF HIGH MODULI AT THE JOINT SURFACES (THIN CORTICES). THE LOWER DENSITY WITHIN THE METAPHYSES UNDERLINES THE NECESSITY OF PROPER AND SUFFICIENT FIXATION INSTRUMENTATION IN THOSE ZONES, I.E. FOR INSTANCE MORE SCREWS AND ESPECIALLY LOCKING SCREWS ARE BENEFICIAL FOR A MORE POROUS SUBSTRATE. 89

FIGURE 2-14: EXAMPLE OF ONE TRANSVERSE IMAGING SLICE WITH BONE AND SURROUNDING TISSUE AND A PHANTOM WITH MINERAL CYLINDERS OF KNOWN DENSITY FOR CALIBRATION OF IMAGE INTENSITY TO APPARENT DENSITY. 89

FIGURE 2-15: COLLAPSE OF THE FRACTURE GAP WITH CONTACT OF THE PROXIMAL AND DISTAL SEGMENTS FOR A 10 MM DIAPHYSEAL GAP UNDER WALKING LOADS WITHOUT ADDITIONAL SUPPORT WITHIN THE FRACTURE GAP. 90

FIGURE 2-16: PLATE PLACEMENT IS NOT TRIVIAL AS THERE IS NO UNIVERSAL ALGORITHM. SURGICAL TECHNIQUES VARY AND THUS PLATE PLACEMENT MAY VARY STRONGLY. WE TRIED TO PLACE THE PLATE WITH A SMALL DISTANCE BETWEEN THE PLATE AND THE BONE (CLEARANCE) TO ALLOW FOR FREE PLATE BENDING. HOWEVER, THIS BONE-PLATE DISTANCE SHOULD REMAIN SMALL OVER THE WHOLE PLATE LENGTH TO AVOID EXCESSIVELY LONG FREE BENDING LENGTHS OF INDIVIDUAL SCREWS. FURTHERMORE, EXCESSIVE DISTANCE OF THE PLATE FROM THE BONE RESULTS IN DECREASED PLATE STRENGTH AHMAD ET AL. (2007). 91

FIGURE 2-17: EXAMPLE OF A SCREW MODEL PLUS INTERFACES TO PLATE AND BONE (BONE NOT SHOWN). LEFT: WHOLE PLATE WITH MULTIPLE SCREWS AND THEIR CONNECTIONS VIA MULTI-POINT CONSTRAINTS. RIGHT: DETAIL OF PROXIMAL PLATE TIP WITH ONE SCREW AND ITS MULTIPLE CONNECTIONS. 92

FIGURE 2-18: TOP: SCHEMATIC CUT OF A DYNAMIC LOCKING SCREW (DLS)..... 93

FIGURE 2-19: THE DYNAMIC LOCKING SCREWS WITH MULTIPLE CONTACTING PARTS WERE SIMPLIFIED WITH A TUBE-TO-TUBE CONTACT WITH SPECIAL ITT31 ELEMENTS, COMPARE THE IMAGES ABOVE IN [HTTP://WWW.LHE.NO/DOWNLOAD/ABAQUS_TUBE-TO-TUBE_MODELING.PDF](http://www.lhe.no/download/abaqus_tube-to-tube_modeling.pdf), LAST ACCESSED 18. SEPTEMBER 2018. ON THE RIGHT YOU CAN OBSERVE OUR IMPLEMENTATION IN ABAQUS/CAE. 93

FIGURE 2-20: SCHEMATIC APPEARANCE OF STRUCTURAL BEAM MODELS OF SCREWS, WHICH ARE CONNECTED TO SUBSTRATE BONE AND PLATE. ON THE LEFT FOR A STANDARD LOCKING SCREW AND ON THE RIGHT FOR A DYNAMIC LOCKING SCREW. 94

FIGURE 2-21: FINITE ELEMENT MODEL IMPLEMENTATION (CENTER, RIGHT) OF THE *IN VITRO* EXPERIMENT BY DÖBELE ET AL. (2014) ON THE LEFT. 95

FIGURE 2-22: COMPARISON OF DISPLACEMENT MEASUREMENT RESULTS FROM DÖBELE ET AL. (2014), LEFT, AND OUR NUMERICAL SIMULATION, RIGHT, OF A CYLINDER WITH A LATERAL PLATE UNDER AXIAL-BENDING LOAD FOR TWO DIFFERENT SCREW TYPES: LOCKING SCREWS (BLUE) AND DYNAMIC LOCKING SCREWS (RED). 96

FIGURE 2-23: SINGLE SCREW MODEL ROTATING AROUND THE SCREW HEAD WITH A MEASUREMENT-MATCHED ROTATIONAL SPRING STIFFNESS ADDITIONALLY TO SCREW SHEAR-BENDING. 96

FIGURE 2-24: WHEN A DISPLACEMENT CONSTRAINT IS APPLIED TO ONE NODE OF A COMPLIANT ELEMENT (LOW MODULUS), REACTION FORCES LEAD TO HIGH DEFORMATION OF THIS ELEMENT. THIS WAS SOLVED BY DISTRIBUTING THE CONSTRAINT ON MULTIPLE NODES. 97

FIGURE 2-25: DIFFERENT VIEWS OF THE REPRESENTATION OF THE BONES AND THE CONSIDERED MUSCLES FOR THE INVERSE DYNAMICS ESTIMATION OF THE MUSCLE AND JOINT FORCES AT THE FEMUR. MUSCLES AT OTHER BONES THAT WERE USED FOR CALCULATION ARE NOT SHOWN. 99

FIGURE 2-26: LEFT: SCALED LOADS (RED) FOR 45% OF THE GAIT CYCLE (MAXIMUM HIP JOINT LOAD) WITH ADDITIONAL MUSCLE LOADS, ESPECIALLY RELEVANT AT THE GREATER TROCHANTER. 99

FIGURE 2-27: OVERVIEW OF THE TESTING PROCEDURE. 101

FIGURE 2-28: FROM LEFT TO RIGHT: EXAMPLE OF VALIDATION SPECIMEN OF A DISTAL FEMUR WITH LATERAL PLATE FIXATION, EMBEDDED IN PMMA (WITH PURPLE CLAY TO ALLOW FREE PLATE MOTION). CT-IMAGES WERE OBTAINED AFTER TESTING TO VERIFY INTEGRITY AND FOR MODELLING. FLUOROSCOPIC IMAGES SHOW THE SCREW POSITION (NUMBER OF HOLES 9,7,5,3 MARKED) AND THE EMPTY SCREW HOLES OF PREVIOUS TESTING. 102

FIGURE 2-29: LEFT: TEST RIG SET-UP FOR TORSIONAL TESTING. 104

FIGURE 2-30: MATERIAL MAPPING OF VALIDATION SPECIMENS WITH A MULTI-BIN APPROACH (LEFT) AND A REDUCED MAPPING TWO-BIN APPROACH SIMILAR TO SIMPLIFIED MODELS THAT WERE PUBLISHED BEFORE (SPEIRS ET AL., 2007)..... 105

FIGURE 2-31: VALIDATION REGRESSION RESULTS OF IFM SEPARATED ACCORDING TO LOAD AND MATERIAL MAPPING MODEL..... 107

FIGURE 2-32: POOLED VALIDATION REGRESSION RESULTS OF IFM FOR THE TWO MATERIAL MAPPING MODELS.	108
FIGURE 2-33: INTERFRAGMENTARY MOVEMENT BETWEEN DEFINED NODES (LEFT IN RED, CORRESPONDING PAIRS AT THE PROXIMAL SEGMENT NOT SHOWN) WERE EVALUATED FOR THE MEDIAL AND LATERAL POINT PAIRS. WHEN IDENTIFYING THE CORRESPONDING THE LOCATIONS, AN ERROR MIGHT BE INTRODUCED BY MISMATCHED POINT CORRESPONDENCE (RIGHT, ERROR IN LOCATION SYMBOLISED BY THE EXTENSION OF THE BLUE CIRCLES).	109
FIGURE 2-34: OVERVIEW OF BONE AND PLATE DEFORMATION. LEFT: INTACT BONE DEFORMATION UNDER PHYSIOLOGICAL LOADING SCALED 5 TIMES FOR CLARITY. THE ISTHMUS OF THE BONE IS DEFLECTED LATERALLY. RIGHT: LOCKING PLATE FRACTURE FIXATION UNDER PHYSIOLOGICAL LOADING SHOWING SPLINTING OF THE BONE AND LESS LATERAL DISPLACEMENT OF THE SHAFT, 3 TIMES SCALED.	113
FIGURE 2-35: AXIAL FORCE AT THE DLS HEAD (LONGITUDINAL SCREW DIRECTION) FOR DIFFERENT SCREW CONFIGURATION OVER THE HEALING COURSE.	114
FIGURE 2-36: RESULTING SHEAR FORCE AT THE DLS HEAD (LONGITUDINAL SCREW DIRECTION) FOR DIFFERENT SCREW CONFIGURATION OVER THE HEALING COURSE.	114
FIGURE 2-37: REALISTIC FATIGUE FAILURE MECHANISMS (DAMAGE PATTERN) OF A DYNAMIC LOCKING SCREW DURING PHYSIOLOGICAL LOADING. EXCESSIVE VON MISES STRESS IS SHOWN IN RED (QUANTITATIVE LEGEND PURPOSEFULLY NOT SHOWN, NO SYSTEMATIC EVALUATION OF OPERATIONAL STRENGTH USING S-N OR WÖHLER CURVES). LEFT: ABOUT 200N OF SHEAR AND TRACTION LOAD, ADJACENT TO AN EXTENDED FITTING AT THE PIN, CAN LEAD TO A FATIGUE FAILURE AND BREAKAGE AT THE END OF THE PIN. RIGHT: FATIGUE FAILURE AT THE SCREW HEAD UNDER SHEAR AND COMPRESSIVE LOAD WOULD REQUIRE COMPRESSIVE FORCES HIGHER THAN 260N WITH 200N SHEAR.	117
FIGURE 4-1: SCHEMATIC REPRESENTATION OF A DISTAL FEMUR FRACTURE WITH UNCLEAR OPTIONS FOR SCREW PLACEMENT.	135
FIGURE 4-2: PLATE WORKING LENGTH (PWL: HERE 3 EMPTY SCREW HOLES ON THE RIGHT) IS THE DISTANCE BETWEEN THE TWO SCREWS CLOSEST TO THE FRACTURE ON EITHER SIDE OF THE FRACTURE, HERE WITH 62 MM ON THE LEFT AND 102 MM IN THE CENTER.	135
FIGURE 4-3: DIFFERENT SCREW PLACEMENTS ARE POSSIBLE WHEN A LONG PLATE IS CHOSEN FOR A DISTAL FEMUR FRACTURE. LEFT TO RIGHT: CLINICAL EXAMPLE OF DISTAL FEMUR FRACTURE FIXATION IN A X-RAY CONTROL. THREE SCREW PLACEMENT VARIATIONS.	136
FIGURE 4-4: PEARSON CORRELATIONS (RIGHT TABLE) OF DIFFERENT SCREW DISTANCES WITHIN THE PLATE (LEFT, A-D) VERSUS IFM COMPONENTS (AXIAL=Z, SHEAR) AT DIFFERENT POSITIONS (ANTERIOR, POSTERIOR, LATERAL, MEDIAL) AS POINTED OUT IN THE CENTER FOR DIFFERENT SCREW TYPES PROXIMALLY (LS VERSUS DLS). NOTE THAT PLATE WORKING LENGTH (A) SHOWS THE STRONGEST CORRELATIONS.	137
FIGURE 4-5: THE AXIAL IFM UNDER THE PLATE (LEFT) AND OPPOSITE THE PLATE (RIGHT) FOR TWO DIFFERENT SCREW TYPES IN THE PROXIMAL SHAFT. COMPARE FIGURE 4-2, AND FIGURE 4-4: LETTER "A" SIGNIFIES THE PLATE WORKING LENGTH OR EMPTY SCREW HOLES ACROSS THE FRACTURE.	138
FIGURE 4-6: THE RATIO SHEAR/AXIAL IFM UNDER THE PLATE (LEFT) AND OPPOSITE (RIGHT) FOR TWO DIFFERENT SCREW TYPES IN THE PROXIMAL SHAFT. COMPARE FIGURE 4-2, AND FIGURE 4-4: LETTER "A" SIGNIFIES THE PLATE WORKING LENGTH OR EMPTY SCREW HOLES ACROSS THE FRACTURE.	139
FIGURE 4-7: SCHEMATIC SHOWING AN INCREASE IN SHEAR COMPARED TO AXIAL MOVEMENT WITH HIGHER PLATE WORKING LENGTH. RESULTING SHEAR (MOTION IN FRACTURE PLANE) IS THE VECTOR ADDITION OF THE RELATIVE MOTION IN THE TWO DIRECTIONS IN THE FRACTURE PLANE. AXIAL MOVEMENT IS THE MOTION IN Z-DIRECTION, ORTHOGONAL TO FRACTURE PLANE.	139
FIGURE 4-8: LOCAL IFMS WITH ITS COMPONENTS IN- AND OUT-OF- PLANE DETERMINE LOCAL STRAIN WITH ITS COMPONENTS AS A FUNCTION OF FRACTURE SIZE AND SHAPE.	140
FIGURE 4-9: DIFFERENT MODELS OF FRACTURE CONFIGURATION WITH BRIDGING GAP TISSUE. THE RESULTING IFM HAS THE COMPONENTS IN-PLANE (IPM) AND OUT-OF-PLANE (OPM).	141
FIGURE 4-10: COMPONENTS OF IFM (LEFT: OUT-OF-PLANE, RIGHT: IN-PLANE) FOR DIFFERENT FRACTURE ANGLES (FRONTAL PLATE), DIFFERENT GAP SIZES (1 MM OR 3 MM) AND DIFFERENT PLATE WORKING LENGTHS.	141
FIGURE 4-11: DIFFERENCE IN VOLUME FOR AN IDEAL CYLINDER (LEFT) AND REAL BONE SAMPLE (RIGHT) WITH CUTTING ANGLE AND GAP SIZE (HEIGHT).	142
FIGURE 4-12: VOLUME-NORMALISED IN-PLANE COMPONENT OF IFM (SHEAR MOVEMENT) FOR DIFFERENT FRACTURE ANGLES (FRONTAL PLATE), DIFFERENT GAP SIZES (1 MM OR 3 MM) AND DIFFERENT PLATE WORKING LENGTHS ON THE LEFT VERSUS MEAN DEVIATORIC STRAIN OF GAP TISSUE.	143
FIGURE 4-13: CALCULATED FRACTURE ANGLES FOR MINIMUM IN-PLANE AND MAXIMUM OUT-OF-PLANE IFM USING DATA FROM THE SYSTEMATIC SCREW PLACEMENT ANALYSIS. THE TABLE HEADINGS L, M, P, A STAND FOR LATERAL, MEDIAL, POSTERIOR, ANTERIOR POSITIONS IN THE FRACTURE GAP, COMPARE FIGURE 4-4, FIGURE 4-7.	144
FIGURE 4-14: VOLUME-NORMALISED OUT-OF-PLANE COMPONENT OF IFM (NORMAL MOVEMENT) FOR DIFFERENT FRACTURE ANGLES (FRONTAL PLATE), DIFFERENT GAP SIZES (1 MM OR 3 MM) AND DIFFERENT PLATE WORKING LENGTHS ON THE LEFT VERSUS MEAN HYDROSTATIC (MEAN OF PRINCIPAL STRAINS) OF GAP TISSUE.	144

FIGURE 4-15: PROCEDURE SET-UP FOR TESTING THE EFFECT OF AN ADDITIONAL LAG SCREW NEXT TO LOCKED PLATING COMPARED TO ONLY LOCKED PLATING: A, LAG SCREW GROUP, B, LOCKING PLATE GROUP, C, LAG SCREW GROUP WITH INCREASED PLATE WORKING LENGTH, D, LOCKING PLATE GROUP WITH INCREASED PLATE WORKING LENGTH. 145

FIGURE 4-16: OUT-OF-PLANE MOVEMENT RESULTS FOR TESTS WITH OR WITHOUT LAG SCREW NEXT TO A LOCKING PLATE FOR DIFFERENT LOADS AND DIFFERENT WORKING LENGTHS..... 146

FIGURE 4-17: IN-PLANE MOVEMENT RESULTS FOR TESTS WITH OR WITHOUT LAG SCREW NEXT TO A LOCKING PLATE FOR DIFFERENT LOADS AND DIFFERENT WORKING LENGTHS. 146

FIGURE 4-18: PLATE CURVATURE DOES NOT FIT ALL PATIENTS AND MIGHT LEAD TO NON-UNIFORM, AND ALSO PARTIALLY LARGE CLEARANCES BETWEEN PLATE AND BONE ESPECIALLY AT THE PLATE TIPS..... 147

FIGURE 4-19: RECONSTRUCTION OF PLATE POSITION BASED ON EDGE-MATCHING FROM A SINGLE-PLANE X-RAY IMAGE USING A 3D BONE AND PLATE MODEL WITH MODEL-BASED RSA, MEDIS SPECIALS B.V., NETHERLANDS (MOEWIS ET AL., 2012)..... 148

FIGURE 4-20: EFFECT OF MECHANICAL TESTING CONDITIONS. TOP: SIMPLE AXIAL-BENDING MODEL OF A LATERAL PLATE WITH LOCKING SCREWS ON THE LEFT AND DYNAMIC LOCKING SCREWS ON THE RIGHT, LEADING TO APPRECIABLY DIFFERENT DEFORMATIONS (=TISSUE STIMULATION) OF COMPLIANT GAP TISSUE. BOTTOM: COMPLEX PHYSIOLOGICAL LOADING MODEL OF A LATERAL PLATE WITH LOCKING SCREWS ON THE LEFT AND DYNAMIC LOCKING SCREWS ON THE RIGHT, LEADING TO HARDLY NOTICEABLE DIFFERENCE IN DEFORMATION (=TISSUE STIMULATION) OF COMPLIANT GAP TISSUE..... 149

FIGURE 5-1: LOCKING PLATE PLACEMENT LATERALLY (LEFT) MAY LEAD TO MEDIAL BONY SUPPORT UNDER LOAD (RIGHT). 164

Chapter 1. Background of fracture healing

Overview of fracture healing, general introduction to bone tissue and fracture fixation, background of mechano-biology and outline of a coherent fracture treatment

How can fracture healing work?

Relevant publications:

*Mehta, M., Lienau, J., Heyland, M., Woloszyk, A., Fratzl, P., & Duda, G. (2010). Quantitative spatio-temporal callus patterning during bone defect healing using 4D monitoring. *Bone*, 47, S101-2.*

*Mehta, M., Checa, S., Lienau, J., Hutmacher, D., & Duda, G. N. (2012). In vivo tracking of segmental bone defect healing reveals that callus patterning is related to early mechanical stimuli. *Eur Cell Mater*, 24, 358-71. (Acknowledged M. Heyland)*

*Frisch, J. T. (2012). *Frakturheilung bei Immuninsuffizienz* (Doctoral dissertation, Freie Universität Berlin). (Acknowledged M. Heyland)*

*El Khassawna, M. S. T. (2013). *Cellular and molecular analysis of fracture healing in a neurofibromatosis type 1 conditional knockout mice model* (Doctoral dissertation, Humboldt-Universität zu Berlin). (Acknowledged M. Heyland)*

*Heyland, M., Mehta, M., Toben, D., & Duda, G. N. (2013). Microstructure and homogeneity of distribution of mineralized struts determine callus strength. *Eur Cell Mater*, 25, 366-79.*

1.0. Overview

Within this dissertation, mechanical issues related to bone fracture fixation (osteosynthesis¹) are discussed, mainly concerning the preservation and adapted exploitation of the regenerative capacity of bone tissue with special attention to biological requirements for fracture healing.

1.0.1. General Background

A bone fracture is a macroscopic separation of bone and trauma to surrounding tissue resulting from mechanical overload. A world incidence of bone fracture of about 9.0-22.8/1000/year (roughly 1-2% per year) has been found (Court-Brown and Caesar, 2006, Donaldson et al., 1990, Sahlin, 1990, Melton III et al., 1999). However, the fracture incidence varies strongly for different fracture locations, between sexes and geographic regions. Increased fracture rates occur in young male adults caused mainly by their lifestyle (motor vehicle or sport accidents) and elderly individuals due to motor control issues, and especially women due to osteoporosis (Singer et al., 1998, Court-Brown and Caesar, 2006). Today, the treatment of most fractures is reliable and efficient. Nevertheless, a few fracture types and attendant circumstances still pose problems in some cases.

1.0.2. Problem

The challenge of modern osteosynthesis¹ consists of distinguishing potential problem fractures from simply treatable fractures just as well as treating the fractures and the revision cases. Empirically found risk factors have helped to identify certain fracture types that may pose difficulties. Currently, medical treatment of most fractures of the same kind occurs in a standard fashion. Additional care and effort has to be invested if the fracture shows signs of delayed or absent healing. There have been investigations on ideal fracture healing conditions and the scientific community roughly knows about the general framework of sound fracture healing (Epari et al., 2007, Giannoudis et al., 2007, Matthews et al., 2008, Geris et al., 2010a, Augat et al., 2005, Einhorn, 1995). Although there have been basic approaches by different working groups, neither scientists nor professional foundations or research

¹ Literally from Greek [όστέον σύνθεσις = ostéon sýnthesis]: bone (re-)assembly, in medical terms consisting of:
1. Reduction, i.e. the restoration of appropriate bone-joint alignment, i.e. set the fractured bone segments, and
2. Internal fixation, i.e. retention of proper alignment (with implants) under load.

societies have fully transcribed the implementation of a required osteosynthesis stiffness into clinical guidelines to create an adapted osteosynthesis implant structure to achieve an adequate tissue stimulation.

1.0.3. Goals

The intention of the following analyses is to find general working principles of fracture fixation for successful, expeditious and robust fracture healing, and apply those principles to patient-specific configurations of fracture fixation. In detail, the importance of a coherent fracture treatment is established with consideration of the regenerative capacity as well as the stimulation of healing. Fracture treatment variables for mechano-therapy are identified and their influence on fracture healing is evaluated, finding key elements of fracture treatment. Based on those key features, strategies of fracture treatment are identified and validated numerically.

Overall, the influence of fixation parameters and their control for mechano-therapy are assessed. Examples using clinical *in vivo* data show the capacity and compare the performance of finite element models, biomechanical tests and an analytical tool to assess the role of adapted fixation conditions for fracture treatment. A discussion of future perspectives of fracture mechano-therapy, its control and monitoring will elucidate potential developments in the field of mechano-therapeutics.

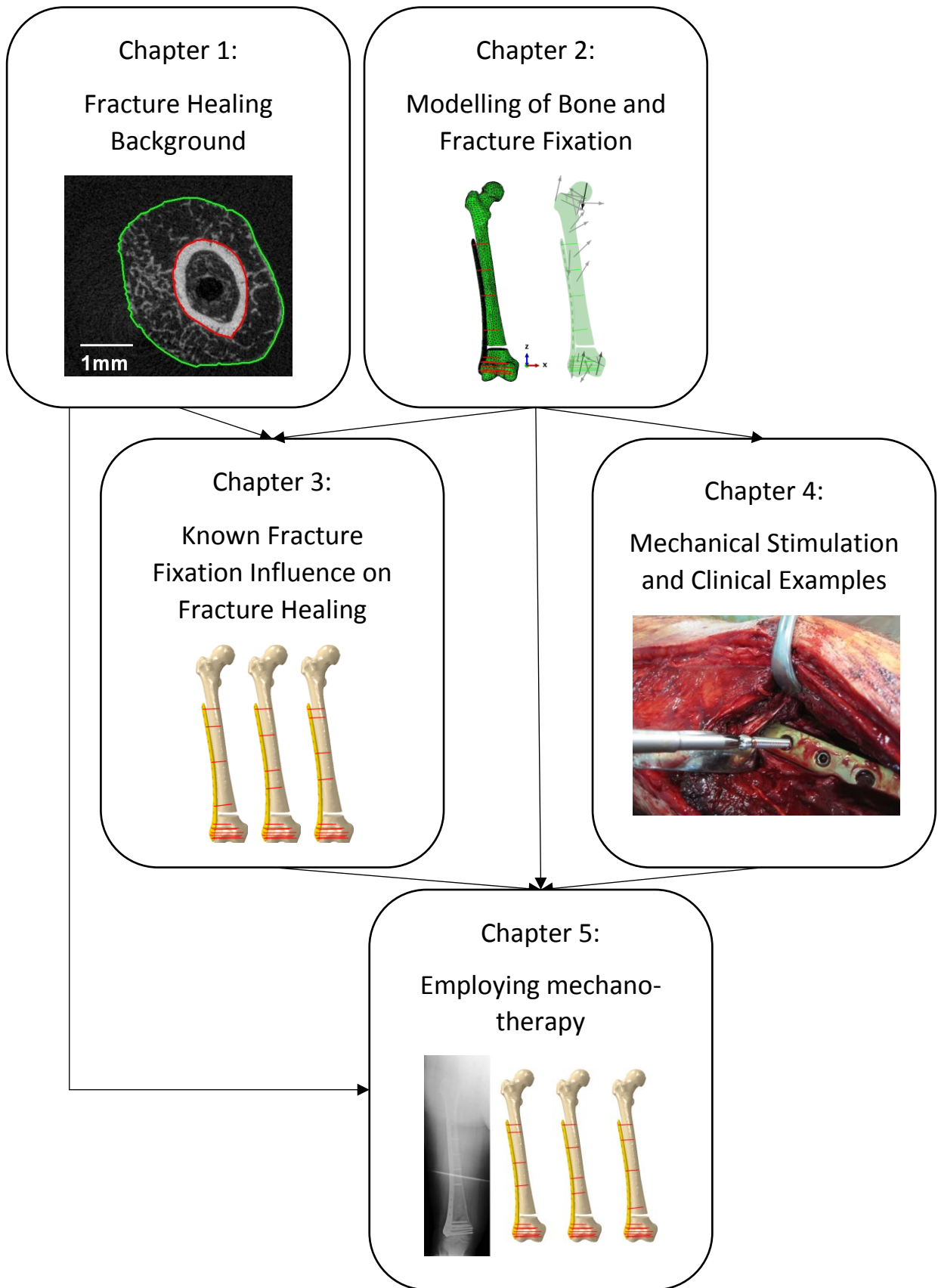
1.0.4. Scope

This research covers computational modeling approaches of current standard fixations of long bones, especially locking plate fixations with generic and patient-specific geometry and under generic and patient-specific physiological load with different means of screw-bone fixation, especially for exemplary problem fractures of the femur and their validation through *in vitro* experiments and comparison to reported individual cases from the literature.

1.0.5. Hypotheses

1. Fracture fixation parameters (type of fixation, position, material, and configuration) influence mechano-biological stimulation in the form of interfragmentary movement and interfragmentary strain at the fracture zone.
2. Physiologically realistic models of fracture fixation can be created using finite element models that can describe the mechano-biological tissue stimulation.
3. The configuration of locked plating fracture fixation has a reliable mechanical influence on the
 - a) initial interfragmentary movement components and
 - b) initial strain at the fracture site.
4. A distinct construct configuration (screw type and placement, plate position) of internal locked plating fracture fixation leads to a desired biologically adapted mechanical stimulus (according to basic research) within the fracture gap for a certain fracture model (fracture type configuration).
5. Different fracture models can be fixated in a reproducible way with internal locked plating so that they reproducibly and robustly lead to a destined range of mechanical stimulation at the fracture site.
6. The mechanical environment of orthopedic fracture fixation can be controlled reliably so that the mechanical stimulus at the fracture site can be controlled with sufficient robustness (within desired mechanical range).
7. A coherent fracture treatment (mechano-therapy) can be established as a compromise of adapted mechano-biologic stimulation, minimal iatrogenic trauma, necessary reduction and fixation strength.

1.0.6. Graphical Outline of the Thesis



1.1. Fracture healing

1.1.1. Overview

The remarkable and complex physiological process of fracture healing may reconstitute a connection of separated bone parts with functional new bone tissue for many fractures (Figure 1-1). Primary (direct) and secondary (indirect) bone fracture healing can be differentiated on grounds of the healing pathway running through different tissue types. About 5-10% of long bone fractures however, do not heal adequately swift, misplaced or not at all, resulting in delayed union, mal-union, non-union or other physical impairment up to amputation or even death (Rodriguez-Merchan and Forriol, 2004, Tzioupis and Giannoudis, 2007). Orthopedic fracture care can treat most of such critical fractures by applying reduction and fixation with implants, holding the fractured bone fragments in place, and impeding infections at the same time. Such an osteosynthesis should provide a mechanically and biologically favorable environment for successful (*restitutio ad integrum*), expeditious (quick initiation and completion) and reliable (robust) fracture healing.

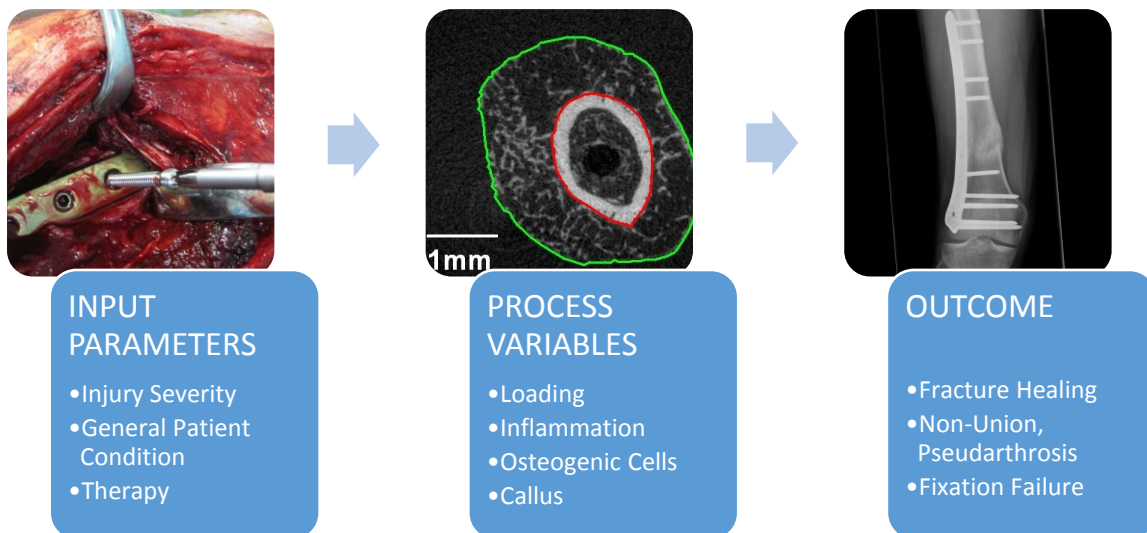


Figure 1-1: Qualitative illustration of the complex process of fracture healing. Left: Surgical intervention as one form of clinical fracture management². Center: Callus cross-section as assessed during research in an animal model³. Right: Healing result controlled by a clinical X-ray⁴.

² Clinical images were provided by PD Dr. med. Sven Märdian from university hospital of Charité - Universitätsmedizin, Berlin, Germany.

³ Research image from Julius Wolff Institute for Biomechanics and Musculoskeletal Regeneration, Charité - Universitätsmedizin, Berlin, Germany.

⁴ Clinical images were provided by PD Dr. med. Sven Märdian from university hospital of Charité - Universitätsmedizin, Berlin, Germany.

1.1.2. Basic anatomy of bone

Bone tissue properties represent a compromise of both necessary stiffness to limit the strain and thus leading to a more efficient whole-body dynamics, and elasticity for shock absorption and fracture risk reduction. Bone mass is minimized for weight reduction through load-adaptive remodeling of bone morphology. Thus, depending on the location and function, bone structure and composition vary.

1.1.2.1. Extracellular structure of bone tissue (bone matrix)

Hydroxyapatite⁵, collagen⁶, proteoglycans⁷, non-collagenous proteins and water consistently form the main components of bone. These components are not distributed uniformly, but heterogeneously in porous structures and with anisotropic (mostly with almost orthotropic) material properties (Felsenberg, 2001, Doblaré et al., 2004, Fratzl and Weinkamer, 2007, Currey, 2002).

Bone is a biologically synthesized nano-composite with a strong hierarchical structure over many orders of magnitude. The following table (Table 1) illustrates the bone structure, adapted from Weiner and Wagner (1998), Martin et al. (1998):

⁵ specifically considered carbonous, apatitic calcium phosphate with amorphous phases similar to that of hydroxyapatite or dahllite

⁶ structural protein, polycondensated polymer with frequent occurrence of the amino acid glycine, in bones, skin, tendons, ligaments type 1, i.e. two alpha-1 chains and one alpha-2 chain, configured via hydrogen bonds to triple helices, called tropocollagen molecules, which assemble into microfibrils and via covalent bonds to collagen fibers and collagen fiber bundles

⁷ macro-molecules from proteins and carbohydrates which stabilize and regulate molecule movements, store growth factors within the extra cellular matrix, attract ions, attract water molecules via osmosis, and inhibit mineralization

Table 1: Hierarchical structure of bone tissue.

Order of magnitude (size, amount)	Structure
few <i>nm</i> - ca. 100 <i>nm</i>	Main components:
ca. 40-50%	Hydroxyapatite ⁵ : $\text{Ca}_5(\text{OH})(\text{PO}_4)_3$
ca. 30%	Collagen ⁶
ca. 20-30%	Water: H_2O
few %	Others (proteoglycans, other proteins, etc)
few 100 <i>nm</i>	Mineralized fibers (collagen fibers with external mineral phase)
some 100 <i>nm</i>	Fiber bundles
some more 100 <i>nm</i>	Arrangement of fiber bundles
>10 μm	a) Trabeculae in cancellous bone b) Osteons (Havers-systems) in compact bone
>100 μm	Bone tissue either shows high or low porosity, two types: a) trabecular or spongy bone (50-95% porosity), mostly in cuboidal bone, flat bone and at the end of long bones b) cortical or compact bone (5-10% porosity, different pores)
>1 <i>mm</i>	Whole bone Long bones: a) epiphysis: rotund, bulgy end of a long bone, joint with adjacent bone b) metaphysis: narrow interlayer with of a long bone with growth plate c) diaphysis: midsection of a long bone, hollow bone shaft filled with bone marrow and adipose fat

1.1.2.2. Bone cells

The outer surface of the diaphysis and metaphysis of long bones is formed by the periosteum, a well perfused and sensitive (potentially pain-causing) connective tissue containing fibroblasts and the cambium, a layer of undifferentiated pluripotent cells. The periosteum is involved in bone growth and bone healing. A similar tissue at the inner bone surface is called endosteum. These boundary areas contain mesenchymal osteoprogenitor cells (bone precursor cells) which may differentiate into

osteoblasts (bone forming cells) or chondrocytes (cartilage forming cells). Osteoclasts (bone resorbing cells) originate from blood cells. Most of the constant remodeling of bone tissue takes place in trabecular bone at the surface of the struts (trabeculae). Compact bone is remodeled via Haversian systems with canals (nutrient channels). While osteoclasts dissolve existing bone tissue through acid secretion and proteolysis, which results in tunnels, blood vessels grow inside and osteoblasts build a new osteon in a lamellar fashion (ring layers, Haversian system). Osteoblasts eventually transform into osteocytes, inactivated bone lining cells (Felsenberg, 2001, McKibbin, 1978). Such active conversion processes with cell and matrix interactions adapt the material of bone to the predominant mechanical loads (remodeling) and repair structural defects (Einhorn, 1998, Augat et al., 2005).

1.1.3. Primary fracture healing

A primary (direct) treatment of bone fracture requires precise anatomical reposition with a vascularized minimal fracture gap or no gap at all. Only a tiny distance between the fracture ends of less than 1 mm with proper implant stiffness is acceptable (MacLeod and Pankaj, 2018), and especially with rigid implants, bone tissue compression of about -0.1% (avoiding loss of fixation) to less than approximately -2% has to be achieved, corresponding to the approximate yield strength of bone tissue (Reilly and Burstein, 1975). Immobilization is required (or what is clinically known as absolute stabilization), i.e. only tiny displacements or none at all, which is ensured through bony contact support in the presence of tiny fracture gaps (and flexible fixation), or with rigid fixation in the absence of a remaining fracture gap. The healing in these cases occurs by direct bridging of the bone defect and interlinking (Willenegger et al., 1971, Marsell and Einhorn, 2011), which might actually be considered as direct bone remodeling (McKibbin, 1978). This is often hard to realize in clinical practice, often at the cost of compromising the biological capacity through iatrogenic trauma caused by large access and extensive metal hardware.

1.1.4. Secondary fracture healing

Mostly, at least to some degree, secondary (indirect) bone healing with bridging tissue formation occurs even in well-fixed fractures, especially when small gaps (larger than 0.5-1 mm) are present. The newly formed fracture tissue is called callus. Secondary fracture healing passes through inter-

connected stages of the healing process (Table 2) (Willenegger et al., 1971, Greenbaum and Kanat, 1993, Schindeler et al., 2008).

Secondary fracture healing initially recovers a minimum support function rapidly through the formation of a soft, but wide callus, neglecting the optimal form regarding for instance weight and perfusion effort. There seems to be a connection between callus size and composition and interfragmentary movement (Comiskey et al., 2013, Comiskey et al., 2012, Comiskey et al., 2010, Comiskey, 2010, García-Aznar et al., 2007). The formation of cartilage (i.e. a passively provided tissue) may compensate the limited perfusion capabilities. Diffusion - supported by cyclic mechanical tissue dilatation causing increased fluid flow - may sustain the cartilage tissue. A slow conversion to woven bone and ultimately to lamellar bone results in a well-adapted functional structure. In order to achieve robust fracture healing, first a rapid recovery of force transmission is implemented and then, while maintaining the functional performance of the structure, constraints are optimized (for example strain, mass, volume, metabolic effort). The improvement of fracture healing consequently is a complex optimization problem. The objective function (biomechanical competence) is fuzzy, i.e. there are neither single definite target values nor parameter limits available that guarantee successful treatment and the influences of many parameters (fixation, signaling proteins, etc.) are not completely understood.

Table 2: Overview of the inter-connected stages of the secondary healing process.

Healing stage	Process
<i>Fracture hematoma formation</i>	blood clot formation, minimal mechanical stabilization, inflammatory response (inflammation)
<i>Soft callus formation (granulation and chondrogenesis)</i>	angiogenesis (neovascularization), cell recruitment (migration and differentiation), periosteal proliferation, anti-inflammatory response, cartilage formation from mesenchymal (pluripotent) cells from periosteum and bone marrow, soft callus
<i>Hard callus formation (ossification of periosteal callus)</i>	intramembranous (desmal) osteoid formation and mineralization, woven bone
	endochondral cartilage degradation, formation of new bone tissue and mineralization, hard callus
<i>Callus remodeling</i>	bone restructuring according to the load for months to years, lamellar bone

As a result of the concomitant trauma of a fracture, hematoma formation occurs, which develops granulation tissue. According to the bone anatomy, new bone formation then typically starts at the periosteal and endosteal surfaces of the cortical bone in the so-called soft callus. Immediately after the fracture event, the mesenchymal stromal cells (MSCs) which reside in the surrounding soft tissue disperse into the fracture zone, multiply and migrate within the fracture. Given sufficient vascular perfusion, this bone formation proceeds guided by chemical and mechanical stimuli in all directions throughout the fracture gap. Depending on the biological and mechanical conditions, MSCs differentiate into fibroblasts, chondrocytes and osteoblasts and those cells synthesize the extracellular matrix of their corresponding tissue and determine the further course of healing. The ossification takes place (temporarily shifted) from different initial tissues. During desmal or intramembranous ossification in the connective tissue, MSCs transform into osteoblasts, which build new rudimentary bone (osteoid). During endochondral ossification in cartilage, tissue blood cells (monocytes) and MSCs migrate to the site and differentiate into chondroclasts (cartilage-destroying cells) or osteoblasts respectively. Bone tissue gradually replaces the cartilage tissue. Intramembranous bone formation can be observed predominantly close to cortical bone, but adjacent to zones of endochondral ossification. Newly formed mineralizing callus tissue may enclose a variety of tissue types including fibrocartilage, cartilage, granulation tissue, intramembranous bone and calcifying cartilage, which will eventually remodel into fully mineralized bone tissue (Claes and Heigele, 1999, Augat et al., 2005).

In the presence of a fracture gap, interfragmentary movement and secondary fracture healing may occur. The callus formation starts in some distance from the center of the fracture gap through intramembranous bone formation at the periosteum and endosteum. Subsequently, when the callus diameter increases and the callus grows towards the fracture, the predominant type of ossification changes to endochondral ossification. The callus supports the fracture through an increased cross-sectional area of the bridging tissue (improved structural properties) and by tissue differentiation (gradually improving material properties). As the rigidity of the callus increases, the interfragmentary movement decreases in (often non-linear) relation to this. Eventually, the callus tissue solidifies and the hard callus bridges the bony fragments. This reduces the interfragmentary movement to such a low level that bone formation may occur in the fracture gap. The rate of reduction of interfragmentary movement appears to be related to the initial interfragmentary movement, with larger, though restricted, interfragmentary movements having a faster decline rate (Claes et al., 1998, Augat et al., 2005). One could thus presume that many risk factors for fracture-healing complications might be associated with loading and movement of the musculoskeletal structure itself.

1.1.5. Complications in fracture healing

Aside from early local or systemic complications that are often associated to the fracture trauma itself such as compartment syndrome, embolism or infections, late problems are in the focus here, which are really problems with bone healing itself. Fractures that do not heal adequately swift are termed delayed unions. If the union of the fragments fails to appear in a period of 6 months, the fracture is called a non-union. Based on the amount of tissue that is formed, one may categorize into atrophic (no tissue formed) or hypertrophic non-union or pseud-arthritis, which is a false joint formation that requires further intervention. A mal-union of bone fragments may occur or develop if joint or fragment alignment and bone length are not properly reconstructed (anatomic reposition, reduction = primary loss of fixation) or maintained during loading (insufficient fixation, or excessive load = secondary loss of fixation).

Confounding factors of fracture healing time and outcome can be fracture-trauma-dependent (e.g. location, type, geometry), and/or quality-of-surgery-and-treatment-dependent (e.g. access, choice of fixation, tissue damage), or related to patient attributes and lifestyle (e.g. age, sex, diabetes, use of medications such as corticosteroids and non-steroidal anti-inflammatory drugs (NSAIDs), smoking, excessive alcohol use, and poor nutrition), (Hernandez et al., 2012), (Figure 1-2, left). Apparently, the surgeon can hardly influence the emergence of fracture and patient attributes, so surgeons should focus on the quality of treatment and surgery under consideration of the other factors. It has to be respected that each patient requires adjusted, stratified treatment procedures according to general health status, muscle mass, disease status (e.g. diabetes mellitus, osteoporosis, infection), medication use (e.g. NSAIDs), lifestyle (e.g. smoking, alcohol abuse), local fracture type and status. An appropriate mechanical stimulation of fracture hematoma and fracture callus has to be achieved through adapted fixation and loading with respect to the regenerative capacity (Duda et al., 2001) (Figure 1-2, right).

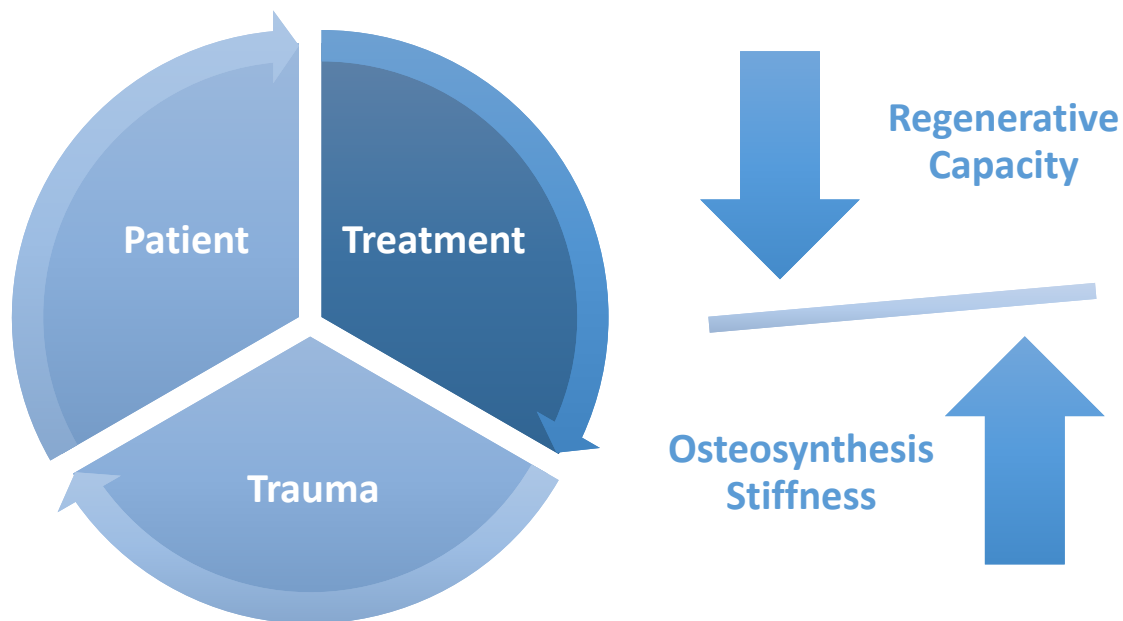


Figure 1-2: Left: The complex process of fracture healing is influenced by confounding parameters involving the patient (characteristics), trauma and treatment. Right: Surgeons define the proportions how much they favor biology (regenerative capacity, minimizing iatrogenic trauma) at the expense of the achievable mechanical stiffness and clinical stability (i.e. ultimate failure strength and retention of alignment), (Duda et al., 2001).

Diabetes, non-steroidal anti-inflammatory drug use, and a recent motor vehicle accident are most consistently associated with an increased risk of a fracture-healing complication (Hernandez et al., 2012). There is general agreement on risk factors for fracture healing concerning surgeon opinion (Bhandari et al., 2012), literature and epidemiologic data (Hernandez et al., 2012), but there are still consistently high complication rates for a few specific fracture types (Kanakaris and Giannoudis, 2010). Comparably rare, but often considered complicated fractures due to the delicate and mostly compromised soft tissue envelope are for instance fractures of the distal femur, proximal tibia, tibial diaphysis, tibial plafond, talus and calcaneus (Court-Brown and Caesar, 2006). Despite modern osteosynthesis procedures, for years about 5-15% of all tibia fracture patients show fracture healing impairments such as absent or delayed healing, pseudarthrosis and infections (Puno et al., 1986, Pheiffer and Goulet, 2006). Additionally, fractures associated with osteoporosis and frailty are critical. Kammerlander et al. (2012) reported for a series of 43 geriatric patients in their 80s after distal femur fracture a 50% mortality at the 5-year follow-up, a frequent loss of independence, and only 18% of patients who can walk without help (Kammerlander et al., 2012, Ehlinger et al., 2013). Thus, it might be corroborated that special care should be taken to preserve the soft tissue envelope during surgery, or somehow otherwise support the biological potential if the presence or viability of osteogenic cells has been compromised.

If a fracture shows signs of delayed or absent healing, it remains difficult to assess the time point for further intervention as there is a lack of consensus in the definitions of delayed union and non-union (Bhandari et al., 2012). A reliable prediction of healing and the identification of healing problems early on is necessary. The prediction of fracture union of treating surgeons shows very high sensitivity, but only humble specificity (0.50 for tibia, 0.25 for femur), i.e. non-unions appear as false positives in cases when union was expected quite frequently so that union was correctly predicted in only 72.7% of the cases (Squyer et al., 2016). Risk factors for non-union have been identified (Santolini et al., 2015), including:

- an open method of fracture reduction,
- open fracture,
- presence of post-surgical fracture gap,
- smoking,
- infection,
- wedge or comminuted types of fracture,
- high degree of initial fracture displacement,
- lack of adequate mechanical stiffness provided by the implant used,
- fracture location in the poor zone of vascularity of the affected bone,
- and the presence of the fracture in the tibia.

First approaches such as the NURD Calculator⁸ (O'Halloran et al., 2016), or the Non-Union Scoring System (Calori et al., 2008, Calori et al., 2014)⁹ that consider different such parameters in a scoring system (Thevendran et al., 2015) are helpful to assess the total complication risk and identify the need for supplemental treatment. However, the current scoring systems are mostly subjective, additive counts that do not sufficiently consider details of the individual patient-specific mechanical environment, and they especially do not consider the (multiplicative) interplay of regenerative capacity (potential for healing) and biomechanical stimulation (excitation of healing impulse).

⁸ Compare <http://shocknurd.org>, last accessed 14th November 2018,

Also compare congress abstract:

https://ota.org/sites/files/legacy_abstracts/ota16/OTA%20AM16%20Poster%20029.pdf, last accessed 14th November 2018,

Also compare journal manuscript: Ross, K. A., O'Halloran, K., Castillo, R. C., Coale, M., Fowler, J., Nascone, J. W., Sciadini M. F., LeBrun C. T., Manson T. T., Carlini A. R., Jolissaint, J. E. (2018). Prediction of tibial nonunion at the 6-week time point. *Injury*, 49(11), 2075-2082.

⁹ Compare the mobile phone application *LEG-NUPS* – Leeds-Genoa Non-Union Predicting Score based on Calori, Giannoudis et al. (<https://itunes.apple.com/US/app/id1082773804>, last accessed 30th July 2018).

1.2. Trauma parameters

The extent of trauma strongly influences the treatment choice and the prognosis. One of the most dominant mechanical factors on fracture healing is the fracture geometry, described by fracture type (including shape and location) and gap size (Augat et al., 2005, Claes et al., 1998).

1.2.1. Fracture type classification

There are various classification systems for bone fractures, based on cause, historic nomenclature and others, but a comprehensive, systematic classification of fractures of long bones has been established 1958 by the Arbeitsgemeinschaft für Osteosynthesefragen (AO)¹⁰, and is nowadays generally used in clinical practice as well as scientific publications. In anglophone regions, the OTA (Orthopaedic Trauma Association) classification¹¹, an extended and adapted version of the AO-classification is generally used.

The classified description of a bone fracture in the AO (or OTA) nomenclature consists of four digits. Additional coding may describe associated skin, soft tissue or vascular-nervous tissue damage.



Figure 1-3: Fracture example of AO classification type 33-A1.2 – spiral fracture at the distal metaphyseal femur.

The first number describes the affected body region, for instance 3=upper leg, i.e. femur or patella. The next number details the exact localization and differentiates proximal fractures (1), shaft fractures (2, diaphyseal) and distal fractures (3). The following letter A-C characterizes the complexity of the fracture. The delineation of fracture complexity depends on the localization in the shaft or joint region, but generally describes the fracture geometry according to groups such as transverse, oblique, or spiral. The subsequent number distinguishes into simple, multi-fragmentary and complex fractures (Figure 1-3)¹².

¹⁰ <https://www.aofoundation.org>, last accessed 30th July 2018.

¹¹ <http://ota.org/research/fracture-and-dislocation-compendium>, last accessed 30th July 2018.

¹² Clinical images were provided by PD Dr. med. Sven Märdian from university hospital of Charité - Universitätsmedizin, Berlin, Germany.

Fracture classifications have their legitimate place in education, grading of fractures, communication of *relative* severity of fractures and corresponding treatment alternatives (Andersen et al., 1996). However, fractures with the same AO classification may still differ substantially. Equating one classification with one type of management in an absolute fashion would appear to be an overextension of the capabilities of this classification tool; also the use of these classifications for direct comparisons of different published series may be beyond the capacity of any of the fracture classifications studied (Andersen et al., 1996). The AO Surgery Reference¹³ gives current delineation of different fractures with the corresponding indications and the common available treatment options in detail. New classification systems for non-union surgery try to enable comparability between patients concerning severity, treatment options and prognosis (Calori et al., 2008, Calori et al., 2014). The current classifications focus on a phenomenological description of the trauma or an injury mechanism, but they rarely translate directly (bijectively) to a certain therapy. The role of fixation for treatment prognosis, especially properly adjusted patient-specific initial fixation has not been accurately described yet. The non-union classification system mainly handles cases after they failed to initially succeed (Calori et al., 2014).

1.2.2. Gap size and interfragmentary movement

Mechanical boundary conditions play an important role during bone fracture healing. Experimental studies, mostly in sheep, rats or mice, have identified numerous mechanical parameters such as gap size, strain rate and strain magnitude that may affect the process of healing (Claes et al., 1998, Duda et al., 2003a). The mechanical environment is determined by the local stress and strain within the fracture tissue. However, the local stress and strain is not directly accessible. Therefore, the mechanical environment is described by global mechanical factors, e.g. gap size and interfragmentary movement (IFM). In experimental studies, small fracture gaps up to 3 mm were beneficial for a fast and successful healing process, while larger gaps over 3 mm resulted in decreased size of the periosteal callus and reduced bone formation in the fracture gap and thus delayed fracture healing (Augat et al., 1998, Claes et al., 1997). The precise role of IFM and local strain will be elucidated in the section 1.5 Mechano-biology of fracture healing.

¹³ <https://www2.aofoundation.org/wps/portal/surgery>, last accessed 30th July 2018.

1.2.3. Injury severity

The general degree of trauma severity can be quantified using for instance the injury severity score (ISS). This score may describe polytrauma with generally decreased perfusion and systemic inflammation, which may lead to impaired fracture healing. The degree of local trauma and the healing status is evaluated based on radiographic and clinical parameters without a definitive (scoring) standard for the detailed definition of local biological (such as cell numbers, cell viability, etc.) or mechanical (such as tissue strain) conditions of fracture-healing (Bhandari et al., 2012, Corrales et al., 2008).

1.2.4. Vascularization and angiogenesis

Fractures usually occur together with damage to the soft tissue envelope and disruption of vascularization. However, sufficient vascular supply is a prerequisite for the fracture repair process as blood supply delivers oxygen, nutrients and some systemically derived cells to the fracture site and ischaemia results in delayed fracture healing (Hankenson et al., 2014). The biochemical milieu involves complex interactions among local and systemic regulatory factors such as growth factors or cytokines (Augat et al., 2005). Vascularization is hampered by instability in the fracture healing zone (Claes et al., 2003, Claes et al., 2002, Lienau et al., 2005, Augat et al., 2005), but improved through adequate mechanical stimulation (Bieler, 2011). General local differences in perfusion have been suggested to lead to increased complication risks associated with certain fracture locations such as distal femur and distal tibia (Santolini et al., 2014).

1.3. Patient parameters

Patients show many different attributes that influence the emergence of the fracture and the healing process.

1.3.1. Demographics (Age and Sex)

Age is not a consistent contributor to high complication risk. However, specific complications (e.g. implant failure such as screw-pull-out or secondary bone fractures) are associated to age-related diseases such as osteoporosis (Chao et al., 2004). Some publications indicate age as a risk factor for non-union (Santolini et al., 2015) while others indicate that bone fracture non-union rate decreases with increasing age (Zura et al., 2017a): It seems that non-union rates increase until the 4th decade and then decrease after the 5th or 6th decade of life (Zura et al., 2017b, Wenger and Andersson, 2018). The analysis of non-union rates in relation to age is biased, based on the variance of fracture rates for respective locations at different ages.

Sex is associated to different lifestyles and vulnerability to certain circumstances: Young men suffer more often from motor vehicle accidents or sport accidents while older women sustain more osteoporotic fractures in fall events (Court-Brown and Caesar, 2006). Some studies have found an association of non-union risk to male sex (Hernandez et al., 2012, O'Halloran et al., 2016), which might also be associated to smoking, alcohol abuse, and insufficient or over-loading due to less or more compliance, different attitude towards pain or different muscle status. However, the found differences between sexes, which these given reasons might potentially cause, may also occur between different patients independent of sex.

1.3.2. Comorbidities and clinical parameters

Systemic inflammation

Patients with rheumatoid arthritis, diabetes mellitus, multiple trauma or sepsis may show systemic inflammation which can increase fracture healing time and the rate of complications such as non-unions (Claes et al., 2012).

Chronic diseases

Diabetes, hepatitis, or HIV-infection are associated with an increased risk of fracture non-union (O'Halloran et al., 2016, Ricci et al., 2014, Hernandez et al., 2012). Dialysis treatment is not associated with fracture healing complications, and the evidence for diabetes is weak and might need more specification of the disease status (Rodriguez et al., 2014, Santolini et al., 2015). Peripheral vascular disease led to an increased mal-union risk (Hernandez et al., 2012), possibly due to altered pain

perception and overloading (mechanical cause) or minimal perfusion and (locally) disturbed cell differentiation, proliferation and bone remodeling (biological cause) or a combination of both.

Medication

Many drugs have been shown to affect bone healing in the disadvantage of the patient such as corticosteroids, chemotherapeutic agents, non-steroidal anti-inflammatory drugs (NSAIDs), antibiotics, anticoagulants and those drugs which reduce osteoclastic activity (Pountos et al., 2008).

Biomarkers

Several groups of cells¹⁴ (Reinke et al., 2013), and certain molecules (Pountos et al., 2013, Sousa et al., 2015, Hankenson et al., 2014) and genes¹⁵ (Dimitriou et al., 2011, Dimitriou et al., 2013) have been investigated as predictors of fracture non-union. Limited available data do not yet encourage the routine use of any of the existing markers for a risk assessment of non-union, but this is currently implemented and tested in the first steps within the clinical routine.

1.3.3. Lifestyle

Obesity

Obesity, i.e. a BMI¹⁶ > 30 kg/m², represents a major risk factor for healing complications (Ricci et al., 2014, Rodriguez et al., 2014), especially in combination with a steel plate (vs. more flexible titanium

¹⁴ Terminally differentiated CD8(+) effector memory T (TEMRA) cells (CD3(+)CD8(+)CD11a(++)CD28(-)CD57(+) T cells) as found in peripheral blood, which aggregate as a result of an individual's immune response to lifelong antigen exposure, negatively affect bone regeneration in humans. Those TEMRA cells accumulate in the fracture hematoma and produce interferon-gamma/tumor necrosis factor-alpha, which inhibit osteogenic differentiation and survival of human mesenchymal stromal cells. The individual adaptive immune profile (experienced immune system) may strongly impair the endogenous bone regeneration. Source: REINKE, S., GEISLER, S., TAYLOR, W. R., SCHMIDT-BLEEK, K., JUELKE, K., SCHWACHMEYER, V., DAHNE, M., HARTWIG, T., AKYUZ, L., MEISEL, C., UNTERWALDER, N., SINGH, N. B., REINKE, P., HAAS, N. P., VOLK, H.-D. & DUDA, G. N. 2013. Terminally differentiated CD8(+) T cells negatively affect bone regeneration in humans. *Sci Transl Med*, 5, 177ra36.

¹⁵ Two specific genotypes (G/G genotype of the rs1372857 SNP, located on NOGGIN and T/T genotype of the rs2053423 SNP, located on SMAD6) as well as polymorphisms within the PDGF gene are associated with a greater risk of fracture nonunion (p=0.02, OR=4.56 and p=0.04, OR=10.27, respectively, after adjustment for age). Source: DIMITRIOU, R., CARR, I. M., WEST, R. M., MARKHAM, A. F. & GIANNOUDIS, P. V. 2011. Genetic predisposition to fracture non-union: a case control study of a preliminary single nucleotide polymorphisms analysis of the BMP pathway. *BMC Musculoskelet Disord*, 12, 44, DIMITRIOU, R., KANAKARIS, N., SOUCACOS, P. & GIANNOUDIS, P. 2013. Genetic predisposition to non-union: evidence today. *Injury*, 44 Suppl 1, S50-3.

¹⁶ Body-Mass-Index (BMI): BMI=mass [kg] / (height [m])²

plate), which may hint at a low mechanical stimulation due to a low activity as a confounding factor for the obesity. This is corroborated by the fact that patients with BMI between 25 and 30 kg/m² show a higher risk of non-union and delayed union while patients with BMI>30 kg/m² only had a higher risk for delayed union and mal-union, but not non-union (Rodriguez et al., 2014). Obese patients (BMI>30 kg/m²) will always transfer higher loads during activities than low BMI patients. This may lead to higher potential for mal-union caused by overloading of the fixation or even fixation failure, but also a high stimulation through high tissue strain. However, a low activity level, especially in the initial phases of fracture healing in combination with smaller loads compared to higher BMI-patients and rigid fixation in the group of patients with BMI 25-30 kg/m² might lead to the increase of healing complications except mal-union.

Compliance

Patient compliance (adherence, cooperation) signifies how well the patient follows the clinical instructions, e.g. for loading, weight-bearing (Braun et al., 2016), protection of the injury, but also medication use etc. Insufficient compliance to the clinician/physician, but also towards pain may cause overloading (in exceptional activities such as early sports) or the likely more serious but largely underestimated problem of insufficient loading (lack of stimulation through immobilization or inactivity) as well as worsening of chronic diseases. When insufficient loading would lead to insufficient stimulation and hypothetically slow or absent healing, surgeons would not detect this early on and would only doubtfully attribute the healing disturbance to an earlier time point of little patient activity (or even worse excessively stiff fracture fixation).

Smoking

Smoking is a controversial parameter concerning fracture healing complications with some evidence for its disadvantage (Santolini et al., 2015), but also some evidence for its indifference (O'Halloran et al., 2016, Rodriguez et al., 2014). Most certainly serious consequences of smoking such as decreased blood perfusion definitely have an effect on the healing process as could be shown for former smokers (Hernandez et al., 2012).

Alcohol

Alcohol shows interesting, but only rather weak effects on the outcome of fracture healing with positive and negative results (Hernandez et al., 2012, Rodriguez et al., 2014, O'Halloran et al., 2016, Santolini et al., 2015). Interesting relationships of an increased risk for fracture-healing complications

with loading and movement might be suggested based on a study by Hernandez et al. (2012). Possibly, persistent brain damage (motor control issues) or insufficient patient compliance in drinkers (alcohol abuse) led to a higher risk of mal-union (former drinkers, adjusted odds ratio, $OR^{17}=2.6$, confidence interval, $CI=0.44-16$; current drinkers, $OR=1.7$, $CI=0.78-3.6$), but interestingly lower risk of non-union (former drinkers, $OR=0.65$, $CI=0.20-2.1$; current drinkers, $OR=0.89$, $CI=0.62-1.3$). One might attribute this to a sufficient mechanical stimulus that may be exerted under unrestricted loading. The restriction of loading (known as partial weight bearing in the clinic) will have to be discussed in detail.

Poor nutrition

Fracture healing is a build-up process that requires sufficient building materials and energy. Thus, the process can be hampered or inhibited by insufficient supply of the required items, specifically the necessary building blocks itself such as calcium for bone mineralization or vitamin D for signal molecules. As the fracture area suffers from low perfusion rates in the initial healing phases, the supply of building materials is improved through mechanical promotion of diffusion and fast angiogenesis, which both require tissue deformation within well-defined limits (Lienau et al., 2005, Geris et al., 2010c, Bieler, 2011, Son et al., 2014a).

1.4. Treatment parameters

Acute treatment of fractures respects the overall condition of the patient, but ultimately seeks to restore the function of the fractured bone. Thus, non-operative treatment is considered first, but operative treatment, i.e. surgical intervention, may become indicated for example if conservative methods fail, the trauma is too extensive or if the fracture is clinically unstable¹⁸, i.e. there is a high displacement or excessive pain. Orthopedic treatment including fixation may even be indicated for an intact bone or a healed fracture if joint alignment needs to be corrected, e.g. to alleviate pain in patients with arthritis (at the hip and knee) as an alternative to joint replacement, especially for younger patients.

¹⁷ Odds ratio (OR): level of association of two properties in a certain population, $OR = (\text{number of people with first and second property} / \text{number of people only with first property}) / (\text{number of people only with second property} / \text{number of people without first or second property})$, $OR > 1$: first property is associated with a higher risk to express second property, $OR < 1$: first property is associated with a lower risk to express second property.

¹⁸ Clinical stabilization implies the bracing with sufficiently stiff instrumentation to allow healing and functionality.

1.4.1. Overview: Fracture fixation instrumentation (Treatment options using fixation)

A comprehensive overview of fracture fixation options is given in Table 3. The term stability is applied here according to its use in clinical practice outlining the degree of load-dependent displacement of the fracture fragment surfaces (Perren, 2002).

1.4.2. Conservative fracture management

Non-surgical fracture care for simple fractures usually consists in the application of either braces or splints or casts from fiberglass or plaster in joint extension, and then usually accompanied by immobilization. This external splinting may lead to loss of reduction for clinically instable fractures during loading and is thus only suited for a limited range of fracture types (Sarmiento et al., 1996).

Table 3: Different concepts of fracture fixation adapted from Wagner (2010).

Principle of fracture fixation (degree of clinical stability)	Method		Technique and implant function	Fracture healing (type)
Absolute stability (high)	Compression	static ¹⁹	Lag screw (conventional screw)	Direct (primary)
			Lag screw and protection plate	
			Compression plate	
		dynamic ²⁰	Tension banding	
			Tension band plate	
			Buttress plate	

¹⁹ Fracture in compression – implant in traction

²⁰ Compression during loading/movement

Relative stability (low)	Splinting	locked ²¹	External splinting	External Fixator ²²	Indirect (secondary)
			Intra-medullary splinting	Intramedullary nail ²³	
			Internal extra-medullary splinting	Standard plate bridging	
		Locking plate bridging			
		un-locked ²⁴	External splinting	Conservative fracture management (cast, extension)	
			Intramedullary Splinting	Elastic nail	
K-wire					

1.4.3. Conventional interfragmentary compression

The goal of conventional (plate) osteosynthesis is to obtain a high clinical stability (i.e. high stiffness, small displacements, high ultimate failure strength) with a rigid plate (stiff metal such as steel) close to the bone (in contact) and/or using screws (interfragmentary screws or screws within the plate, some also crossing the fracture line, or with a neutralization plate to protect interfragmentary lag screws). Compression of the fracture fragments (pre-tension on the plate or interfragmentary screws) is created by different means such as lag screws, eccentrically placed screws within the plate, or an articulated tension device (Cronier et al., 2010).

1.4.3.1. Lag Screws

This screw type is used to compress two fragments directly by pulling a distal fragment onto a proximal fragment in respect to the long axis of the screw. While the ridged part of the screw bites into the distal fragment, the screw shaft near the head moves freely within the over-drilled proximal fragment (often the screw shaft close to the head is smooth) and the screw head pushes the fragments together.

²¹ Locked splinting with control of length, axis and rotation

²² Changeable to dynamic compression

²³ Changeable to dynamic compression, for instance in dynamic locking nail

²⁴ Splinting with partial control of length, axis and rotation

1.4.3.2. Compression Plates

Compression plates and tension bone screws (lag screws) form a common and proven method of osteosynthesis. Surgeons create constructs that press compression plates onto the bone with the purely axially loaded screws. This connection with force transmission by friction between plate, screw and bone can also be pre-loaded perpendicular to the fracture line, resulting in reduction up to close fit of the reduced fracture ends under compression²⁵. A small interfragmentary gap may remain due to incongruence of the fracture surfaces, for instance below 0.5 mm and very small strain within this gap: less than approximately 2% is needed to avoid the destruction of the newly formed bone as tested by Reilly and Burstein (1975). Avoiding any gap altogether and applying appropriate compression (tissue strain approximately 0.1-2%) enables primary bone healing to occur, connecting the fracture ends comparably promptly. Anyhow, the compression underneath the plate may pressure the periosteum, and cause negative remodeling (stress shielding and bone resorption) of the underlying tissue. This pressure may constrict blood supply up to necrosis and thus hinder fracture healing. Assuming a Young's modulus of bone of 1 to 20 GPa and minimum absolute strain of 0.1% as -0.1% axial compression, a stress ($\sigma = E\varepsilon$) of 1 to 20 N/mm² needs to be created using for example a compression plate. Assuming a fracture at the distal femur or the humerus with cortical areas of 500 mm² or 250 mm² respectively and contact zones of 50%, surgeons need to create compression forces of 250-5000 N and 125-2500 N to achieve adequate compression. With exemplary titanium plates ($E=112$ GPa, rectangular cross-section) with 16 mm width and 2.5 mm thickness for the humerus, and 3.2 mm thickness for the femur, this roughly results in plate stress ($\sigma = F/A$) of about 63 N/mm² and 98 N/mm² for the humerus and femur respectively. Compression drill guides need to be adapted accordingly. Let us assume an exemplary screw-hole-eccentricity of 0.5 mm over a 40 mm distance between two plate holes (assuming pure axial compression at the femur and the plate, no plate bending, screw ideally stiff) and an initial fracture gap of 0.3 mm. When axial force is exerted, first the fracture gap will close, leaving 0.2 mm eccentricity. With a bone modulus of 1 to 20 GPa, the plate and bone would exhibit a (total spring) stiffness of about 143 kN/mm + 6.25 kN/mm = 149.25 kN/mm to 143 kN/mm + 125 kN/mm = 268 kN/mm (assuming two parallel springs of stiffness $k=EA/l$ with 50% contact zone of femoral area of 0.5 times 500 mm², plate width of 16 mm and thickness of 3.2 mm, $l=40$ mm, titanium plate). This would lead to forces of about 30 kN to 54 kN for the 0.2 mm displacement, and thus excessively high bone stress. Those numbers vastly exaggerate the needed

²⁵ Reduction or compression can be achieved using for instance a lag screw (screw thread only distally) OR a fully threaded screw and over-drilling the near cortex to the size of the external diameter of the screw (gliding hole) OR compression drill guide for creating eccentrically drilled holes (pre-tension on the plate).

forces, as in reality, there is some plate (and screw) shear and bending, as well as some relative movement of bone and the axial plate stiffness of 143 kN/mm here and the maximum bone stiffness of 125 kN/mm here are both much lower. More realistic estimates of bone and plate-screw stiffness are 20-40 kN/mm and 2-10 kN/mm respectively, which would translate to about 4-10 kN compression force accordingly. However, as necessary compression force (or more importantly tissue stress) is not precisely controlled (and model predictions are not trivial), it is likely that in many cases where a comparably small gap is closed, compression is rather excessive for the bone tissue (but certainly not as high as first calculated above). Most likely, some bone tissue would degrade and bone fragments would just move closer together, also decreasing plate stress and avoiding plate failure. Bone can handle excessive strains through remodeling (resorption of degraded tissue and new tissue formation). Even when most of the eccentricity leads to closure of the gap, it is highly likely that bone tissue will undergo excessive straining. Apparently, designers of eccentric drill guides or eccentric screw holes within plates have realized that the need to close the gap is stronger than the limitation of compressive bone strain. As fatigue strength of titanium is well above 200 MPa or even above 600 MPa for Ti6Al4V (Niinomi, 1998), even with open screw holes and stress concentrations around these holes and local stress increase up to factor 2 (half area), compression plates are initially safe even with comparably small cross-sectional area. When additional bending load is applied, compression plates rely on the load-sharing with the bone. If this load-sharing does not occur, for instance because a gap is bridged, plate stress strongly increases and the plate's cross-sectional area has to increase to ensure safety against plate failure (Meeuwis et al., 2017). The plate area needs to be adapted based on the plate material, bone cross-sectional area, fragment contact zone and consideration if the surgeons apply the plate with assured bony contact. Screws are stressed purely axially if the plate is applied flush to the bone (but the plate might need to be contoured to fit the bone well). When there is a free bending length of the screws (no bracing support in a substrate), screw diameters need to increase as well to be able to resist the additional bending stress (Wagner and Frigg, 2006, Cronier et al., 2010).

1.4.4. Tension bands

By placing a device eccentrically on the convex side (tension side in bending) of a curved bone or on articular fractures where muscles tend to distract the fragments, a tension band system may convert tensile forces into compressive forces onto the bone at the opposite side (MacLeod and Pankaj, 2018). The tension band can consist of loops of wire or cables, suture material, but also intramedullary nails, plates, and external fixators can function according to this principle of closing interfragmentary gaps.

1.4.5. Buttress plates

Commonly used for epiphyseal or metaphyseal fractures, buttress plates enclose a large volume and with a large surface they support weakened, thin cortex. The load is applied orthogonal to the plate through many screws.

1.4.6. External fixators

A strongly proven and comparably easy means of fracture reduction and temporary fixation is the use of external fixators which consist of percutaneous pins or wires which are anchored in the bone on both sides of the fracture and bridged externally with bar frames. This is especially suitable for severe soft-tissue injuries, because an external fixator can be placed comparably fast while creating minimal iatrogenic trauma but may stabilize the fracture zone in relative stability.

1.4.7. Intramedullary nails

Another proven method of osteosynthesis is the application of an intramedullary nail (stiff rod) into the medullary cavity of the bone. This implant may brace the bone structure from within for certain types of fractures. The internal volume can be adapted to the implant geometry through reaming. However, this may compromise the biological capacity for higher mechanical stiffness and strength. Furthermore, the nail can be locked in place with screws or bolts (proximally and/or distally) for higher stiffness. New developments include flexible nail components to allow for controlled axial motion.

1.4.8. Locking fixation

1.4.8.1. Locking plates

An external thread at the screw head and a congruent internal thread inside the plate hole were introduced in 1931 by the surgeon Paul Reinhold (Wolter and Jürgens, 2006). However, modern fixation similar to locking of bars in pedicle screw spinal fixation, i.e. angle-stable fixation in the form

of locked plating for fracture fixation was just widely adopted beginning in the 1990s (Wolter et al., 1999, Seide et al., 1990, Seide et al., 1999, Frigg et al., 2001). An aim was to transfer the force more along or parallel to the long axis of the bone similar to the external Ilizarow ring fixator (Wolter et al., 1999). The biological aspect of fracture healing gained more consideration (Rozbruch et al., 1998). In order to improve local blood supply and avoid negative remodeling under the fixation plate, as well as to promote secondary bone healing, locking plates with angle-stable (locking) screws were introduced, also called internal fixators (Perren and Buchanan, 1995, Seide et al., 1990, Seide et al., 1999, Wolter et al., 1999, Kranz et al., 1999).

According to possible screw orientations, modern locking mechanisms can be differentiated into mono-directional and multi-directional (poly-axial) locking (Cronier et al., 2010). Mono-directional locking is realized by thread-thread blocking (and additional form fit with a conical screw head and plate hole) using a target device during screw cutting to ensure screw-plate alignment (e.g. Locking Compression Plate, LCP by DepuySynthes) or with an additional adjusting screw or cap fixation of the screw head in the plate hole. Multi-directional screw orientation is realized either through:

1) locking by cold welding of a soft titanium alloy of the plate and the harder titanium alloy of the screw head, (e.g. TiFix System from Litos, and the SmartLock System from Stryker). This process may create complications during implant removal (Haidukewych, 2004), or

2) locking by friction or jamming, i.e. with special screw head and plate hole shapes such as equilateral polygons, adjusting screws or caps, flat locking nuts placed at the end of the screw (Yáñez et al., 2010, Yáñez et al., 2012, Cuadrado et al., 2013), etc. Jamming of conventional screws, which are aligned at different angles in a method called fencing, has also been suggested (Windolf et al., 2010). Suzuki et al. (2010) suggested cold welding as a complication for jammed screws as well due to erroneous application (e.g. overtightening) and possibly high cyclic loads.

Although locking plates can be applied with prior compression unto the fracture, they generally function in a unilateral bridging disposition (neutralization plate or as peri-prosthetic protective plate osteosynthesis). Locking plates usually allow some interfragmentary movement. As the locking screws span a clearance (distance between plate and bone), this free screw bending length leads to additional stresses unto the screws (or bolts). As a result, locking screws have an increased diameter compared to a conventional screw (Cronier et al., 2010, Wagner and Frigg, 2006). However, the thread is finer, because function of the locking screw is to resist shear and bending, while the conventional screw resists screw-pull-out when the conventional plates are compressed onto the bone. Most of the interfragmentary movement results from plate bending, and there are strong limitations especially for the motion close to the plate. As a result, locking plates lead to asymmetrical callus formation (Lujan

et al., 2010). Fixation that allows interfragmentary movement (without bony contact support) relies on rapid callus formation because the callus formation prevents or delays fatigue failure of the plate itself (Perren, 2002, Granata et al., 2012). Thus, ways to reduce the stiffness of locked bridge plating constructs were investigated to improve the stimulation of callus formation, such as different screw types, configurations and plate lengths.

1.4.8.2. Dynamic Locking Screws (Far Cortical Locking)

A modification to increase interfragmentary motion are near cortical slots (Sellei et al., 2011, Gardner et al., 2010, Gardner et al., 2009) that allow a locking screw to slide in an elongated hole within the bone close the plate. This way, the locking screw functions as a bending beam between the plate and the trans-cortex of the bone. Major orthopedic companies picked up this simple technique (overdrilling the near cis-cortex and locking within the far trans-cortex) and further amplified and standardized the principle with special screw designs. In these special screws for locking plates (e.g. MotionLoc Screw, Zimmer), the threaded purchase is achieved only within the far cortex. The rest of the screw shaft is smooth and reduced, acting as a cantilever beam with a stop angle when the screw shaft contacts with the near cortex of the bone and the stiffness rises suddenly. The dynamic locking screws (DLS, DepuySynthes) implement a similar concept. Here, the threaded screw part is formed by a large diameter envelope with a smooth small diameter cantilever beam within. One tip of the beam is rigidly connected to the locking plate and the other tip is joined to the far side of the envelope. The smooth beam can bend up to the stop angle when it contacts the inner wall of the envelope.

1.4.8.3. Other dynamic locking implants

A less rigid (anisotropic stiffness) plate with different torsion/bending and axial stiffness due to (degradable) polymer inserts has been suggested (Ferguson et al., 1996, Bottlang et al., 2016, Uhthoff et al., 2006). This working principal is similar to the dynamic or semi-rigid screws, but utilizing standard locking screws that lock into flexible, suspended sliding elements within the plate (Potter, 2016). Furthermore, an axially sliding plate has been suggested (Sun et al., 1998) that is supposed to allow axial motion, but to hinder bending and torsion. Additionally, a similar self-dynamizable internal fixator has been tested that only applies axial dynamization when a screw purposefully loosens (Mitkovic et al., 2012, Mitković et al., 2017).

1.4.8.4. Additional locking plate: double plating or plate next to nail

The addition of a second, medial or anterior locking plate has been suggested for high strain situations (Perren, 2015) for distal femur fractures (Jazrawi et al., 2000) or for peri-prosthetic fractures (Lenz et al., 2016, Wähnert et al., 2017). The second medial or anterior plate, which might have to be inserted through a more traumatic access next to a lateral locking plate, has shown success in the treatment of distal femoral non-unions (Holzman et al., 2016). However, there are some limitations to the placement of a medial plate at the femur to avoid the risk to injure the femoral artery (Kim et al., 2014, Jiamton and Apivatthakakul, 2015). The combination of a locking plate with other implants such as an intramedullary nail for intertrochanteric fractures also showed favorable results (Eberle et al., 2012).

1.4.9. Miscellaneous other instrumentation

Numerous other implants and devices can be used independently, but are mostly used as supplements for fracture fixation such as cables, wires, sutures, staples, bone cerclages, Thabe titanium cerclage bands or extension arms in the presence of an endoprosthesis stem.

Shape memory implants with a temperature-change induced change of structure have been tried, i.e. for an adaptable stiffness (Pfeifer et al., 2013, Decker et al., 2015, Müller et al., 2015, Determann, 2016) or creating interfragmentary compression (Tarniță et al., 2010). Such adjustable or self-adjusting implants may also serve to minimize trauma through smaller surgical access and uniqueness of surgery due to automatic or controlled implant assembly or adjustment (unfolding similar to balloon catheter or shaping similar to stents) within the patient and without the need for additional surgery to remove/add a screw etc. for dynamization/stabilization later on.

In a sense, such implants prepared the ground for more intelligent implants (using sensors and potentially actuators). Next to implants that monitor the healing process with telemetric systems (Faschingbauer et al., 2007, Seide et al., 2012, Fountain et al., 2015, Windolf et al., 2014), it would also be possible to automatically allow for an adapted tissue stimulation. Examples for this could firstly be a direct stimulation approach using for instance ultrasound (low-intensity pulsed ultrasound: LIPUS) to deform the tissue periodically with an attachment device to the fixation. Secondly, an indirect approach could influence the patient activities' dynamics with variable implant stiffness (for instance strain-rate dependent stiffness using a non-Newtonian fluid) creating more guided kinematics and possibly higher muscular co-contraction. Thirdly, local stimulation at the fracture could be adapted by

changing fixation implant characteristics for instance using partial material degradation. Such novel implants may also allow for desired and adapted dynamization²⁶ (Wolter et al., 1999) or inverse dynamization (decreasing movement), either actively using actuators or passively converting muscle and joint forces using the (directional) implant stiffness (components) as a control factor as suggested (Epari et al., 2007, Epari et al., 2013).

1.4.10. Rehabilitation activities (Loading)

Patients can actively manage their loading situation for a good portion, i.e. through the choice of a certain activity. The general pattern of loading in form of a resulting joint force vector with minimal deviations in orientation remains consistent for routine activities at the lower limbs. At the hip joint, there is less than 15 degrees variation in the sagittal plane and less than 10 degrees variation in the frontal plane of average peak load orientation during the following activities: walking, stairs climbing, stair descending, standing up, sitting down, standing on one leg, knee bend. Only the variation in the transverse plane is larger than 40 degrees (Bergmann et al., 2010). However, patients cannot control (or more precisely: reliably reduce) the load intensity (magnitude) robustly (Vasarhelyi et al., 2006, Ebert et al., 2008).

Anyhow, multiple studies established resultant internal fracture gap loading as a major factor for local tissue stimulation and fracture healing outcome (Claes et al., 1998, Klein et al., 2003, Schell et al., 2005). There is evidence that resulting tissue stimulation as a consequence of the total load can partially be regulated through the control of the osteosynthesis stiffness (Epari et al., 2007). This is important, because most non-unions appear at the lower limb (Giannoudis et al., 2015) and are likely associated with the mechanical stimulation. In a study by Giannoudis et al. (2015), 89% of the non-union patients were affected at the lower limb (femur 55%, tibia 34%). Mainly with the revision of the fixation in 83% of the cases, Giannoudis et al. could achieve a union rate of 98.4%. Management of loading (chosen activities) may represent one major factor that provides a basic requirement when implant stiffness is to be adapted for improved tissue stimulation. Patients need to be active and load the fracture zone through basic, commonplace activities or rehabilitation activities in order to create a load. Otherwise, hardly any tissue deformation for stimulation can occur irrespective of the fracture fixation stiffness. Usually, surgeons stipulate 6-8 weeks of partial load bearing after fracture, i.e. the

²⁶ Dynamization in medical terms refers to a method or strategy that increases interfragmentary movement or compressive loading to promote bone healing in fractures. This can be achieved for instance by removing selected screws or changing the fixation altogether.

patient should not exceed an equivalent of 15-25 kg of ground reaction force using crutches for instance. This does not necessarily markedly reduce the internal joint loads: Average hip joint unloading using crutches aggregates to 17%, although it may amount to up to 53% unloading for individual patients (Damm et al., 2013). Partial weight bearing in patients does not reliably unload the defect zone and there is no direct relationship between interfragmentary movement magnitudes and ground reaction forces in patients (Duda et al., 2003a). Through precise muscular control, bone deformation might be controlled actively using crutches, as shown with consistently correlating ground reaction forces to tibia bending strain in trained, healthy volunteers with intact bone (Ganse et al., 2016). Duda et al. (2003a) assumed that the use of crutches or other methods for partial load bearing might help to avoid extremely high loads (through additional mindfulness and balance aid) rather than strikingly reduce the peak forces, especially in patients that suffer pain and muscle weakness.

Adapted rehabilitation programs for certain fractures (and accompanying iatrogenic muscle trauma caused by fracture access) are recommended to selectively strengthen muscles and neuro-muscular control (Paterno and Archdeacon, 2009) and to stimulate the healing process. However, the rehabilitation protocols are usually poorly documented and the evidence for the efficacy of a specific type of physiotherapy is weak (Smith et al., 2009). Preventive muscle strength training prior to surgery might alleviate issues with muscle weakness and overloading. Surgeons usually encourage full load bearing (without crutches) after 12 weeks. The gain in ground reaction force during healing may be a consequence of the healing itself and on the other hand, higher activity will lead to increased tissue stimulation and presumably faster healing. Ankle fracture patients with higher activity and loading (high performers) reached time to full weight bearing after 6 weeks significantly earlier than the low performers (lower activity and loading); Strong correlations between pain (different scoring systems) and weight bearing were observed over 3 months (Braun et al., 2016). This connection of healing and function can be compensated through very stiff fixation that allows early function by stress-shielding the healing zone, reducing pain, but also strongly limiting the stimulation. As a result, such systems that show improved early function do not necessarily reflect faster (structural) healing. What needs to be considered in detail for rigid fixations is that the increase in function (and the decrease in pain) cannot be used as control variable for healing anymore, which sets the endpoint of fracture healing as even more uncertain.

1.5. Mechano-biology of fracture healing

1.5.1. Overview

Numerous mechanical and biological factors influence the fracture healing process and the development of non-union, e.g. excessive motion, a large interfragmentary gap >3 mm, restricted blood supply, severe periosteal and soft tissue trauma (Geris et al., 2010b). All those parameters directly influence either the survival, migration or stimulation of the involved cells. Provision of the necessary cells and survival of the tissue is a requirement for healing, but the stimulation of the cell proliferation and differentiation regulates the course, speed and robustness of healing.

When surgeons use an implant to stabilize²⁷ a fracture, the result is a mechanical system that directly influences the biology of fracture healing. The implant's main function is to brace the fracture zone in terms of limiting displacements and avoiding failure (re-fracture); so the osteosynthesis should transfer the load until the bone regains the ability to fulfil this function and consolidates the fracture. Aims of an osteosynthesis are the restoration of joint congruency, realignment of mechanical axis deviations and mechanical support of fracture healing, eventually to render the implant unnecessary. The general influence of the mechanical environment on fracture healing is known (Goodship and Kenwright, 1985, Kenwright and Goodship, 1989). Interfragmentary movement (IFM) within the fracture zone can stimulate fracture healing (Claes and Heigele, 1999). Unfavorable movement can also impede or even prevent healing, depending on the type of movement and fracture geometry (e.g. gap size) (Augat et al., 2003, Claes et al., 1997). When cyclically loaded, elastic deformations of the implant occur and this leads to relative fragment movements and tissue deformation in the fracture gap. Therefore, the stiffness of the osteosynthesis, which is chosen by the surgeon, significantly influences the healing process (Willie et al., 2011, Epari et al., 2007). An important issue that also has to be considered is the restricted blood supply and contact necrosis caused by excessive (plate) compression onto the bone (Perren, 2015, Perren et al., 1988).

Experimental findings suggest that less callus forms with a generally stable fixation, whereas a larger callus forms with a rather unstable (meaning deformable) fixation (Claes et al., 1995, Duda et al., 2003a). Animal experiments show that IFMs between 0.2 mm and 1 mm in transverse fracture gaps (osteotomies) of 1 mm to 3 mm respectively stimulate satisfactory callus formation. The corresponding interfragmentary strain ($IFS=IFM/gap$) for good bone healing ranges approximately from 20% to 40%

²⁷ Fracture stabilization is a clinical term that refers to splinting/fixation in order to achieve proper wound healing.

(Claes et al., 1997, Claes et al., 1995, Goodship and Kenwright, 1985, Wolf et al., 1998, Augat et al., 2005). Strains of approximately 5% to 10% stimulated less callus formation and led to slower bone healing (Claes et al., 1997, Claes et al., 1995, Augat et al., 2005, Claes, 2011). At the cortex underneath plates, the interfragmentary movement is dramatically reduced to values in the order of 0.07 to 0.2 mm, which for fracture gaps of 3 mm or more led to low IFS and a reduced or deficient bone formation in the cortical fracture gap close to the plate (Stoffel et al., 2003, Claes, 2011). Increasing movement stimulated callus formation but did not improve tissue quality (Claes et al., 1998). IFM stimulates healing, but the ideal range likely varies across stages of bone healing; while early loading and high IFM initiates a large amount of periosteal callus and cartilage, it also delays healing compared to moderate initial IFS around 30% in a 1mm gap (Willie et al., 2011). Larger fracture gaps (greater than 5 mm) in general displayed delayed healing. In contrast to smaller gaps, larger gaps needed lower IFS through more stable fixation for an uneventful healing (Claes et al., 1997, Claes, 2011). A closure of the fracture gap or even contact between the fragments leads to an enhanced fracture healing (Claes et al., 1997, Harrison et al., 2003, Markel and Bogdanske, 1994, Claes et al., 2009). However, this procedure does not allow one to discriminate between the effect of closing the fracture gap or a changed IFM (Claes et al., 2009). IFM is known to decrease rapidly while the callus forms and mineralizes (Kenwright et al., 1991, Dailey et al., 2012). Especially shear movements (e.g. torsion) are critical at the fracture site because the healing process can apparently be impeded (Schell et al., 2005, Epari et al., 2007). Abundant periosteal callus formation resulting in a high structural area moment may reduce especially bending and torsion and thus compensate for some shear (Park et al., 1998) and even lead to accelerated fracture healing compared to unfavorable, excessive axial motion. As a result, it can be concluded that excessive axial motion is more critical than moderate shear motion, as moderate shear will just create a large callus that eventually stiffens the construct. As this adds to the stiffness non-linearly, the healing process may proceed at a high rate once the soft callus grows. However, excessive shear movement resulted in healing with delayed bone formation in the fracture gap, decreased periosteal callus formation and inferior mechanical stability compared to healing with proper axial movement (Augat et al., 2003, Augat et al., 2005). The effects of shear compared to axial motion appear to be sensitive to timing, magnitude and/or gap size (Augat et al., 2005). A possible explanation for the negative effect of interfragmentary shear movement on fracture healing may lie in the assumption that too large shear movements may handicap the ingrowth of an adequate intramedullary blood supply and therefore lead to delayed healing (Duda et al., 2001). Generally, too high IFM is unfavorable. High axial IFM might be better tolerated in a multi-fragmentary fracture because the IFM movement is shared by several fracture gaps and therefore reduces IFS in each gap (Perren, 2002).

There have been quantitative assessments of tissue differentiation as a function of local tissue strain using different components of strain (e.g. longitudinal direction) or strain invariants (minimum or maximum principal strain, hydrostatic or volumetric/dilatational strain, and distortional strain as second invariant of the deviatoric strain tensor or octahedral shear strain), which often correlate especially in simple loading models. Intramembranous bone formation occurs for the strain (major component) smaller than approximately 5% and small hydrostatic pressure (≈ 0.15 MPa). Strains less than 15% and hydrostatic pressure of more than 0.15 MPa stimulated endochondral ossification. Multiple study authors hypothesized that gap size and the amount of strain and hydrostatic pressure along the calcified surface and fluid flow in the fracture gap are the fundamental mechanical factors involved in bone healing (Claes and Heigele, 1999, Claes et al., 1998, Prendergast et al., 1997, Goodship et al., 1998, Lacroix and Prendergast, 2002, Geris et al., 2010b). Current approaches focus on deviatoric strain (e.g. octahedral shear strain) in conjunction with fluid flow with cartilage formation (endochondral ossification) for less than for instance 5% shear strain and formation of immature bone for less than 2.5% shear strain (Epari et al., 2006b, Isaksson et al., 2006, Kim et al., 2012, Steiner et al., 2013).

1.5.2. Fracture fixation mechanics

1.5.2.1. Control of mechanical conditions

The historical development of fixation principles had initially led to a neglect of fracture biology (Perren, 2002, Marsh and Li, 1999). Cells need to be able to migrate to the fracture site, survive under little perfusion, proliferate and differentiate into stiffer tissue while being deformed strenuously. A strong emphasis on fracture biology succeeded the period of pure mechanical fixation with little detailed examination of mechanical conditions (Marsell and Einhorn, 2011, Hankenson et al., 2014). Currently, the assignment of a certain type of fixation can only control the mechanical conditions well at the fracture site on a routine basis if the principle of absolute stability (i.e. high rigidity) is chosen for treatment. The gap is reduced and the fragments are compressed (with moderate control of the magnitude of compression force using for instance a torque-limiting wrench). If the surgeon chooses fixation for secondary fracture healing, surgeons may accentuate fracture biology. Mechanical conditions are not well controlled and especially tissue deformation may vary substantially. In case of fixation for secondary fracture healing, clinicians consider fracture configuration, but they do not routinely evaluate and document the remaining gap size and fracture angle and the fixation is not explicitly adapted to these parameters. The internal loads (muscle and joint loads) in relation to

fracture orientation, as well as the resulting osteosynthesis stiffness (3D-components) are only considered for a few locations such as the proximal femur where major problems have arisen (Calori et al., 2014) and where the incentive to find empirical solutions was strong due to the high numbers of critical patients. However, surgeons, as well as most researchers do not explicitly follow the principal connections between loading, stiffness and resulting strain (mechanical stimulation). Nonetheless, there are empirical guidelines that often seem arbitrary, but have generally come out successful (Sonderegger et al., 2010). Those general guidelines may not be ideal for individual patients and may especially fail for borderline indications. The number of complications that most likely relate to mechanical issues remains high for many fracture locations such as at the tibia and the distal femur (Elliott et al., 2016).

1.5.2.2. Evaluating healing progress

A parameter that quantifies the degree of healing or union as the ratio between the current value of the stiffness in any direction and the one corresponding to the fully bonded interface in that direction has been suggested in numerical studies (Alierta et al., 2014) and for *in vitro* measurements. Although properties such as stiffness of a healing fracture provide a direct and clinically relevant measure for fracture healing (Hente et al., 2003), their application will in the near future be limited to clinical studies or research settings (Augat et al., 2014). Even if whole bone stiffness can be measured *in vivo* in the initial healing stage, the whole-bone stiffness of the fractured bone is very sensitive to the variation of callus stiffness at the fracture site; when callus modulus reaches 15% of the intact bone, the whole-bone stiffness rises up to 90% that of the intact bone (Chen et al., 2015). The clinical assessment of healing occurs based on radiographs and direct clinical examination without a definitive standard (Bhandari et al., 2012, Corrales et al., 2008). This makes numerical approaches more crucial, because improvements to the fixation and its application are masked by a large variability in the assessment of stiffness and healing time and only the extreme cases of fixation failures or non-union stand out.

1.5.2.3. Regenerative potential and stimulation

As indicated, the research community often regards the fracture healing process as guided by parameters from the sectors patient, trauma, and treatment (Figure 1-2). For example, obesity

(BMI>30), open fracture, occurrence of infection, and use of a stainless steel plate for fixation are significant independent risk factors (Rodriguez et al., 2014). In this study by Rodriguez et al. (2014), it was found that when none of these variables are present (titanium instead of stainless steel); the risk of non-union requiring intervention is 4%, but increases to 96% with all mentioned factors present.

A different approach would be to consider the fracture healing process as a dynamic control process (Figure 1-4) with the regenerative healing potential (as a plant in control theory) and also the excitation of the dynamic system (stimulation of healing and disturbing signals), which are both influenced by all sector parameters (patient, trauma, treatment), (Figure 1-5). With this approach, the time until healing (or risk for complications) is a function of potential and stimulation. This can qualitatively describe good, moderate and bad healing in a simple way: when healing potential (controller: cellular response + plant: consequences of cellular response) is low, even a good stimulation can only achieve a poor to moderate result; when stimulation is inappropriate, even ideal healing potential is wasted.

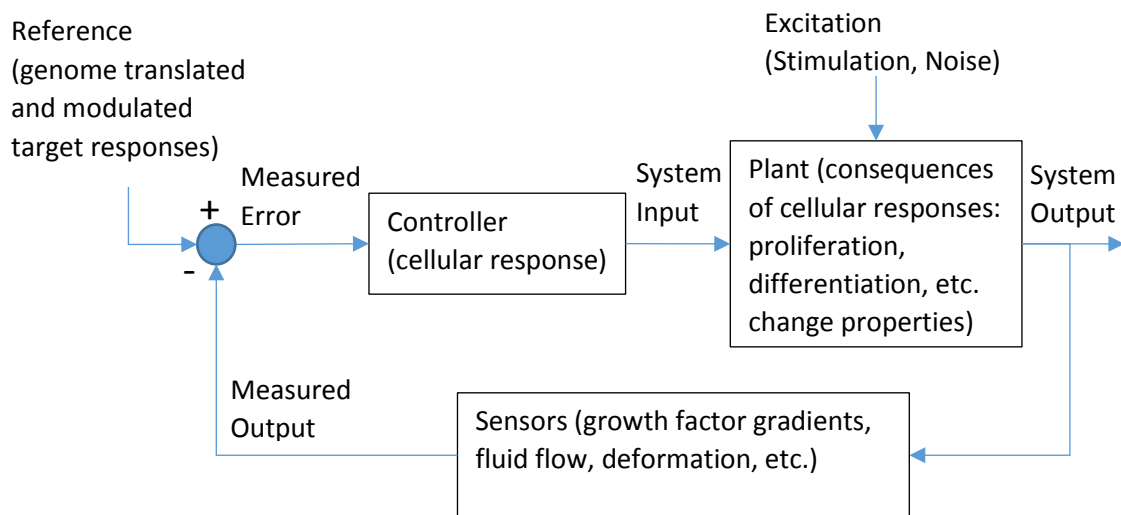


Figure 1-4: Analysis of fracture healing considering the fracture as a dynamic system and the healing process as a feedback control loop with the special feature that both the plant (regenerative tissue) and the controller signal are both dynamically changing.

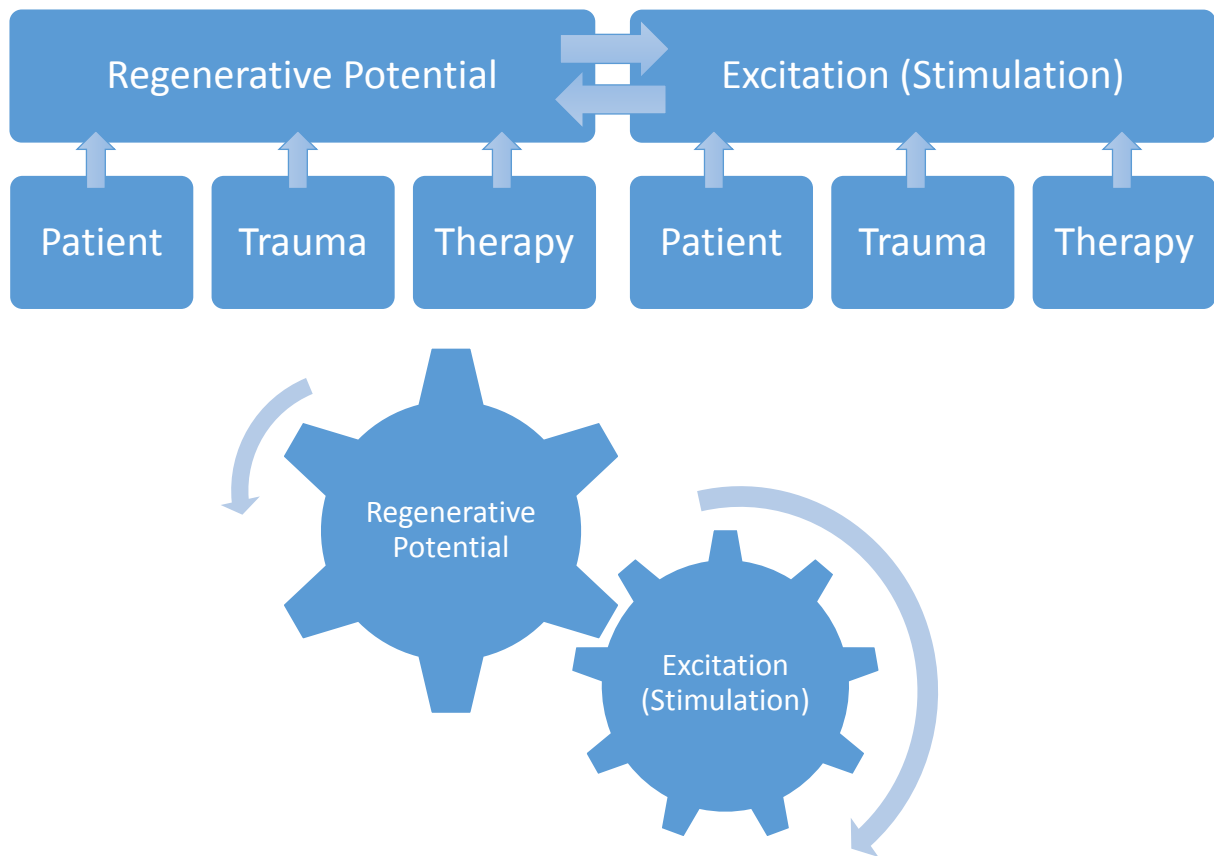


Figure 1-5: Neither the fracture biology nor the local stimulation or the mechanical conditions alone can explain all fracture complication cases. The interacting variables of regenerative potential and excitation determine the healing result together, thus the patient-, trauma- and therapy-specific risk factors are not necessarily additive.

1.5.2.4. Fixation and stimulation

Mechanical stiffness (component-wise) of the osteosynthesis fixation (Duda et al., 1998, Kassi et al., 2001) has been shown as a predictive parameter for the outcome of mechano-biological stimulation for transverse 3 mm osteotomy fractures in sheep (Epari et al., 2007). However, the range of suitable mechanical fixation stiffness components is sensitive to the fracture gap size (Steiner et al., 2014), with greater robustness of fracture healing for smaller gaps (≤ 3 mm, especially < 1 mm) and little margin for suitable fixation stiffness for large gaps (> 3 mm). This might explain the higher number of complications with rising gap size, but the existence of singular favorable healing cases even for large gaps: Large gaps may just show a higher sensitivity to fracture fixation stiffness (components) with a much smaller margin of appropriate values. However, exceeding a certain gap size (which remains to be determined), additional treatment using scaffolds or grafts or else is definitely required (Giannoudis et al., 2007).

The adapted fracture healing process has to be considered as a Pareto efficiency problem, which has to find a balance between creating/conserving biological potential for healing and avoiding additional trauma caused by surgical access (e.g. to reduce the fracture gap) and splinting implants (Figure 1-6). A larger access, that allows more control of the reduction (bone re-setting) and placement of a high stiffness fixation construct, leads to a disproportionately high depletion of healing potential. Developments in fracture fixation and the surgical access, such as intramedullary nailing and also locked plating (Beltran et al., 2015) allow to escape the Pareto frontier and potentially improve the fracture healing process further by maintaining a high regenerative healing potential through minimized iatrogenic trauma and at the same time ensure correct joint alignment. An additional free parameter of the clinical degree of relative stability²⁸ (i.e. stiffness components) emerges with improved flexible fixation that determines the amount of healing stimulation, which together with the regenerative capacity provides for the fracture healing. Now the race between healing and implant fatigue has to be examined and some evidence hints that the stiffness of the osteosynthesis should and can be adapted to the circumstances, i.e. controlled in a certain range (Epari et al., 2007) for fast and robust healing through adapted stimulation. At the same time, this more compliant design will lead to early fatigue if callus fails to appear. Tools that are available for the clinician to further promote healing include growth factors, scaffolds (grafts), mesenchymal stromal cells and the control of the mechanical environment, which was coined as the Diamond concept (Giannoudis et al., 2007, Giannoudis et al., 2015).

²⁸The term stability is applied here according to its use in clinical practice outlining the degree of load-dependent displacement of the fracture fragment surfaces (PERREN, S. M. 2002. Evolution of the internal fixation of long bone fractures: the scientific basis of biological internal fixation: choosing a new balance between stability and biology. *J Bone Joint Surg Br*, 84B, 1093-110.).

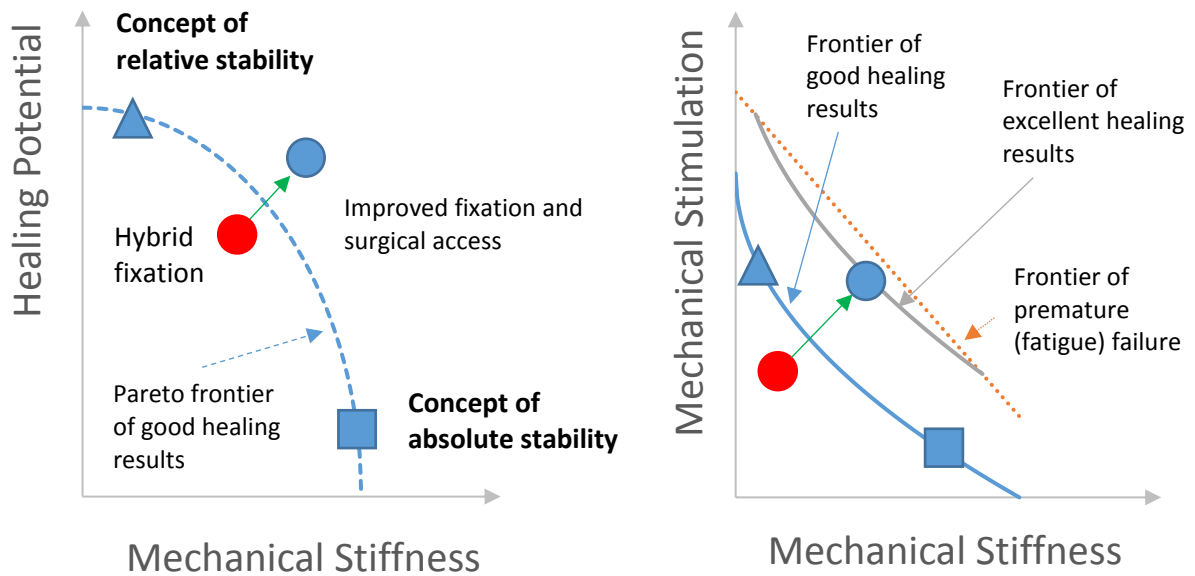


Figure 1-6: Schematic diagrams for fracture treatment parameters, LEFT: Compromise of creating high stiffness construct versus preserving healing potential has led to the two diametrically opposed principles of surgical fixation: absolute stability (blue square) versus relative stability (blue triangle) ensuring Pareto optimal choice of fixation (Pareto frontier dashed in blue denotes good healing results). A hybrid fixation often led to a decrease of stiffness and healing potential and less favorable results (red circle). Novel (dynamic) fixation (blue circle) may preserve healing potential (regenerative capacity) maintaining alignment at the same time. RIGHT: Now, the osteosynthesis stiffness can be controlled to adapt the movement that leads to stimulation and healing (Epari et al., 2007) because the healing potential is maintained in a fixation that retains the alignment.

Generally, there are the antagonistic fixation modes of fracture compression (principle of *absolute stability*) and fracture bridging (principle of *relative stability*). Apparently, when fracture compression with sufficient osteosynthesis stiffness is possible, only a tiny gap has to be closed and little volume has to be regenerated. For some simple fractures, this is easily possible and then leads to fast fracture healing. This type of fixation needs an intact bone remodeling process and is not robust for many fracture types: If an appreciable post-surgical gap remains, healing will be delayed or held off if there is no or little callus formation (Lim et al., 2016, Drosos et al., 2006, Santolini et al., 2015). In fact, many fractures with small gaps show some secondary fracture healing, although surgeons targeted a direct healing, but fortunately, such cases are often supplied with sufficiently flexible fixation. On the other hand, Kubiak et al. (2006) proposed that locked plates which are usually used as bridging plates (principle of *relative stability*) over a gap, are comparable with extremely rigid external fixators and run the risk of becoming “nonunion generators”. Furthermore, fracture fixation using compression and employing very stiff implants may enable very fast full function through load-sharing of the implant. Only the time point for implant removal is hard to assess and even fully functional initial osteosynthesis may fail late (Henderson et al., 2011a).

For many fracture types such as comminuted fractures or defects, fracture compression is not possible and considerable gaps remain. Then, if the regenerative potential is sufficient, secondary fracture healing via callus formation is a robust process that is controlled by the tissue strain, which is determined by osteosynthesis stiffness.

The osteosynthesis stiffness depends on the fixation implant material (e.g. steel / titanium) as well as on the implant geometry (e.g. cross-sections, position), bony support (contact, scaffold, graft, gap tissue stiffness) and on the selected implant configuration (e.g. screw number / arrangement). Kassi et al. (2001), Duda et al. (1998) suggested to consider the 3D stiffness matrix of constructs to evaluate the resulting interfragmentary movement (strain) caused by specific implants with specific configurations under specific load²⁹.

The surgeon also has to balance the need for maintaining the endosteal / periosteal blood supply versus achieving a high stiffness, e.g. with nails (stiff beam) that can be inserted into the reamed (for increased support and size standardization) or the un-reamed intramedullary canal. This is similar for conventional plates that can lead to periosteal necrosis when pressed too tightly to the bone or screws in the plate may loosen on the other hand. While conventional screws compress the plate against the bone, locking screws resist shearing on the entire length of the screw (Cronier et al., 2010). Intramedullary nailing is superior (in general terms of stiffness and strength) to plating from the principal mechanical point of view (central support vs. lever support) and provides earlier weight bearing, but an unlocked, unreamed nail also causes high shear movements (Claes, 2006, Nourisa and Rouhi, 2016). In addition, in order to insert the nails, surgeons have to create an additional drill hole, engaging into the medullary canal where major cell populations reside. To avoid additional trauma, support the biological potential and achieve a robust osteosynthesis stiffness even in compromised (osteoporotic) bone, surgeon can choose locking plates (MacLeod et al., 2014). Such locking fixations seek to maintain a certain elasticity to stimulate bone healing (Cronier et al., 2010) and preserve the biological potential through minimal access and limited or no bone-plate contact.

There is a current discussion about dynamic fixation³⁰ conditions (Potter, 2016), i.e. the tissue deformation that is allowed or aspired. There exists a quantifiable cause-and-effect relationship between the rate of bone healing and the (initial) mechanical stimulus (Comiskey et al., 2010) caused by tissue deformation through implant flexibility. Callus formation is associated with 3-D fracture-site

²⁹ Abstract submitted to 11th Congress of the German Society of Biomechanics (Deutsche Gesellschaft für Biomechanik), 3-5 April 2019 in Berlin: Could timely fracture healing be achieved by adapting the 3D fixation stiffness matrix? (Mark Heyland, Adam Trepczynski, Georg N. Duda)

³⁰ The clinical term “dynamic fixation” means the preservation of relative motion using devices that control the motion in a certain range and originates from spinal surgery.

motion at twelve and twenty-four weeks (Elkins et al., 2016): Longitudinal motion promotes callus formation at twelve and twenty-four weeks while shear inhibits callus formation at twelve and twenty-four weeks. An adapted axial stiffness and a high shear stiffness improve the fracture healing results (Schell et al., 2005, Epari et al., 2007). For example, titanium plate constructs with a comparably short bridge span (plate working length) result in greater longitudinal motion with less shear than steel plates or longer bridge spans, and are associated with greater callus formation (Elkins et al., 2016).

1.5.2.5. Fixation failure mechanisms

Conventional screws compress the plate onto the bone while locking screws function as multiple parallel bolts, similar to a hayfork that can lift a material with weak interlinkage (Cronier et al., 2010). The diameter of a locking screw is greater and its thread finer with resistance to shearing increased by factor 2 and to flexion (bending) by factor 3 (Cronier et al., 2010). Conventional non-locking screws may fail one after the other when toggled and a single screw's thread purchase limits the failure strength. For locking fixation, all locking screws must shear through bone simultaneously, so that the construct only fails as a whole with potentially higher ultimate strength. The strength of fixation equals the sum of all locking screws' resistance to shear at the interface to the bone. However, for sufficient bone quality (with regard to bone mineral density), conventional screw constructs may exhibit higher load to failure (Miller and Goswami, 2007). While conventional constructs display decreasing load to failure as bone mineral density decreases, the load to failure shows little fluctuation with changing bone mineral density for locking constructs (Kim et al., 2007, Miller and Goswami, 2007), Figure 1-7.

Due to their working principle, bridging plates and locked fixators must carry higher bending and torsional loads than compression plates which results in high implant stresses that occur at the level of the fracture, especially without fragment contact (Stoffel et al., 2003, Chao et al., 2013, MacLeod and Pankaj, 2018). As a result, such fixation implants strongly rely on callus formation for load-sharing support (MacLeod et al., 2015).

Construct strength vs. bone quality as a function of construct type

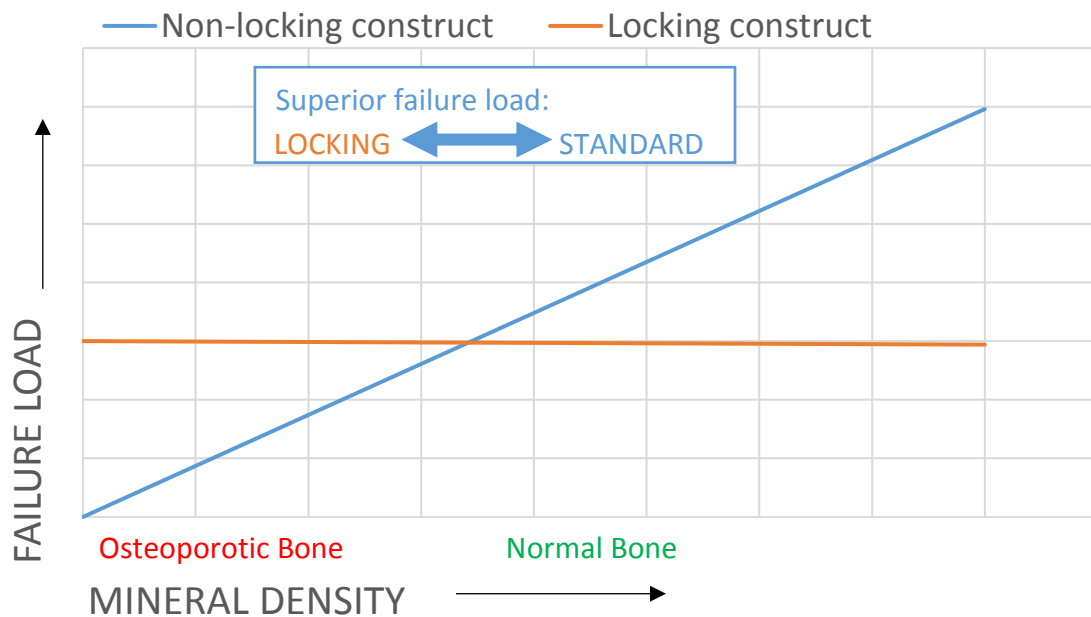


Figure 1-7: Schematic of construct ultimate strength vs. bone quality as a function of construct type adapted from measurements of Kim et al. (2007) and the review of Miller and Goswami (2007) suggesting higher ultimate strength for non-locking constructs in normal bone quality (density above 0.55 g/cm^3) and consistently high ultimate strength even for low bone quality (e.g. osteoporotic bone).

The design of internal fixation implants constitutes a complicated procedure involving the optimization of performance measures while physiological design constraints are imposed which are typically not present in other technical fields (Arnone et al., 2013). The classic engineering approach to minimize the maximum implant stress (distribute stress unto the whole assembly) for maximum lifespan and to avoid fatigue through stiff assemblies is foiled in secondary fracture healing because the tissue can regenerate, but needs the deformation (stimulation) to initiate abundant callus formation and heal. Thus, in the end, short-termed elevation of implant stress and increased tissue stimulation may prove advantageous over the classical engineering approach (MacLeod et al., 2015). Thus, classical biomechanical laboratory tests that do not consider the healing (gain in regenerative tissue) can only be used to define minimum implant standards (ultimate strength) to ensure initial implant survival. On the other hand, implant fatigue evaluations without the consideration of the healing (e.g. callus) are not meaningful, but they can only estimate the time to failure when healing fails to appear. To optimize implants in terms of (biomechanically tested) fatigue life implementing thicker, stiffer implants is unreasonable as it may impair the intended healing process and will eventually lead to failure anyhow. While experimental *in vitro* studies show that stiffer plates can bear more loading cycles (Hoffmeier et al., 2011, Schmidt et al., 2013), clinical results indicate that stiffer plate constructs tend to lead to plate

failures (Button et al., 2004, Hak et al., 2010b, Tan and Balogh, 2009). An explanation was suggested by MacLeod et al. (2015)³¹: stiffer constructs fail in the clinics, although *in vitro* the failure rate is lower than for more flexible plates, because *in vitro* there is less plate bending and lower strain for stiffer constructs. However, in the physiological setting such stiff plates maintain higher strain over a long time in later healing phases (load sharing with callus according to stiffness). Additionally, there is the intensifying effect that more flexible plates lead to faster callus formation (Lujan et al., 2010). In the light of these results, it is doubtful that suggestions like design modifications such as filling of plate holes to minimize plate stress (Anitha et al., 2015) are reasonable, as the plate flexibility may lead to the rapid increase in gap tissue stiffness and thus to unloading of the plate. It is also questionable if additions such as screw hole plugs may at all increase fatigue life even just in the *in vitro* set-up (Firoozabadi et al., 2012). Such modern locking plates are designed to share the load, i.e. they exhibit what would be conventionally considered as an insufficient fatigue life. The fatigue limit of an isolated locked plate constructs equaled 1.9 times body weight for an average 70-kg patient over a simulated 10-week postoperative course (Granata et al., 2012) while physiological (normal walking) loads easily exceed 2 times body weight, even with crutches after only 4 weeks post-surgery (Damm et al., 2013). Thus, implant fatigue life at high physiological loads does not need to outlast the whole fracture healing process or until the expected time point of full consolidation, except when there is insufficient callus tissue formed or mineralized to share the load.

³¹ At the World Congress of Biomechanics in Boston 2014, I was fortunate to become acquainted with the young Scottish researcher Alisdair (Ali) R. MacLeod who presented a poster showing a simple analytical model to estimate the longitudinal component of interfragmentary movement (MACLEOD, A. R. & PANKAJ, P. A simple analytical tool to optimise locking plate configuration 7th World Congress of Biomechanics, 2014 Boston.). We had a few talks and I mentioned that callus or regenerative tissue, even despite its initially small stiffness, cannot be omitted in analyses. At the 2015 congress of the European Society of Biomechanics (ESB) in Prague, I was quite joyfully surprised that Alisdair presented models with different plate stiffness that explained the discrepancy in expected stress and fatigue failure between clinical *in vivo* experience and *in vitro* tests. These differences were found to be a result of the callus formation within the fracture gap. I like to believe the inspiration for this study originates from my insistence on the importance of regenerative tissue stiffness, which was gained from my first modeling approaches and results; however, I cannot be sure. We have been talking to each other via e-mail and each year at the ESB congress since and 2016 in Lyon, I suggested to him that perfusion of passively supplied tissues such as the intervertebral disc or cartilage might not only depend on mechanical load cycles, but also on variations in blood pressure. Thus, sports or physical activity or other means of widely diversifying the blood pressure (high-low fluctuations) such as intermittent antihypertensive drugs may be a highly effective tool for (early) tissue regeneration (of mostly passively supplied tissues). So far, I could not muster the necessary instruments for such a large scale study including long-term blood-pressure measurements that would be needed to test this hypothesis, but I haven't seen a publication by Alisdair either.

1.5.3. Algorithms of fracture healing

Empirical animal experiments and clinical data suggest the deduction of prevalent hypotheses, which a number of studies corroborate using further data:

- 1) the controlled and well-regulated initial, early loading (and strain determined by fixation stiffness, preferably low shear, moderate longitudinal strain) is important for expeditious secondary fracture-healing (Mehta et al., 2012, Goodship et al., 1998) because it leads to a moderately large callus;
- 2) the later (over-)loading (high strain, especially high shear) during regeneration may delay fracture healing, and inverse dynamization (Epari 2013, Willie 2011) leads to faster callus consolidation;
- 3) the correct repositioning of fragments and maintenance of correct joint alignments is crucial, especially under loading to avoid mal-union;
- 4) the fixation failure is usually caused by callus inhibition and can be minimized through improved stimulation for callus formation, especially initial stimulation.

Testing of such hypotheses has been made much easier through implementation and validation of numerical simulation using fracture healing algorithms.

There is no unified theory of tissue regulation, but in the tradition of phenomenologically described adaptation processes, fracture healing can be described as an advancement of Wolff's law, Frost's concept of the "mechanostat", and Perren's strain theory (Elliott et al., 2016). Bone adapts to the stimulation it receives in multiple interleaved feedback control pathways. Modern algorithms are predicated on theories of tissue differentiation based on concepts by Roux, Pauwels, Huiskes, Weinans, Prendergast, Lacroix, Carter, Claes, and Heigele (Suárez, 2015). Mechanical invariants of tissue deformation such as octahedral shear strain and volumetric strain serve as control variables. Prendergast et al. (1997) described how fluid flow can amplify cellular deformation. However, healing simulation as a function of only deviatoric strain accurately predicted the course of normal fracture healing, which suggests that the deviatoric strain component may be the most significant mechanical parameter to guide tissue differentiation during indirect fracture healing (Isaksson et al., 2006). Additionally, when neglecting fluid flow, the uncertain perfusion and diffusion rates that are highly sensitive to local porosities and permeabilities do not have to be dubiously guessed, making the models easier to handle, less complex and all remaining input variables well-founded. Furthermore, fluid flow providing cells with oxygen and nutrients is a dynamic process that requires the consideration of time-dependency of load such as loading rates and tissue characteristics such as relaxation time, which may play a role in bone formation (Chaudhuri et al., 2016, Darnell et al., 2017).

However, if cell survival is ensured, initial tissue formation as predicted by the mechano-biological theories is dominated by the deformation stimulus (Epari et al., 2006b). This can be seen in a much higher sensitivity to tissue shear strain versus fluid flow (Byrne et al., 2011) or the ability to predict healing results based on solely deformation for different load cases (Steiner et al., 2013).

Generally, most healing algorithms follow a general pattern (Suárez, 2015):

- 1) mechanical model calculating the mechanical state of the tissue (stress/strain, flow velocities, and pressures),
- 2) diffusion/proliferation/differentiation model estimating the motion/number of cells and bio-signals due to concentration gradients,
- 3) reaction model predicting the change in tissue phenotype and stiffness,
- 4) iterate beginning @1)

Computer models can simulate the increasing callus size and delay in healing when there is a larger gap size, and the very small callus volume and non-union when the gap is increased further as observed by Claes et al. (1998). Pre-defined callus domains in models of bone healing mechano-biology may cause strain artefacts (Wilson et al., 2015), thus callus growth should be modeled and pre-defined callus domains should be avoided. Callus size and shape are determined by minimum principal strain through an optimization approach (Comiskey et al., 2012). Minimum principal strain as a main stimulus for tissue differentiation (neglecting suggested stimuli such as local stress or fluid flow) shows good qualitative and quantitative agreement with the histological findings (Suárez, 2015, Duda et al., 2005). Models are able to predict the temporal evolution of the callus stiffness for different gap sizes. This correspondence between results and experiments suggests that the observed effects can be explained largely by the mechano-biological algorithm used in such models (Gómez-Benito et al., 2005). Vetter et al. (2011) compared the effect of different stimuli (volumetric strain, deviatoric strain, greatest-shear strain, and principal strain) for tissue differentiation and found that all of these could accurately predict bone healing within a range of thresholds (Betts and Müller, 2014).

Models for fracture healing have become increasingly complicated and validation of those models is often insufficient (Betts and Müller, 2014, Isaksson, 2012). The potential of simulation tools for patient-specific pre-operative treatment planning has been demonstrated before (Byrne et al., 2011, Nasr et al., 2013). However, the translation of computational models to the clinics is very limited because the scope of the existing models and the requirements of clinical modeling do not match, patient-specific parameter identification is complicated and flawed, and validation of models is insufficient (Carlier et al., 2015a). Simple models (with fewer assumptions and/or less input parameters) that consider the known limitations may represent general phenomena of fracture healing with sufficient accuracy

(Mehboob et al., 2013, Mehboob and Chang, 2014, Son et al., 2014b, Son et al., 2014a, Mehboob and Chang, 2015). However, a wide range of specific cases that involve impairment of cell migration or metabolism can only be represented by complex computational models (Carlier et al., 2015b).

1.6. Time response of fracture healing

1.6.1. Fracture healing cascade interplay with fixation

The functioning fracture-healing cascade reduces the strain in the fracture zone over time. The initially formed tissue in the gap is very compliant with fracture haematoma modulus of less than 0.1 MPa (Steiner et al., 2014, Chaudhuri et al., 2016, Darnell et al., 2017), and the strain is mainly reduced by callus area increase. This is not very fast and effective, and the direct placement of stiffer regenerative tissue (with small or no callus) is more effective for faster healing (through primary fracture healing). However, this requires strongly reduced strain (through adequate fixation) and very small gaps around or less than 1 mm. Reduced strain leads to differentiation of stiffer tissue, more accurately: stiffer tissue can be formed and maintained, because the strain is lower, reducing the strain even more.

Gap strain, the deformation (mostly compression) across the gap, can be reduced by parameters that either increase the gap length or decrease motion. Gap length can be increased by fracture comminution and/or imperfect reduction. Due to the reduced bone strain and interrupted supply after fracture, opposing bone surfaces close to the fracture undergo resorption, thus increasing gap width and decreasing gap strain (Perren, 2015). Bone resorption (decrease of mineral content, degradation of bone) at and close to the fracture site occurs and can be demonstrated radiologically or by nano-indentation (Leong and Morgan, 2008). This can decrease the local modulus and increase gap length. If at the same time, global motion does not increase as a result of this absorption, gap strain may be reduced. Strain reduction then, in turn, may lead to the return of relative stability³² (Egol et al., 2004, Perren, 1979). Reduced gap strain allows formation of new connective tissue with a high strain tolerance. Osteosynthesis stiffness increases markedly to the power of three of the diameter in bending and torsion, or with the diameter for axial stiffness with increasing callus size (Perren, 2015). This may reduce strain even further and allow woven and eventually cortical bone to build up.

³² Relative stability as a clinical term refers to the control of relative fragment motion within a healthy range that generates proper tissue deformation eventually leading to fracture healing. In this sense, stability refers to the progressive decrease of motion and strain at the fracture gap over time, while instability would mean a permanently low stiffness and interfragmentary motion under load.

Insufficient straining does not induce the healing cascade, while too high straining induces large callus formation, but it may not be able to bridge the gap or mineralize sufficiently to reduce the straining further. For very small transverse gaps of 1 mm or less, a proper strain distribution can be achieved with very high shear stiffness (> 500 N/mm) and high axial stiffness (> 3500 N/mm) of fixation (principle of absolute stability³³). In the presence of larger transverse gaps around 3 mm, there is a narrow strip of optimal stiffness for the axial component around 1500-2500 N/mm and shear > 400-500 N/mm (Steiner et al., 2014, Epari et al., 2007).

If there is too low initial IFM or the reduction of IFM occurs too fast, an atrophic pseud-arthritis may develop, because little bone is formed at the ends of bone, while in the (large) fracture gap, IFM suits only for fibrous connective tissue (high shear component). However, a common cause for an atrophic pseudarthrosis is often a loss of blood supply with severe periosteal and soft tissue trauma (Claes et al., 2002). The callus does not grow sufficiently to reduce IFM inside the gap further. A hypertrophic pseud-arthritis may develop if the initial IFM is too high, especially the shear components. Plenty of soft callus tissue is added, but this does not lead to a (local) decrease of tissue strain to a level that enables bone formation (Claes et al., 2009).

The strain depends on external load application (determined by patient activities) and osteosynthesis stiffness (determined by fixation and fracture gap-tissue stiffness). As the future development of gap-tissue stiffness depends on current strain, this is a feedback control loop: future strain depends on external load and stiffness of tissue and instrumentation that led to current strain which results in new tissue formation and stiffening. External load is an input variable that patients cannot sufficiently control, so that the stiffness of the implant has to control the stress to avoid implant failure and regulate tissue stimulation. In this feedback control system, fracture fixation may serve as a stabilizer of external load variations or changes caused by disturbance variables of the control process, i.e. allow but limit interfragmentary movement. The goal of fracture fixation is to find an adapted stiffness solution for fast healing, i.e. largely independent of variations of load application. The stiffness of the healing tissue has to be increased through stimulation, i.e. the current strain has to be initially allowed but continually decreased until bone is formed. However, especially at the beginning of healing, the fixation has to clinically stabilize the whole area. Initially, fixation implants take up comparably high loads and should allow a definite (minimum principal) strain of about 20% - 40% of the regenerative tissue for secondary fracture healing or < 2% for primary fracture healing (Claes, 2017b, Claes, 2017a, Claes, 2011, Reilly and Burstein, 1975). This should lead to abundant new tissue formation and avoid destruction of tissue. It has to be noted that at the beginning of healing, minimum load may be exerted

³³ Absolute stability as a clinical term means anatomic reduction of the fracture gap and interfragmentary compression with (macroscopic) absence of fracture motion under physiological load using a stiff fixation.

due to muscle weakness and low patient activity, potentially establishing the need for comparably flexible fracture fixation.

Ideally, as loads rise, construct stiffness has to increase with the load, so that the low initial stiffness allows moderate strain for small initial loads, but another high stiffness takes up later higher loads. This might be achieved through gap closure and contact with direct load transfer. Recent technical innovations such as biphasic stiffness implants like Far Cortical Locking (FCL) or Dynamic Locking Screws (DLS) have a low stiffness state, and a high stiffness state (maximum stiffness similar to locking screws). This represents a mechanically controlled adaptive biphasic stiffness solution. The high stiffness can take up high loads leading to moderate deformation. Similar to locked plating, excessive strains are prevented and reliably transferred parallel to the vulnerable regenerative tissue. The low stiffness for lower loads allows for sufficient flexibility for secondary fracture healing. Thus, the strain rises as a function of loading, and rising tissue stiffness leads to more load-sharing of tissue. This way, overloading as well as under-stimulation of the regenerate tissue are in principle reduced.

The surgeon determines implant stiffness and healing pathway. This relative stability and secondary bone healing are the goals of “biologic fixation techniques” with bridging fixation provided by splints, casts, external fixators, intramedullary nails, and locked plating constructs that all decrease gap strain by controlling motion while tolerating an increased gap length (Egol et al., 2004). While a rigid fixation may lead to improved healing, an extremely rigid fixation actually suppresses bone formation, as well as a moderately flexible fixation promotes healing (Claes et al., 2009). A well-controlled flexible fixation can enhance callus formation, thus potentially improving the healing process, whereas an excessively unstable fixation can even lead to non-union (Claes et al., 1995, Kenwright and Goodship, 1989, Augat et al., 2005). There is some clinical evidence that locked plate constructs might be unduly stiff to reliably promote fracture-healing (Lujan et al., 2010). Bottlang et al. (2010), Lujan et al. (2010) report that 19% of femoral fractures that became non-unions exhibited less callus formation, while maintaining stable implant alignment. They suggest that callus inhibition rather than implant failure is the primary cause of these non-unions with 37% of all fractures showing no or very little callus at six months after surgery. The most prominent location of inhibited callus formation was close to the plate where the asymmetric gap closure characteristic of unilateral bridge-plate constructs causes the least interfragmentary motion. Deficient healing is likely caused by the high stiffness and asymmetric gap closure of locked-plate constructs (Bottlang et al., 2010). As this load-shielding may prevent stimulation, callus formation might be hampered and implant failure might be more likely. A mechanical study evaluating the mechanical endurance of human femora stabilized with 14-hole broad 4.5 mm locking plates found that constructs with load sharing (fragment contact) resisted 20 times more cycles than the constructs with an 8 mm segmental diaphyseal gap (Chao et al., 2013). Fixation

constructs with fewer screws and even a longer plate working length are not automatically more compliant, and do not inevitably lead to greater gap motion as fragment contact, bone-plate contact or bony support have to be evaluated as well. Furthermore, in non-locking constructs, the contact between the plate and the bone segments causes the concentration of the bending moment between the ends of the bone segments. That means the effective plate working length (unsupported area of the plate) may be reduced to equal roughly the gap width, regardless of the positioning of the screws. The physical offset of a locking plate without contact enables a locking plate to bend along the whole distance between the two screws close to the fracture (Chao et al., 2013).

Locking plates undergo comparably large elastic deformation compared to conventional plates and lead to high strain conditions in the fracture gap that may not be suitable for all fracture types (Duffy et al., 2006), potentially also leading to excessive strain. As a result, the use of an interfragmentary lag screw is not in contradiction to the locking compression principle because in certain fracture patterns the interfragmentary range of motion might exceed optimal parameters (Horn et al., 2011). Such a lag screw can be used to reduce the gap size and deformation under load (Märdian et al., 2015b). Especially in conditions where a complete reduction of the gap cannot be guaranteed, this bridging with additional lag screw might be favorable as even a thin fracture gap (1 mm) with no contact between the fracture sites after plating decreases stiffness exponentially compared to fragment contact (Oh et al., 2010). Contact at the fracture surfaces of $\geq 50\%$ is necessary to avoid undue stress concentration in a compression plate, which underscores the importance of creating maximum contact between fracture surfaces while using compression plates, because the decrease in stiffness depends more on the extent of the bone defect than gap size (Oh et al., 2010).

Locking implants (angular-stable fixation) may reduce the rate of implant related failure compared to conventional compression plates (Frigg et al., 2001). Callus emergence and stiffening are accelerated with lower axial stiffness of the osteosynthesis construct. Torsional shear movements are hampered better than with an (unlocked) intramedullary nail (Pekmezci et al., 2014, Mehling et al., 2013) and higher fatigue strength is not necessary due to the expeditious bony callus support. Although reamed intramedullary nailing standardizes the canal structure, allows for larger nails, leads to better implant fit and higher stiffness (Hoegel et al., 2012), it interferes with bone vascularity (Schemitsch et al., 1994). The high shear deformation with unreamed intramedullary nails could be reduced by using a stiff implant material and an angle-stable nail-screw fixation (Wehner et al., 2011). However, locking plates have the advantage that they lead to abundant tissue stimulation even for transverse fractures and lower loads with high failure strength even in osteoporotic patients. In contrast, locked nails may tolerate higher loads due to the central support and allow for early weight-bearing, but are suited better for oblique or spiral fractures (Augat et al., 2008, Alierta et al., 2016, Nourisa and Rouhi, 2016).

It has been proposed to flexibly stabilize a fracture during the early stages of healing to stimulate the formation of a larger periosteal callus, and then to increase fixation stiffness (inverse dynamization) and thus enabling a more rapid mineralization of the tissue (Epari et al., 2013, Bartnikowski et al., 2017, Bartnikowski, 2016). Potentially, this inverse dynamization might represent a physiological process that surgeons exploited unknowingly all along. Non-locked screws tilt around an axis within the more distant cortex and this leads to marked resorption where the screw moves while the screw thread in the far cortex, near the axis of rotation does not show bone resorption (Perren, 2002). This process of excessive transverse screw load, movement, resorption, more movement, leads to increasing tissue stimulation with the response of callus formation corresponding to the amount of displacement or instability. Thus, it could be argued that many constructs that aim for absolute stability do represent fail-safe constructs with relative stability, but may reach absolute stability once the deformation is reduced by tissue aggregation and differentiation. This would represent an initial (fast) dynamization and subsequent inverse dynamization to a stiff construct. This view can be substantiated by callus formation in many fixations that aimed for primary fracture healing. In secondary fracture healing, surgeons schedule the necessary movement from the start, but the precise amount and quality of tissue deformation is not yet considered in clinical practice. At this point, it should be clear that fixation has to be adapted patient-, trauma-, and treatment-specifically and that all fixation options such as intramedullary nails, locked or un-locked plating may all show advantages in certain situations. The advantage of rigid internal fixation lies in the precise restoration of anatomy which is important in articular and peri-articular fractures and for instance for preserving radial bow in fractures of the forearm (Zehnder et al., 2009). Simple fracture patterns are generally more amenable to conventional plating rather than locked plating (Zehnder et al., 2009), although the hybrid use of locking plates and lag screw or positional screws is also an option (Horn et al., 2011, Märdian et al., 2015b, Wenger et al., 2017, Yang et al., 2015, Chung et al., 2016). For some fracture patterns such as comminuted fractures involving metaphyseal bone at the proximal humerus and distal femur, locking plates have replaced conventional standard plates as the preferred method of fixation (Zehnder et al., 2009).

Dynamic/rigid fixation configurations for secondary/primary healing respectively differ in their healing (time) response (Figure 1-). While there occurs faster healing for rigid stabilization for primary healing initially, faster dynamic healing happens after 50 days (Alierta et al., 2016). Eventually, the total construct stiffness has to strongly increase to facilitate bone healing, which can be achieved biologically through a large or very stiff callus or through instrumentation (Bartnikowski, 2016). Although there are some differences, locking plates function similar to external fixators (Schmal et al., 2011), so as a result locking plates have also already been used extra-corporally (Kloen, 2009). Studies with external fixators have shown that longitudinal motion and shear have competing effects on callus

formation. This was also confirmed for titanium plate constructs with a bridge span shorter than 80mm, which demonstrated significantly greater callus at twelve and twenty-four weeks than longer plate working lengths that led to more shear (Elkins et al., 2016). Increasing bridge span preferentially increased shear at the fracture, which was found to be inversely associated with callus formation (Elkins et al., 2016, Märdian et al., 2015a). Fractures that fail to heal usually maintain alignment and form less callus, suggesting callus inhibition rather than hardware failure is the primary problem (Henderson et al., 2011b)

Schematic increase in stiffness according to fixation principle:

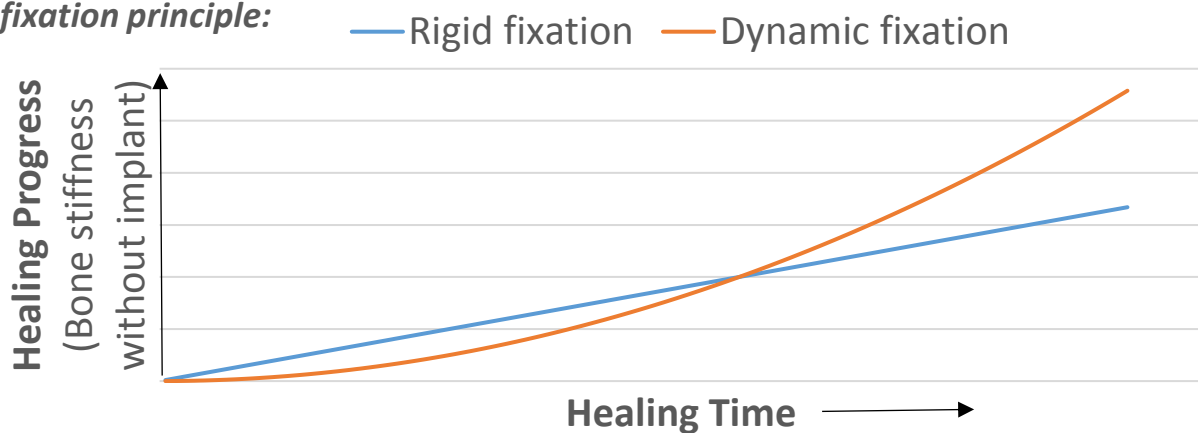


Figure 1-8: Schematic time progress of healing shows that using different fixation principles leads to different time-kinematics of stiffness increase: initially low rate of improvement for dynamic fixation¹, but in later stages much stronger increase of stiffness in later stages for dynamic fixation.

1.6.2. Specific, adapted fracture fixation

1.6.2.1. Patient-specific bone structure and material properties

Although patient bone geometries, i.e. the general anatomy characteristics, are similar in the absence of deformities, the exact geometric structures may vary strongly in size and shape (Ehlke et al., 2015). Additionally, bone shape adapts to the major loading trajectories over time, leading to different bone shapes in elderly compared to younger subjects³⁴. This leads to large differences in lever arms as well

³⁴ Compare poster at the 8th World Congress of Biomechanics Dublin 2018: Mark Heyland, Annabell Bähr, Georg Duda, Sven Märdian; Femur anatomy features in structural analysis: the position of Trochanter major as a risk factor for periprosthetic femoral shaft fractures? <https://app.oxfordabstracts.com/stages/123/programme-builder/submission/20085?backHref=/events/123/sessions/13&view=published>, last accessed 21. November 2018

as different relations of lever arms. As a result, patient-specific loading may vary during the same activity as different muscles with different lever arms are active as well as fracture risk may vary substantially with the different bone geometries.

Additionally, there are differences between patients in bone and callus microstructure (Mehta et al., 2010, Mehta et al., 2012, Mehta et al., 2013) and nanostructure (Gupta et al., 2006, Fratzl and Gupta, 2007, Fratzl and Weinkamer, 2007). A common disease especially in elderly women is osteoporosis. Bone becomes more susceptible to fracture, as the two competing mechanisms of bone adaptation, degradation and formation, do not balance each other anymore. The reduced bone quality presents the surgeon with fixation problems (Chao et al., 2004). There are also numerous diseases such as neurofibromatosis type 1 that affect bone quality and fracture healing (Mehta et al., 2013).

Bone quality strongly influences the strength of many types of fracture fixations (i.e. bone stiffness and strength, often correlated to bone stiffness). For example, standard screw-plate strength rises linearly with bone density (Miller and Goswami, 2007, Kim et al., 2007, Hördemann, 2010). However, modern locking fixation abrogates this correlation and leads to high construct strength consistently (Miller and Goswami, 2007, Kim et al., 2007, Hördemann, 2010). As this is widely independent from bone density, such fixation is well suited for osteoporotic patients (MacLeod et al., 2016c, MacLeod et al., 2014).

For fracture healing stimulation, bone quality did not significantly influence interfragmentary motion (IFM) with less than 8% difference (MacLeod et al., 2016c). Much of this difference can be attributed to the larger cross-section of osteoporotic bone used in this study (6.8% larger than healthy bone) resulting in an increased distance of the plate from the loading axis (higher bending lever arm). As a result, for the prediction of IFM and within a certain range of acceptable bone densities, the geometry or anatomy of a fractured bone is more decisive than its material properties.

1.6.2.2. Specific loading situation

Joint and bone loading strongly depend on the physical activity, bone geometry and are also determined by body weight (BW). However, internal loads may even differ to a considerable degree between subjects with similar BW (Trepczynski et al., 2014, Taylor et al., 2004, Heller et al., 2005b, Heller et al., 2001b, Heller et al., 2001a, Heller et al., 2005a, Heinlein et al., 2009, Bergmann et al., 2010, Bergmann et al., 2001, Bergmann et al., 2014). Variations in hip joint loading of most hip patients during all common activities other than walking and stair climbing are comparably small except during stumbling and implants should mainly be tested with loading conditions that mimic walking and stair

climbing (Bergmann et al., 2001). The average patient loads the hip joint with about 240% BW (percent of body weight) when walking at about 4 km/h and with slightly less when standing on one leg (Bergmann et al., 2001). Walking may lead to an average peak force of about 1800 N and the high peak force is about 3900 N (Bergmann et al., 2010). Measured knee joint forces for level walking range about 180-280% BW, with axial forces of about 220-250% BW and substantially lower shear forces of up to about 30% BW (Bergmann et al., 2014, Fregly et al., 2012, D'Lima et al., 2012). The maximum torque varies for different activities and body weight at the hip or knee, but generally does not exceed about 10, rarely 20 Nm (Bergmann et al., 2014, Bergmann et al., 2010). Using fixation implants with torsional stiffness of 2-5 Nm/degree, this leads to maximum angular displacements of only a few degrees (2-5 degrees, possibly up to 10 degrees) without consideration of any regenerative gap-tissue stiffness or bony support, as most fractures are not orthogonal to the torsional rotation axis. *In vivo* measurement with external ring fixation revealed consistent twist angles below 1.5 degrees for different activities 10 to 14 days postoperatively (Duda et al., 2003a).

MacLeod et al. (2016c) found that strain at the screw-bone interface, plate stress, and IFM all increase non-linearly with load, which indicates that patient body weight should be taken into account when selecting a plate type and screw configuration (MacLeod et al., 2016c).

Immediate full weight bearing of more than two times body weight appears critical as the fatigue limit of a locked plate construct equaled 1.9 times body weight for an average 70-kg patient over a simulated 10-week postoperative course (Granata et al., 2012). Thus, the protection of the fixation implant needs bony support through gap closure or advancing size or material properties of callus tissue. However, for most patients, lateral locking plate fixation at the distal femur over a small gap leads to fast and successful healing after early mobilization without bone grafting with low rates of infection (Kolb et al., 2008, Kregor et al., 2004, Poole et al., 2017). A high healing rate might be attributed to the appropriate mechanical stimulation that leads to abundant callus formation unloading the plate at due time. Successful, but purely mechanical management of failure cases substantiates this (Poole et al., 2017).

The direct measurement of plate deformation as an indirect metric of tissue deformation in a patient that was mobilized with partial weight-bearing (10 kg ground reaction force equivalent) revealed high loads during partially active exercises (Faschingbauer et al., 2007). As a result, physiotherapy continued passively and the therapists trained the patient to avoid movements with high implant loads until consolidation (Seide et al., 2012, Faschingbauer et al., 2007). This indicates muscle forces dominate the internal load. Under certain circumstances, internal forces can correlate with external ground reaction forces. D'Lima et al. (2012) monitored knee forces *in vivo* and compared the reduction in knee

forces with the reduction in ground reaction forces. They found that peak tibial forces correlated with peak ground reaction forces; however, even at pressure settings that reduced ground reaction force to 10%, peak tibial forces remained above 0.5 x BW (D'Lima et al., 2012).

Interfragmentary motion is not significantly changed by partial weight-bearing; ground reaction force does not sufficiently correlate with the interfragmentary stimulus (Duda et al., 2003a). As various tasks (different patient activities) lead to clear differences in ground reaction forces, the interfragmentary movements were hardly different in axial compression, shear and twisting around the long axis of the tibia for patient with external ring fixators (Duda et al., 2003a, Duda et al., 2003b). Duda et al. (2003a) stated that specifically the amplitudes of gap movements during co-contraction illustrate the role of the muscles during loading of the healing bone: simple co-contractions of only the gastrocnemii muscles resulted in movement magnitudes comparable to those occurring during standing up and walking. As interfragmentary movements were similar during partial weight bearing and walking slowly, it seems that muscle forces dominate the mechanical environment at the defect site (Duda et al., 2003b).

Subjects with intact muscles and good muscular control can minimize co-contraction and bone deformation, as was demonstrated with a correlation of tibia deformation and ground reaction forces (GRFs), but the magnitude of GRF is hard to control by subject and especially patients with (muscle) trauma (Ganse et al., 2016, Ebert et al., 2008, Hurkmans et al., 2007).

As a result, the wide range of hip joint force unloading that was achieved using crutches (mean -17%, individually but to -53%) is not surprising (Damm et al., 2013), as it strongly depends on the patient. However, also overloading with crutches (vs. no crutches) was observed (Damm et al., 2013). Muscular internal forces (for stabilization) create surprisingly high loads³⁵ (Faschingbauer et al., 2007), possibly higher than during any other activity. Partial weight-bearing combined with untrained, inappropriate muscular stabilization (i.e. inefficient control of fracture displacements with high co-contraction) might lead to excessive loading. Unduly careful partial-weight bearing with imbalanced muscle status or disturbed muscular control might paradoxically even lead to excessive muscular stabilization loads, even though the ground reaction forces appear low. Excessive muscle loads might fracture bones (Hartkopp et al., 1998) and it has been expressed before that such maximum co-contraction in elderly patients with a good muscle status might occur during ineffective stumbling-recovery events³⁵. Measurements in patients stabilizing their leg with full muscle force in the thigh resulted in similar

³⁵ Compare internal hip forces during stumbling event, OrthoLoadDatabase: <https://orthoload.com/database/>, file search: JB4541A. <https://www.youtube.com/watch?v=LoRHwwV6XCE>, last accessed: 21 November 2018.

forces when the heel was put on the ground to bear full weight, as there is a control mechanism that reduces the muscle load when additional load is applied (Faschingbauer et al., 2007).

1.6.2.3. Specific mechano-biological stimulation

The internal load does not necessarily directly correspond to the specific quantity nor quality of the local mechano-biological stimulation at the fracture. The specific gap size (Steiner et al., 2014) and orientation relative to the load (Pauwels, 1935) in combination with the gap bridging stiffness (tissue over the gap and fixation) play a major role when it comes to the specific local strain.

Furthermore, the general patterns of mechanical signals that influence bone-healing progression are known. However, there is a need to further investigate the species-specific, or even patient-specific (gender, clinical status, age) mechano-biological regulation of bone regeneration (Borgiani et al., 2015, Checa et al., 2011), i.e. especially the thresholds of strain for tissue proliferation and differentiation.

1.6.2.4. Reasonability of patient-specific modeling

While bone anatomy and material distribution vary among patients, this leads to different relative positions of bony landmarks, and different lever arms. Additionally, muscle control and activities differ between patients, leading to changes in loading magnitude and direction. As fracture configuration (type, size, and orientation) differs as well as fracture fixation stiffness, different tissue strain can be expected.

Bone shape models or image reconstruction may cover the different bone shapes. Material distributions can be derived from imaging or models, with assumptions such as a two layered material, or inhomogeneous distribution with many material classes, isotropy or anisotropy according to material (fabric) orientation or strain-gradients (iterative modeling with initial isotropic model or a reasonable anisotropic assumption). Displacement constraints, measured internal loads, and sophisticated methods to account for the boundary conditions (such as inertia relief) enable static or quasi-static simulations of well-controlled loading situations that can similarly be achieved in the gait lab and compared for validity. As a result, local bone tissue strain can be assessed patient-specifically (Szwedowski et al., 2012). Multi-physics models may simulate bone metabolism and the result of changes can be explained based on changes at a low length-scale (e.g. cell metabolism).

The patient-specific modeling enables the access and comparably easy changes to multiple levels from nano-scale to macro-scale (multi-scale). Multi-physics models that consider for instance mechanical deformation and fluid flow as well as cell numbers and types are possible (finite element, fluid dynamics, lattice computer models). The extension to fuzzy input is possible to cover the biological variability within patients. Patient-specific models can be validated based on real clinical cases. Large data stacks (CTs, gait data) can be used to create the models, but the issue of many uncertain assumptions (esp. boundary conditions) remains. Often, a lack of certain aspects that are not modeled to avoid complexity, such as muscular stabilization (Phillips, 2009, Phillips et al., 2007), leads to an instability or unrealistic outcome in models (Bayoglu and Okyar, 2015), which is compensated by feedback control loops in reality. Thus, simplified or even (deliberately) unrealistic assumptions are made to avoid unmanageable model complexity. The specialized sub-models avoid too many assumptions of uncertain or unknown aspects, but need a number of idealizations. Many biological processes are highly robust, which signifies for the modeler that sensitivity (or robustness) often trumps accuracy. The input and output are both fuzzy, so there exists a high validation effort. Most golden standards are empirical, and there is a need for clear analytical background stories. Many unrealistic models (with a small margin of validity) exist that do not clearly state their limitations. In summary, the individual aspects of the modeling process need to be scrutinized in order to be able to make clear statements how fixation conditions can be connected to tissue strain and fracture healing.

Chapter 2. Modelling fracture fixation

Modelling and validation of fracture fixation mechanical behavior

How can fracture fixation and resulting tissue stimulation be modeled?

Relevant publications:

Heyland, M., Duda, G. N., Schaser, K.-D., Schmoelz, W. & Märdian, S. (2016). Finite element (FE) analysis of locking plate fixation is a valid method for predicting interfragmentary movement. Podium presentation. 22nd Congress of the European Society of Biomechanics (ESB 2016), July 10-13 2016, Lyon. <https://esbiomech.org/conference/index.php/congress/lyon2016/paper/view/714>

Heyland, M., Trepczynski, A., Duda, G. N., Zehn, M., Schaser, K.-D., & Märdian, S. (2015). Selecting boundary conditions in physiological strain analysis of the femur: Balanced loads, inertia relief method and follower load. Medical engineering & physics, 37(12), 1180-5.

Märdian, S., Schaser, K. D., Duda, G. N., & Heyland, M. (2015). Working length of locking plates determines interfragmentary movement in distal femur fractures under physiological loading. Clinical biomechanics (Bristol, Avon), 30(4), 391-6.

Ehlke, M., Heyland, M., Märdian, S., Duda, G. N., & Zachow, S. (2015). Assessing the relative positioning of an osteosynthesis plate to the patient-specific femoral shape from plain 2D radiographs. Podium presentation. Proceedings of the 15th Annual Meeting of CAOS-International, June 17-20, 2015, Vancouver. [http://www.caos-international.org/2015/papers/CAOS%202015%20-%20Paper%20%20\(71\).pdf](http://www.caos-international.org/2015/papers/CAOS%202015%20-%20Paper%20%20(71).pdf)

Ehlke, M., Heyland, M., Märdian, S., Duda, G. N., & Zachow, S. (2015). 3D Assessment of Osteosynthesis based on 2D Radiographs. Podium presentation by Stefan Zachow. 14. Jahrestagung der Deutschen Gesellschaft für Computer- und Roboterassistierte Chirurgie (CURAC 2015), September 17-19 2015, Bremen. https://opus4.kobv.de/opus4-zib/files/5621/ZIBReport_15-47.pdf

Heyland, M., Duda, G. N., Trepczynski, A., Dudé, S., Weber, A., Schaser, K.-D. & Märdian, S. (2014). Winkelstabile Plattenfixation für typische Problemfrakturen des distalen Femur: in silico Analyse verschiedener Schraubenauswahl und -belegungen um die Osteosynthesesteifigkeit zu kontrollieren. Podium presentation. Deutscher Kongress für Orthopädie und Unfallchirurgie (DKOU 2014) 28.10. - 31.10.2014, Berlin. <http://www.egms.de/static/en/meetings/dkou2014/14dkou073.shtml>

Heyland, M., Duda, G. N., Trepczynski, A., Schaser, K.-D. & Märdian, S. (2014). Locking plate osteosynthesis fixation configurations for typical problem fractures of the distal femur: in silico analysis of different simulated screw selection and placement to control osteosynthesis stiffness. Poster. 7th World Congress of Biomechanics (WCB 2014), July 6-11 2014, Boston.

2.1. Analytical mechanical models of fracture fixation

Different types of fracture fixation such as conventional plating, locked plating or intramedullary nailing have different mechanical functional principles with inherent advantages and disadvantages (Cronier et al., 2010, Egol et al., 2004). One major group of osteosynthesis implants are bone screws which operate just as conventional mechanical machine screws or lag screws. Conventional (cortical or cancellous) bone screws press a plate or another over-drilled bone fragment unto the bone surface and are stressed in tension. The behavior can be modeled just like mechanical screw-plate-systems in a pure tension-compression bolted joint diagram (spring model).

Locking screws act as bolts (beams) and can be loaded in different ways: tensioned, compressed, sheared, twisted and bent just like locking plates or intramedullary nails. However, the dominant load is bending or torsion. The resulting locking screw or plate behavior from uniaxial loads can be modeled for these implants as beam deformation. The structural behavior of a single implant can be tested uniaxially for instance in cantilever bending and shearing tests *in vitro* and compared to analytical and *in silico* calculations.

2.1.1. Cantilever beam bending

A cantilever beam with uniform cross section is loaded with force F at the free end A and fixed at the other end B. The deflections of the beam remain small in a linear case and in comparison to the length, width and height of the beam. The material of the beam is linear elastic, isotropic, and homogeneous.

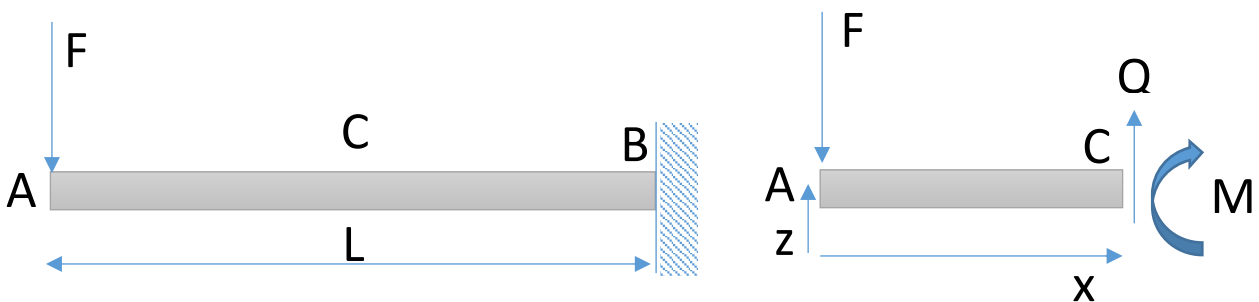


Figure 2-1: Cantilever beam with single load at the end.

With the free-body diagram (Figure 2-), the resulting moment M can be found:

$$M(x) = Fx$$

Using Euler-Bernoulli beam theory, the (elastic) curve $w(x)$ describes the deflection of the beam in the z direction at distance x :

$$EI \frac{d^2w}{dx^2} = -Fx$$

Integration in x , leads to:

$$EI \frac{dw}{dx} = -\frac{1}{2}Fx^2 + c_1$$

At the fixed end B, there is $x=L$ and $dw/dx=0$, so that $c_1 = \frac{1}{2}FL^2$:

$$EI \frac{dw}{dx} = -\frac{1}{2}Fx^2 + \frac{1}{2}FL^2$$

Integrating in x , we get:

$$EIw = -\frac{1}{6}Fx^3 + \frac{1}{2}FL^2x + c_2$$

At B, $x=L$, $w=0$:

$$0 = -\frac{1}{6}FL^3 + \frac{1}{2}FL^3 + c_2$$

$$c_2 = -\frac{1}{3}FL^3$$

We obtain the following elastic curve equation:

$$EIw = -\frac{1}{6}Fx^3 + \frac{1}{2}FL^2x - \frac{1}{3}FL^3$$

$$w = \frac{F}{6EI}(-x^3 + 3L^2x - 2L^3)$$

For the deflection at A for $x=0$, we obtain:

$$w_A = -\frac{FL^3}{3EI}$$

So, the maximum bending deflection w of a simple single-side fixed support (unconfined at free end) cantilever beam and free length L , Young's modulus of E , under end load F can be analytically given as:

$$w_{max} = -\frac{FL^3}{3EI}$$

With a circular cross-section (diameter d) and a second moment of area for circular section:

$$I = \frac{\pi d^4}{64}$$

For a single bending screw with a single fixed support, the load, the geometry and the material modulus can describe the deformation w as follows:

$$w = -\frac{64FL^3}{3E\pi d^4} = -\frac{64}{3\pi} \cdot F \cdot \frac{L^3}{d^4} \cdot \frac{1}{E}$$

If we consider this small deflection in bending as a linear spring stiffness in the orthogonal (z) direction, we get:

$$k = abs\left(\frac{F}{w}\right) = \frac{3\pi d^4 E}{64L^3}$$

2.1.2. Braced cantilever beam bending

Moving on to another case: A cantilever beam with uniform cross section is loaded with force F at end A and is confined to move only in z -direction and fixed at the other end B.

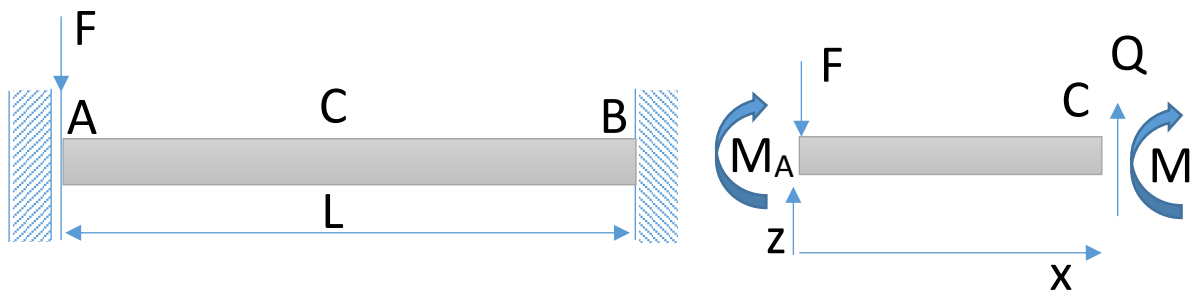


Figure 2-2: Beam with a load and a confined curvature at one end and one fixed end.

The reaction force at B must be $-F$, with the free-body diagram (Figure 2-2, symmetrical moment), it can be found:

$$M(x) = Fx - M_A = Fx - \frac{1}{2}FL$$

Using Euler-Bernoulli beam theory, the (elastic) curve $w(x)$ describes the deflection of the beam in the z direction at distance x :

$$EI \frac{d^2w}{dx^2} = -Fx + \frac{1}{2}FL$$

Integration in x , leads to

$$EI \frac{dw}{dx} = -\frac{1}{2}Fx^2 + \frac{1}{2}FLx + c_1$$

At the fixed end B, there is $x=L$ and $dw/dx=0$, so that $c_1=0$:

$$EI \frac{dw}{dx} = -\frac{1}{2}Fx^2 + \frac{1}{2}FLx$$

Integrating in x , we get

$$EIw = -\frac{1}{6}Fx^3 + \frac{1}{4}FLx^2 + c_2$$

At B, $x=L$, $w=0$:

$$0 = -\frac{1}{6}FL^3 + \frac{1}{4}FL^3 + c_2$$

$$c_2 = -\frac{1}{12}FL^3$$

We obtain the following elastic curve equation:

$$EIw = -\frac{1}{6}Fx^3 + \frac{1}{4}FLx^2 - \frac{1}{12}FL^3$$

$$w = \frac{F}{12EI}(-2x^3 + 3Lx^2 - L^3)$$

For the deflection at A for $x=0$, we obtain:

$$w_A = -\frac{FL^3}{12EI}$$

So, the maximum bending deflection w of a simple cantilever beam with single fixed support and confined curvature $dw/dx=0$ at the loose end, and free length L , Young's modulus of E , under end load F can be analytically given as

$$w_{max} = -\frac{FL^3}{12EI}$$

With a circular cross-section (diameter d) and a moment of inertia for circular section:

$$I = \frac{\pi d^4}{64}$$

For a single bending screw, the load, the geometry and the material modulus can describe the deformation w as a mechanical stimulus as follows:

$$w = -\frac{16FL^3}{3E\pi d^4} = -\frac{16}{3\pi} \cdot F \cdot \frac{L^3}{d^4} \cdot \frac{1}{E}$$

If we consider this small deflection in bending as a linear spring stiffness in the orthogonal (z) direction, we get:

$$k = abs\left(\frac{F}{w}\right) = \frac{3\pi d^4 E}{16L^3}$$

So the difference in maximum deformation (stiffness) of unilaterally fixed beam between a confined and an unconfined bending of the loose end could be calculated with factor 4.

2.1.3. Screw stiffness (effective diameter)

A simple cantilever beam bending test was carried out using different locking screws (test performed and data retrieved from Synthes, Figure 2-3). The bending stiffness was evaluated for a 50 mm screw sample, which was clamped at the screw head, and the free end was moved orthogonal to the long axis of the screw. The orthogonal displacement was recorded, synchronized with the applied load.

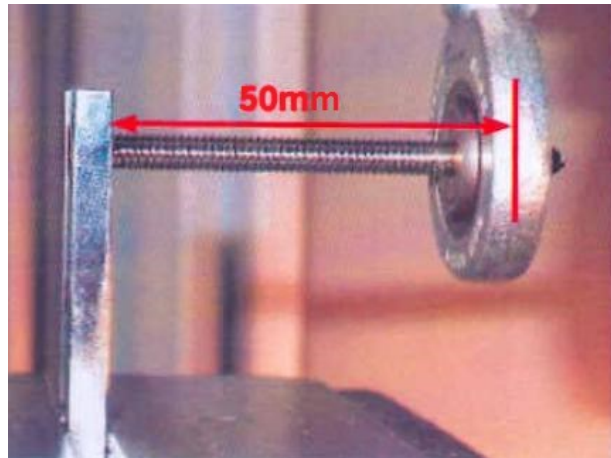


Figure 2-3: Test set-up for cantilever bending of a single screw. Load was applied as a force at 50 mm distance.

With the known screw bending stiffness of the screws (shear can be neglected because $L \gg d$), an effective diameter of the beam can be calculated, solving the following equation for d :

$$k = \frac{3\pi d^4 E}{64L^3}$$

$$d = \sqrt[4]{\frac{64L^3 k}{3\pi E}}$$

Table 4 shows bending test results (stiffness) and effective diameter for different screw types.

Table 4: Single screw bending stiffness for 50 mm cantilever bending test.

Screw Type, free bending length <i>L = 50 mm</i>	Measured bending stiffness	Material properties	Effective diameter
Steel locking screw (LS)	56 N/mm	$E_{\text{Steel}}=187 \text{ GPa}$	$d_{\text{LS, Steel}}=3.99 \text{ mm}$
TAN (titanium alloy) locking screw	39 N/mm	$E_{\text{TAN}}=112 \text{ GPa}$	$d_{\text{LS, TAN}}=4.15 \text{ mm}$
CCM (cobalt--chromium-molybdenum alloy) DLS 5.0	27 N/mm	$E_{\text{CCM}}=224 \text{ GPa}$	$d_{\text{DLS, CCM}}=3.18 \text{ mm}$

The shear-bending stiffness of the DLS for a similar test with 6 mm free length resulted in a measured 5,466 N/mm between 500N-1500N. The pin touches the sleeve starting at approximately 200N.

2.1.4. System spring stiffness

When multiple spring elements are coupled, the total stiffness can be calculated as follows:

For coupling in series: $\frac{1}{k_{total}} = \sum_{i=1}^n \frac{1}{k_i}$; For parallel coupling: $k_{total} = \sum_{i=1}^n k_i$

With the following notation (Figure 2-4), we can model a total system stiffness (one-dimensional):

- Stiffness for the screws (for LS/DLS): k_{si} , with i for confined (B) / unconfined (D) case, i.e.

(k_{SB} for confined screw bending because the bone acts against free bending and k_{SD} for unconfined screw bending, because the screw can bend freely over the defect),

- Stiffness for a part of the plate between two screws, k_{pi} , with i parallel to bone (B) or defect (D),

(k_{PB} for a plate part parallel to bone, and k_{PD} for a plate part parallel to the defect),

- Stiffness for a defect, the notation k_D ,
- and for bone, the notation k_B .

The screw-plate-element in series has a combined stiffness as follows:

$$\frac{1}{k_{SP}} = \frac{k_S + k_P}{k_S \cdot k_P}, \quad k_{SP} = \frac{k_S \cdot k_P}{k_S + k_P}$$

When a defect/bone is considered parallel to k_{SP} :

$$k_{bridge} = k_{D/B} + k_{SP}$$

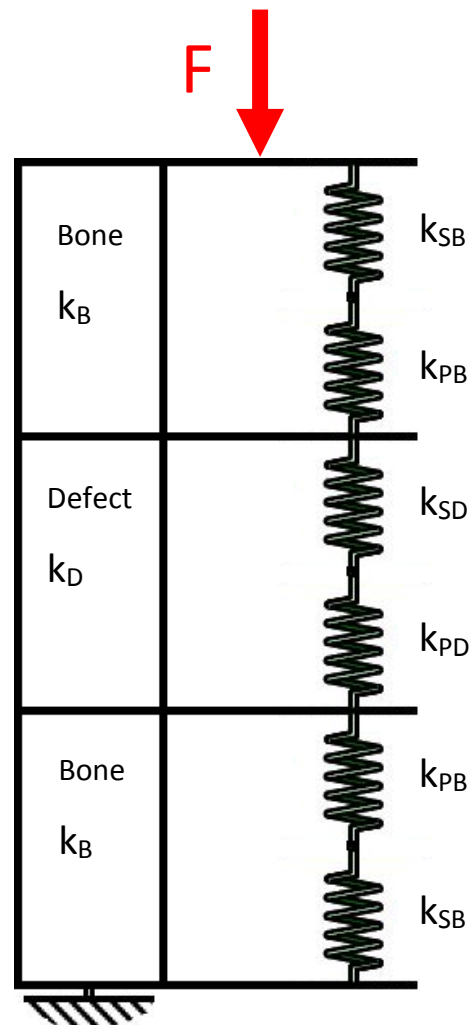


Figure 2-4: Schematic spring system of fracture fixation.

The total stiffness (or flexibility) of n elements bridging bone or defect can be calculated with:

$$\frac{1}{k_{total}} = \sum_{k_i}^n \frac{1}{k_{Di/Bi} + \frac{k_{Si} \cdot k_{Pi}}{k_{Si} + k_{Pi}}}$$

The role of individual parameters within this simplified spring system can be interpreted for a number of cases.

2.1.4.1. Defect bridging

When only a defect bridged with a plate is considered, the following total system stiffness results:

$$k_{bridged\ defect} = \frac{k_D(k_{SD} + k_{PD}) + k_{SD} \cdot k_{PD}}{k_{SD} + k_{PD}} = k_D + \frac{k_{SD} \cdot k_{PD}}{k_{SD} + k_{PD}}$$

The stiffness of the defect bridging is complex and crucially dependent on the individual components of stiffness of the osteosynthesis fixation (k_{sp}), i.e. screw (bending) stiffness and plate (bending) stiffness and defect stiffness (Figure 2-5). Stiffness of the defect bridging is mostly influenced by the osteosynthesis fixation alone if the defect stiffness is small (close to zero). For higher stiffness of tissue within the defect, defect stiffness may strongly add linearly to the total stiffness.

The following assumptions of fixation component stiffness are not validated at this point of time and represent educative guesses! The following analyses need to be revisited when parameters were

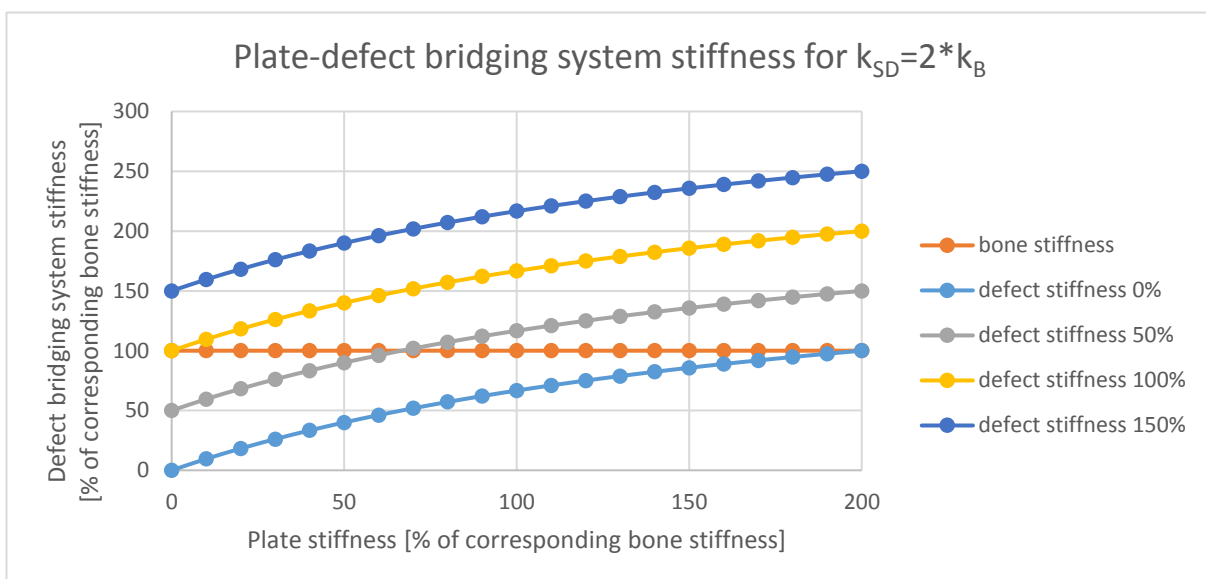


Figure 2-5: Stiffness of defect bridging for varying plate stiffness (screw stiffness constant) and varying tissue compliance over the fracture (defect stiffness).

identified reliably. At this point, the results show the relative qualitative relationships, but the shown values should not be used for decision making.

2.1.4.2. Bony bridging

When only a bony bridging with a plate is considered, the following total system stiffness results:

$$k_{bridged\ bone} = \frac{k_B(k_{SB} + k_{PB}) + k_{SB} \cdot k_{PB}}{k_{SB} + k_{PB}} = k_B + \frac{k_{SB} \cdot k_{PB}}{k_{SB} + k_{PB}}$$

The stiffness of the bony bridging is determined by bone stiffness plus the combination of plate stiffness and screw stiffness, and the structure is stiffer than the bone itself (Figure 2-6).

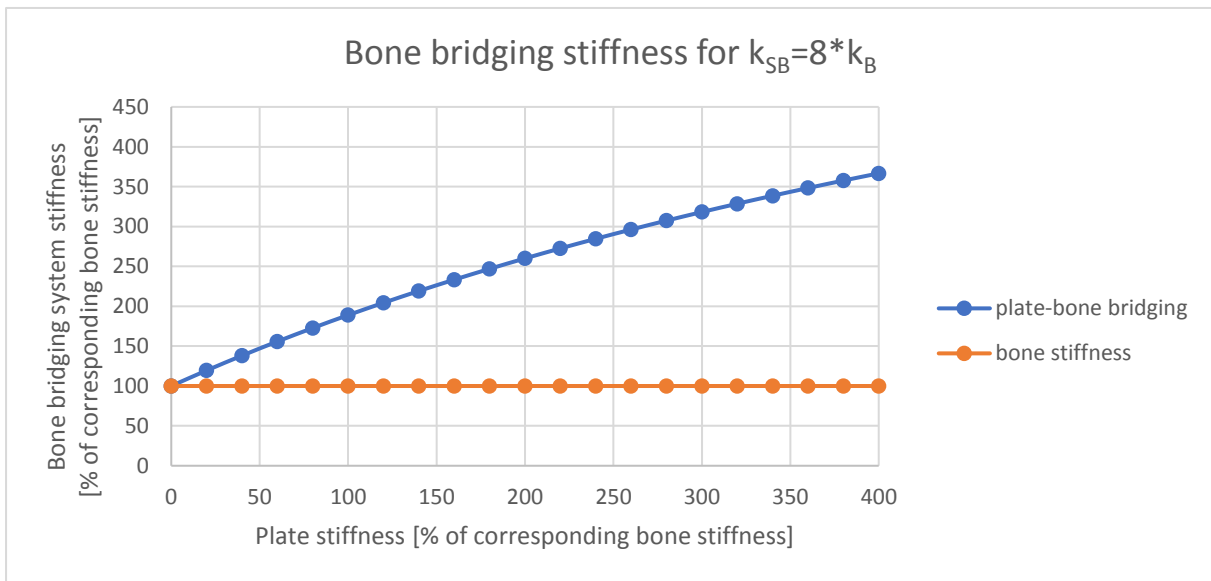


Figure 2-6: Stiffness of bony bridging for varying plate stiffness (screw stiffness constant).

2.1.4.3. Considering multiple parts of bony bridging and defect bridging

The total stiffness (or flexibility) of n elements bridging bone and one defect can be calculated with:

$$\frac{1}{k_{total}} = \frac{1}{k_D + \frac{k_{SD} \cdot k_{PD}}{k_{SD} + k_{PD}}} + \frac{n}{k_B + \frac{k_{SB} \cdot k_{PB}}{k_{SB} + k_{PB}}} = \frac{1}{k_{PB}} + \frac{n}{k_{PD}}$$

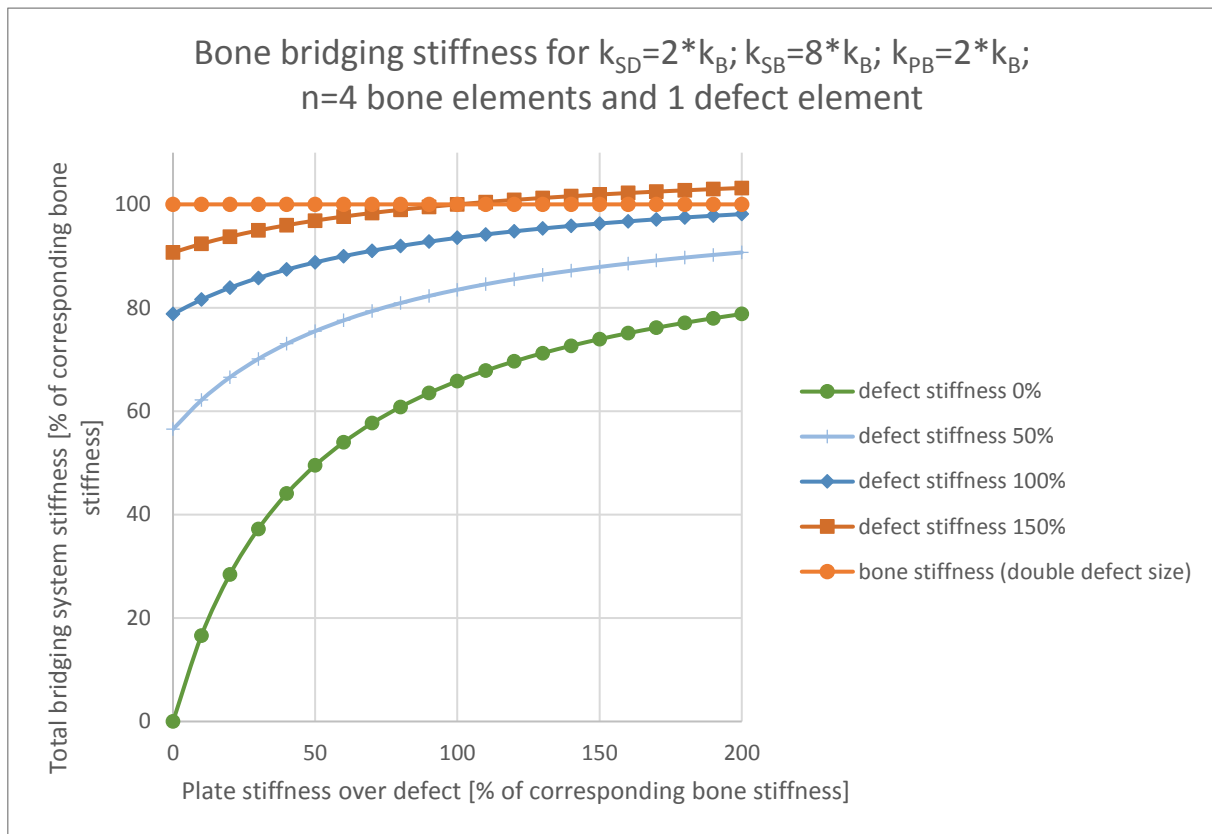


Figure 2-7: Total stiffness of bony bridging and defect bridging for varying plate stiffness (screw stiffness constant).

Even for this simple case, the stiffness is complex (Figure 2-7). Generally, the stiffness of the plate over the defect determines the total stiffness. Total stiffness rises further with increasing defect stiffness.

In biological studies during fracture healing, an overshoot of defect gap stiffness has been observed when bone or callus was mechanically tested without fixation and compared to the contralateral intact bone (Wehner et al., 2014). This might be explainable on purely mechanically grounds as an effect that the total bridging system stiffness is increased until it reaches approximately normal bone stiffness (and the tissue in the gap is remodeled accordingly). With fixation over the defect zone, e.g. 100% plate stiffness of corresponding intact bone stiffness, the total system stiffness reaches 100% of intact bone stiffness (for the assumed parameters given above) for 150% of defect stiffness (Figure 2-7) relative to intact bone stiffness (150% of apparent stiffness of native bone, i.e. from material + structural sources). With initially minor material quality of the regenerative tissue (low modulus, inefficient microstructure), a large callus must form strongly exceeding the original cross-sectional area on intact, native bone.

When different fixation stiffness, e.g. different plate stiffness over the gap is chosen, different amounts of such an overshoot (excessive defect stiffness) might be expectable. For our model and

the assumed parameters, a plate stiffness of approximately 250% over the defect (relative to 100% intact bone stiffness with similar size) which is a very stiff fixation, would yield no stiffness overshoot. In contrast, a minimal fixation stiffness over the defect would enable 100% of stiffness overshoot (Figure 2-8) because the flexible fixation would share most of the load and the tissue stimulation would be attenuated. For plate stiffness over the defect higher than 250% of intact bone stiffness, tissue in the fracture gap would most likely only slowly approach intact bone stiffness without an overshoot, given the assumed input values here are reasonable.

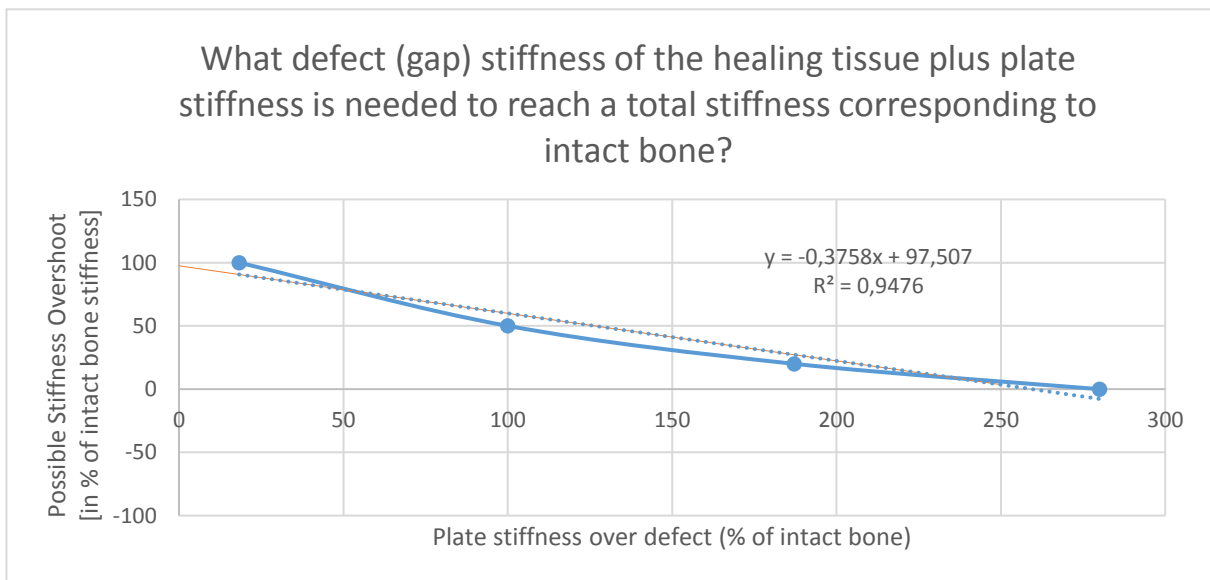


Figure 2-8: Excess defect stiffness compared to intact bone stiffness during fracture healing relative to plate stiffness for the given assumptions above.

With this maximum total stiffness of about 200% of intact bone stiffness related to low screw-plate fixation stiffness over the defect, one might estimate the maximum callus size (assuming no further biological issues). Let us assume, on the one hand 20% modulus for the callus, and on the other hand intact bone stiffness as a target value (100% modulus). Axial stiffness depends on the product of modulus and area with intact bone outer radius $R=14\text{ mm}$ and inner radius $r=5\text{ mm}$:

$$\frac{E_{Callus}A_{Callus}}{E_{Bone}A_{Bone}} = 2.0$$

$$\frac{E_{Callus}A_{Callus}}{E_{Bone}A_{Bone}} = \frac{0.2E_{Bone}}{E_{Bone}} \cdot \frac{\pi(R_{Callus}^2 - r^2)}{\pi(R_{Bone}^2 - r^2)} = 2.0$$

$$\frac{(R_{Callus}^2 - r^2)}{(R_{Bone}^2 - r^2)} = 10$$

$$R_{Callus}^2 - r^2 = 10(R_{Bone}^2 - r^2)$$

$$R_{Callus} = \sqrt{10 \cdot R_{Bone}^2 - 9r^2} = \sqrt{10 \cdot (14 \text{ mm})^2 - 9 \cdot (5 \text{ mm})^2} = 41.7 \text{ mm}$$

For the given values in this example, the callus should not exceed about (41.7 mm/14 mm=2.98) 300% of the initial bone radius. In reality, there really seems to be a relation between (maximum) callus size and bone size, but without any quantification in the literature.

Sophistication and parameterization of such analytical mechanical models requires detailed knowledge on influential factors and sensitivity of parameters in order to be able to make justified assumptions. Thus, more complex models are needed to show justification of assumptions.

2.2. Finite element analysis

The previous models rely on a number of assumptions. Models that are more complex can directly measure the impact of those assumptions and their sensitivity for different input parameter combinations by excluding or including those assumptions and assessing the difference in output. In the following pages, physiologically realistic finite element models of secondary fracture fixation are created through:

- Implementation of realistic geometry
- Implementation of physiological boundary conditions (especially loading)
- Implementation of physiological bone material properties
- Implementation of realistic implant behavior
- Validation of subject-specific finite element (FE) models against *in vitro* experiments
- Discussion of modelling process automation & abstraction (reduction of complexity)
- Implementation of patient-specific realistic models from standard parameters

The finite element method was chosen, because it is widely used and well automated in numerous convenient software packages. So far, each model has to be developed individually, but a general procedure of a FE analysis can be described as follows:

1. Pre-processing:
 - a. Problem definition and idealization
 - b. Data assimilation and parameter identification
 - c. Specification of the analysis and model creation
2. Solution: Solving equations and deriving variables
3. Post-processing: Sorting, printing, plotting, checking and interpreting results

General guidelines for finite element studies in the biomechanical field have been published (Erdemir et al., 2012, Viceconti et al., 2005, Cristofolini et al., 2010).

2.2.1. Idealization

The idealization process simplifies aspects of the system, which is modeled. It has to be respected that those simplifications or approximations in the model will lead to errors and the modeling approach has to be justified and validated to make sure that the interpretation of the model results can answer the research question. For instance, mechanical loads can be represented with sufficient accuracy as concentrated forces (Polgar et al., 2003), but only if the stress/strain around the load application point is interpreted accordingly and the volume of interest is located at sufficient distance. A simple model (e.g. with fewer parts or input values) can be handled much easier than a more sectioned model and a modeling engineer should always seek to make it as simple as possible and just adequately complex for the required needs. Complex models with a high number of parts and possible interactions need a high number of input values that have to be defined for open parameters. Continuing the example of mechanical loads that appear as distributed loads, those require a definition of the application area as well as an intensity distribution across this area while concentrated loads require just an application point and an intensity. If the parameter identification is insufficient for a complex model, it may produce less accurate results than a simple model, which additionally allows easier performance of validation and parameter identification.

How is musculoskeletal modelling different from general mechanical modelling?³⁶ Almost all input is fuzzy and numerous: meaning geometrical dimensions, effects of boundary conditions, and material properties can often neither be measured directly nor very accurately, but all those inputs are fortunately well bounded. Furthermore, biological systems consist of multiple feedback loops. As a result, an appropriate sensitivity of a model often trumps the accuracy: many input value variations will often lead to similar results, but distinct combinations lead to different clusters of results. Thus, it is more reasonable to use many perturbations of a simple model compared to few complex model variations to identify those clusters of input parameter sets leading to beneficial or adverse outcomes. Musculoskeletal models often use rigid body assumptions, and just when evaluating soft tissue behavior, complex material models are employed.

The maxim that medical doctors act upon is helping the biology, not replacing it and doing as little as possible, but as much as needed. They try to find designs that help win the race for healing, not those

³⁶ The FE-Net (Thematic Network, funded by the European Commission) reported in 2005 that the bio-medical technology challenges in FE “include a general lack of credible data, ill-understood scale effects and the ability of material to change behaviour in response to environment.”
<https://www.nafems.org/about/projects/past-projects/fenet/industry/bio/>, last accessed 7 December 2018.
https://www.nafems.org/downloads/FENet_Meetings/St_Julians_Malta_May_2005/fenet_malta_may2005_bio_medical.pdf, last accessed 7 December 2018.

that last (without healing), as those will eventually lead to revision as almost all implants will fail in fatigue at some time point.

Many complex boundary conditions exist, as the body is not classically assembled, but develops and changes over time, exploiting regeneration, but also suffering degeneration. The human body is a dynamic system that adapts its load, movement and deformation, as well as structure constantly. Loading for examples depends on the movement kinematics and those fluctuate with high variability between patients and activities. However, does the internal load reflect these variations at all? In many cases, we do not know yet.

The failure mechanisms of tissue, but also medical devices are usually complex and simple functional principles can hardly be established, but for a few limited cases.

Common issues of idealization are usually questions of complexity (number of interesting parts or loads), linearity (interactions of parts and load), or dimension (degrees of freedom).

Realistic 3D geometry representation may play a crucial role when in bone formation compared to only 2D geometry (Hsu et al., 2018b). For our modeling approach, due to the increasing lever arm during plate bending, geometric non-linearity will be considered. Bone material is inhomogeneous and a mesh representation requires sufficiently fine meshes and homogenization of parameters over each elements' size. Details of idealization are discussed for the specific modeling issue as follows.

2.2.2. Parameter identification

The input values that are assigned to the model parameters have to be determined comprehensibly through direct measurement or deduction. In the field of biomechanics, input parameters are often estimated based on disputable grounds, especially internal loads, geometry, boundary conditions and material properties. Biological values (model input) may vary over a large range. Model sensitivity tests can provide an indication for the importance of an accurate parameter identification as they specify the prediction uncertainty of the model when an input parameter is varied. Let us assume a general polynomial relationship between input and output of a model and an error in parameter identification of 10%, which are likely in a biological context. If we assume a linear relation then the error progression will yield also 10% error, but if the polynomial is dominated by a second-order term, the error may increase to (1.10^2) 21% and for a dominant 4th order term to (1.1^4) 46.4%. Thus, at this point, work should be invested in basic model validation and parameter identification (e.g. reducing input error <10%) much more strongly than in model sophistication (finding best predictive function e.g.

polynomial exponent). Imagine the real (ideal) input as 1.00 and the ideal model as $out = inp^{2.20}$. The measured input error is +10% and the current model is $y = x^2$. We now improve the input error by 10% to obtain an input of 1.09, or we improve the error of the model (exponent) by 10% to 2.02. As a result, we obtain for the first case an resulting error: $(1.09^2 - 1.00^{2.2}) = 18.81\%$ while for the second case: $(1.10^{2.02} - 1.00^{2.2}) = 21.23\%$. It is obvious that for higher exponents the difference in error will increase even more. Thus, it is important to reduce both errors equally, as well as in the modeling assumptions and in the parameter identification.

2.2.3. General procedure of model creation

The general procedure of biomechanical model creation is described as follows, adapted from (Schileo et al., 2008).

- 1) Deduction of bone anatomy (definition of bone geometry), e.g. through CT segmentation,
- 2) Geometry simplification (idealization) and NURBS³⁷ extraction,
- 3) Automatic meshing, (Schileo et al. 2007, 2008); choice of element type and refined meshing,
- 4) Definition of material properties through the densitometric calibration of the CT dataset with a phantom (Kalender, 1992), and element-specific application of an empirical density–elasticity relationship (Morgan et al., 2003), spatially distributed material properties and a numerical integration algorithm for mapping data sampled of the CT grid onto the FE mesh (Taddei et al., 2007),
- 5) Placement of bone and fixation hardware,
- 6) Creation and definition of fasteners (screws), internal constraints, contact etc.
- 7) Definition of boundary conditions (loads, displacement constraints)
- 8) Output requests
- 9) Translation of pre-processing into computational model
- 10) Created model ready for solving

In our modeling approach, the procedure was not executed sequentially (Figure 2-9), but required some cross-referencing and iterations.

³⁷ Non-uniform rational B-Splines, which define surfaces in space in computer graphics.

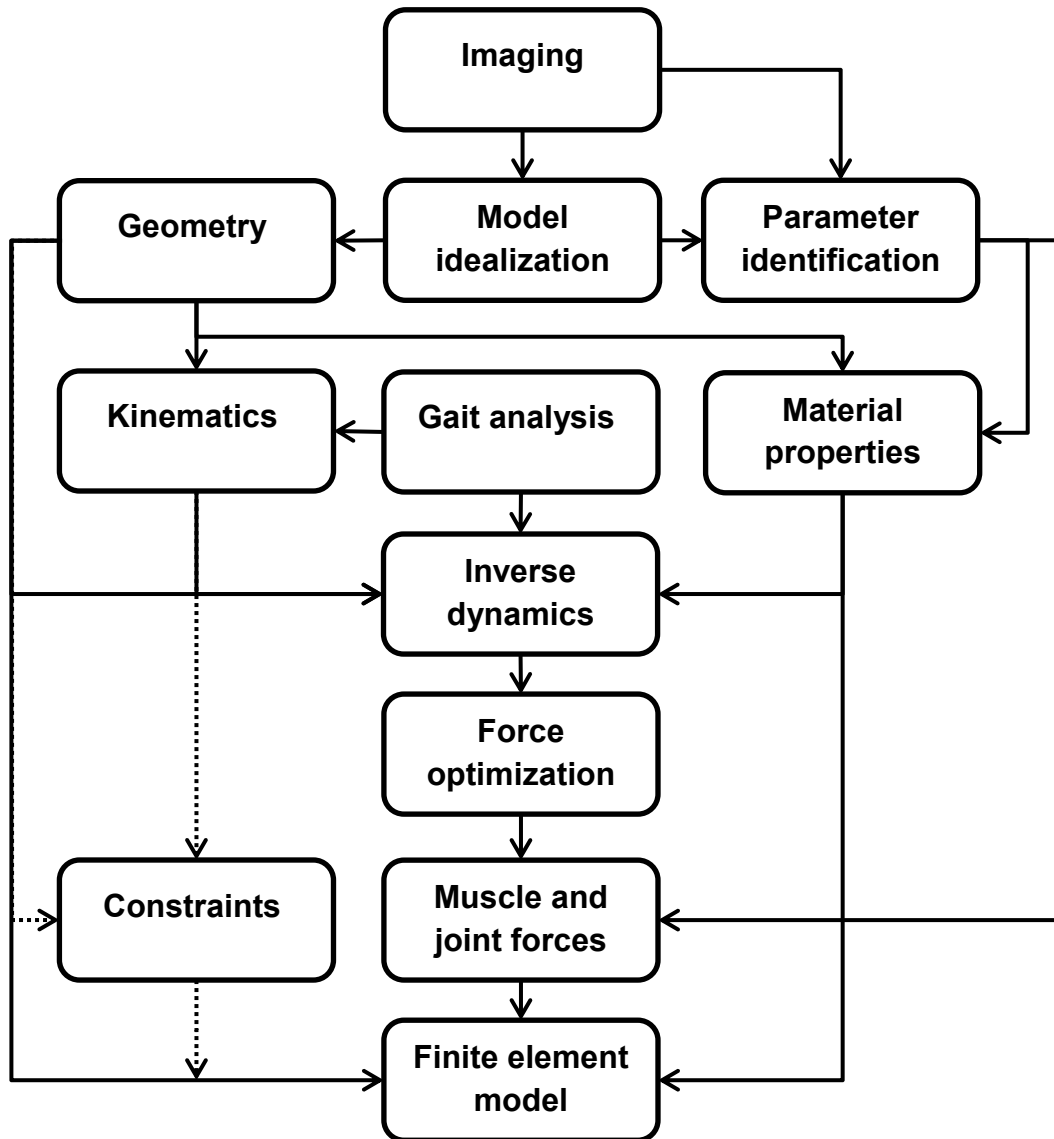


Figure 2-9: Schematic steps of a biomechanical finite element model creation.

There are many different modeling parameters that have been discussed in the literature (Grant, 2012, MacLeod et al., 2016b, Chen et al., 2017, Alierta et al., 2014, Wittkowske et al., 2017, Poelert et al., 2013). We will briefly exemplify our approach towards single modeling issues here.

To quantitatively analyse the influence of fixation configuration (screw position, screw type, plate working length, plate material), fracture configuration (fracture slope, and gap size) and loading conditions on interfragmentary movement (IFM) in a locking plate construct of a distal femur fracture, geometrically nonlinear, (quasi-)static finite element (FE) models were developed.

2.2.4. Modeling of patient specific geometry

The specific geometry of each patient is different. However, for fixation mechanics, mostly the distances (lever arms) between the load application and fixation placements and interactions carry the most importance (Trepczynski et al., 2012, Kutzner et al., 2013). Such characteristic landmarks however, can only be identified with high accuracy if the patient anatomy is known in 3D-space. The standard method of modeling patient specific geometry consists of reconstruction from imaging. For bone tissue, usually CT-image slices are either manually segmented or machine-learning is used on segmentation and those stacked label-slices are reconstructed to solid bodies. A more sophisticated way uses statistical shape models based on principal component analyses of manually segmented bones that are fit to one specific bone model with a specific topology. The resulting principal components are varied based on likelihood in the ground-truth-data-set and fitted into the image data set. With the second approach, characteristic topological points can be defined and automatically fitted to the specific patient data.

Using input data from quantitative computed tomography (qCT), the software Amira v5.3 (Visage Imaging, San Diego, USA) was used for segmentation and smoothing of the imaging data (Figure 2-10). Bone tissue area was manually selected on imaging slices of different planes. For selection, image intensity was varied until bone tissue appeared prominent. Interpolation tools and curve smoothing tools in the Amira software were used to match the bony anatomy more closely. Manual correction, especially at the meta- and epiphyses was necessary to exclude adjacent tissue. Manual segmentation remains a cumbersome necessity. Alternatives such as machine-learning segmentation or statistical shape models require excessive preliminary work with the disadvantage that their accuracy still strongly depends on 3D-image quality. Human manual segmentation may compensate for many issues of image quality such as metal hardware imaging artefacts or bony defects. Furthermore, such automated techniques can only capture reliably in their output what was initially included within the ground-truth data set such as bony apophytes.

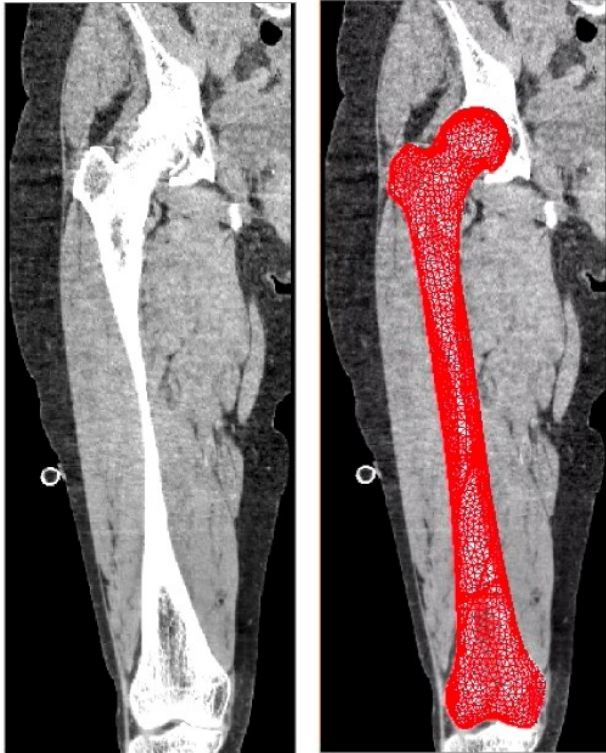


Figure 2-10: Left: Imaging data (qCT), here frontal plane, served as data source for segmentation, which was performed manually, per slice directly on the data set, separating bone tissue from other tissues based on image intensity and general shape of the bone.

Right: The bone mesh was positioned in the CT-coordinate system and all other parts were added and positioned accordingly.

Geomagic Studio 10 (Geomagic, Morrisville, USA) was employed for reprocessing and creation of Non-Uniform-Rational-B-Spline (NURBS). If the whole bone as segmented from Amira is used in the models, this step is not necessary, as Amira can produce high-quality tetrahedral meshes. However, later changes to the orphan mesh are difficult and can be simplified by creating a NURBS-representation of the bone first (Figure 2-11). Then, cuts or creation of screw holes, defects, etc. can be performed easily directly within the pre-processing software. As an example, the addition of a hip prosthesis that requires cutting at the femoral head and subtraction of the cavity for the prosthesis and bone cement would be challenging when performed on the mesh as it requires moving nodes and not only removing elements. Much easier, the solid body geometry of the reconstructed NURBS-bone can be imported, the head can be cut with sophisticated software tools and the hip prosthesis (or an enlarged model to leave a margin for bone cement) can be subtracted from the bone, leaving a solid body model that can be manipulated even further. Furthermore, meshing within the pre-processor enables the user to adapt the mesh so that a number of analyses (e.g. with different fracture configuration) can be performed simply by manipulating (such as removing) different element sets. Thus, even at an early time point in geometry creation, the desired analyses should already be clear to avoid complicated additions at later stages.

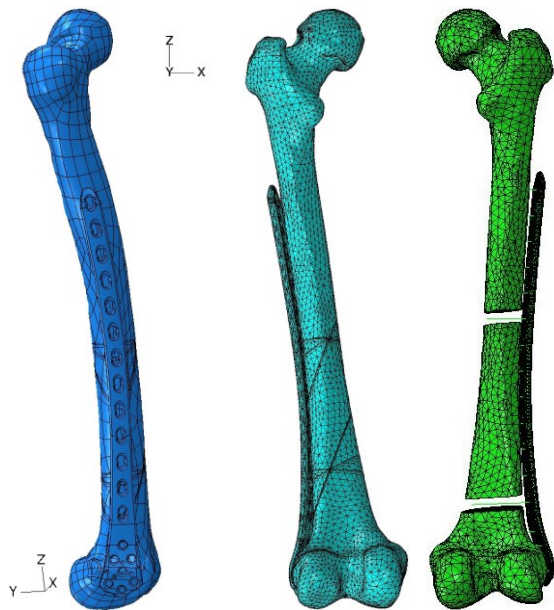


Figure 2-11: Left (blue): Representation of the femur geometry with splines allows import to pre-processing software and positioning of other hardware relative to bone (here a plate).

Center (turquoise): Pre-processing software allows adaptation of mesh and creation of element sets, so that different fracture gap sizes and fracture angles can be implemented within the same model, yielding better control and comparability of the results as different element sub-sets can be removed to vary fracture configuration with otherwise identical model (very similar mesh).

Right (green): Manipulations such as Boolean operations (e.g. subtraction of bony defects such as a fracture gap) can be handled much more conveniently before mesh creation and variations of the mesh should be considered during meshing.

Amira v5.3 (Visage Imaging, San Diego, USA) or Abaqus/CAE v.6.9-12 (Dassault Systèmes, Vélizy-Villacoublay, France) were used for discretization of the geometry. Preliminary testing with first-order tetrahedral elements revealed excessively stiff constructs. Ramos and Simoes (2006) could show for the proximal femur that experimental strains were well correlated with numerical ones using second order tetrahedral finite elements. Polgar et al. (2001) conclude in their study that linear tetrahedral elements should be avoided and quadratic tetrahedral elements ought to be chosen for finite element analysis of the human femur with the coarsest possible T10 mesh compatible with accuracy to minimize computer capacity and CPU time. Our models were meshed with second-order tetrahedral elements (C3D10) with strong refinement in areas of high local curvature similar to other studies (Wieding et al., 2012, Hölzer et al., 2012, Miramini et al., 2015a, Miramini et al., 2016, Speirs et al., 2007). The initial mesh seed was set to a few millimetres resulting in characteristic element lengths well below 2 mm, and minimum several 100k DOFs for the bones. This mesh was verified to be suited to yield consistent results in reaction forces, surface strain and displacement with finer meshes (Figure 2-12). Moazen et al. (2013) found that solutions converged on the parameters of interest with less than 5% error (axial stiffness, torsional and bending rigidities) with approximately 400,000 total elements. Hölzer et al. (2012) state that integral and qualitative conclusions can be drawn from subject-specific FE models with coarser meshes, but they also show best results for element length between 1 and 2 mm. For fine material distribution and good convergence, element edge lengths around or just below 2 mm were suggested before (Polgar et al., 2001, Wieding et al., 2012, Arnone et al., 2013).

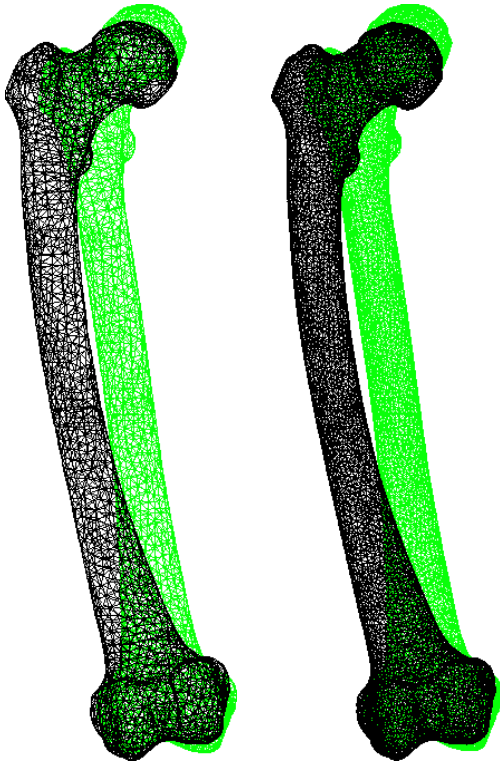


Figure 2-12: All meshes have element edge lengths well below 2 mm for most elements. For mesh size sensitivity testing, different characteristic element lengths were implemented: 1.67 mm, 240798 DOFs, left, or 1.37 mm, 459825 DOFs, 1.10 mm, 894900 DOFs, right. The reaction forces, surface strain and displacement with finer meshes are consistent with the coarser meshes, allowing the use of the models with fewer DOFs and faster computation, compare (Heyland et al., 2015b).

2.2.5. Modelling of patient specific material properties

Model results are sensitive to material property definition. However, for the prediction of IFM, the geometry of a fractured bone is much more critical than its material properties within a reasonable range (MacLeod et al., 2016c).

Bone material is not isotropic, but can be represented by orthotropy (Cowin and Mehrabadi, 1989, MacLeod et al., 2016c). Realistic material property assignment (e.g. orthotropy) is very important for the FE analyses of small bone specimens or uncommon loading directions, whereas in global FE analyses, this assignment can be simplified to an isotropic bone model, if the inhomogeneous material model is used (Baca et al., 2008). This simplification is reasonable as the definition of orthotropy requires additional (uncertain) input such as local axes for each element and markedly more time and effort than an isotropic model. Predicting a stiffness tensor from a scalar density value remains difficult. In a semi-automated procedure, San Antonio et al. (2012) base the directions of the axes of orthotropy on computed principal stresses and achieve stress distributions differences of maximum 7.6% while the local changes in the strain distributions could be much higher (maximum 27%) compared to an isotropic model. Yang et al. (2010) also report that the differences between isotropic and orthotropic material property assignments are significant in some local regions (Von Mises stress maximum 13.25% and nodal displacement maximum 15.04%) where maximum values did not occur.

The exact amount of deviation differs depending on comparative parameter, loading conditions, and mesh refinement. Experimental results agree in terms of strains and displacements with computed FE models with either inhomogeneous orthotropic properties or empirically based isotropic properties (Trabelsi and Yosibash, 2011); only the strains within the femoral neck are sensitive to isotropic versus orthotropic properties in FE results.

For an inhomogeneous isotropic material model, the Young's modulus and Poisson ratio of each element need to be determined. Yosibash et al. (Yosibash et al., 2007) performed a sensitivity analysis concerning Poisson's ratio ranging from 0.01 to 0.4 and determined a negligible effect on displacements and strain, thus, a standard value of 0.3 or similar can be chosen.

2.2.5.1. Homogenization of bone tissue

Patient-specific material properties with inhomogeneous material properties need the basis of local CT-attenuations or another source of intensity distribution. For calculation of local Young's modulus, first local intensities are used to determine local bone density and then empirical relationships can be used to estimate local Young's modulus of each element (Pankaj, 2013). A comprehensive algorithm including validation of this material mapping approach has been described by the Rizzoli group from Bologna (Taddei et al., 2006a, Taddei et al., 2006b, Taddei et al., 2007, Schileo et al., 2007, Helgason et al., 2008, Schileo et al., 2008, Cristofolini et al., 2010). They found a great model sensitivity to the implemented density–elasticity relationship (Schileo et al., 2007) with the best empirical density–elasticity relationship obtained by Morgan et al. (2003) when compared to other reported regressions:

$$E[MPa] = 6850\rho^{1.49}; \quad \rho \left[\frac{g}{cm^3} \right] \quad \text{Equation 2.1}$$

We implemented this material mapping approach and first found a significant correlation between the qCT image density (in Hounsfield Units) and the mineral density of a known phantom ($R^2 > 0.99$; $p < 0.001$) which formed the base for a specific linear regression formula for each image scan to calculate the apparent mineral density (Figure 2-14). Then, a non-homogeneous material distribution (material mapping approach) was modelled based on averaged image densities over each mesh element (averaging based on 64 points with sample scalar field function in Amira software) and local apparent mineral densities were calculated. These acquired equivalent densities were calibrated according to Schileo et al. (2008) and an empirical density-isotropic stiffness relation from femoral neck tissue was used as described by Morgan et al. (2003) to calculate local Young's modulus of each

element according to Equation 2.1. This gives material property estimates resulting in numerical output that is in accordance with experimental measurements (Cristofolini et al., 2010). Finally, the materials were rounded and grouped into bins (size 50 MPa) according to a range of moduli resulting in more than 400 material definitions (Figure 2-13).

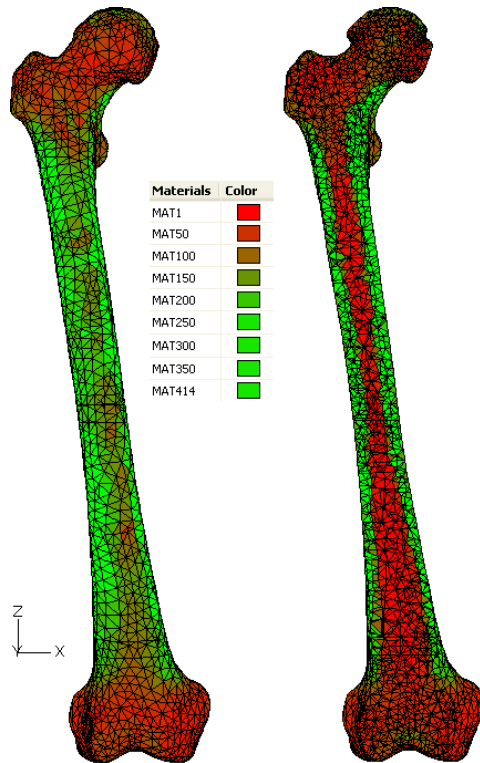


Figure 2-13: Modelling result example of material mapping approach yielding 414 bins of 50 MPa size with rising Young's modulus from red to green, on the left for the femoral surface, on the right for a cut of the femur. Note the high material modulus of the diaphyseal cortex and the lower moduli at the meta- and epiphyses with small areas of high moduli at the joint surfaces (thin cortices). The lower density within the metaphyses underlines the necessity of proper and sufficient fixation instrumentation in those zones, i.e. for instance more screws and especially locking screws are beneficial for a more porous substrate.

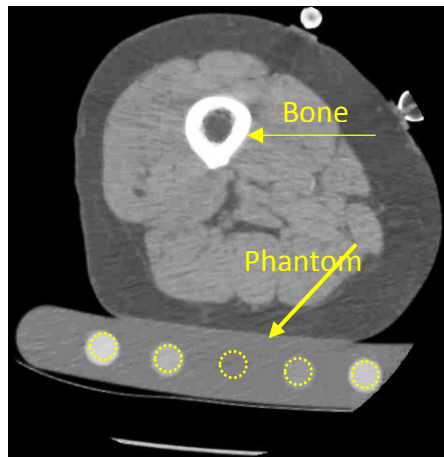


Figure 2-14: Example of one transverse imaging slice with bone and surrounding tissue and a phantom with mineral cylinders of known density for calibration of image intensity to apparent density.

2.2.5.2. Modelling of regenerative tissue

Initially, the simulation of comminuted fractures without cortical support was implemented at the distal femur. The fracture was created with different osteotomy gap sizes such as 10 mm, because this

distance has been shown to avoid cortical contact while loading (Chao et al., 2013) or 3 mm between the distal and proximal fragments by removing elements 68mm above the lateral condyle (location of the first plate hole at the shaft). Without any additional supporting structure but a lateral plate, full weight-bearing during gait would lead to collapse of the gap (Figure 2-15).

It was aspired to mimic conditions representing 60-80 days postoperatively when patients are able to walk with full weight bearing. Four diagonally spanning spring elements (anterior–posterior and medio-lateral) with a stiffness of 80 N/mm each in axial and 40 N/mm in shear direction were introduced at the fracture gap, similar stiffness to measured stiffness in patients with external ring fixators (Duda et al., 2003a, Duda et al., 2003b). It should be mentioned here that most macroscopic simulations at the whole bone level that focus on the fixation neglect regenerative tissue³⁸ and rather reduce the loads to avoid collapse of the gap.

Later, assumptions of low tissue stiffness with homogeneous Young's modulus of the tissue within the gap of for instance 1 MPa or 10 MPa were implemented as well with 3 mm or 1 mm fracture bridging sizes.

2.2.6. Plate model



Figure 2-15: Collapse of the fracture gap with contact of the proximal and distal segments for a 10 mm diaphyseal gap under walking loads without additional support within the fracture gap.

³⁸ At the 2015 congress of the European Society of Biomechanics (ESB) in Prague, Alisdair MacLeod presented models with different plate stiffness that explained the discrepancy in expected stress and fatigue failure between clinical *in vivo* experience and *in vitro* tests. These differences were found to be a result of the callus formation within the fracture gap. I like to believe the inspiration for this study originates from our talk at the World Congress of Biomechanics 2014 in Boston and my insistence on the importance of regenerative tissue stiffness, which was gained from my first modeling approaches and results.

The fracture gap was stabilised with the model of a laterally bridging plate such as the LISS-DF (less invasive stabilising system for distal femur, DePuy Synthes, Zuchwil, Switzerland), LCP-DF or similar plates according to the manufacturer's recommended surgical technique³⁹ (Figure 2-16). Typical mesh size of the plate are more than 50,000 tetrahedral elements (C3D10). In later implementations, we could see the importance of plate deformation rather than bone deformation. We used coarser meshes for the bone (still sufficiently fine to allow for the homogenization of the bone tissue to be able to distinguish cortical from trabecular areas), and fine meshes for the plate. The material model of the plate was isotropic, homogeneous with a Young's modulus of 110GPa for titanium plates and 187GPa for steel plates, and a Poisson ratio of 0.3.



Figure 2-16: Plate placement is not trivial as there is no universal algorithm. Surgical techniques vary and thus plate placement may vary strongly. We tried to place the plate with a small distance between the plate and the bone (clearance) to allow for free plate bending. However, this bone-plate distance should remain small over the whole plate length to avoid excessively long free bending lengths of individual screws. Furthermore, excessive distance of the plate from the bone results in decreased plate strength Ahmad et al. (2007).

Left: Plate model of a 13-hole Locking Compression Plate (Depuy Synthes) with combination holes for potential hybrid fixation.

Center: Positioned plate on bone model (in red, not meshed, only NURB-representation).

Right: Second view of plate on bone model. Only placement in multiple planes ensures correct plate position.

³⁹For reference, see manufacturer's manuals:

http://synthes.vo.llnwd.net/o16/LLNWMB8/INT%20Mobile/Synthes%20International/Product%20Support%20Material/legacy_Synthes_PDF/DSEM-TRM-0614-0094-2a_LR.pdf, last accessed 17 September 2018.

http://synthes.vo.llnwd.net/o16/LLNWMB8/INT%20Mobile/Synthes%20International/Product%20Support%20Material/legacy_Synthes_PDF/016.000.235.pdf, last accessed 17 September 2018.

http://synthes.vo.llnwd.net/o16/LLNWMB8/INT%20Mobile/Synthes%20International/Product%20Support%20Material/legacy_Synthes_PDF/016.000.358.pdf, last accessed 17 September 2018.

2.2.7. Screw model and its interfaces

Beam elements represent the screws with structural and material properties adapted to published data (Döbele et al., 2014) and unpublished data provided by the screw manufacturer (Figure 2-3, Table 4). The screw-plate and screw-bone interfaces were realised using beam multi-point-constraints (Figure 2-17) as previously described (Wieding et al., 2012).

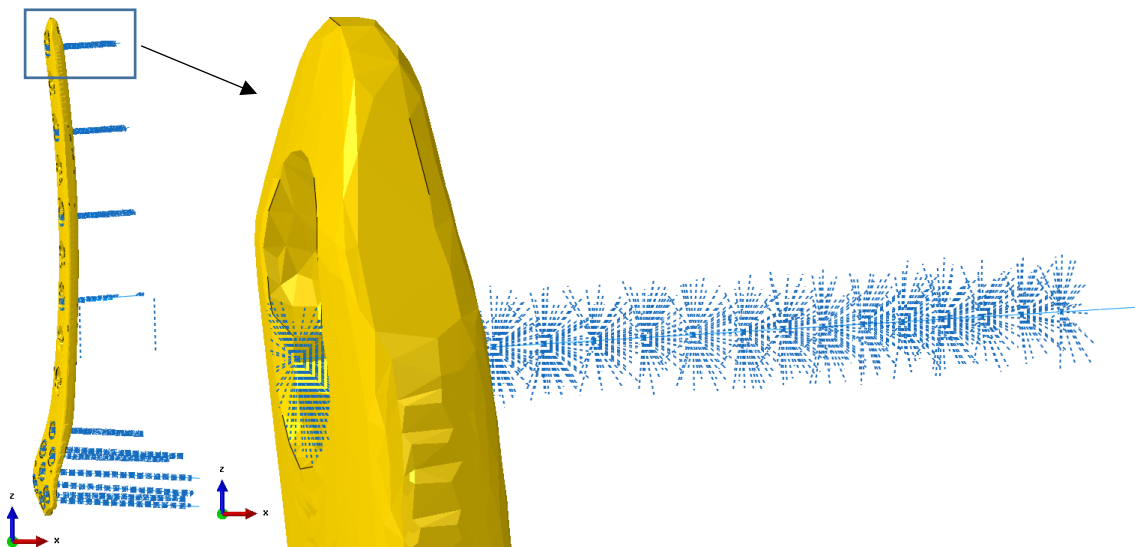


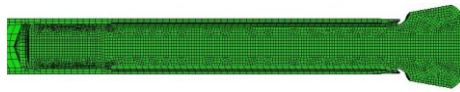
Figure 2-17: Example of a screw model plus interfaces to plate and bone (bone not shown). Left: Whole plate with multiple screws and their connections via multi-point constraints. Right: Detail of proximal plate tip with one screw and its multiple connections.

2.2.7.1. Individual screw model

For modeling and validating individual screw behavior, we assimilated test data of different individual screws loaded in a defined way. These single screw shear-bending tests (Figure 2-3) were used to simplify the screw to beam elements (Figure 2-17, Figure 2-18) with defined properties matching the displacement results *in vitro* versus *in silico*. We have chosen to model fewer details as this is less complex and less time consuming. Such simplified models for the screws reduce the modelling effort strongly without compromising result quality when evaluating only the global load-deformation behavior (MacLeod et al., 2012b): There is a strong impact on the local stress-strain environment within the bone in the vicinity of the screws (local stress/strain differences), but we do not evaluate this. Local stress/strain distribution around screws requires a local detail model (Wieding et al., 2012).



Figure 2-18: Top: Schematic cut of a dynamic locking screw (DLS).



Center: Detailed finite element model of an individual DLS (tip not shown).



Bottom: Simplified structural screw model with much less computational effort.

Dedicated detail models of bony microstructure are a special domain to evaluate very localized strain and even failure (Steiner et al., 2017, Steiner et al., 2016, Steiner et al., 2015, Ruffoni et al., 2012), Nolte 2013 (CADFEM GmbH)⁴⁰.

The special difficulty of modeling the multi-part DLS could be conquered using special ITT31 elements in tube-to-tube contact as generally described by Lars Hansen (Figure 2-19) in http://www.lhe.no/download/Abaqus_Tube-to-Tube_modeling.pdf, last accessed 18th September 2018.

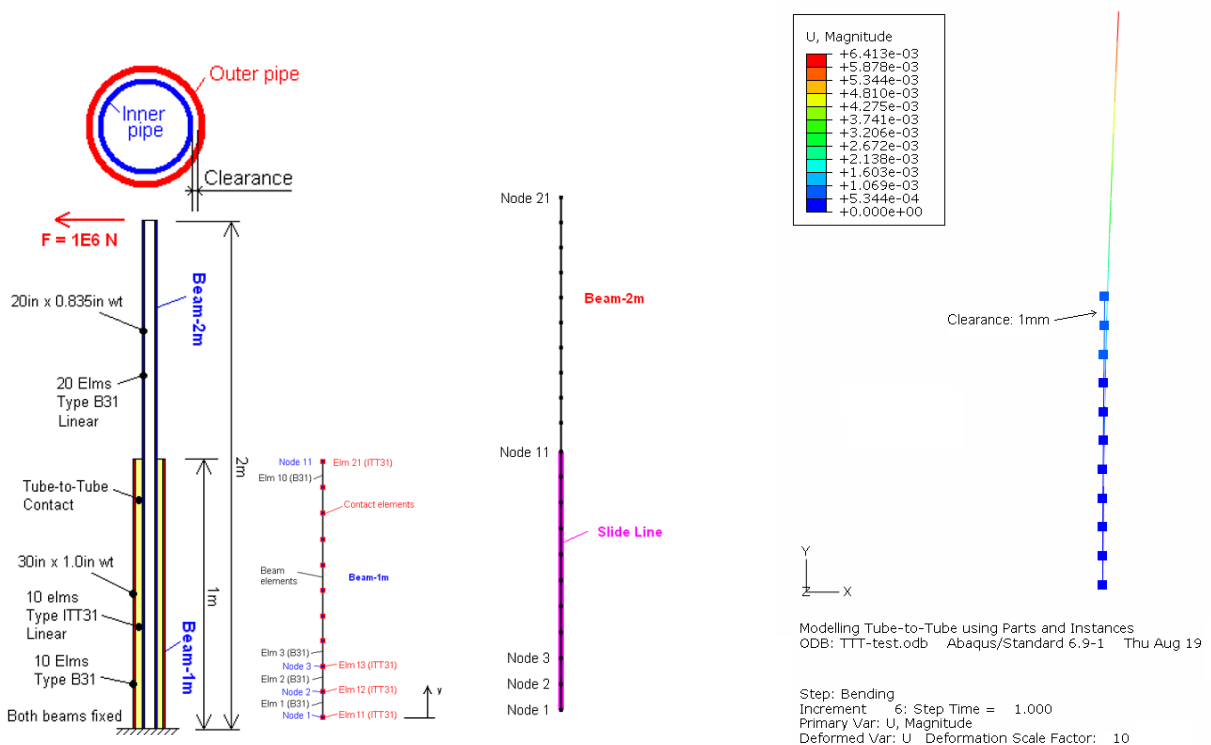


Figure 2-19: The dynamic locking screws with multiple contacting parts were simplified with a tube-to-tube contact with special ITT31 elements, compare the images above in http://www.lhe.no/download/Abaqus_Tube-to-Tube_modeling.pdf, last accessed 18. September 2018. On the right you can observe our implementation in Abaqus/CAE.

⁴⁰ Nolte 2013: Simulation method to investigate the bone-screw interface at pedicle screws in vertebrae. https://www.nafems.org/downloads/nwc13/abstracts/212_Nolte.pdf, last accessed 18th September 2018.

2.2.7.2. Screw-bone model

Surgical pre-drilling size (not tapped) is quite large (4.3 mm) compared to the 3.8 mm recommended tapping drill size of a metric standard screw with the same nominal diameter of 4.5 mm. A larger initial hole leads to less compression of the surrounding tissue (Grant, 2012) and a comparably strain-less in-laying of the screw into the bone tissue should preserve the structural integrity of the bone microstructure, but it still compresses the bone to higher densities around the screw threads. This justifies the modeling of bonded contact of the screw surface (modeled as a simple cylinder or threaded) to the bone surface (modeled with a subtraction hole at the screw position). Simple bonded interfaces (Bottlang and Feist, 2011, Stoffel et al., 2003, Wehner et al., 2011) prevent separation of upper surface from bone and reduce movement as the bone underneath is compressed and the bone above stretched under tensile loads (Grant, 2012). A direct connection of a structural screw model to the bone tissue to gain a reinforced structural screw-bone model constitutes another modeling option. A structural representation of the screw, which connects screw nodes rigidly or even with a certain adjustable interface stiffness to bone nodes at the outer surface diameter of the screw might more realistically capture the tensioning of the upper part and the compression of the part below the screw/bolt in transverse shear loading of the bolt.

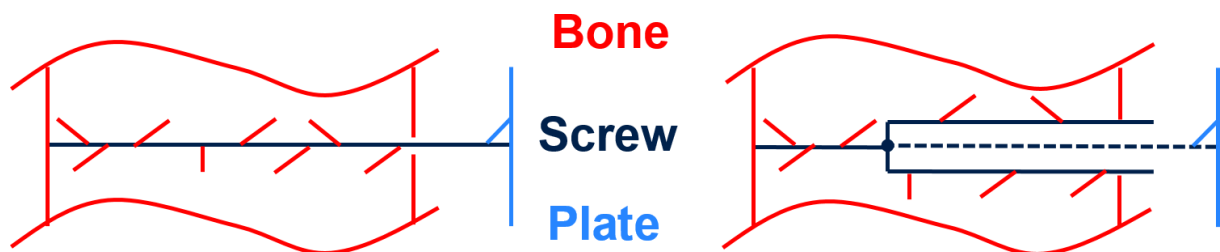


Figure 2-20: Schematic appearance of structural beam models of screws, which are connected to substrate bone and plate. On the left for a standard locking screw and on the right for a dynamic locking screw.

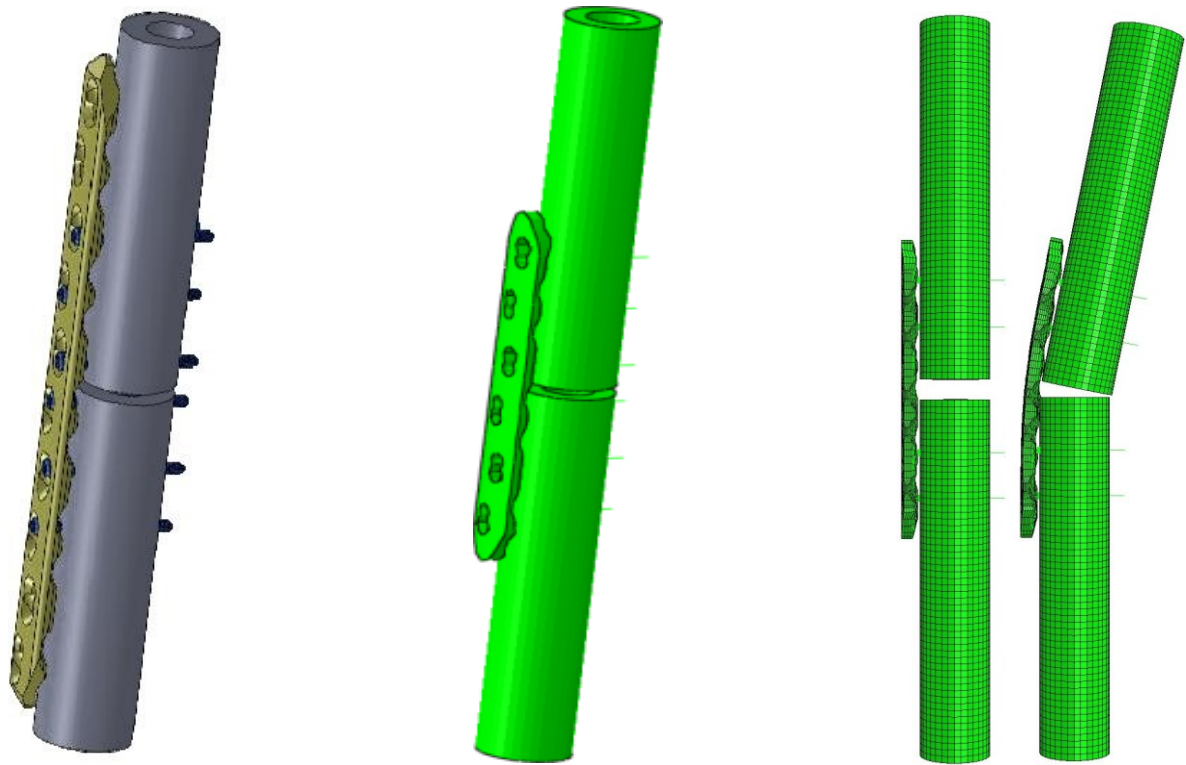


Figure 2-21: Finite element model implementation (center, right) of the *in vitro* experiment by Döbele et al. (2014) on the left.

Instead of a full screw threaded geometry, but resorting to a fully structural screw representation, the computational size and complexity of the model is dramatically reduced without necessarily reducing its accuracy (Wieding et al., 2012). The idealization of structural screw representation with direct connection to the surrounding support material via point constraints is justifiable and advantageous (Wieding et al., 2012), (Figure 2-20). For a simple model of plate bending (Figure 2-21), we achieved good agreement to measured results in terms of displacements mainly caused by plate deformation with the screw models and screw-interface model we implemented for different screw types (Figure 2-22).

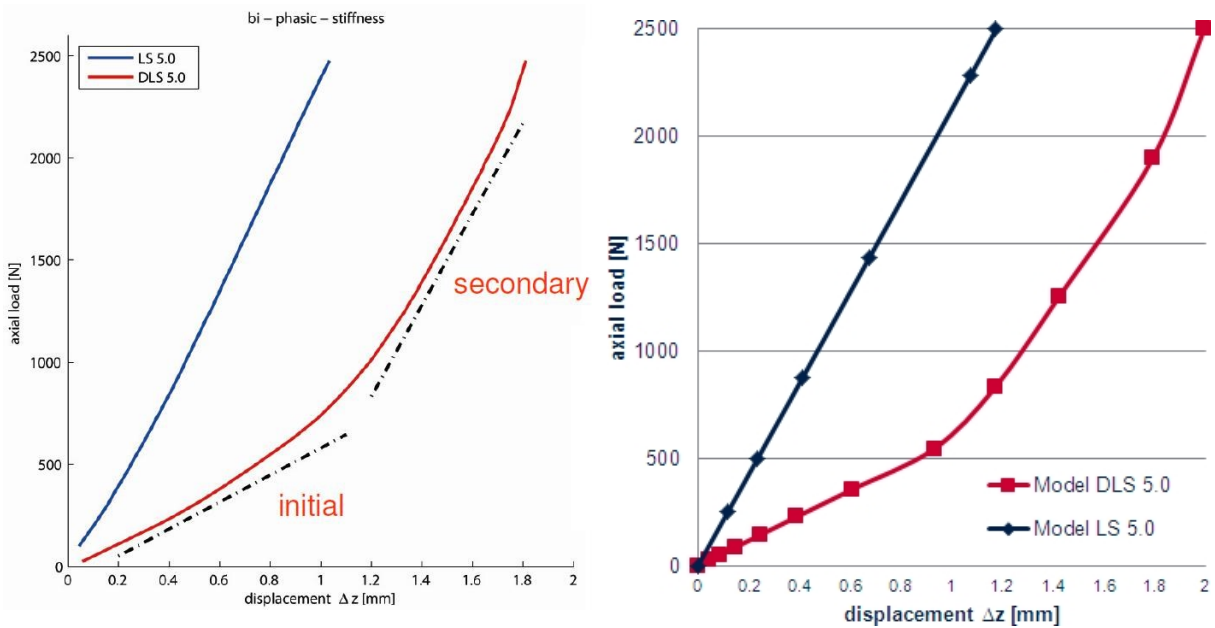


Figure 2-22: Comparison of displacement measurement results from Döbele et al. (2014), left, and our numerical simulation, right, of a cylinder with a lateral plate under axial-bending load for two different screw types: locking screws (blue) and dynamic locking screws (red).

2.2.7.3. Screw-plate interface

For all further investigations here, angular stability of the screw head within the plate was assumed and the screw head was rigidly linked to the plate hole using multiple multi-point constraints (Figure 2-17).

More recent evaluations, with other plates and other poly-axial (variable angle) locking mechanisms, showed the need for an additional rotational spring stiffness letting the screw head rotate within the plate (Figure 2-23), which leads to reduced stiffness.

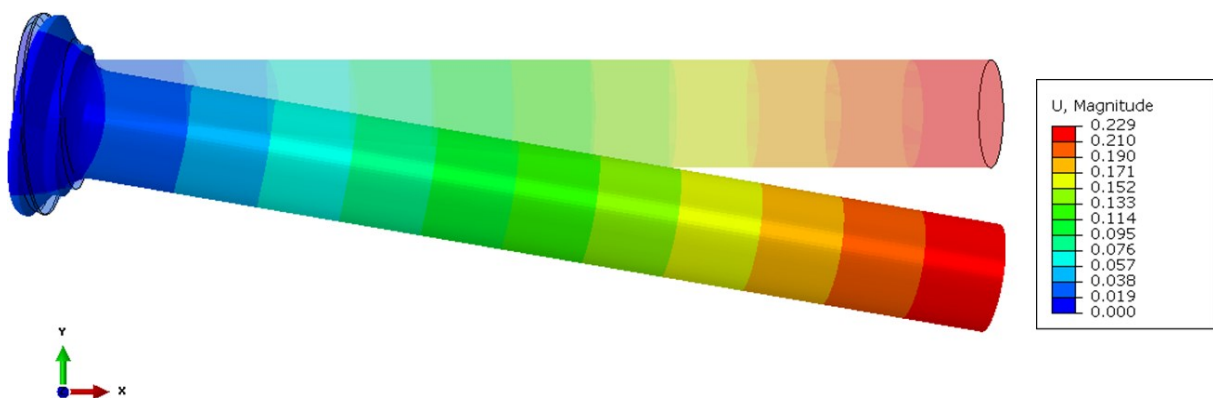


Figure 2-23: Single screw model rotating around the screw head with a measurement-matched rotational spring stiffness additionally to screw shear-bending.

2.2.8. Physiologically based boundary conditions of the femur

2.2.8.1. Mechanical constraints

For a statically determinate equilibrium, 6 degrees of freedom need to be constrained. Otherwise, the whole structure could move in space.

2.2.8.2. Displacement constraints

The method of loading is critical and responsible for much of the difference in reported stiffness values, or in failure loads (MacLeod et al., 2018a, Grant et al., 2015). For our investigations, the empirically found, but physiologically based boundary conditions of (Speirs et al., 2007) were used. Those displacement constraints have been used in previous studies showing physiological strains (Bayoglu and Okyar, 2015, Szwedowski et al., 2012). Although those boundary conditions are not fully physiological, they ensure a certain physiological deformation and the reaction forces necessary to perform this deformation are reasonably low (Speirs et al., 2007).

One potential problem we have encountered when combining the material mapping approach and the singular point constraints by Speirs et al. (2007) was that the elements where reaction forces appear could be excessively distorted (Figure 2-24) when they happened to be assigned comparably low Young's moduli. The source of this error might be surface or partial volume artefacts during segmentation. Distributing the displacement constraint unto a larger number of nodes fixed this error.

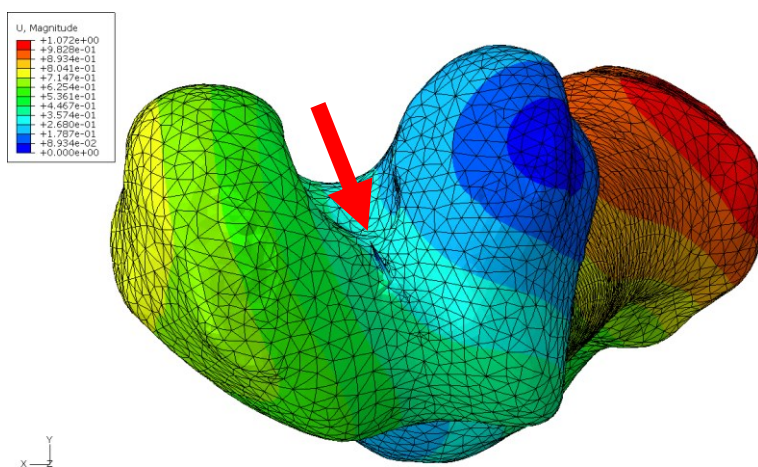


Figure 2-24: When a displacement constraint is applied to one node of a compliant element (low modulus), reaction forces lead to high deformation of this element. This was solved by distributing the constraint on multiple nodes.

2.2.8.3. *Inertia relief*

An alternative to displacement constraints is the inertia relief method for the analysis of unsupported systems such as flying objects⁴¹, vehicles in flight, or even individual robotic arms. This method allows for an acceleration (additionally to or instead of a reaction force). It could potentially also be used to validate the finite element results based on gait lab measurements of individual motion segments such as a leg or an arm where their acceleration is measured independently. However, mass distribution has to be validated as well as it influences the inertia relief calculation. ABAQUS offers the capabilities of inertia relief analysis (Documentation Abaqus 6.8, 2008) and we have reported results in a published study (Heyland et al., 2015b).

2.2.8.4. *Muscle and joint loads*

A data set with gait cycle data, quantitative computed tomography (qCT) and ground reaction force data of a representative patient from a previously published study was chosen. The measured parameters were comparable to the data published elsewhere (Boyer et al., 2012, Szwedowski et al., 2012). Based on this data, a validated model of the lower limb was scaled to match the body weight (e.g. 716 N) of the patient. Internal muscle and joint forces (Figure 2-25), (Heller et al., 2001a, Heller et al., 2001b) were estimated using inverse dynamics. The muscle and joint contact forces for the time point of 45% of a gait cycle of a specific patient in normal level walking were extracted from this validated musculoskeletal model and applied to the corresponding FE model nodes.

According to Saint-Venant's principle, the difference between the effects of two different but statically equivalent loads onto the surface of an elastic body becomes very small at sufficiently large distances from the area of load application and may only lead to significant changes in strain and stress locally around the direct area of load application. According to Timoshenko, for a cantilever beam, a relevant length of decline of the error can be approximated with one beam diameter. Thus, we used concentrated loads analogous to the inverse dynamics model, without the need for further uncertain parameters for load distribution. Main loads were the joint loads at the hip and knee and major muscle

⁴¹This can be rocket science! Our article on inertia relief was cited by rocket scientists (HEYLAND, M., TREPCZYNSKI, A., DUDA, G. N., ZEHN, M., SCHASER, K. D. & MÄRDIAN, S. 2015b. Selecting boundary conditions in physiological strain analysis of the femur: Balanced loads, inertia relief method and follower load. *Med Eng Phys*, 37, 1180-5.):

Dongyang, C., Abbas, L. K., Xiaoting, R., & Guoping, W. (2018). Aerodynamic and static aeroelastic computations of a slender rocket with all-movable canard surface. *Proceedings of the Institution of Mechanical Engineers, Part G: Journal of Aerospace Engineering*, 232(6), 1103-1119.

loads appeared at the greater trochanter (Figure 2-26), confirming previous simplifications in models using only those major loads (Bayoglu and Okyar, 2015, Speirs et al., 2007).

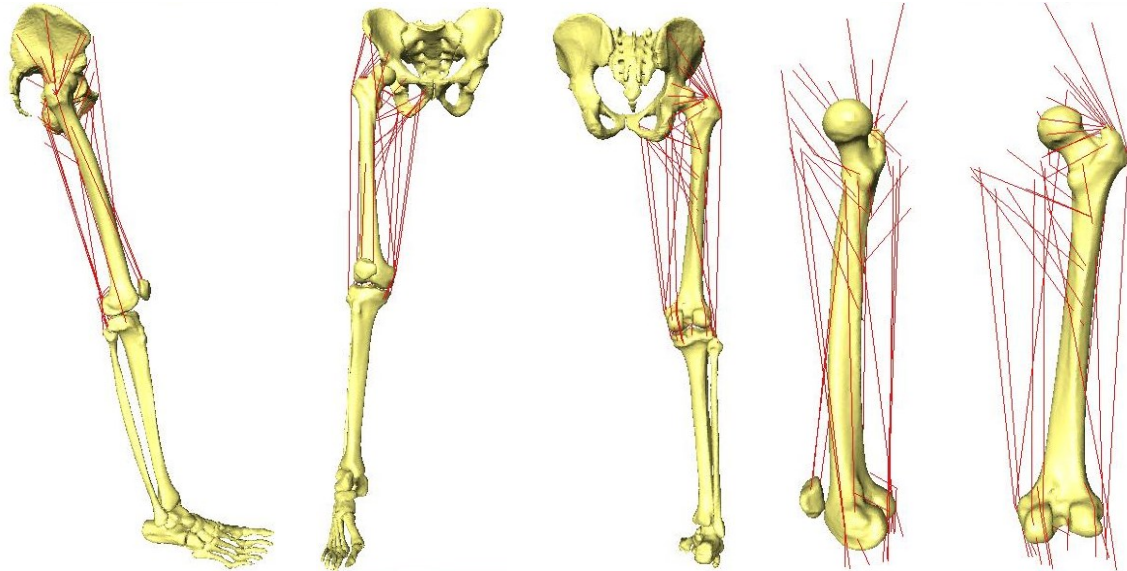


Figure 2-25: Different views of the representation of the bones and the considered muscles for the inverse dynamics estimation of the muscle and joint forces at the femur. Muscles at other bones that were used for calculation are not shown.

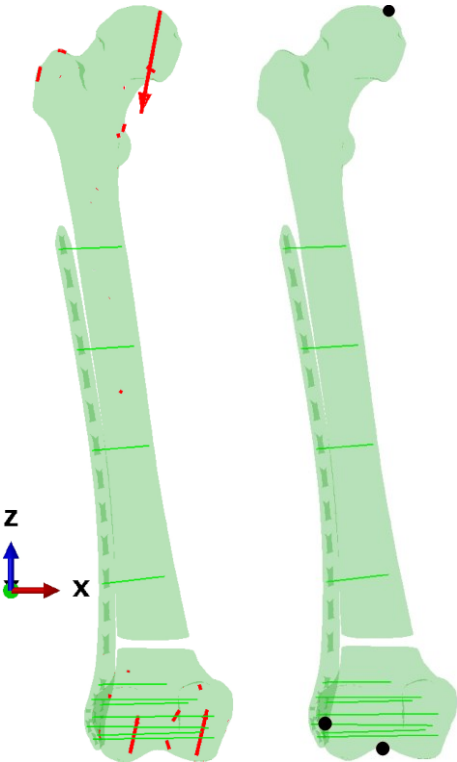


Figure 2-26: Left: Scaled loads (red) for 45% of the gait cycle (maximum hip joint load) with additional muscle loads, especially relevant at the greater trochanter.

Right: Displacement constraints (black) at the hip and knee according to Speirs et al. (2007) leading to additional reaction forces.

2.2.8.5. Contact interfaces

We tried to avoid contact interfaces, as the precise physical validation especially *in vivo* remains out-of-scope for our studies. We placed the plate at a considerable distance of a few millimeter from the bone, so the possible contact between plate and bone should be minimal or even avoided. Furthermore, we checked for contact between the proximal and distal segments at the gap, so either a large gap was chosen to avoid contact or the gap was bridged with elements.

2.2.9. Validation of modelling approaches

Fixation stiffness determines interfragmentary movement (IFM), which may guide secondary bone fracture healing. However, in the literature, fixation stiffness strongly varies even for similar fixations due to different boundary conditions (MacLeod et al., 2018b, Grant, 2012, Grant et al., 2015). So even for well-defined boundary conditions, is our finite element modelling approach valid then? Do measurements and simulations match?

In the framework with another study (Märdian et al., 2015b), biomechanical *in vitro* cadaver tests were carried out on 5 pairs of fresh frozen human distal femora (Figure 2-27). Locked plating constructs composed of distal femur, locking plate, conventional locking screws and/or semi-rigid dynamic locking screws with a distraction defect model were tested in different bridge plating configurations under axial (bending-)compression and torsion. The overall stiffness and local IFM of locked plating and dynamic locked plating for two different working lengths (free plate bending length over the fracture) were assessed for each principal loading mode. Computer tomography scans were prepared. Based on this image data, sample-specific finite-element models of the 10 bones were created. The bones were loaded *in silico* with the same loading scenarios as *in vitro* and the local IFM at the lateral cortex (directly under the plate) and at the medial cortex (opposite the plate) were evaluated. The differences between *in vitro* experiments and *in silico* model results were compared and provide the basis for a discussion of model validity in terms of agreement of IFM.

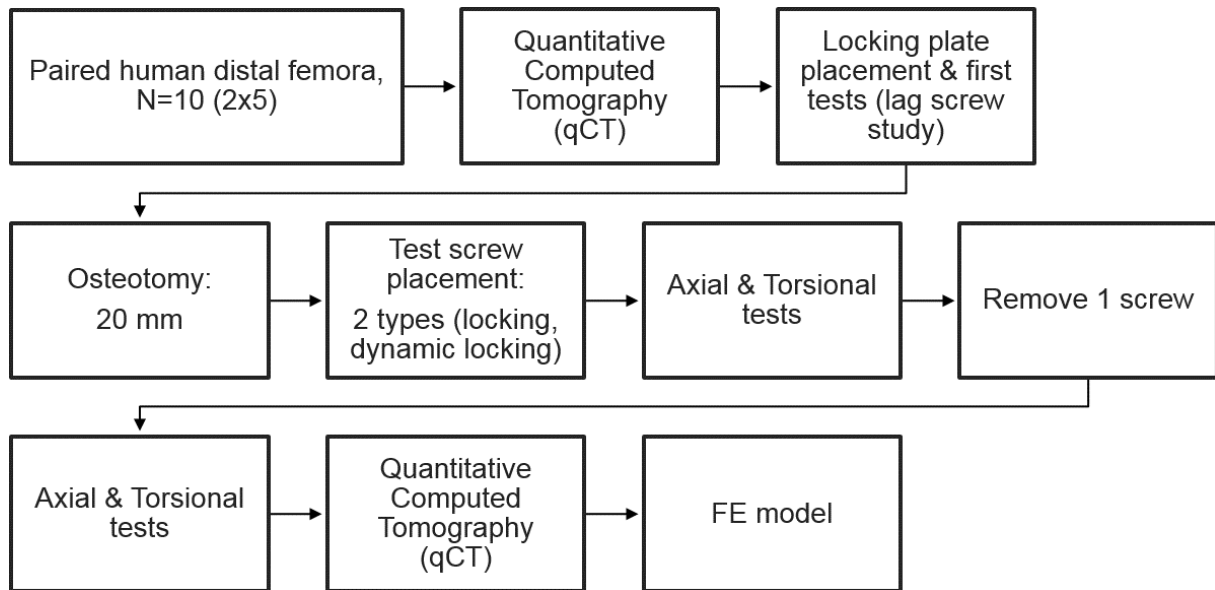


Figure 2-27: Overview of the testing procedure.

2.2.9.1. *In vitro* tests

Specimen preparation

Paired, fresh frozen human distal femora of 1 male, and 4 female donors with an average age at death of 71, and a standard deviation of 9 years, were chosen. Left and right distal femora were each assigned to different screw type test groups to avoid any bias caused by bone morphology. Specimens were derived from the local anatomy department and all donors gave informed consent prior to death. All preparations and tests were performed at the local department of trauma surgery at Innsbruck, Austria. After explantation, the distal femora were cleaned from surrounding soft tissues mechanically and stored at -30 °C. To exclude bone pathologies and to determine bone mineral density, the bone specimens were subjected to quantitative Computed Tomography (qCT) scans (LightSpeed VCT 16, GE Healthcare, Milwaukee, USA). Prior to testing, the bones were thawed overnight at 6 °C and prepared at room temperature just before testing started.

Implant placement

As described previously (Märdian et al., 2015b), prior to testing, a 9-hole locking plate (LCP-DF, Synthes, Oberdorf, Switzerland) was placed relative to the intact bone according to the manufacturer's recommended surgical technique. Drill guides were used for each screw to ensure the correct pre-

determined direction. All screws were placed bi-cortically. The distal part of the plate was fitted with all possible conventional locking screws (n=7), identical for all bones. Distal femur condyles were embedded in poly-methyl-methacrylate (PMMA, Technovit 3040, Heraeus Kulzer, Wehrheim, Germany) within conically shaped cuboid molds with the epicondyles orientated parallel to the bottom of these molds. Modelling clay (Carl Weible, Schorndorf, Germany) was wrapped around the distal and proximal tip of the plate and the surrounding bone to allow free plate movements and prevent fixation of the plate caused by the PMMA (Figure 2-28). The femur was adjusted, so that the loading axis of the testing machine was aligned through the center of the condyles for proximal embedding. The bones were then repeatedly, quasi-statically tested with loads up to 1000 N or 4 Nm for a different research question (Märdian et al., 2015b). Afterwards, the two femur fragments (proximal and distal) were distracted and new screws were applied within completely fresh holes within the bone which were offset by 20 mm to the existing screw holes from the previous tests. Various configurations bridging the distraction defect model with the 9-hole locking plate and 7 conventional locking screws (LS) in the distal plate holes were created:

- Group 1a) 4 LS in holes 3, 5, 7, and 9 proximally;
- Group 1b) same configuration as 1a) but LS from hole 3 was removed;
- Group 2a) 4 dynamic locking screws (DLS) in holes 3, 5, 7, and 9 proximally;
- Group 2b) same configuration as 2a) but DLS from hole 3 was removed.



Figure 2-28: From left to right: Example of validation specimen of a distal femur with lateral plate fixation, embedded in PMMA (with purple clay to allow free plate motion). CT-images were obtained after testing to verify integrity and for modelling. Fluoroscopic images show the screw position (number of holes 9,7,5,3 marked) and the empty screw holes of previous testing.

Loading

All tests were performed with a servo-hydraulic material testing machine (MTS, 858 Mini Bionix II, Eden Prairie, MN, USA). The different locking plate constructs were loaded in axial (bending-) compression up to 500 N/1000 N, at a rate of 30 mm/min with 2s dwell time using a ball-joint proximally and a hinged joint distally. With modification to the boundary conditions with a X-Y-table distally, the locking plate constructs were also loaded in torsion (Figure 2-29) up to 2 Nm/4 Nm at a rate of 30 deg/min, alternately in internal and external direction with 2s dwell time at nominal load. Each construct was tested for 5 cycles with 10 N controlled preload. The angle of rotation (deg), applied torque (Nm) for the rotational testing as well as the axial displacement (mm) and applied compression (N) were recorded by the testing machine (TestStar, MTS; sampling rate 20 Hz). Global bony integrity was verified for all specimens with additional qCT scans after the biomechanical tests.

Evaluation of *in vitro* tests

Digital image correlation was performed using the system PONTOS 5 M (GOM, Braunschweig, Germany). Using marker points on the bone surface (Figure 2-29), 3D motion of the relative interfragmentary movement (IFM) was detected with the optical measurement system PONTOS 5 M (GOM, Braunschweig, Germany). For the synchronized load cycles with the testing machine, IFM was calculated between maximal and minimal load. The tracked points were assumed to be located on rigid bodies (distal and proximal bone fragment). The relative movement of single target point positions directly under the plate lateral, and opposite at the medial side were calculated based on the movement of the PONTOS measured point movements. There were more than three measurement points per fragment available, so the rigid body movements of the two bone fragments were calculated through minimization of the error of target point movement relative to all measured point movements using the generalized reduced gradient method (GRG solver) in Microsoft Excel (MS Excel 2010, Microsoft, Redmond, Washington, USA).



Figure 2-29: Left: Test rig set-up for torsional testing.

Right: PONTOS camera image with marker points for evaluation of relative movement.

2.2.9.2. *In silico models*

The *in vitro* tests were modeled using specimen-specific imaging data. Two loading scenarios each and two different screw placements (working length variations) for each of the two tested screw types (Group 1 and 2) for the five bones yields a total of 40 models. IFM at the cis-cortex underneath the plate (lateral) and at the trans-cortex opposite the plate (medial) were assessed for the reduced loads (500 N / 2 Nm) and the full loads (1000 N/ 4 Nm). Quasi-static, 3D models were calculated using the solver Abaqus Standard v.6.12-2 (Dassault Systèmes, Vélizy-Villacoublay, France).

Geometry

Quantitative Computed Tomography (qCT) data of the tested bones was employed to create specimen-specific finite element models. Geometry of the proximal and distal fragment of the femur and their positions were derived from qCT through semi-automatic segmentation based on image intensity and manual inspection with Amira v5.3 (Visage Imaging, San Diego, USA). Plate geometry was derived from CAD data and its specimen-specific individual plate position was assessed through surface registration using the qCT data sets using Amira v5.3 (Visage Imaging, San Diego, USA). Geometry was meshed with tetrahedral elements using Amira and imported to Abaqus/CAE v.6.12 (Dassault Systèmes, Vélizy-Villacoublay, France) to change the mesh to second-order tetrahedral elements (C3D10). Total element

Material mapping

Reduced material mapping

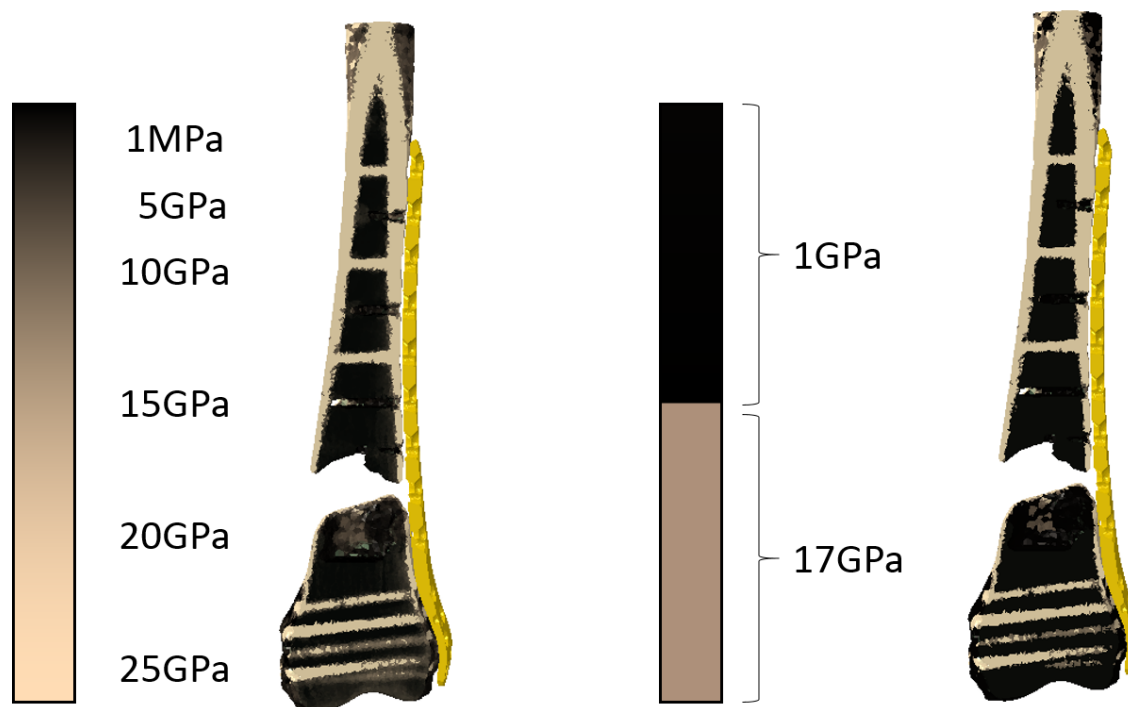


Figure 2-30: Material mapping of validation specimens with a multi-bin approach (left) and a reduced mapping two-bin approach similar to simplified models that were published before (Speirs et al., 2007).

numbers for the bone vary based on bone size from 382,328 to 534,827 elements. The plate element numbers vary between 59,636 and 60,952 elements.

Material properties

A material mapping approach (inhomogeneous material distribution) with isotropic behavior (of each single element) was realized using the local image intensity from qCT and a linear regression with a mineral density phantom ($R^2 \geq 0.996$, $p < 0.001$) according to an established method (Schileo et al., 2008; Schileo et al., 2007; Taddei et al., 2007). For calculation of element-specific Young's modulus, a regression of local stiffness to modulus from the femoral neck including cortical and trabecular bone was chosen (Morgan et al., 2003) with the addition of a cut-off at 1MPa and 25GPa to attenuate for imaging artefacts caused by the plate and screws. Minimal material modulus was set at 1MPa for all elements below the cut-off and maximal bone modulus was set at 25GPa. Poisson's ratio was set at 0.3 for all materials. Materials were grouped into bins (of size 50MPa) according to a range of modulus resulting in more than 500 material definitions. To test sensitivity to material modeling, material definitions were reduced to two materials with modulus of 1GPa for material of density below 1.28 g/cm³ (corresponding to 10GPa in the material mapping model) and modulus of 17GPa above the density threshold (Figure 2-30). Plate material was defined with an isotropic modulus of 112GPa.

Screw models

Screws were modeled as structural beam elements. Material properties of the screws were set as isotropic modulus of 112GPa for LS and 224GPa for DLS. Structural properties were calculated from screw geometry and validated using *in vitro* experiments from the literature (Döbele et al., 2014). Dynamic screws were modeled using tube-to-tube contact with ITT31 elements and a Slide Line. The interfaces between screws and plate or bone were implemented using beam multi-point-constraints (Wieding et al., 2012).

Boundary conditions

Local coordinate systems were constructed from screw landmarks on the PMMA mold from qCT pointing from left to right in X-direction, to proximal in Y-direction and from posterior to anterior in Z-direction. This coordinate system conforms to the PONTOS coordinate system (Döbele et al., 2012b, Döbele et al., 2014). The load application point was created as a reference point within each individual local coordinate system at a defined distance above the distal femur where the load would have been applied through the test rig. At this point, either 1000N in local negative Y-direction, or both 10N in negative Y-direction and 4 Nm around the local Y-axis (both directions consecutively) were applied as the different loading scenarios. At the bottom, two reference points anterior and posterior of the bone were created where support through the bearing occurred in the *in vitro* tests. At these points, displacement constraints were applied: for axial (bending-) compression, both points were pinned; for torsion only the X-Z-movement was permitted. The reference point at the top was coupled to the top of the proximal fragment through a kinematic constraint. The reference points at the bottom of the bone were coupled to the anterior and posterior surface of the distal bone fragment via a kinematic constraint. Contact between the plate and the bone surface was implemented to avoid penetration.

Statistical analysis

IBM SPSS Statistics v.18.0 (IBM Corporation, Armonk, New York, United States) was used to compute Pearson's correlations of *in vitro* experimental results and *in silico* model results.

2.2.9.3. Validation results

The regression of *in silico* IFM (medial and lateral) and experimental IFM (at corresponding points) yield significant linear relations, with a coefficient of 0.8321 and 0.313 offset ($R^2 = 0.9417$) for the axial loading and the material mapping model and a coefficient of 0.8364 and 0.334 offset ($R^2 = 0.9403$) for the axial loading and the reduced material mapping model (Figure 2-31). The model IFM tended to be lower than the measured IFM, so the FE models tend to be stiffer than the real specimens in axial loading. For torsion loading, there are significant linear relations as well, with a coefficient of 1.0562 and -0.1571 offset ($R^2 = 0.8222$) for the material mapping model and a coefficient of 1.0653 and -0.1598 offset ($R^2 = 0.8288$) for the reduced material mapping model (Figure 2-31). The model IFM tended to be slightly higher than the measured IFM in torsion, so the FE models tend to be more flexible than the measured stiffness. The error of the regression was higher in torsion than for axial loading. The combined regression model has a coefficient of 0.9086 and 0.08 offset ($R^2 = 0.9003$) for the material mapping model and a coefficient of 0.9163 and 0.087 offset ($R^2 = 0.9011$) for the reduced material mapping model (Figure 2-32).

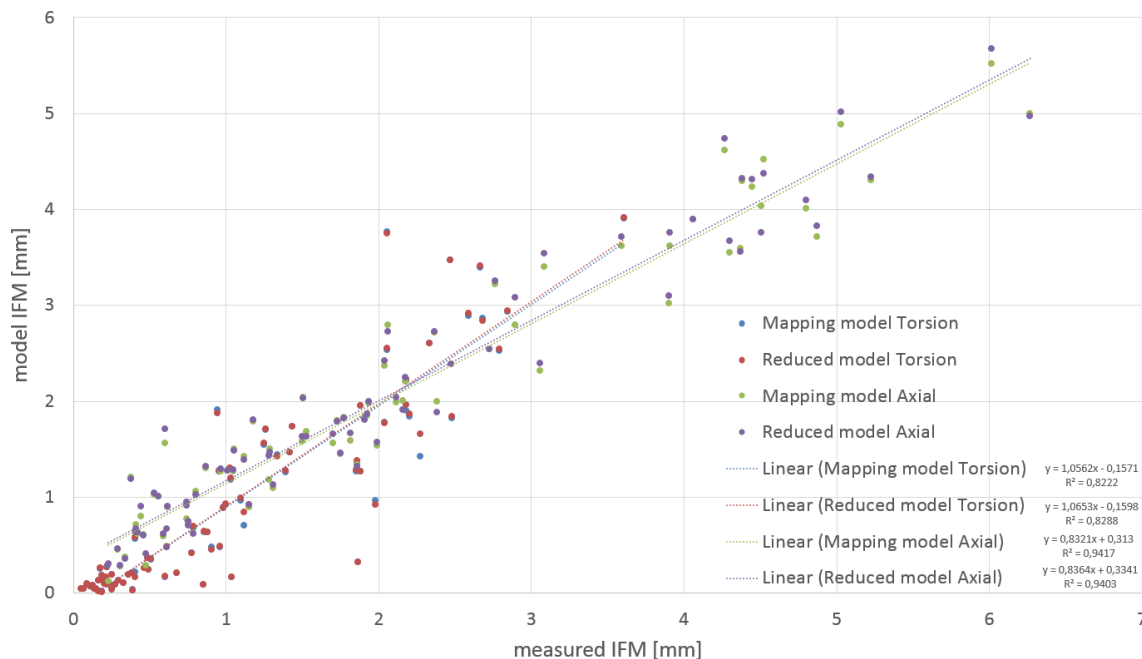


Figure 2-31: Validation regression results of IFM separated according to load and material mapping model.

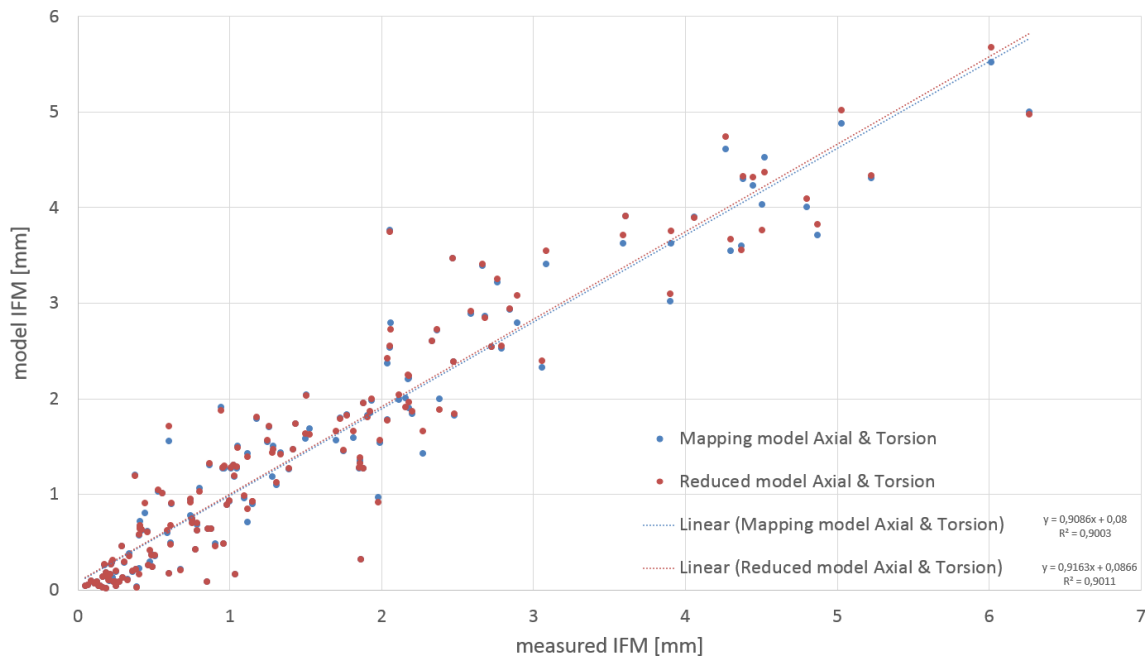


Figure 2-32: Pooled validation regression results of IFM for the two material mapping models.

2.2.9.4. Discussion of validation results

We set out to show the validity of *in silico* distal femur fixation models in relation to corresponding *in vitro* experiments. With adequate models, we may commit our research to the mechano-biological effects of fixation such as different screws or plate working lengths or even further optimize fixation 3D-stiffness through implant design changes.

Although numerous computational models have been published, limited knowledge exists on how to employ screw placement and elastic screws as powerful tools in fracture care. One may attribute this in part to incomplete understanding due to insufficient parameter identification and validation which leads to arbitrary modelling approaches that do not assess sensitivity to different aspects of their models and thus lead to widely dispersed results that are valid only for special cases and are often unrealistic for (physiologically) altered input parameters.

The 3D-registration exhibits possible errors caused by PONTOS camera measurement errors and the neglected deformation of the surface. The accuracy of the PONTOS system is around $5\mu\text{m}$ (Döbele et al., 2012b). Our own brief validation using a calibrated micrometer gauge confirmed that within the calibration plane, the relative movement of marker points can be tracked with a mean accuracy $<3\mu\text{m}$. However, the deviations perpendicular to the main calibration plane can be much higher for a

single marker point (<75 μm). However, with our approach, individual measurement errors will have little influence due to the high number of tracking points.

What showed to be much more influential was the definition of the reference points and their matching between the measurement and the model. Our initial matching was based on point identification in the CT images and yielded weaker results⁴² than more dedicated identification using multiple points and axes with a 3D-check. Furthermore, we planned to fit the model geometry into the PONTOS-data of point clouds, which was unsuccessful due to the uncharacteristic shape of the femur (especially in rotation, but also in z-translation direction). Thus, we identified the position of reference points of the PONTOS data visually using the camera data. This might introduce another error, as exact point correspondence between measurement and model cannot be guaranteed (Figure 2-33). For future investigation, to acquire the position of relevant points on physical specimens and match them to the corresponding FE model, high-precision digitisers have been suggested (Cristofolini et al., 2010). Characteristic device geometry with markers attached to the samples might serve the same purpose. *In vitro* validation of FE models of long bones may be further improved with more accurate determination of evaluation and force application points (Juszczak et al., 2010).

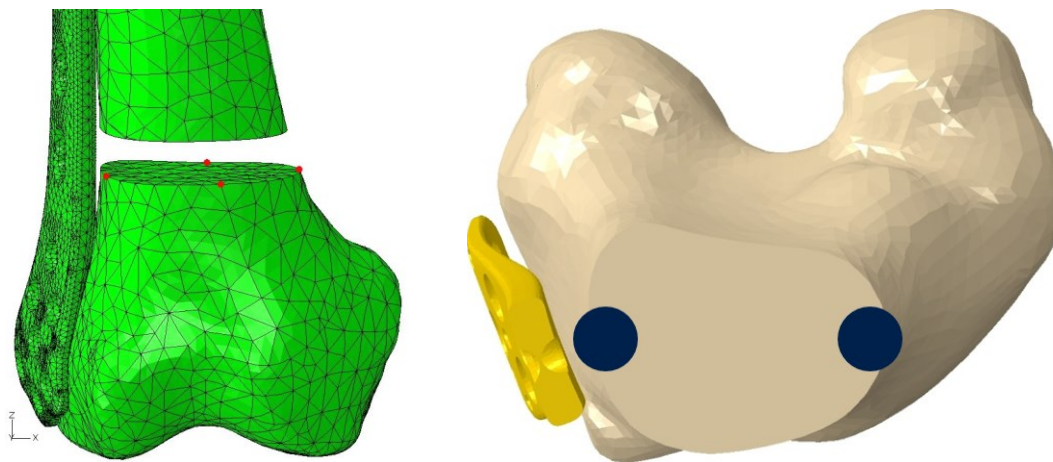


Figure 2-33: Interfragmentary movement between defined nodes (left in red, corresponding pairs at the proximal segment not shown) were evaluated for the medial and lateral point pairs. When identifying the corresponding the locations, an error might be introduced by mismatched point correspondence (right, error in location symbolised by the extension of the blue circles).

⁴²Heyland, M., Duda, G. N., Schaser, K.-D., Schmoelz, W. & Märdian, S. (2016). Finite element (FE) analysis of locking plate fixation is a valid method for predicting interfragmentary movement. Podium presentation. 22nd Congress of the European Society of Biomechanics (ESB 2016), July 10-13 2016, Lyon. <https://esbiomech.org/conference/index.php/congress/lyon2016/paper/view/714>

The considered load cases do not represent physiological loading sets, but they may represent components of physiological loading, both in quality and quantity⁴³. Although the chosen boundary constraints are artificial, they do not substantially limit the normal deformation as suggested by Grant et al. (2015), Grant (2012). For other boundary conditions, it may become necessary to measure the local reaction forces (Juszczak et al., 2010). For physiological loading, either the boundary conditions according to Speirs et al. (2007) have shown empirical evidence, especially if the load case is well-balanced, or the method of inertia relief can be used if for instance a moving reference frame from gait analysis can be used for additional validation (Heyland et al., 2015b).

The comparison of the material mapping binned into more than 400 material groups or just 2 revealed hardly any difference. Thus, for future studies, we can reliably investigate interfragmentary movement with just a two-material model of bone under the assumption that we can identify the dense areas reliably. Homogenization of bone tissue with only one or two resultant bone material properties may correctly predict IFM, but may lead to a great difference in local load transfer (at interfaces) and may lead to false conclusions if the gap tissue and its local tissue strain is considered. The material mapping approach can more accurately represent the local differences in material properties and thus may lead to a more realistic tissue strain distribution.

Our analyses show that mechanical conditions within locking plate constructs can be strongly influenced through screw type and location. Further analyses have to be performed in order to formulate general recommendations of fixation choice and specific screw placement for various fracture types in order to control fixation stiffness reliably in mechano-biological fracture care. Some mostly empirical evidence can be gathered from the literature though.

⁴³ The loading that is derived from musculoskeletal models has shown its worth when unexpected failure cases of the dynamic locking screw occurred and were investigated in 2013 by Synthes. https://www.mdco.gov.hk/textonly/english/safety/recalls/recalls_20130614b.html, last accessed 3 December 2018.

A biomechanical lab-test was prepared in order to provoke such screw failures to understand the mechanism of failure. The loading in silico of the screws was evaluated and could not find a particular reason why the screws could have failed. The full story and how those innovative screws failed in an innovative way is described in section 2.2.9.5, confirming our loading model which was not included in the laboratory validation tests.

2.2.9.5. *Direct clinical relevance of the loading model: Estimation of screw failure loads*

Problem

In some cases, breakage on the lower edge of the flexible pins of the dynamic locking screws (DLS) were observed:

"Medical Device Safety Alert: Synthes Dynamic Locking Screw Stardrive

Medical device manufacturer, Synthes, has issued a medical device safety alert concerning certain lots of the Dynamic Locking Screw Stardrive \varnothing 3.7mm, self-tapping, Cobalt-chrome alloy (CoCrMo), sterile [length 22mm to 70mm] and \varnothing 5.0 mm, self-tapping, Cobalt-chrome alloy (CoCrMo), sterile [length 32mm to 90mm].

The manufacturer received several complaints and investigations showed breakage at the bottom of the pin of the Dynamic Locking Screw (DLS). The breakages are recognized during planned implant removal of the whole construct after successful healing. There is the potential that the breakage of a DLS may result in a mal-union or non-union requiring additional medical intervention. In a worst case scenario there is the potential for permanent impairment to occur in the presence of a mal-union or non-union.

Serious injury described as soft tissue damage/irritation and prolonged surgical procedures have been reported as a result of DLS breakage. However, no known events of permanent impairment have been reported due to the breakage of a DLS.

According to the local supplier, the affected products were distributed in Hong Kong.

If you are in possession of the affected products, please contact your supplier for necessary actions.

Posted on 14 June 2013"

Source: http://www.mdco.gov.hk/textonly/english/safety/recalls/recalls_20130614b.html, last accessed 3 December 2018.

This was discovered after successful healing when removing the screws. Why and how those failures occurred was unclear. The observed mode of failure were high-cycle fatigue breaks, so that a rather medium-sized, cyclical load was assumed.

Methodology

In finite element models, forces at the screw head of the DLS were extracted. First, we suspected a large plate-bone distance as the most proximal screws were affected. However, this did not prove to be reasonable in the observed cases. Assuming full load bearing (normal walking with low qualitative variance of forces over the gait cycle, so a time point at 10% of the high load gait cycle was chosen) with an surgically optimal placed plate, the following cases were simulated to capture the maximum forces on the DLS in the healing process:

- 1) distal osteotomy without fragment contact (initial situation post-op),
- 2) as 1) but with medial obstruction (local callus formation modeled with a flexible spring element),
- 3) as 2) but with 3 stiffer spring elements (increase in callus formation, stiffening),
- 4) intact bone with osteosynthesis plate (condition shortly before implant removal).

Various typical screw configurations (various screw assignments) in the titanium plate were simulated, starting from the distal hole to the proximal:

- A) 3,8,9 (proximally tightly packed);
- B) 3,4,9 (tightly packed distally) and
- C) 3,6,9 (evenly distributed).

Results

The load on the femoral head is essentially a combination of axial force, a-p and m-l shear force. The intact femur (without plate fixation) bends slightly under load, medially under pressure (compressed) and laterally under tension (Figure 2-34).

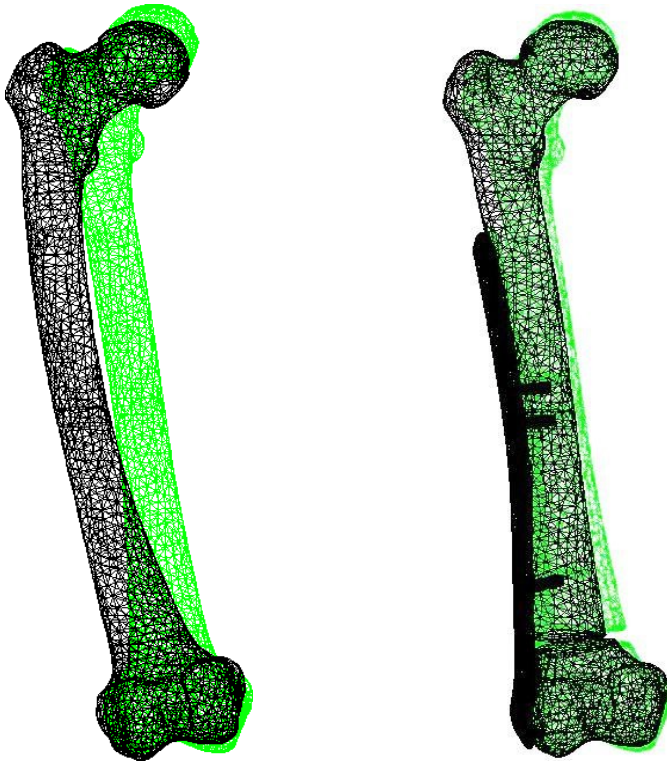


Figure 2-34: Overview of bone and plate deformation. Left: Intact bone deformation under physiological loading scaled 5 times for clarity. The isthmus of the bone is deflected laterally. Right: Locking plate fracture fixation under physiological loading showing splinting of the bone and less lateral displacement of the shaft, 3 times scaled.

In the case of plate fixation, the loading situation is significantly more complex (e.g., proximally DLS, distally locking screws, metaphyseal osteotomy). Lateral stiffening by the plate results in reduced bending of the proximal fragment caused by axial force, but relative movement of the fragments, not only axially but also orthogonally thereto (shearing motion and tilting of the upper fragment, torsional motion). The extent of axial relative movement, the extent of shear and torsion depends on the screw configuration.

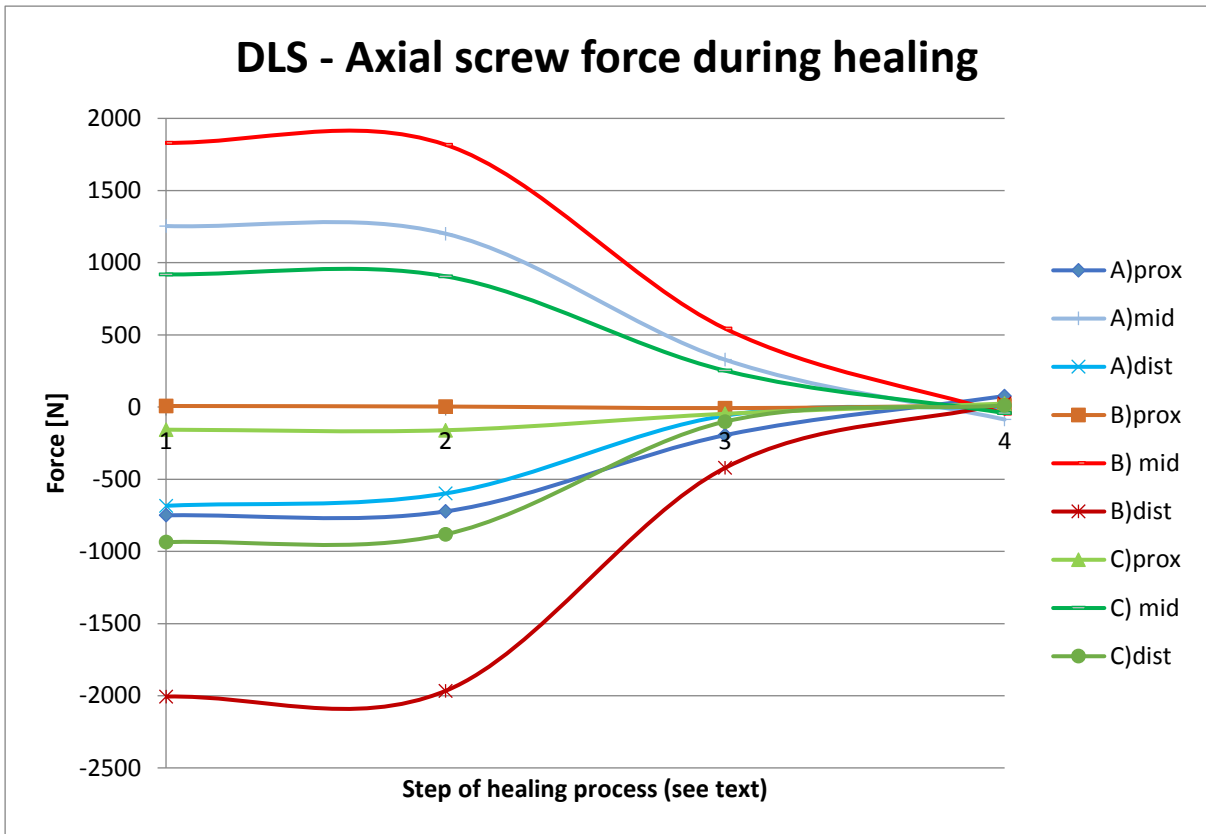


Figure 2-35: Axial force at the DLS head (longitudinal screw direction) for different screw configuration over the healing course.

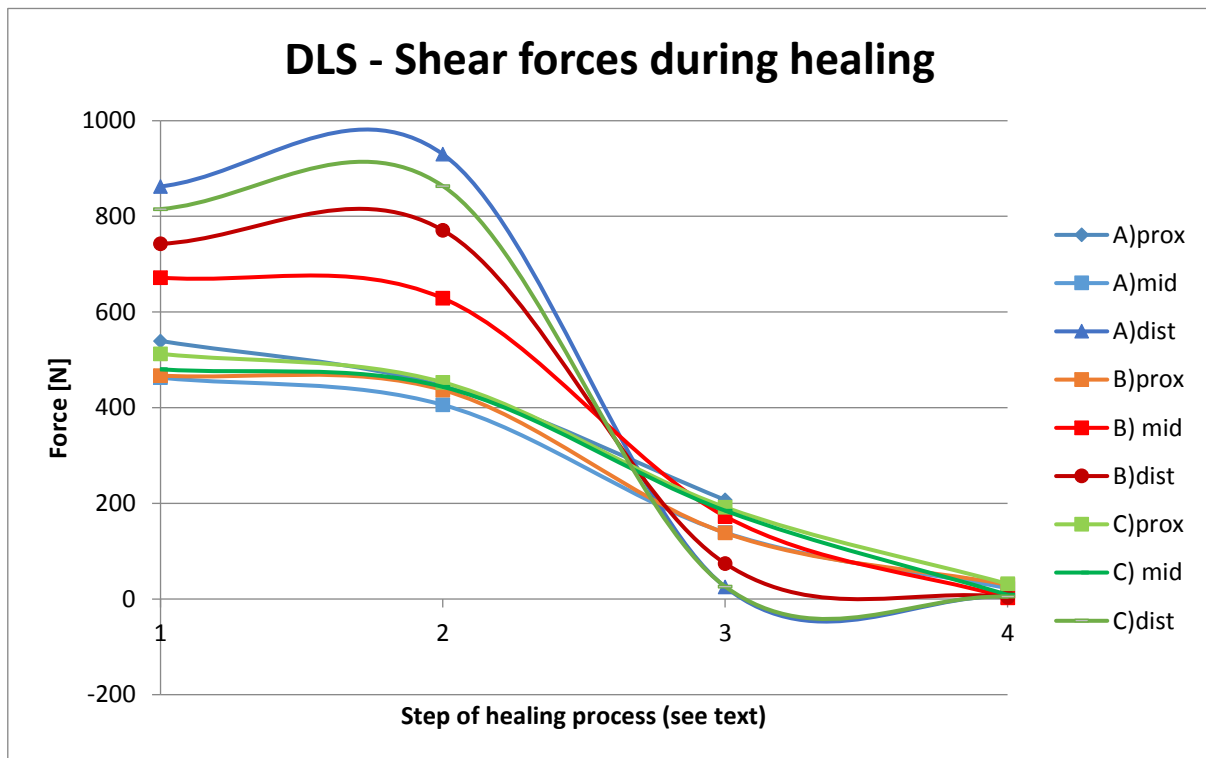


Figure 2-36: Resulting shear force at the DLS head (longitudinal screw direction) for different screw configuration over the healing course.

Initially, a distally high screw density (configuration B) leads, according to our model, to the highest loads of the mid- and distal screw head (Figure 2-35). This is accompanied with considerable shear force (Figure 2-36).

However, if the first two steps are passed quickly, a slow healing in step 3 lasts much longer. Let us focus on step 3 of healing. The highest shear forces are seen in the proximal screws and in the middle screws. Focusing on those screws with high shear force, especially, a proximally high screw density (configuration A) leads, according to our model, to a comparably high tensile load of the proximal screw (a few hundred Newton over almost the entire healing process). In the other configurations it is not the proximal screw that has the highest traction.

Table 5: Axial and shear forces during healing at the dynamic locking screw head. Highest traction forces (negative value) and highest shear forces during healing step 3 (presence of callus) are marked bold/red.

AXIAL FORCE [N]	HEALING STEP				SHEAR FORCE [N]	HEALING STEP			
CONFIGURATION	1	2	3	4	CONFIGURATION	1	2	3	4
A) PROX 9	-750	-723	-195	76	A) PROX 9	540	445	207	33
A) MID 8	1254	1201	328	-86	A) MID 8	463	406	139	23
A) DIST 3	-684	-598	-59	3	A) DIST 3	863	930	25	5
B) PROX 9	7	4	-7	11	B) PROX 9	467	437	138	30
B) MID 4	1830	1818	544	-46	B) MID 4	672	629	173	3
B) DIST 3	-2006	-1966	-421	25	B) DIST 3	743	771	74	4
C) PROX 9	-157	-160	-46	24	C) PROX 9	513	453	192	32
C) MID 6	919	906	252	-41	C) MID 6	480	444	185	9
C) DIST 3	-936	-881	-101	12	C) DIST 3	815	863	26	5

Discussion

Our results, combined with the failure pattern of the DLS pins, suggest that the DLS pins may be very sensitive to axial traction and may fail to function due to fatigue in conjunction with medium-high shear forces. This is supported by the fact that, in the case of the proximally packed plate the axial tension and shear on the proximal screw head remain high during healing at a few hundred Newtons with many load cycles (walking of the patient). This could explain why the proximal screw breaks, but not the distal screw, which could initially be loaded much more heavily.

Our model with optimally placed plate cannot satisfactorily recapitulate the failure of the DLS pins for distally packed screw mounts, because in this case the tensile load of the proximal screw is very low.

An altered distance of the plate to the bone can significantly affect the loading of the plate and also the screws. Even with slight inclination of the plate or specific bone shape, different distances of the individual screws to the bone would result. In the case of large distances, this tends to increase the

load on the plate and, in the case of small distances, it is more likely to increase the load on the screws. With very small distances of the screw heads to the bone, a significant increase in the axial screw force can result, with other bone shape and / or plate inclination the remaining screws can also be relieved from loading. We were able to understand this in our in silico experiments and the x-ray images of the pin breaks also underline the presence of this influencing factor. In initial calculations, the local reduction of the plate-bone distance with decreasing distance leads to an increase of the axial force on the screw. This may account for some 10N here, thus increasing the axial load on the proximal screw, while e.g. at the same time the axial load of the distal screw could be lowered. This could explain the failure of evenly distributed screw mounts, but even so, in the case of a distally packed configuration, it would be more likely to break the distal DLS.

In the concrete cases of failure, the configurations have uniformly distributed screw assignments. In one case, both external screws (proximal and distal) are also broken, which would be consistent with this explanatory approach. In a second case, the second proximal screw is broken, which could be explained by a small distance to the bone.

A single influence parameter cannot explain the present failures of the DLS pins in our model. We believe that the fractures of the DLS pins are probably a combination of homogeneous to proximally high screw density in the plate in combination with (locally close to the broken screws) small distances between plate and bone, and possibly also particularly strong muscle strength (higher internal forces, through e.g. limited motor control, or high physical activity). We would expect initially somewhat reduced loads, and after successful and advanced callus stiffening at full load bearing with very many load cycles, the screw head axial forces of at least -100 to more than -200N with simultaneous shear forces around 200N at the proximal screws might be the cause of failure. By contrast, the middle screw would experience comparable shear and higher axial loads, but just compression and no traction. Although the distal screw experiences almost similar tensile loads, there are significantly lower shear loads.

So, based on our assumptions, no particularly obvious overloading was observed. We concluded that there must be a high fatigue stress followed by a singular high stress, but failure could (also with damage accumulation) only be expected if stresses would have been elevated further, through a notch or another factor. Pure loading conditions in vivo were not enough for this failure. We speculated that especially the most proximal DLS might be susceptible to a notch at the pin under tension and shear of a couple of hundred Newton with many loading cycles (damage accumulation) and then breakage through singular overload. In 2014, with a model of a single DLS, we could identify two different possible failure modes of the DLS (Figure 2-37).

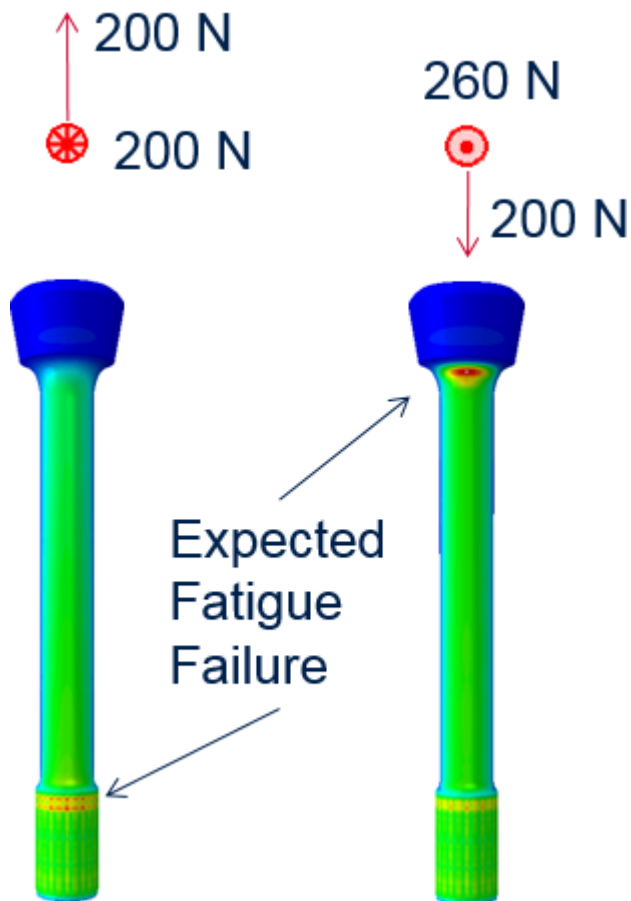


Figure 2-37: Realistic fatigue failure mechanisms (damage pattern) of a dynamic locking screw during physiological loading. Excessive Von Mises stress is shown in red (quantitative legend purposefully not shown, no systematic evaluation of operational strength using S-N or Wöhler curves). Left: About 200N of shear and traction load, adjacent to an extended fitting at the pin, can lead to a fatigue failure and breakage at the end of the pin. Right: Fatigue failure at the screw head under shear and compressive load would require compressive forces higher than 260N with 200N shear.

Chapter 3. Mechanical constraints of the biology of healing

Identification of mechano-biologically relevant parameters for mechano-therapy

What is known to be biomechanically important for fracture healing?

Relevant publications:

Heyland, M. (2018). Brief Commentary on Mechano-Biological Fixation. Journal of investigative surgery: the official journal of the Academy of Surgical Research, 1-2.

Heyland, M., Duda, G. N., Märdian, S., Schütz, M., & Windolf, M. (2017). Stahl oder Titan bei der Osteosynthese. Der Unfallchirurg, 120(2), 103-109.

Heyland, M., Duda, G. N., Schwabe, P. & Märdian, S. (2016). Influence of fracture angle on interfragmentary movement. Podium presentation. 22nd Congress of the European Society of Biomechanics (ESB 2016), July 10-13 2015, Lyon.

<https://esbiomech.org/conference/index.php/congress/lyon2016/paper/view/719>

Märdian, S., Schaser, K. D., Duda, G. N., & Heyland, M. (2015). Working length of locking plates determines interfragmentary movement in distal femur fractures under physiological loading. Clinical biomechanics (Bristol, Avon), 30(4), 391-6.

Heyland, M., Duda, G. N., Haas, N. P., Trepczynski, A., Döbele, S., Höntzsch, D., Schaser, K.-D. & Märdian, S. (2015). Semi-rigid screws provide an auxiliary option to plate working length to control interfragmentary movement in locking plate fixation at the distal femur. Injury, 46, S24-S32.

Heyland, M., Duda, G. N., Schmoelz, W., Schaser, K.-D. & Märdian, S. (2015). Mechanical behavior of different locking plate fracture fixation options at the distal femur. Poster. 21st Congress of the European Society of Biomechanics (ESB 2015), July 5-8 2015, Prague.

Heyland, M., Duda, G. N., Trepczynski, A., Dudé, S., Weber, A., Schaser, K.-D. & Märdian, S. (2014). Winkelstabile Plattenfixation für typische Problemfrakturen des distalen Femur: in silico Analyse verschiedener Schraubenauswahl und -belegungen um die Osteosynthesesteifigkeit zu kontrollieren. Podium presentation. Deutscher Kongress für Orthopädie und Unfallchirurgie (DKOU 2014) October 28-31 2014, Berlin. <http://www.egms.de/static/en/meetings/dkou2014/14dkou073.shtml>

Heyland, M., Duda, G. N., Trepczynski, A., Schaser, K.-D. & Märdian, S. (2014). Locking plate osteosynthesis fixation configurations for typical problem fractures of the distal femur: in silico analysis of different simulated screw selection and placement to control osteosynthesis stiffness. Poster. 7th World Congress of Biomechanics (WCB 2014), July 6-11 2014, Boston.

3.1. Literature overview

The 10 most common and important risk factors for fracture non-union in long bone fractures based on the hierarchy of level of evidence are (Santolini et al., 2015):

1. an open method of fracture reduction,
2. open fracture,
3. presence of post-surgical fracture gap,
4. smoking,
5. infection,
6. wedge or comminuted types of fracture,
7. high degree of initial fracture displacement,
8. lack of adequate mechanical stability provided by the implant used,
9. fracture location in the poor zone of vascularity of the affected bone,
10. and the presence of the fracture in the tibia.

The most important factors seem to be associated to vascularity and angiogenesis, as it could be argued that all parameters change perfusion or are influenced by blood supply. Sufficient blood supply forms a basic prerequisite for regenerative processes as those processes are carried out by living cells. However, out of those 10 risk parameters, number 3, 6, 7, and 8 are related to mechanical conditions and number 10 has a mechanical component. It seems to be of utmost importance to first secure the blood supply of the fracture area through adapted and suitable fixation that minimizes iatrogenic trauma and secondly achieve mechanical stiffness within a certain window adapted to the fracture configuration.

3.1.1. Mechanical parameters that influence fracture healing

The evolution of fracture fixation and the overall clinical patient care respecting and preserving the biological capabilities is ongoing at a high speed with significant reductions in complications (Matthews et al., 2008). However, the understanding of the physiological response to injury, bone biology, biomechanics and implants is mostly gained through empirical studies. Standardization of procedures and implants are needed to make group interventions comparable, treatment economically reasonable and easily performable even by inexperienced surgeons especially in times of precision medicine (patient-specific care). Patients are different. There is an impressive diversity in the

armamentarium of fracture instrumentation with the main implants being screws, intramedullary nails, and plates. Each type of fixation implant bears its specific advantages and disadvantages. Predictive factors of fracture non-union for different fixation construct characteristics have been reported: for instance plate length and screw placement, cortical contact, as well as implant material (Rodriguez et al., 2014). However, are such risk factors meaningful without further context? As an example, the mechanical working principles of locking plates are different from conventional plate-screw systems (Egol et al., 2004). This means that recommendations for optimal screw placement for conventional plates are not readily transferable to locking plate constructs (Fitzpatrick et al., 2009). The conventional compression plates that have been widely used since the 1960s are successful for the most part, but there are some limitations such as the need for adequate bone quality and extensive soft-tissue stripping (Kubiak et al., 2006). The introduction of locked plating (Frigg et al., 2001, Frigg, 2001, Frigg, 2003) has added a versatile option for trauma fixation especially for improved strength in osteoporotic bone (Fulkerson et al., 2006). For almost a decade, locked bridge plating has been equated with secondary fracture healing due to the higher elastic deformation of locking plate constructs compared with conventional plating systems (Marti et al., 2001). It was advocated that on the one hand, locked plates may increasingly be indicated for indirect fracture reduction, diaphyseal/metaphyseal fractures in osteoporotic bone, bridging severely comminuted fractures, and the plating of fractures where anatomical constraints prevent plating on the tension side of the bone (Egol et al., 2004). While on the other hand, conventional plates may continue to be the fixation method of choice for peri-articular fractures which demand perfect anatomical reduction, and certain types of non-unions which require increased stability (with the clinical meaning of limited relative motion within the elastic range) for union (Egol et al., 2004). However, other advantages of locking plates such as the minimally invasive plate osteosynthesis (MIPO) have also led to the use of a locking plate in conjunction with lag screws for primary fracture healing (Horn et al., 2011). The fracture fixation options are manifold, and they are increasing, while a comprehensive algorithm for fixation choice is lacking. The literature offers many studies on different influential mechanical parameters of fixation on construct stiffness and fracture healing outcome.

3.2. Screw configuration

As screw configuration influences construct stiffness, it directly affects the fracture healing process (Nasr et al., 2013). With eccentric cantilever beam bending, it has to be considered that the bone cis-cortex (close to plate) moves less than the far trans-cortex meaning apparent stiffness can vary greatly depending how it has been derived (MacLeod et al., 2012a, Grant et al., 2015). Additionally, screw

configuration influences the amount and distribution of stress within the fixation implant (Ibrahim, 2010). Older bone with thinner cortex and compromised material properties produce higher stresses for the same screw configuration (MacLeod et al., 2012a).

3.2.1. Screw number

More than three locking screws on either side of a long bone fracture only marginally increase axial stiffness and more than four screws only slightly increase torsional rigidity (Stoffel et al., 2003, Freeman et al., 2010, Heyland et al., 2015a, Lee et al., 2014, Meeuwis et al., 2017). Our investigations with a distal femur fracture model revealed a stiffness increase from 3 to 4 locking screws in the shaft to be less than 5%, while using 5 instead of 4 dynamic locking screws, the stiffness increase was below 10% (Heyland et al., 2015a). For humeral fractures, even two locking screws per fragment might be sufficient to achieve proper fixation (Hak et al., 2010a). Adding more screws may alleviate stress concentrations around screw holes for certain screw configurations; however, care should be taken not to overly increase the construct stiffness and thus create excessive plate stress (MacLeod et al., 2012a). Thus, for long bone fractures of the lower extremities, usually four bicortical screws per (shaft) fragment are used while for the upper extremities usually three bicortical screws are used. Collinge et al. (2011) recommend for distal femur fracture four well-spaced bicortical screws in the shaft segment and five or more screws (mostly locking) in the small condylar/articular segment. For peri-prosthetic femoral fractures ten cortices of fixation have been recommended (Wood et al., 2011). Stiffness of locking plate fixation is not dominated by screw number, but plate working length, i.e. the placement of the screws closest to the fracture (Hsu et al., 2018a).

3.2.2. Screw placement

The plate working length, determined by the placement of screws close to the fracture, is the most important determinant of construct apparent stiffness, plate and screw stress (MacLeod et al., 2012a, Stoffel et al., 2003, Märdian et al., 2015a, Heyland et al., 2015a, Wee et al., 2017, Wittkowske et al., 2017, Lee et al., 2014), and fatigue life for titanium plates (Hoffmeier et al., 2011). A medium plate working length (leaving 1-2 screw holes unfitted over the fracture) reduces the construct stiffness moderately but can increase the implants lifespan remarkably. Plate working length has a greater effect than plate material or plate thickness within the current clinical range to modulate construct stiffness and IFM (Moazen et al., 2011).

Additionally with few screws, for instance two, the position of an additional middle screw on either side of the fracture significantly influenced axial stiffness; the closer this screw was positioned towards the fracture site, the stiffer the construct for axial compression while torsional rigidity was unaffected by the position of the middle screw (Stoffel et al., 2003). With a higher screw number, altering the spacing of the middle screws has only minor effect on the stiffness of the construct (Krishnakanth, 2012, Heyland et al., 2015a). Screw placement and plate properties substantially affect regions of high strain around the screw-bone interface in locked plating (MacLeod et al., 2016c) where osteoporotic bone was found to be more sensitive to screw spacing (the distance between first two screws closest to the fracture site, on either side of the fracture) than healthy bone. The need for sufficient screw spacing has been voiced before, mostly indirectly through recommendations of filling fewer than half of the plate holes with screws (Gautier and Sommer, 2003). MacLeod et al. (2016c) suggests a screw spacing of one or two empty screw holes to reduce strain. Certain plate-screw densities defined as the ratio of holes in the plate to the number of screws applied across the plate have been suggested before, e.g. 0.5 (Wood et al., 2011).

In bridge plating technique, the highest stress concentrations for the screws generally occur close to the fracture gap (Stoffel et al., 2003). The stress in the screw can be reduced if the fragments can be adapted for contact between the fracture surfaces during dynamic loading and increasing the bridging length can further reduce the stress on the plate and the screws and hence improve fatigue failure (Stoffel et al., 2003).

Different studies evaluated that diverging locking screw configurations are leading to: firstly, bone failure rather than screw pull-out, higher stiffness, and lower failure load in an osteoporotic bone model (Bekler et al., 2008), and secondly, reduced pull-out static and cyclical loading capacity (Kääb et al., 2004, Wähnert et al., 2011). Using locked fixation in minimally invasive plate osteosynthesis (MIPO), such divergent screw placements are avoided with a target aiming device (Kääb et al., 2004). Screw arrangement can be further altered with a staggered screw hole pattern in the plate. Such a bi-planar screw configuration improves the torsional strength of diaphyseal plate fixation relative to a planar configuration in both osteoporotic and normal bone so that with bi-planar fixation, unicortical screws provide the same fixation strength as bicortical screws in non-osteoporotic bone (Denard et al., 2011).

A crossed non-locking screw configuration ("fencing") as an alternative to locking screw fixation was suggested leading to comparable fatigue performance as angular stable (locked) plating, but larger motion in the fracture gap (Windolf et al., 2010).

Proximal screw pullout or loosening has been described as the most common form of implant failure of unicortical locking screws. A potential explanation for this is the eccentric screw placement in context with plate placement that creates a proximal offset, i.e. the screw is not placed through the center of bone and the bone purchase is insufficient (Beingessner et al., 2011, Kolb et al., 2008, Kregor et al., 2004, Schandelmaier et al., 2001).

When using locking screws in the epiphysis, excessive screw length should not be risked, because it is generally poorly tolerated (Cronier et al., 2010).

3.2.3. Screw type

Locking screw constructs show consistent, robust results in a large window of different bone qualities (Miller and Goswami, 2007, Uhl et al., 2008) and are more suited to be used for situations with compromised bone quality such as for osteoporotic patients (Zehnder et al., 2009, MacLeod et al., 2014). However, for bone mineral densities above approximately 0.55 g/cm^3 conventional non-locking screws exhibit higher load to failure in torsion (Miller and Goswami, 2007). Locking screws may show more difficulties with removal due to cold welding or screw head stripping (Suzuki et al., 2010) especially with unicortical screws. A potential reason may lie in plate bending and adaptive bone response due to the local straining.

Although bicortical screw fixation may increase torsional stiffness in a locking plate construct, torsional stiffness is likely more dependent on plate metal composition than on screw length with given plate thickness of clinical plates (Beingessner et al., 2011). Unicortical locked constructs are prone to screw pullout while bicortical locked constructs are prone to screw breakage at the plate-bone interface (Denard et al., 2011). Unicortical screw type affects the mechanical stiffness of the femur to a higher extent than the material type of the locking plate, especially shear interfragmentary strain (Reina-Romo et al., 2014).

Using unlocked (conventional, lag) and locked screws within one construct requires to place the unlocked screws first (lag before locking). The screw type close to the fracture determines torsional stiffness and maximum axial force to failure (Cui et al., 2014). However, a hybrid screw configuration with locking screws close to the fracture does not seem to lead to inferior construct strength compared to an all-locking configuration (Goswami et al., 2011, Dalstrom et al., 2012, Doornink et al., 2010, Freeman et al., 2010, Patel, 2008). When using locking screws for the less dense distal metaphysis, plate strain in lateral plating of supracondylar femur fractures can be decreased by using four non-

locking screws proximal to a comminuted fracture (McLachlin et al., 2017). An option for simple fracture patterns is the use of a lag screw perpendicular to the fracture line through both fragments to achieve fragment compression using a locking plate for additional bridging resulting in higher stiffness and especially reduced shear deformation (Märdian et al., 2015b). As a higher plate working length increases the compliance of the construct, which can be beneficial in comminuted fractures, excessive construct flexibility should be avoided in transverse or short oblique fractures. This may strongly increase interfragmentary strains, especially the shear component (McLachlin et al., 2017). In such simple fractures, conventional (plate) screws can be inserted through stab incisions near the fracture lines to improve local stability and construct stiffness.

Far cortical locking screws, dynamic locking screws or near cortical slots may reduce stiffness and generate more homogeneous interfragmentary motion, and retain the strength of a locked plating construct (Doornink et al., 2011, Freude et al., 2014, Gardner et al., 2010, Heyland et al., 2015a, Krishnakanth, 2012, Nanavati and Walker, 2014, Sellei et al., 2011). The effect of such semi-rigid screws is more pronounced for stiffer plate materials such as steel versus titanium (Döbele et al., 2010, Heyland et al., 2017).

Also, in intramedullary nail fixation, the use of locking screws may lead to large increase in stiffness (Epari et al., 2007) which has been associated with a modulation of the fracture healing result.

3.3. Plate/nail configuration & material

The bending behavior of an osteosynthesis depends on the cross-section, the geometrical form, and the modulus of elasticity as well as on the plate/nail position relative to the bending direction of the composite system (Gautier et al., 2000).

3.3.1. Plate placement and length

Collinge et al. (2011) grouped potential errors of plate placement at the distal femur into six cases:

- 1) too valgus,
- 2) too anterior,
- 3) too rotated,

4) too distal,

5) too flexed or extended,

6) or too far off bone.

Plate length is not a consistent determinant of construct stiffness or plate stress but rather the screw placement within the plate is more limited with a shorter plate: A sufficient plate length should be chosen to enable adapted proper screw placement. For proper plate-screw densities (defined as the ratio of holes in the plate to the number of screws applied across the plate) to be around 0.5 (Wood et al., 2011) this requires sufficient plate holes. Plate span width ratio defined as plate length to fracture length has been recommended to be larger than 3 for comminuted and about 8-10 for simple fractures (Wood et al., 2011).

The plate-bone distance shows discrepancy between the condylar area and the diaphysis and minimally invasive plate placement can hardly be improved by computer-assisted navigation (Al-Ahaideb et al., 2009). Increasing the distance from the plate to the bone from 2 mm to 6 mm and a shorter plate resulted in a decreased axial stiffness and torsional rigidity, but the influence of a larger plate-bone distance was less marked for larger working lengths (Stoffel et al., 2003). Significantly increased plastic deformation during cyclical compression and lower construct failure loads were measured when a locking plate was applied 5 mm from the bone versus flush or 2 mm from the bone (Ahmad et al., 2007).

Excessively long plates or placement (e.g. far anterior near the knee or too distal) can lead to painful encroachment of the plate onto the muscles (e.g. the extensor mechanism at the knee) or to intra-articular screw placement into the intercondylar notch or patellofemoral joint (Collinge et al., 2011). Especially placement of the distal end of locking plates in inappropriate positions may result in high risk of rotational mismatch and plate impingement (Song et al., 2012). This also often led to problems with proximal unicortical screw failure (Khalafi et al., 2006, Beingsner et al., 2011, Kolb et al., 2008, Kregor et al., 2004, Schandelmaier et al., 2001, Button et al., 2004).

Epiphyseal plate placement may conflict with pre-determined screw direction as there are potential problems such as joint penetration, conflict between screws, extra-articular conflict. Variable angle (poly-axial) locking screws were proposed notably for the use for the ankle and the foot (Cronier et al., 2010).

For peri-prosthetic fractures, sufficient plate length that overlaps the prosthesis by 6 cm is mandatory to avoid excessive plate stress (Strauss et al., 2008, Walcher et al., 2016).

3.3.2. Plate/nail material

Stainless steel plates are far more durable (more loading cycles to failure with higher load) than identical shaped grade-2 titanium plates *in vitro* (Hoffmeier et al., 2011), but steel plates lead to significantly stiffer constructs (Heyland et al., 2017). When exchanging titanium for steel in an experimental locking plate fixation, especially axial stiffness (-44%) is reduced compared to shear stiffness (-29% to -34%), (Krishnakanth, 2012), p.77.

Plate modulus and initial loading conditions have to be jointly considered together to achieve the most appropriate plate modulus (Kim et al., 2012). Furthermore, plate modulus and fracture angle have to be adjusted for optimal tissue stimulation with the need of a comparably flexible plate for more transverse fracture line and a little stiffer plate for an oblique fracture line (Kim et al., 2011). Additionally, plate material has to be considered together with bridge span (plate working length) as increasing bridge span preferentially increases shear at the fracture (Elkins et al., 2016, Märdian et al., 2015a, Krishnakanth, 2012). Excessive shear was found to be inversely associated with callus formation (Elkins et al., 2016).

Plate material was found to have a high contribution regarding the overall factor of safety (Arnone et al., 2013). However, the precise role of plate material has been controversially discussed. Plate material can influence the interfragmentary strain for 3 mm gap fractures, but not 1 mm gap fractures (Miramini et al., 2015b). Within a FE model, the change in the material property of the plate and screws from titanium to steel increased the bending stiffness by 30% and torsional stiffness by 73%, which was accompanied with a reduction in fracture movement of 37% in bending and 34% in torsion on the lateral side of the bone (Moazen et al., 2011). Stainless steel as plate material was identified as a risk factor of non-union in distal femoral fractures treated with locked plating (Rodriguez et al., 2014). Combined plate design and material variables have a highly significant influence on the risk of non-union because they determine the construct rigidity which affects the tissue stimulation (Rodriguez et al., 2016). Elkins et al. (2016) compared constructs that maximized longitudinal motion relative to transverse motion in FE analysis (titanium constructs with a bridge span of less than 80mm) to other cases in a series and found that titanium constructs with a short bridge span (less than 80 mm) demonstrated significantly greater callus at twelve and twenty-four weeks. These results suggest that plate material is associated with callus formation with greater affinity than increasing bridge span (Elkins et al., 2016, Lujan et al., 2010) as larger plate working length will increase shear over-proportionally compared to axial IFM. As titanium plates lead to more callus formation compared to

steel plates (Henderson et al., 2011b), the titanium plate shares more load with the regenerative tissue at an earlier time point (MacLeod et al., 2015).

The addition of a medial locking plate plus bone graft next to a lateral plate to treat distal femoral non-unions has achieved a high union rate (Holzman et al., 2016). Such a double plating technique creates very stiff constructs (Jazrawi et al., 2000) with comparable to or even higher stiffness than locked intramedullary nailing (Kaspar et al., 2005) and can only be recommend for small remaining gaps ≤ 2 or 3mm depending on location and attendant circumstances (Lim et al., 2016, Drosos et al., 2006). Thus, full reduction or a scaffold or graft should be indicated for substantial bone defects and such stiff fixation conditions.

The positive effect of low-modulus plates compared to high-modulus plates on the healing performance reduced when blood vessel growth at the fracture site was considered (Son et al., 2014a), which suggests that stiffer fixation bears the advantage of increased angiogenesis.

Further opportunities may lay in alternative materials with different material properties such as CF/PEEK composites with highly anisotropic mechanical properties (Mehboob and Chang, 2014, Son and Chang, 2013). Carbon fiber–reinforced polymer (PEEK) plates show encouraging short-term results in the treatment of distal femur fractures with a comparable nonunion, reoperation, and hardware failure rate to those treated with stainless steel plates (Mitchell et al., 2018).

3.3.3. Nail / plate design

Implant design goes hand in hand with implant application and positioning. The issue of canal reaming for nails at the expense of biological capacity for higher achievable mechanical stability has been discussed: Unreamed nailing resulted in extremely low axial and high shear strain for distal tibia shaft fractures without additional fragment contact and was regarded as critical from a biomechanical perspective (Duda et al., 2001). As an intramedullary nail may lead to high shear movements (Nourisa and Rouhi, 2016), locked nails were introduced that should improve especially the torsional stiffness (Kaspar et al., 2005, Höntzsch et al., 2014). A novel nail with controlled axial interfragmentary motion may also provide axial interfragmentary motion while retaining high torsional stiffness (Dailey et al., 2012, Dailey et al., 2013).

Hemi-helical plate design has been suggested (Fernández, 2002)⁴⁴ wrapping around the bone and altering the screw planes, thus increasing pull-out strength and changing displacement and local regenerative tissue stimulation (Krishna et al., 2008). Recent evaluations have shown that stiffness components (in bending) can be modulated through combinations of straight and helical plate (Perren et al., 2018), which could enable the surgeon to specifically adapt the fixation stiffness to the needs of the fracture configuration and patient characteristics.

Plate stiffness, ultimate and fatigue strength *in vitro* are determined by plate design (Otto et al., 2009, Schmidt et al., 2013). This does not necessarily translate directly to the whole construct strength *in vivo* as described for different plate materials. For example, locking buttons (plugs, screw head inserts) that close unused plate holes have shown increased fatigue life of locking plates *in vitro* (Tompkins et al., 2013, Bellapianta et al., 2011), but this has not been shown to lead to fewer complications *in vivo*. On the contrary, locked plating with screws in all its holes shows increased failure rates due to delayed healing or non-union (Kääb et al., 2006, Tan and Balogh, 2009).

Plate failure should usually occur through the (dynamic compression unit) screw hole as this forms a local notch with stress increase (Stoffel et al., 2003). Such fatigue failure can be expedited through corrosion (Thapa et al., 2015).

It has been reported that there is a consistent pattern of mismatch at the proximal part of the 11-hole LCP-DF for Asian patients, which may cause screw misplacement or valgus malalignment at the fracture site (Hwang et al., 2012).

Changes to plate/nail design such as (compliant) inserts or elongated holes to allow for relative motion of the (locking) screws within the plate/nail (similar to the concept of relative motion of the screws relative to the bone) have been suggested, and those concepts are currently being tested and validated (Bottlang et al., 2016, Henschel et al., 2017, Dailey et al., 2013, Dailey et al., 2012, Mitković et al., 2017,

⁴⁴ Compare: Regazzoni, Perren, Fernández (2018): MIO helical plate: technically easy, improving biology and mechanics of “double plating”,
<https://icuc.net/multimedia/Newsletters/Newsletter%2034/Newsletter%2034%20-%20MIO%20helical%20plate%20double%20plating.pdf>, last accessed 23 November 2018.

Perren, Regazzoni, Lenz and Fernández (2018): Double locking plate, surgical trauma and construct stiffness improved by the helical plate,
<https://icuc.net/multimedia/Newsletters/Newsletter%2035/Newsletter%2035%20-%20Double%20locking%20plate.pdf>, last accessed 23 November 2018.

Mitkovic et al., 2012, Augat and von Rden, 2018, Madey et al., 2017, Giannoudis and Giannoudis, 2017).

3.4. Fracture configuration

Many treatment algorithms do not take into account the configuration of the fracture, neither in terms of the type (transverse, oblique or spiral), angle or detailed degree of comminution (Etchels, 2014).

3.4.1. Fracture location

Mehboob and Chang (2018) simulated the healing process of a fractured femoral shaft with different intramedullary nail materials and found that for a transverse fracture angle there is a dependency of callus stiffness increase on fracture location but not for the consistently well-healing oblique fracture: Mid-shaft fractures healed best and transverse distal femur shaft fractures healed worst. This underlines the clinical perception that distal femur fractures represent a critical fracture type and locked plating has been suggested as a treatment option rather than the otherwise favored intramedullary nailing. However, when differentiating for fracture angle, nailing might be an option for oblique distal femur fractures, which remains to be shown.

3.4.2. Fracture size, reduction and cortical contact

Fracture height, or relative position of the fracture within the bone influences the mechanical lever arms and thus the mechanical boundary conditions (Etchels, 2014).

Fracture reduction to restore angles and offset have been repeatedly associated with outcome (Krischak et al., 2003, Horn et al., 2011, Collinge et al., 2011) as it was also shown to affect implant failure risk (Nassiri et al., 2013).

For a large fracture gap, a low stiffness scaffold to support bone growth and an appropriate modulus bone plate should be used to achieve sufficient mechanical stability to bear the body weight (Mehboob and Chang, 2015). Large fracture gaps need to be fixated with higher stiffness in order to yield successful healing results (Mehboob et al., 2013). If a large gap (e.g. 6 mm) is fixated excessively stiff (e.g. using a position screw and locking plate), healing will fail, but dynamization with a more flexible

fixation (e.g. removal of position screw) may rescue this and lead to healing with bridging callus formation (Oh et al., 2011).

3.4.3. Fracture angle

Etchels (2014) showed a non-linear relationship between axial stiffness and fracture angle without any regenerative tissue, with the construct to be stiffest with an approximately transverse fracture. As fracture angle increased, in either direction, the axial component of construct stiffness decreased. The maximum decrease in axial stiffness, caused by the 70 degree proximal lateral to distal medial fracture, was 8% compared to the transverse fracture (Etchels, 2014). The opening and closing of the gap was considered, but not the differences in local tissue strain as no regenerative tissue was implemented. It was concluded that sufficiently large differences occurred across the fracture angle cases to suggest that the fracture angle may have a noticeable effect on the biomechanics of a potential treatment. With simple estimations a better treatment recommendation could be made using a rule of thumb that considered both the angle and direction of the fracture than by using either the fracture bridge distance (working length) or fracture angle alone (Etchels, 2014).

Plate modulus and fracture angle have to be adjusted for optimal tissue stimulation with the need of a comparably flexible plate for more transverse fracture line and a little stiffer plate for an oblique fracture line (Kim et al., 2011). Fracture angle determines healing efficiency together with load and fixation stiffness as those factors control tissue deformation (Son and Chang, 2013). For realistic loads, oblique-fracture-line plate fixation is less effective than transverse plate fixation.

Only for a few special locations and fracture types such as intracapsular proximal femoral and bicondylar proximal tibial fractures (Pätzold et al., 2017) a classification according to fracture angle that directly translates to a certain fixation has been empirically established. However, the mechano-biologic approach of improved local mechanical conditions that would require estimation of tissue strain with different fracture angle and fixation has not been translated into comprehensive surgical treatment algorithms. As a result, without detailed understanding, for example the Pauwels classification for the proximal femur has been repeatedly challenged in recent decades (Parker and Dynan, 1998, Wang et al., 2016), but the reason it might not appear to be valid in all cases simply originates from improved fracture fixation that may eliminate the correlation of shear and fracture angle. There is evidence for this based on a successful non-union therapy (Marti et al., 1989): a Pauwels abduction wedge osteotomy changes a more vertical fracture line to two more horizontal ones, providing compression at the site of non-union.

It could be shown that (unlocked) intramedullary nailing causes more shear (transverse motion) and less axial (longitudinal movement) compared to plate fixation (Nourisa and Rouhi, 2016). Considering the fracture angle, this would potentially mean beneficial tissue strain for more transverse fractures with a locking plate and for more oblique/spiral fractures with an intramedullary nail.

3.5. Loading conditions

3.5.1. Orientation

In a numerical study, Etchels (2014) changed the direction of the load through the femoral head, relative to the hip, knee and ankle for five different adduction angles (calculated relative to the femoral shaft). As adduction angle had a statistically significant effect on the axial stiffness and fracture movement, the direction of load and configuration stiffness component influence might be changed by adduction angle. However, the resulting joint force vector of the average peak load does not change remarkably in its orientation during routine activities at the lower limb (Bergmann et al., 2010) with less than 15 or 10 degrees of variation in the sagittal and frontal plane respectively during the following activities: walking, stairs climbing, stair descending, standing up, sitting down, standing on one leg, knee bend. However, the variation in the transverse plane can be more than 40 degrees, stressing the need for an especially high stiffness component in this direction. The need to further explore individual clinical situations (especially in terms of loading) and the influence on fracture healing caused by different directions of forces has been voiced before (Ganse et al., 2016).

3.5.2. Magnitude

In simulations of fracture healing with intramedullary rods of different stiffness, the initial magnitude of loading has been shown to be the most sensitive factor of healing performance (Son et al., 2014b). There is a need for sufficient load for tissue stimulation to occur. Such loads can be achieved with early weight-bearing. It might be objected that high peak loading during walking might be associated with mal-alignment as it occurs without fixation, but for instance with proper fixation after tibial plateau fracture, peak loading during walking is not associated with fracture fragment migration (Thewlis et al., 2015).

Currently, surgeons usually recommend 6-8 weeks of so-called partial load bearing after fracture. The patient should try to achieve an external equivalent ground reaction force of 15-25kg using crutches for instance. There is no evidence that this robustly reduces the internal joint loads with the same magnitude as the ground reaction forces are reduced compared to normal walking. Measured internal hip joint forces could be reduced by 17% on average when using crutches, although individual values range up to 53% (Damm et al., 2013). There should be general agreement that the effect of so-called “partial weight bearing” in patients is only mild and often overestimated. Restricted external load does not markedly unload the defect zone during normal activities and there is no direct relationship between interfragmentary movement magnitudes and ground reaction forces in patients (Duda et al., 2003a). Admittedly, through precise muscular control, bone deformation might be controlled actively using crutches in trained, healthy volunteers with intact bone (Ganse et al., 2016) where bone deformation consistently correlates with ground reaction forces. The use of crutches or other methods for partial load bearing might help to avoid extremely high loads (through additional mindfulness and balance aid) rather than strikingly reduce the peak forces (Duda et al., 2003a), especially in patients that suffer pain and muscle weakness. However, when the surgical restriction of external load leads to reduced activity or inactivity, the tissue stimulation might be reduced.

Chapter 4. Biomechanical explanations and clinical examples

Sampling of clinical effects with regard or disregard to mechano-therapy

Can fixation stiffness be controlled and are there examples of successful or unsuccessful mechano-therapy from the clinics?

Relevant publications:

Märdian, S., Seemann, R., Schmidt-Bleek, K., Heyland, M., Duda, G. (2019). [Biology and Biomechanics of Fracture Healing and Fracture Fixation] *Biologie und Biomechanik der Frakturheilung und Osteosynthese. Orthopädie und Unfallchirurgie* up2date, 2-2019, 1-21 [In Print].

Rußow, G., Heyland, M., Märdian, S., Duda, G. N. (2019) [Bone fracture healing and clinical loading stability] *Knochenbruchheilung und klinische Belastungsstabilität, OP-JOURNAL* 2019; 35: 1–9 [In Print].

Heyland, M. (2018). Role of Screw Location, Screw Type and Plate Working Length! Podium presentation. Basic Science Focus Forum at the 2018 Annual Meeting of the Orthopaedic Trauma Association (OTA 2018), October 17-20, 2018, Kissimmee (Orlando area), Florida. <https://ota.org/sites/files/2018-08/PRF12%20%280807%29%20OTA%20AM18%20BSFF%20ONLINE%20Pgm.pdf>

Heyland, M. (2018). Brief Commentary on Mechano-Biological Fixation. *Journal of investigative surgery: the official journal of the Academy of Surgical Research*, 1-2.

Heyland, M., Duda, G. N., Märdian, S., Schütz, M., & Windolf, M. (2017). Stahl oder Titan bei der Osteosynthese. *Der Unfallchirurg*, 120(2), 103-109.

Heyland, M., Duda, G. N., Schwabe, P. & Märdian, S. (2016). Influence of fracture angle on interfragmentary movement. Podium presentation. 22nd Congress of the European Society of Biomechanics (ESB 2016), July 10-13 2015, Lyon. <https://esbiomech.org/conference/index.php/congress/lyon2016/paper/view/719>

Märdian, S., Schaser, K. D., Duda, G. N., & Heyland, M. (2015). Working length of locking plates determines interfragmentary movement in distal femur fractures under physiological loading. *Clinical biomechanics* (Bristol, Avon), 30(4), 391-6.

Heyland, M., Duda, G. N., Haas, N. P., Trepczynski, A., Döbele, S., Höntzsch, D., Schaser, K.-D. & Märdian, S. (2015). Semi-rigid screws provide an auxiliary option to plate working length to control interfragmentary movement in locking plate fixation at the distal femur. *Injury*, 46, S24-S32.

Heyland, M., Duda, G. N., Schmoelz, W., Schaser, K.-D. & Märdian, S. (2015). Mechanical behavior of different locking plate fracture fixation options at the distal femur. Poster. 21st Congress of the European Society of Biomechanics (ESB 2015), July 5-8 2015, Prague.

Heyland, M., Duda, G. N., Trepczynski, A., Dudé, S., Weber, A., Schaser, K.-D. & Märdian, S. (2014). Winkelstabile Plattenfixation für typische Problemfrakturen des distalen Femur: in silico Analyse verschiedener Schraubenauswahl und -belegungen um die Osteosynthesesteifigkeit zu kontrollieren. Podium presentation. Deutscher Kongress für Orthopädie und Unfallchirurgie (DKOU 2014) October 28-31 2014, Berlin. <http://www.eqms.de/static/en/meetings/dkou2014/14dkou073.shtml>

Heyland, M., Duda, G. N., Trepczynski, A., Schaser, K.-D. & Märdian, S. (2014). Locking plate osteosynthesis fixation configurations for typical problem fractures of the distal femur: in silico analysis of different simulated screw selection and placement to control osteosynthesis stiffness. Poster. 7th World Congress of Biomechanics (WCB 2014), July 6-11 2014, Boston.

4.1. Fixation stiffness control and limits

Mechanical conditions are crucial for fracture healing (Klein et al., 2003). Conditions within the fracture zone can be characterized by the relative fragment motion. Inter-fragmentary movements (IFM) are determined by fracture geometry, fixation stiffness, and boundary conditions (load). There are two basic approaches to fracture care: absolute fixation for primary fracture healing (direct bridging of Haversian systems of fracture surfaces at close range) or relative fixation for secondary fracture healing via callus formation. However, surgeons may still select from numerous fixation configuration options without detailed information on the mechanical behavior. Modern concepts of fracture fixation, especially for comminuted fractures, aim at respecting the regenerative capacity by minimizing the iatrogenic trauma and producing beneficial strain as a mechanical stimulus onto the tissue. One promising approach are more flexible locking plate constructs which may explicitly allow for IFM in contrast to the conventional compression plates. Instead of screw-plate-substrate fastening with pre-stress, locked plating involves bolts (locking screws) which have proven to exhibit strength advantages in poor bone stock such as in osteoporotic patients (Doornink et al., 2010, Fitzpatrick et al., 2009, MacLeod et al., 2014, Tejwani and Guerado, 2011). Even with this type of fixation, sufficient interfragmentary compression according to the concept of absolute stiffness (limiting tissue deformation to enable primary fracture healing) can be achieved using an additional plate-independent lag screw and a protecting locking plate as internal fixators in simple fracture patterns (Chung et al., 2016, Wenger et al., 2017, Horn et al., 2011, Märdian et al., 2015b), possible to be applied in a minimally invasive fashion. However, more complex fractures such as comminuted fractures cannot be sufficiently reduced through indirect reduction. Small gaps remain and for those, moderate axial (out-of-fracture-plane) movements with minimal shear (in-fracture-plane) movements appear to improve fracture healing while excessive or insufficient movements delay fracture healing as shown for a transverse 3-mm-gap model in sheep (Epari et al., 2007). To allow for generally more IFM and especially more control of axial movements, semi-rigid screws have been introduced (Heyland et al., 2015a, Döbele et al., 2014, Freude et al., 2014, Freude et al., 2013, Döbele et al., 2012a, Döbele et al., 2010, Bottlang and Feist, 2011, Doornink et al., 2011).

Finite element (FE) models of such and other osteosynthesis systems have been created and are currently widely used to assess the principles of operation of different systems (Arnone et al., 2013, Duda et al., 2002, MacLeod et al., 2012a, Moazen et al., 2011, Nasr et al., 2013, Nassiri et al., 2012) to improve the mechano-biological stimulation of the tissue.

4.1.1. Systematic analysis of screw placements and plate working length

Although there are basic guidelines and tips for surgeons, such as using a longer plate, using many screws in the metaphysis and not all screw holes in the shaft (Gautier and Sommer, 2003, Collinge et al., 2011, Smith et al., 2008, Miller and Goswami, 2007, Cronier et al., 2010), the exact screw placement remains somewhat unclear (MacLeod and Pankaj, 2018, MacLeod and Pankaj, 2014). In many cases, many options for screw placement exist (Figure 4-1).

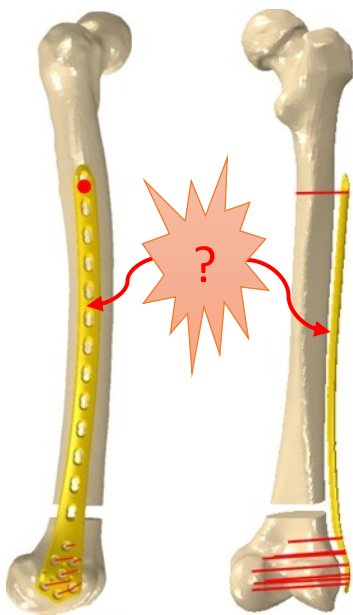


Figure 4-1: Schematic representation of a distal femur fracture with unclear options for screw placement.

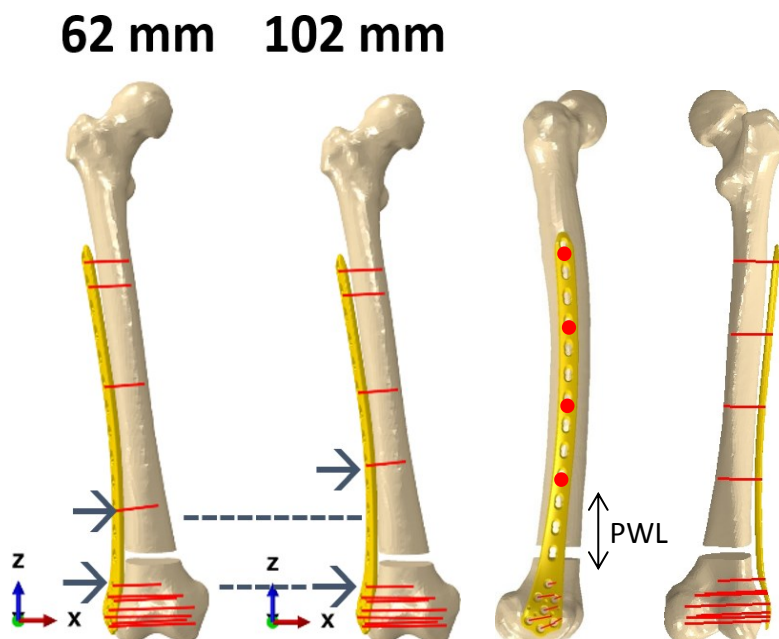


Figure 4-2: Plate working length (PWL: here 3 empty screw holes on the right) is the distance between the two screws closest to the fracture on either side of the fracture, here with 62 mm on the left and 102 mm in the center.

We conducted a systematic analysis of screw placement for a lateral locking plate next to a distal femur fracture (Märdian et al., 2015a)⁴⁵. For all variations, all screw options in the distal fragment of the plate were used (Collinge et al., 2011). At the shaft, the most proximal screw was set across all evaluations (Figure 4-1). Based on clinical experience and published recommendations (Lee et al., 2014, Stoffel et al., 2003), 32 different screw allocations with a total of 4 proximal screws were defined (Figure 4-3). The IFM was evaluated at the lateral (lIFM), medial (mIFM), anterior (aIFM) and posterior (pIFM) side of the fracture zone at defined nodes in both axial (out-of-fracture-plane) and orthogonal shear (in-fracture-plane) directions. Axial IFM and resultant shear IFM were compared within groups of different working lengths and across the groups. The four different working lengths of the plate construct were defined for group A [42 mm], group B [62 mm], group C [82 mm], and group D [102 mm].

IFM changes with fixation configuration

Different screw allocations have a similar qualitative effect on IFM with unequal gap closure, but screw placement significantly affects IFM ($p < 0.05$).

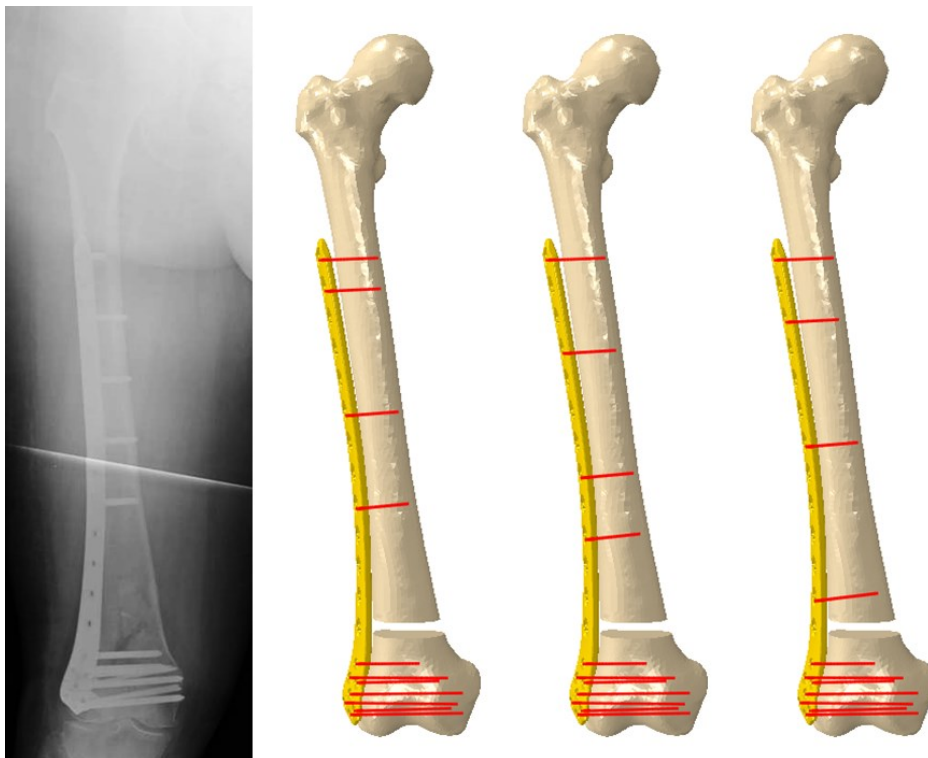


Figure 4-3: Different screw placements are possible when a long plate is chosen for a distal femur fracture. Left to right: Clinical example of distal femur fracture fixation in a X-ray control. Three screw placement variations.

⁴⁵Heyland, M., Duda, G. N., Trepczynski, A., Schaser, K.-D. & Märdian, S. (2014). Locking plate osteosynthesis fixation configurations for typical problem fractures of the distal femur: in silico analysis of different simulated screw selection and placement to control osteosynthesis stiffness. Poster. 7th World Congress of Biomechanics (WCB 2014), July 6-11 2014, Boston.

Plate working length

Especially placement of the first screw proximal the fracture (plate working length, Figure 4-2, Figure 4-4) has a significant effect in changing IFM both cis-cortical (laterally) and trans-cortical (medially), with longer plate working lengths leading to higher IFM ($p < 0.001$), (Figure 4-5).

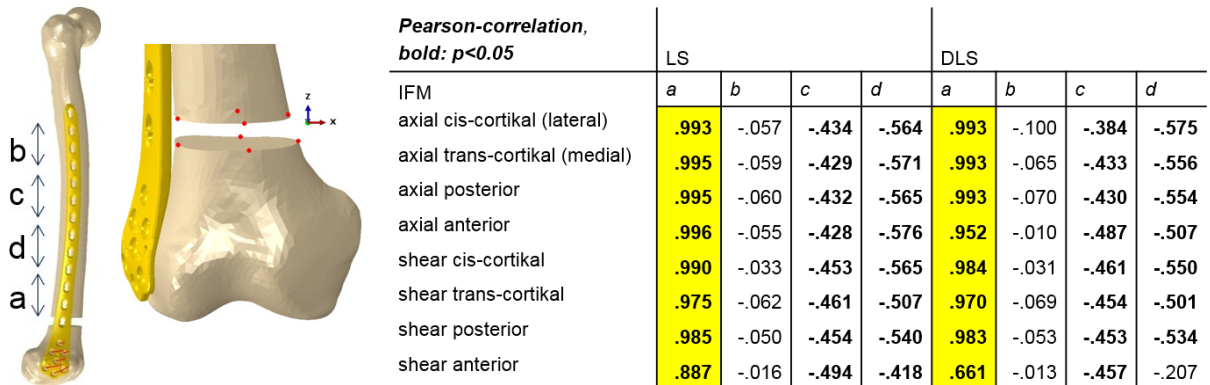


Figure 4-4: Pearson correlations (right table) of different screw distances within the plate (left, a-d) versus IFM components (axial=z, shear) at different positions (anterior, posterior, lateral, medial) as pointed out in the center for different screw types proximally (LS versus DLS). Note that plate working length (a) shows the strongest correlations.

Screw type

Replacing LS with DLS results in increase of cis-cortical (lateral) axial IFM ($p < 0.001$, between +8.4% and +28.1% for the tested screw placements) with minor changes to medial axial IFM ($> -1.1\%$). However, also resultant shear movements significantly increase with higher plate working length over the fracture ($p < 0.001$), as well as the quotient of shear/axial IFM increases for more empty screw holes above the fracture (Figure 4-6). DLS vs. LS may lead to significantly smaller quotients of shear/axial IFM directly under the plate for more than one empty screw hole above the fracture ($p \leq 0.003$), (Figure 4-6).

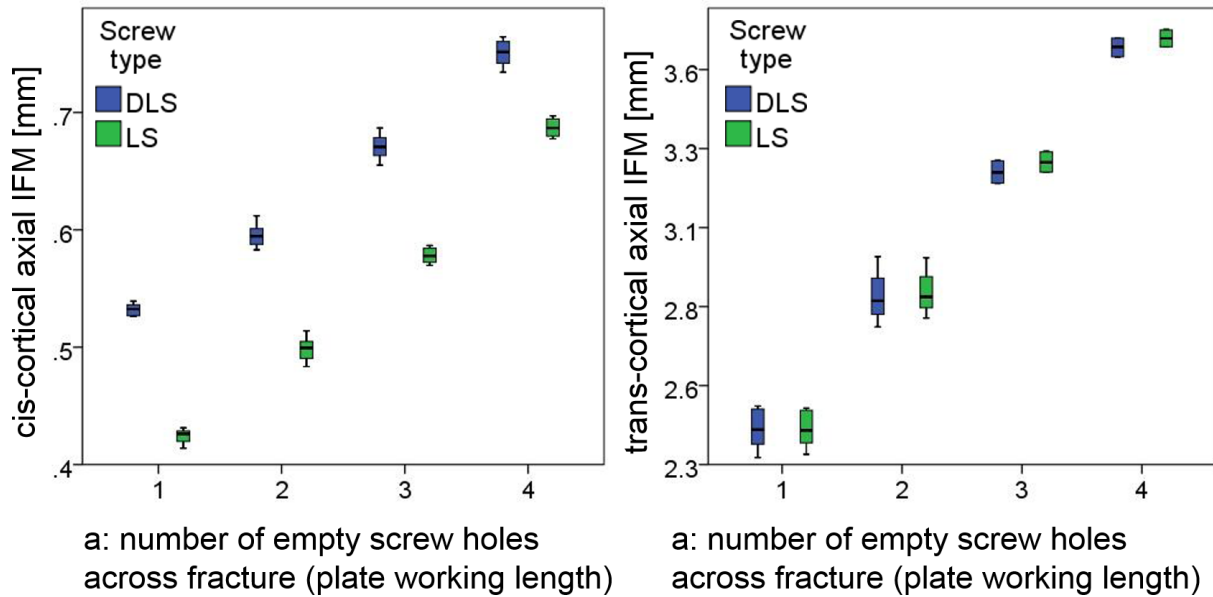


Figure 4-5: The Axial IFM under the plate (left) and opposite the plate (right) for two different screw types in the proximal shaft. Compare Figure 4-2, and Figure 4-4: letter “a” signifies the plate working length or empty screw holes across the fracture.

A wide range of axial and shear stiffness was covered by different fixation options here, but axial and shear stiffness are strongly coupled in locking plate configurations overly restraining axial movements compared to shear (Figure 4-7). Callus growth towards large diameters may compensate excessive shear movements (Plecko et al., 2012).

Limited knowledge exists how to employ screw placement and elastic screws as powerful tools in fracture care. The present findings illustrate a strong influence of screw placement on IFM in a locking plate construct, and confirm especially the influence of plate working length on IFM. Furthermore, DLS instead of LS help to level unequal gap straining and increase cis-cortical axial IFM to some degree. Our analyses show that mechanical conditions within locking plate constructs can be strongly influenced. Further analyses have to be performed in order to formulate general recommendations of screw placement for various fracture types to optimize mechano-biological fracture care.

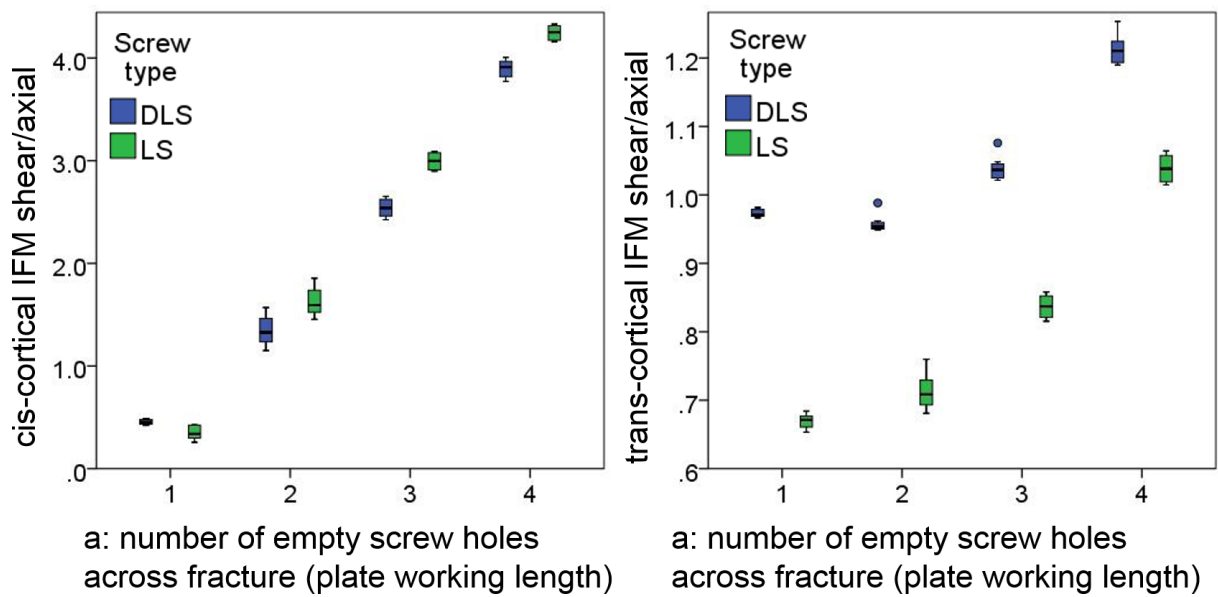


Figure 4-6: The ratio Shear/Axial IFM under the plate (left) and opposite (right) for two different screw types in the proximal shaft. Compare Figure 4-2, and Figure 4-4: letter “a” signifies the plate working length or empty screw holes across the fracture.

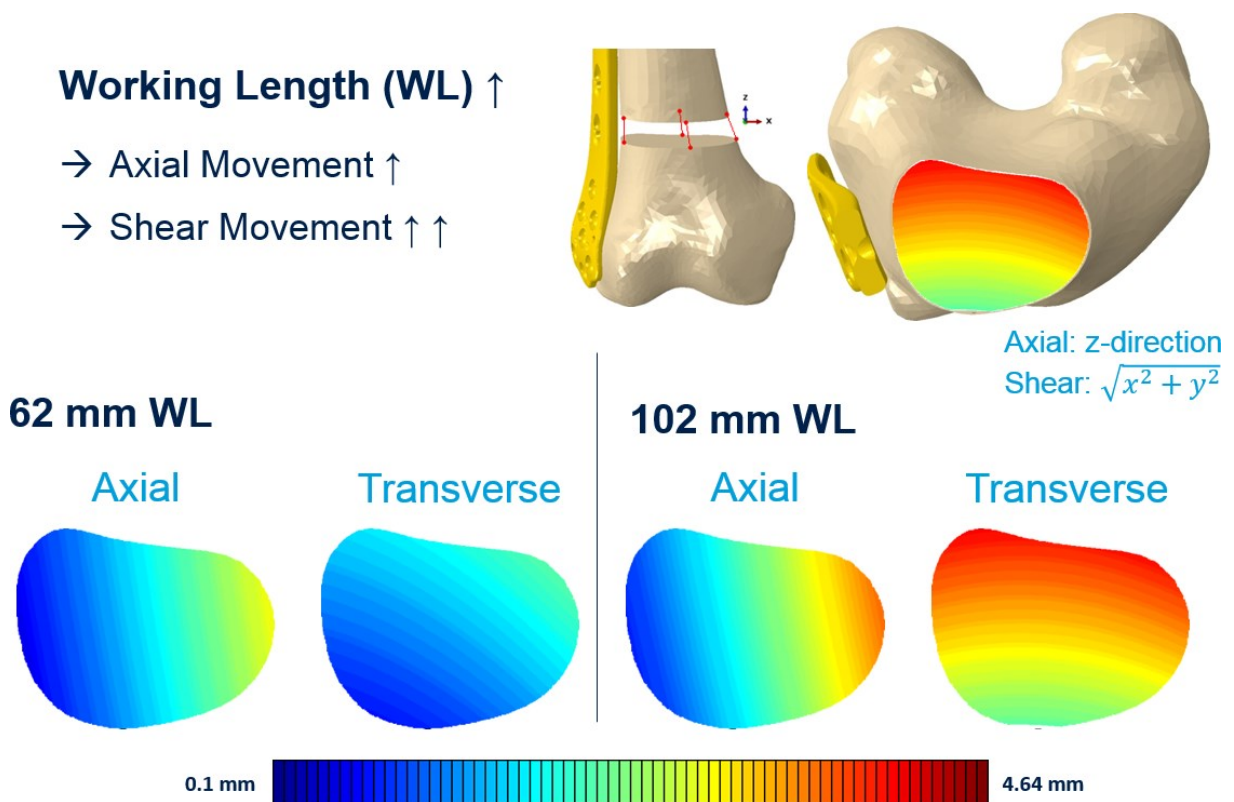


Figure 4-7: Schematic showing an increase in shear compared to axial movement with higher plate working length. Resulting shear (motion in fracture plane) is the vector addition of the relative motion in the two directions in the fracture plane. Axial movement is the motion in z-direction, orthogonal to fracture plane.

4.1.2. Systematic analysis of fracture slope

Not the IFM per se, but the deviatoric strain (distortion, deformation without volume change) impacts tissue differentiation (Isaksson et al., 2006, Isaksson, 2007, Isaksson, 2012), additionally to volumetric components, e.g. hydrostatic strain that impacts cartilage formation. Thus, the fracture gap shape determines how total IFM is subclassified into in-plane-movement (IPM) or shear and out-of-plane movement (OPM) or normal movement (Figure 4-8).

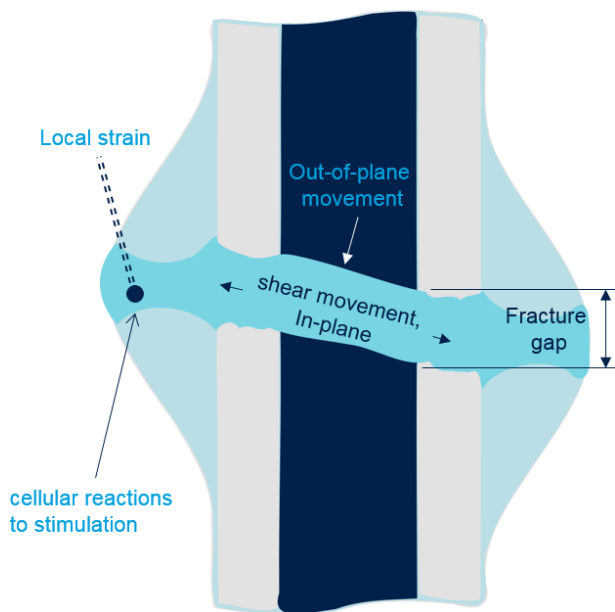


Figure 4-8: Local IFMs with its components in- and out-of- plane determine local strain with its components as a function of fracture size and shape.

We created finite element models with loads corresponding to 45% of the gait cycle (foot push-off) with maximum hip joint contact force during walking considering 41 muscle forces and the main hip and knee joint forces derived from a musculo-skeletal model (Heller et al., 2001b). Displacement constraints of Speirs et al. (2007) were implemented. Isotropic bone material using material mapping was modeled with 24,049 C3D10 elements with Young's moduli between 1 and 22,250 MPa. Plate material was modelled homogeneously with 52,657 C3D10 elements with a Young's modulus of $E=112,000$ MPa. Poisson ratio for all material was 0.3. Screws were represented by beam elements connected with multi-point-constraints to bone and plate. The gap tissue was modelled as an isotropic material with a modulus of $E = 1$ MPa.

Fracture gap slope was varied in the frontal plane between -60 to 60 degrees in 30 degree steps (Figure 4-9) as well as plate working length and gap size (1 or 3 mm).

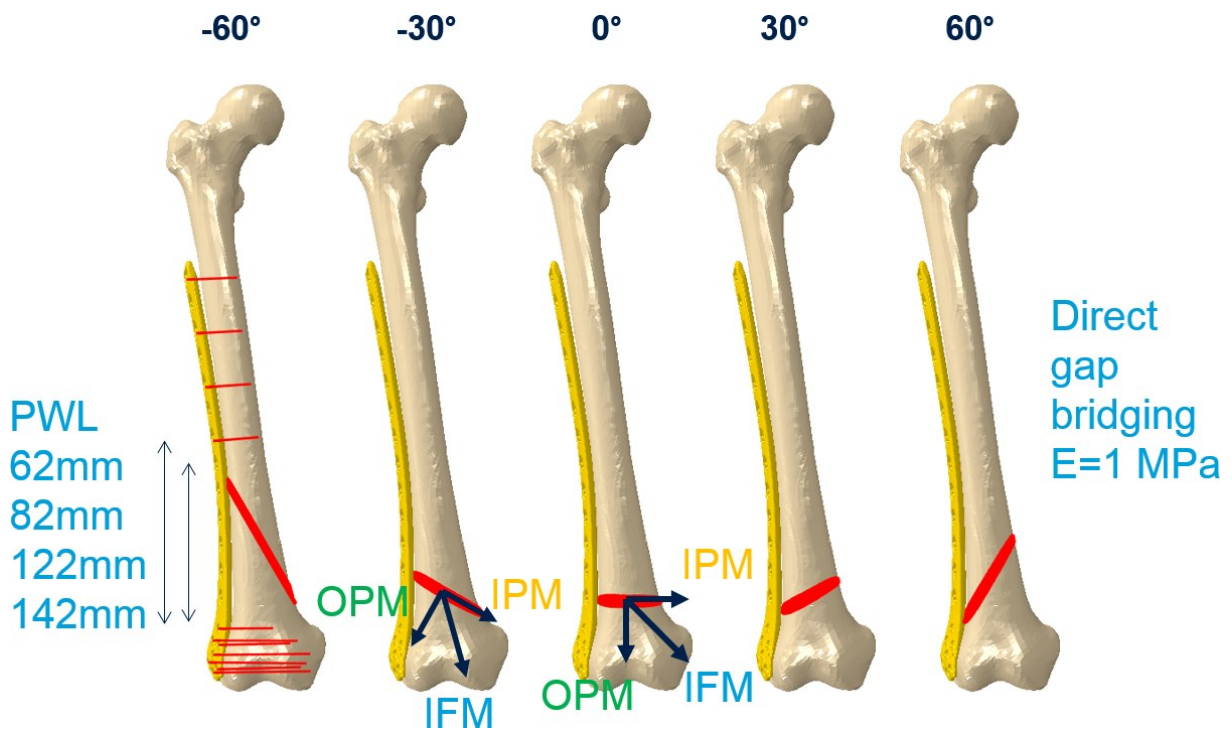
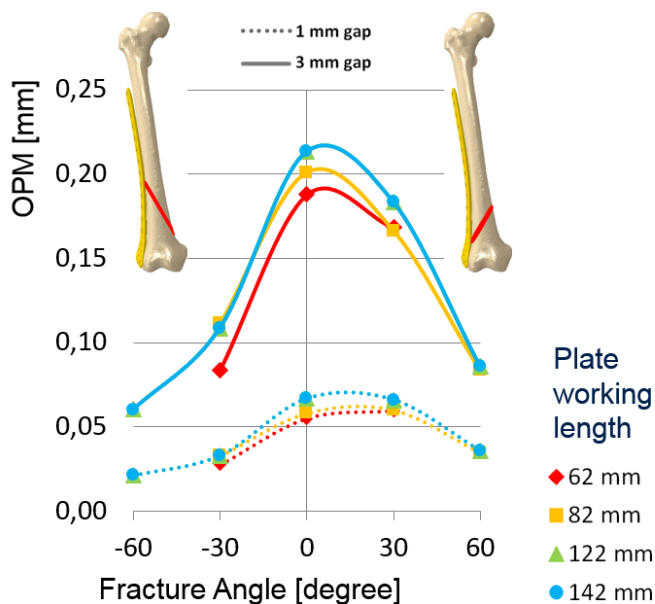


Figure 4-9: Different models of fracture configuration with bridging gap tissue. The resulting IFM has the components in-plane (IPM) and out-of-plane (OPM).

Out-of-plane motion (OPM)



In-plane motion (IPM)

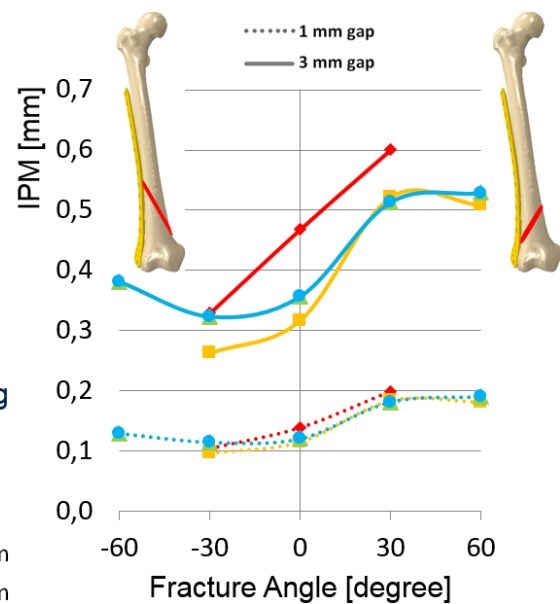


Figure 4-10: Components of IFM (left: out-of-plane, right: in-plane) for different fracture angles (frontal plate), different gap sizes (1 mm or 3 mm) and different plate working lengths.

When evaluating the components of IFM with bridging gap tissue of 1 MPa modulus, we achieve consistent results for different plate working lengths and only high sensitivity to gap size (Figure 4-10). Gaps up to 3 mm usually heal well despite the much higher volume that needs to be regenerated. We decided to normalize for volume as different fracture angles lead to large differences in volume (Figure 4-11). The normalized out-of-plane and in-plane components of IFM follow a similar pattern as the strain invariants that determine fracture healing (Figure 4-12, Figure 4-14).

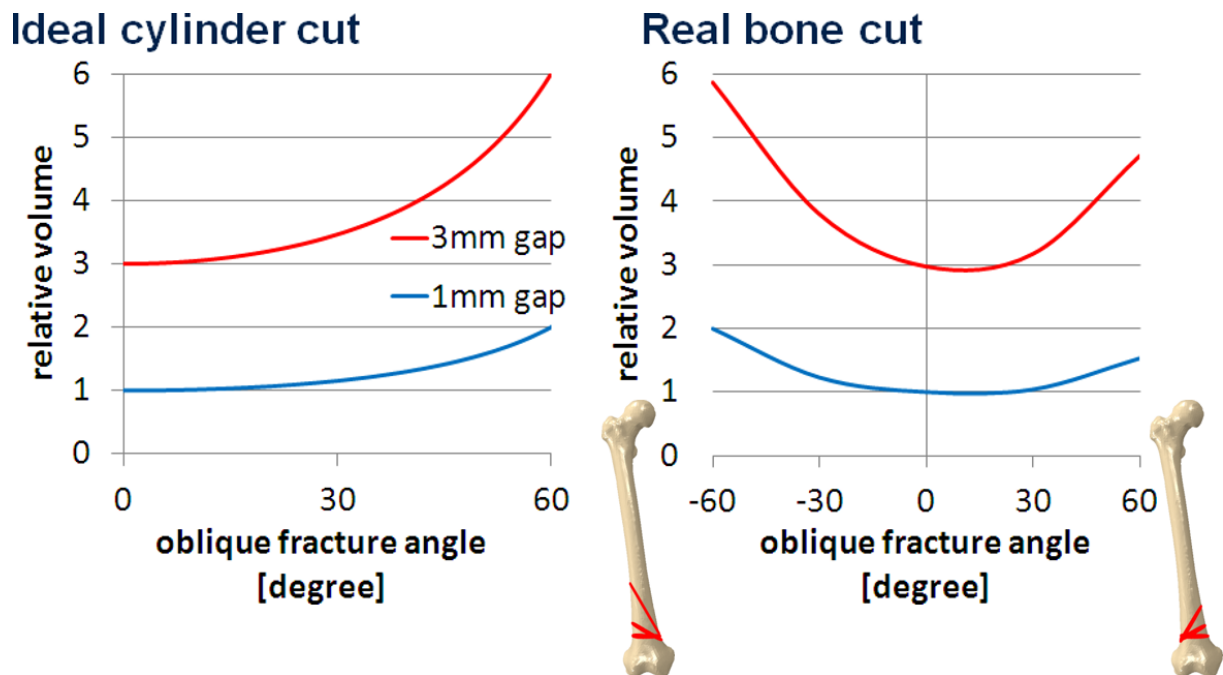
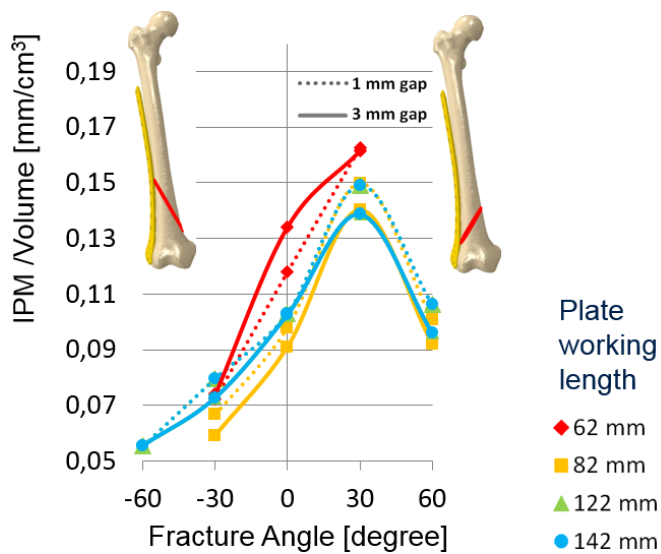


Figure 4-11: Difference in volume for an ideal cylinder (left) and real bone sample (right) with cutting angle and gap size (height).

The clinical evidence, *in vivo* animal studies or *in silico* approaches show controversial results concerning the fracture angle with healing rates of oblique fractures generally worse or equal to transverse fractures (Onnerfalt, 1978, Aro et al., 1991, Aro and Chao, 1993, Nyquist et al., 1997, Son and Chang, 2013). We suggest that IFM components OPM and IPM might serve as surrogate measures for volumetric/deviatoric strain. In a bridged gap as shown here, plate working length seems play a minor role compared to the fracture angle. However in model without gap tissue, fracture angle would determine the ratio of OPM/IPM derivable from total IFM, which is determined by plate working length. Thus, plate working length may determine strain (ratio volumetric / deviatoric) only at an early stage of healing, guiding the later stages of secondary fracture healing (Figure 4-13). Please note that not all fractures angles have a suitable screw placement. Please also note that good stimulation may appear at different location within the fracture gap.

In-plane motion / Volume



Deviatoric strain

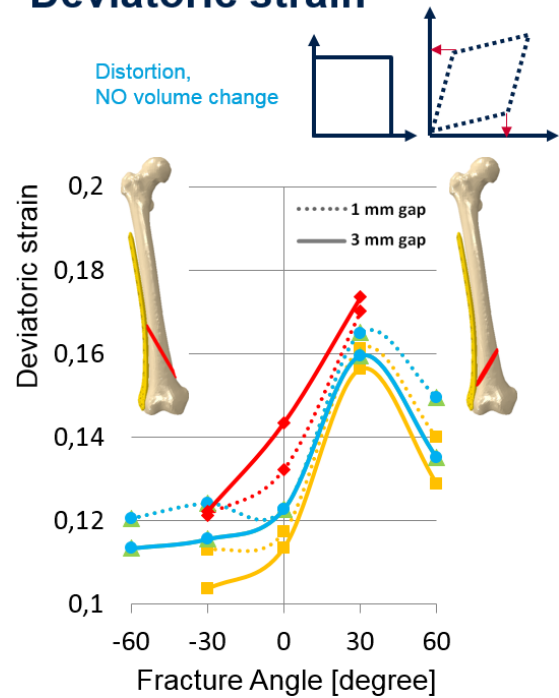
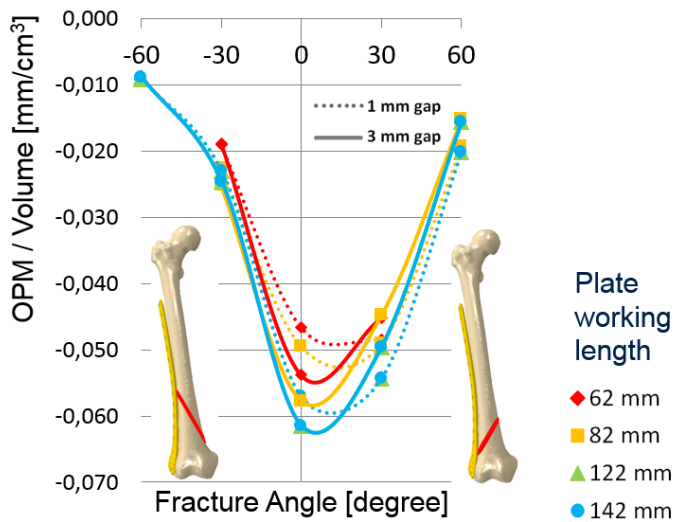


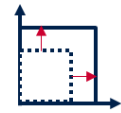
Figure 4-12: Volume-normalised in-plane component of IFM (shear movement) for different fracture angles (frontal plate), different gap sizes (1 mm or 3 mm) and different plate working lengths on the left versus mean deviatoric strain of gap tissue.

We conclude that the orientation of fracture angle is important with unilateral fixation, so that the higher in-plane motion is suffered in fractures with smaller angular deviation to the loading vector. In those fractures, problems might arise as they might not be treatable with the tested hardware. An option for such fractures might be a higher stiffness fixation.

Out-of-plane motion / Volume



Hydrostatic strain



Volume change

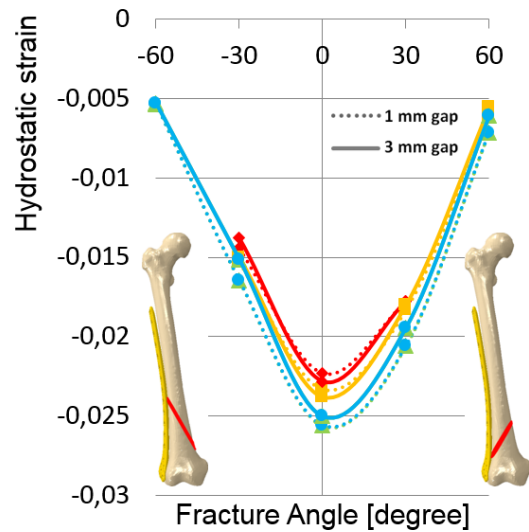


Figure 4-14: Volume-normalised out-of-plane component of IFM (normal movement) for different fracture angles (frontal plate), different gap sizes (1 mm or 3 mm) and different plate working lengths on the left versus mean hydrostatic (mean of principal strains) of gap tissue.

working length	LS, best m-l fracture angle [°], mean α				LS, best a-p fracture angle [°], mean β			
	l	m	p	a	l	m	p	a
42mm	11.8	11.9	29.0	-13.4	-15.5	32.4	26.5	31.5
62mm	56.1	23.5	41.6	8.1	-32.8	29.5	21.1	27.0
82mm	70.4	33.9	51.1	29.0	-45.4	26.5	15.5	21.8
102mm	75.9	43.2	58.3	44.3	-55.5	24.0	9.3	15.9
working length	DLS, best m-l fracture angle [°], mean α				DLS, best a-p fracture angle [°], mean β			
	l	m	p	a	l	m	p	a
42mm	-2.5	15.2	35.9	-23.7	-24.1	43.1	34.1	41.1
62mm	46.6	26.3	45.9	-2.3	-39.4	39.4	27.7	36.3
82mm	65.6	36.2	53.8	20.2	-51.3	36.3	21.4	31.1
102mm	74.0	45.3	60.4	39.7	-59.7	33.7	14.9	25.5

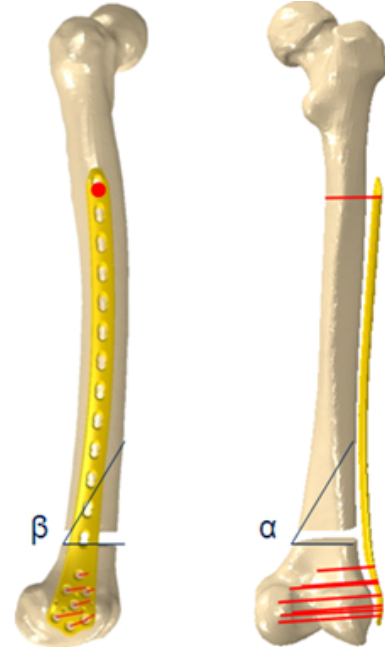


Figure 4-13: Calculated fracture angles for minimum in-plane and maximum out-of-plane IFM using data from the systematic screw placement analysis. The table headings l, m, p, a stand for lateral, medial, posterior, anterior positions in the fracture gap, compare Figure 4-4, Figure 4-7.

4.1.3. Hybrid fixation

Together with the validation, we also conducted an experiment (Figure 4-15) whether a plate independent lag screw could improve fixation stiffness (Märdian et al., 2015b). We tested distal femora in axial compression and torsion as described for the validation.

Experimental Set-up

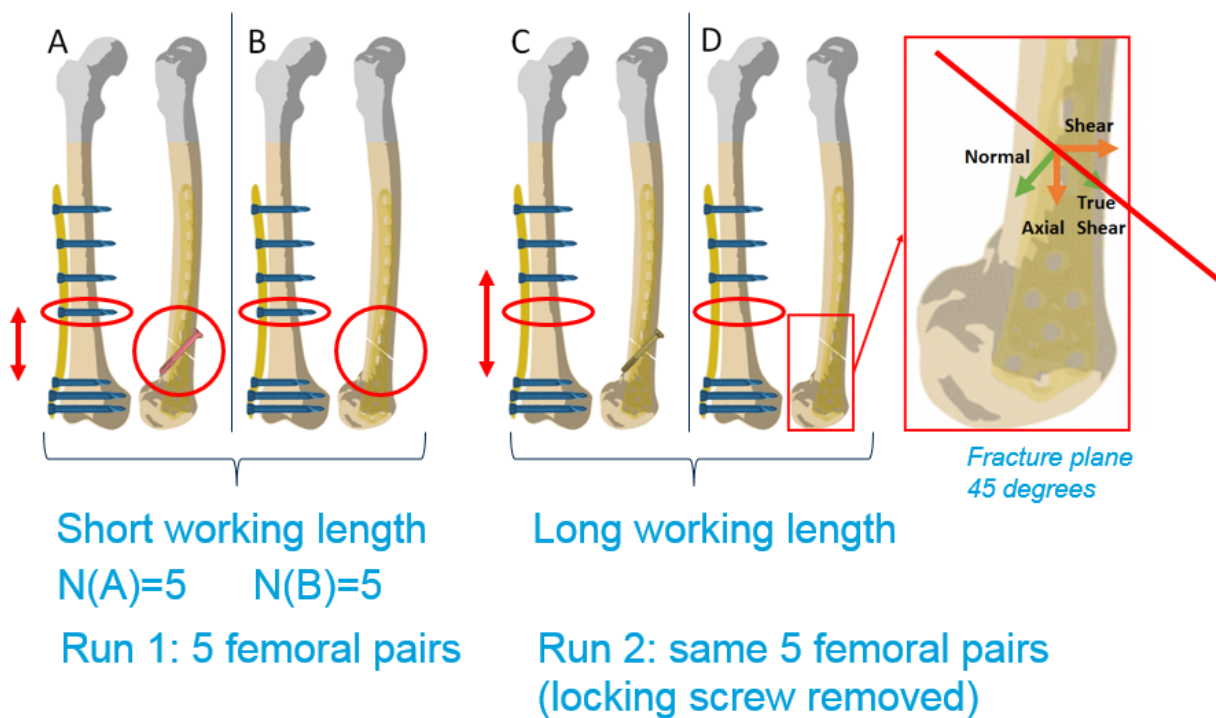
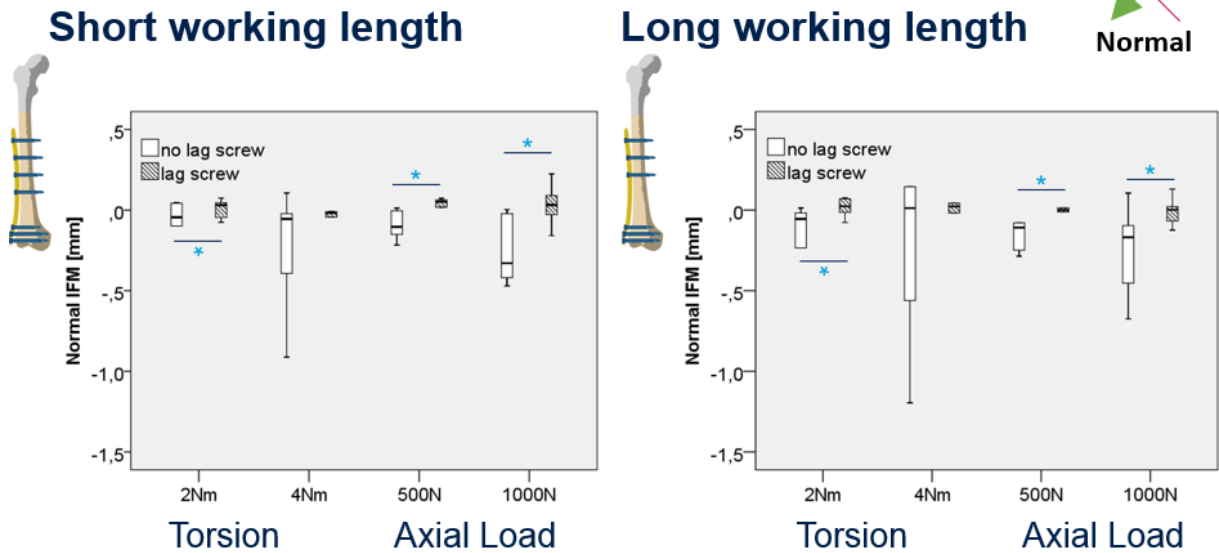


Figure 4-15: Procedure set-up for testing the effect of an additional lag screw next to locked plating compared to only locked plating: A, lag screw group, B, locking plate group, C, lag screw group with increased plate working length, D, locking plate group with increased plate working length.

We evaluated the relative motion of the fracture segments and found that an additional lag screw over the fracture line next to a locking plate as a neutralization plate reduces movement (increases stiffness) and especially shear movement for all loads and both working lengths (Figure 4-16, Figure 4-17). Furthermore, the variance in movement with lag screw is much smaller than without lag screw. Normal IFM without lag screw is negative and tend to open the gap. There are a number of limitations to this test, as only one specific fracture type was tested, with N=5 specimens per group and just the two load cases of pure axial compression-bending or torsion with 2 screw configurations. However, we evaluated the true local movement in real bone and found significant differences for all loads and also tested different plate working lengths. Clinical studies could already show improved healing with a lag screw next to a locking plate without detailed explanation, but suspecting improved stiffness (Wenger

et al., 2017, Chung et al., 2016, Yang et al., 2015). With a lag screw and a locking plate, shorter time to full weight bearing of 11 weeks versus 15 weeks ($p = 0.044$) has also been reported (Horn et al., 2011). Thus, a lag screw fixation next a locking plate might be an option for fractures with inherently high in-plane movement due to their fracture line orientation.

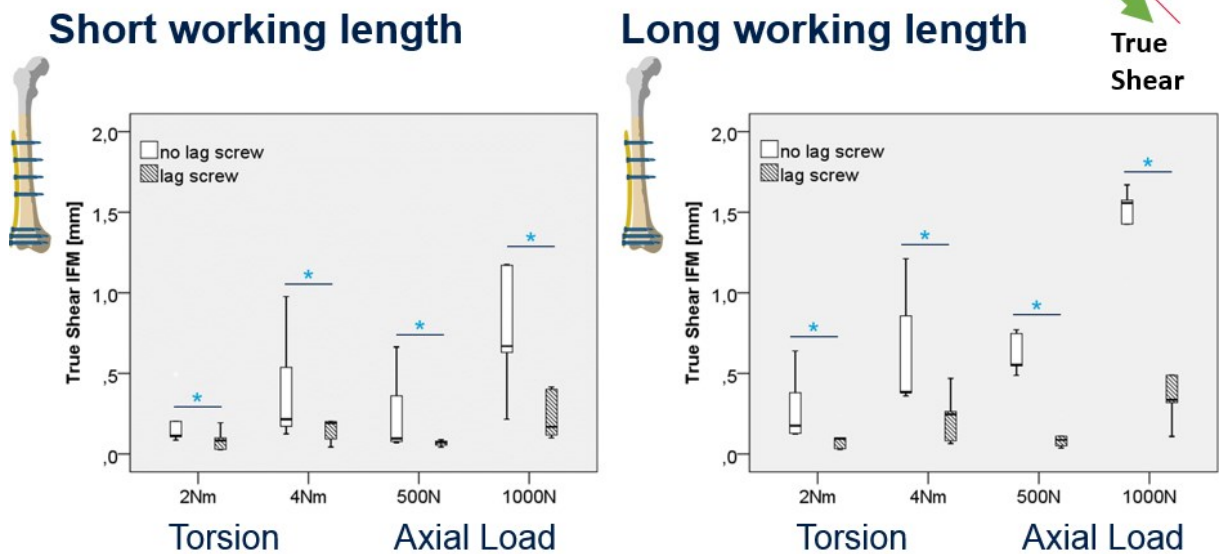
Normal Interfragmentary Movement (IFM)



* $p < 0.05$, Mann-Whitney-U

Figure 4-16: Out-of-plane movement results for tests with or without lag screw next to a locking plate for different loads and different working lengths.

True Shear IFM



* $p < 0.05$, Mann-Whitney-U

Figure 4-17: In-plane movement results for tests with or without lag screw next to a locking plate for different loads and different working lengths.

4.1.4. Further limits of fixation

Pre-contoured plates inevitably must show gradual differences of local bone-plate distance as they cannot fit the whole population. Then, the surgeon or the surgical technique that is used determines willingly or out of necessity if the minimal bone-plate distance occurs proximally, distally or in between at the fracture level. Hwang et al. (2012) report mismatch of pre-contoured locking plate shape with femoral curvature of Asian patients (Figure 4-18), which might prevent proper plate placement with bone-plate distances of less than 5 mm (at all locations) together with long plates altogether, predisposing to implant failure (Ahmad et al., 2007).

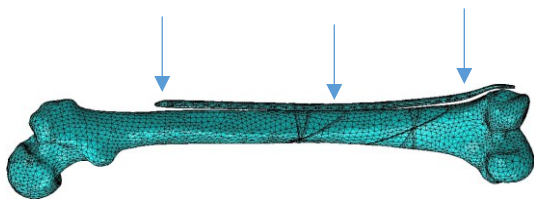


Figure 4-18: Plate curvature does not fit all patients and might lead to non-uniform, and also partially large clearances between plate and bone especially at the plate tips.

We tried to evaluate plate position based on standard clinical imaging (X-ray or fluoroscopy). A tested method from our institute gave mixed results and required a 3D bone model (Figure 4-19). Together with the Zuse institute Berlin, we developed a new method to reconstruct the patient-specific shape of the femur from plain 2D X-rays and assess the relative position the plate to the femur (Ehlke et al., 2015)⁴⁶. With statistical shape and intensity models based on principal component analysis, the variance and range of bone shape and density distribution in a certain cohort is assessed and can be represented with a comparably small set of principal components. To create these models, a number of medical 3D image stacks were segmented. With the principal components, the model can then synthesize 3D geometry and 2D projection images of the most likely anatomy and compare to this to new medical images. We create a matching problem (similarity measure) and can deduct 3D geometry from 2D images. The localization of structures in 3D, even in the presence of noise becomes possible with potential fast-generation of 3D finite element models. Pathologies are not expressed by the model, unless they are contained in the training data. The manual delineation of training sets (segmentation of many data sets) is necessary. The quality of fit cannot be guaranteed. The 3D

⁴⁶ Moritz Ehlke, [Mark Heyland](#), Sven Märdian, Georg N. Duda, Stefan Zachow. 2015. 3D Assessment of Osteosynthesis based on 2D Radiographs. <https://opus4.kobv.de/opus4-zib/frontdoor/index/index/docId/5620>, last accessed 19th September 2018.

Moritz Ehlke, [Mark Heyland](#), Sven Märdian, Georg N. Duda, Stefan Zachow. 2015. Assessing the Relative Positioning of an Osteosynthesis Plate to the Patient-Specific Femoral Shape from Plain 2D Radiographs. <https://opus4.kobv.de/opus4-zib/frontdoor/index/index/docId/5426>, last accessed 19th September 2018.

reconstruction of bone needs a scaling value, which can be given by defined imaging conditions or in our case the size and characteristic shape of the plate, which was imported as a 3D-model. The reconstruction process could not be fully automated for far and still requires some manual correction.

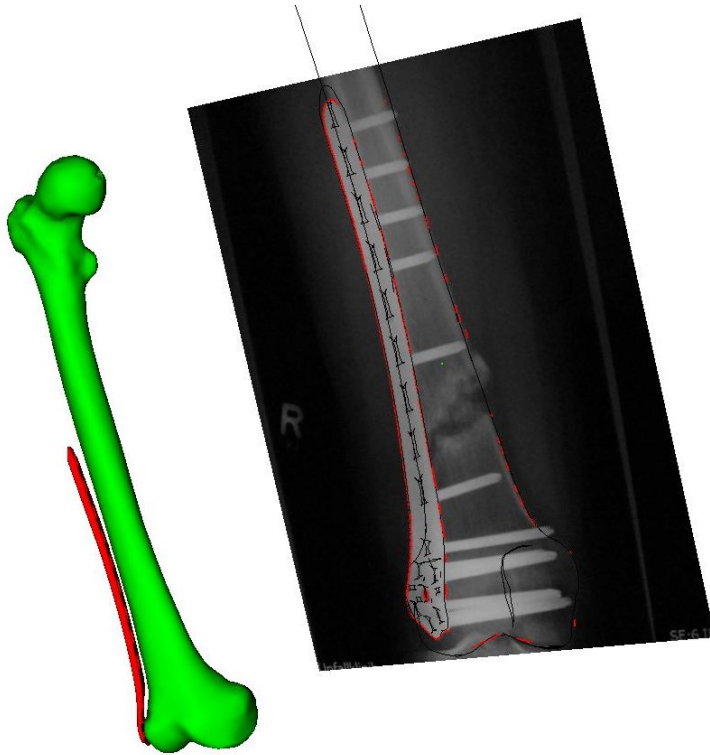


Figure 4-19: Reconstruction of plate position based on edge-matching from a single-plane X-ray image using a 3D bone and plate model with model-based RSA, Medis specials b.v., Netherlands (Moewis et al., 2012).

4.2. Sampling of clinical *in vivo* data for (mechanical) stimulation

The results of innovative implants are often promising when tested under controlled conditions *in vitro*, e.g. with transverse 3 mm osteotomy gaps in sheep (Kaspar et al., 2005, Giannoudis and Giannoudis, 2017). However, the results are rather disappointingly moderate or inconclusive when multi-center studies compare the implants to the Gold standard *in vivo* (Höntzsch et al., 2014) or when simulations model their behavior under realistic conditions (Heyland et al., 2015a). Reasons for this could possibly be attributed to basic differences between the geometrical and boundary conditions in the research set-up and the real clinical cases as well as less control of transient parameters in the clinical setting.

One prime example, although not mechanical, but eye-opening and relevant to fracture care was discovered at our institute while inspecting the immunologic profile of laboratory mice⁴⁷. The adaptive immune system, i.e. the acquired immunity through contact with germs, influences fracture healing capacity (Toben et al., 2011, Reinke et al., 2013). However, many mice in fracture healing studies are kept in aseptic, pathogen-free housing, i.e. a sterile environment. Thus, results of such healing studies do not represent the realistic case with an adaptive immune system.

Döbele et al. (2014) report a 74.4% reduction of initial stiffness (for low loads) and 3.4% reduction of stiffness for higher loads with DLS instead of standard locking screws. When tested under physiological conditions, which operate at the higher loads, the effect of DLS is modest at best (Figure 4-20), but still significant at the cis-cortex, i.e. near the plate (Heyland et al., 2015a).

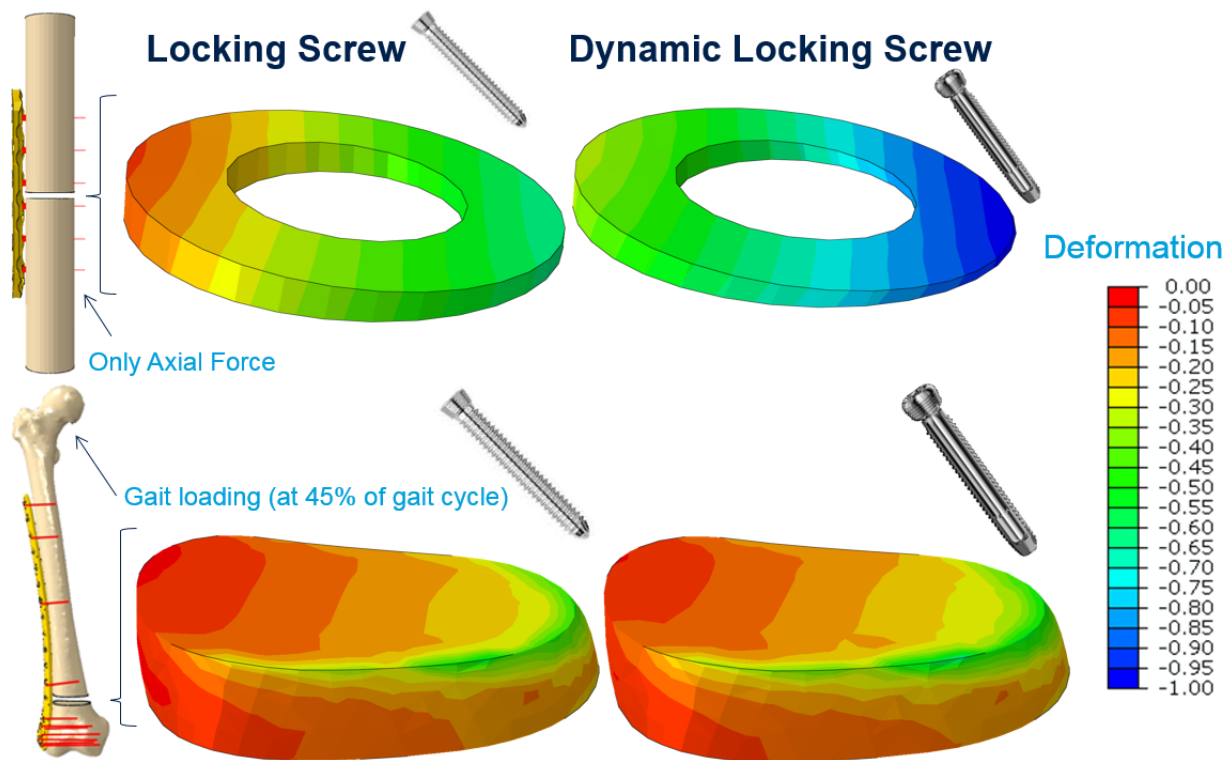


Figure 4-20: Effect of mechanical testing conditions. Top: Simple axial-bending model of a lateral plate with locking screws on the left and dynamic locking screws on the right, leading to appreciably different deformations (=tissue stimulation) of compliant gap tissue. Bottom: Complex physiological loading model of a lateral plate with locking screws on the left and dynamic locking screws on the right, leading to hardly noticeable difference in deformation (=tissue stimulation) of compliant gap tissue.

⁴⁷ I am particularly devoted to this study of the immune system, because I started working as a student at the Julius Wolff institute testing mechanically mice bones for Daniel Toben, who worked on this topic: Toben, Daniel, et al. "Fracture healing is accelerated in the absence of the adaptive immune system." *Journal of Bone and Mineral Research* 26.1 (2011): 113-124.

4.2.1. Dynamization⁴⁸ options

Many devices such as external fixators, plates or intramedullary nails allow for multiple stiffness configurations for example using additional hardware or different screw types or placements. For instance, in a sheep study, a locked intramedullary nail yielded superior healing rates when compared to a conventional nail (Kaspar et al., 2005). When tested in humans, no or only minor differences between the nail types or configurations could be shown (Höntzsch et al., 2014). One main difference between the animal and the human study was the etiology of the fracture, with consistent 3 mm transverse fractures in the sheep and the unspecified distribution of different slopes and fracture sizes in the patients. Let us assume that the locked nail leads to high stiffness (Kaspar et al., 2005) while the unlocked nail allows high IFM. Let us further assume that there are patients with large gaps and fracture orientations firstly almost parallel to the loading vector and secondly rather almost orthogonal to the loading vector. Dividing into those four sub-groups, for the standard nail, we get firstly detrimental stimulation (mostly shear due to high IFM and orientation of the fracture), and secondly beneficial stimulation (mostly normal movement due to high IFM and orientation of the fracture). For the locked nail, we get firstly mildly detrimental stimulation (mostly shear but low IFM) and secondly mildly beneficial stimulation (mostly normal movement but low IFM). Over all groups, comparing standard and locked nail there might be no differences, as some heal well and some show delayed healing. However, the variation should be much higher in the standard nail group, because those two sub-groups would show either very good or very bad stimulation. In contrast, the locked nail group always endures low stimulation in both groups. Unfortunately, we could not evaluate the data based on the suggested sub-groups.

So far, mechano-regulatory strain has often been simplified as the ratio of load and stiffness, but deformation has more dimensions to it. One aspect is the quality: shear (without volume change = distortion) and compression/tension or deformation with volume change (volumetric change). It has been shown now that compression/tension and bending produce high volumetric change while torsion

⁴⁸ Dynamization of fixation is a commonly used procedure to accelerate fracture healing. However, the term dynamization is used for various methods of osteosynthesis modification during the bone healing process. The dynamization by removal of locking screws in intramedullary nailing is performed most frequently. This can lead to a telescopic movement between intramedullary nail and tubular bone, which leads to closing of fracture gaps and compression onto the fracture surfaces. Experimental and clinical studies have shown that this can result in an acceleration of fracture healing. Especially with larger fracture gaps and shapes, which allow a bony support of the fragments, this procedure may be useful. Another method of dynamization is the decrease of osteosynthesis stiffness during fracture healing. This procedure takes place predominantly with external fixators; Here, the flexibility of the osteosynthesis is increased by a partial removal of elements. Study results for this dynamization procedure report beneficial outcome when performed in the late healing phase. With sufficient callus formation, callus bridging and remodeling can be accelerated. CLAES, L. 2018. [Dynamization of fracture fixation : Timing and methods]. *Unfallchirurg*, 121, 3-9.

and shear produce high distortion. Low distortion is beneficial for healing, as it promotes the osteogenic differentiation and high volumetric strains promote cartilage proliferation and mineralization (Isaksson et al., 2006). Thus, a balance of strain and strain quality needs to be found reducing distortion and enabling minimum volumetric stimulation for secondary fracture healing.

As a results, sometimes it is reasonable to decrease stiffness in “dynamization” of the implant, but if high shear components of IFM have to be expected, increasing stiffness of the whole osteosynthesis might be a better option using additional implant hardware (lag screw, additional nail or plate, etc.) or grafts or scaffolds.

4.2.2. Case reports of delayed healing (with possibly unsuccessful fixation)

Button et al. (2004) reports a case of delayed union at 6 months in a 38-year-old woman after a high-speed motor vehicle accident. The Gustilo type II open, comminuted supracondylar femur fracture with intracondylar extension along with a right femoral shaft fracture and right both bone forearm fractures was surgically treated. A deep venous thromboses in both legs developed. Three and a half months after the original procedure, an elective re-operation was performed with autograft, allograft, and growth factor implantation at the fracture site. Five months later, the LISS plate failed while walking. Another revision surgery followed with a locking condylar buttress plate and large fragment DC plate. Six months later, the bony defect is still present on X-ray although she is pain free, ambulating, and has a knee range of motion of 0–110°.

Interpretation: Based on the image in their publication (Button et al., 2004), the fracture line seems to be oriented rather parallel to the main loading vector at the hip. Plate working length seems moderate. Mono-cortical screws are used in the proximal shaft. The plate failed during walking, so load was applied. Despite autograft, allograft, and PDGF placement, healing seems to remain absent. Mechanical conditions might hinder healing with excessively high in-plane movement. A very rigid fixation with additional hardware (e.g. dual-plating) might resolve the issue.

Freude et al. (2014) reports distal tibia fractures treated with LCP and conventional locking screws or dynamic locking screws. The healing results in two mechanically comparable situations with very high plate working length of a 38-year old man with LS and a 67-year old man with DLS yielded complete consolidation for the DLS-fixation after 6 months, while at 11 months the LS-fixation showed callus but incomplete consolidation.

Interpretation: Both are high-angle fractures, and both were treated with a large plate working length, thus enabling high IFM. DLS enable much higher ratios of transverse movement relative to axial movement (Figure 4-6). Thus, for the high fracture angle, the IFM component of in-plane movement with LS might be quite high, while with DLS, it might be lower with much more beneficial normal movement with DLS. An indicator might be callus size, with a small callus (low shear) with DLS and larger callus with LS.

Nassiri et al. (2013) describe three different cases:

- 1) A young man (23) with a transverse fracture (right tibia and fibula, AO 42.A3) after a kick in football was treated with a 4.5 mm Narrow LCP with 10-combi-holes (6 locked screws, two screws at either end of the plate and two screws adjacent to the two middle holes over the fracture site). The two screws adjacent to the fracture and the most proximal screw were unicortical, while the remaining three screws were bicortical. No visible callus formation six months later led to removal of the two innermost screws. Fracture had healed with marked callus formation six months later.

Interpretation: As Nassiri et al. (2013) report in the results of their FE model, axial stiffness decreased by 18% and interfragmentary motion significantly increased with higher PWL with gap closure after removing the two innermost screws, also reducing the stress in the plate to 63% and in the screw to 60%.

- 2) An osteoporotic 74-year-old woman suffered a spiral fracture of the distal femoral diaphysis (AO 32.B1 and was treated by open reduction with a 15-hole LCP Distal Femur Plate using 13 locked screws (one hole in the shaft portion of the plate at the fracture site and one hole in the head of the plate were left unoccupied). Radiographs after 22 weeks revealed plate breakage at the middle part of the original fracture and no callus formation was visible. She underwent IM nailing and after 1 year, there was complete consolidation with marked callus formation.

Interpretation: The very short working length (one unoccupied screw-hole over the fracture site) and the insertion of locking screws at the level of the fracture passing through the fracture line make the construct rigid with an axial stiffness of 2.0 kN/mm (Nassiri et al., 2012): There is little interfragmentary motion which is needed for callus formation (0.09 mm). Nassiri et al. (2013) report maximum Von Mises stress in the plate of 299 MPa at the outer edges in the unoccupied screw-hole over the fracture site, higher than the yield strength of stainless steel (235 MPa). Subsequent failure of the fracture to heal at 22 weeks meant that the stresses experienced by the implant remained high.

We would say that even with a more flexible lateral locking plate fixation, this fracture is critical as its angle is high and oriented from lateral-distally to medial-proximally, predisposing to high in-plane IFM components. Changing to a nail with high transverse components improves the IFM component ratio and increases IFM, so that healing might occur with a large callus.

3) A nun (91) sustained a spiral fracture after a fall to the right distal femoral diaphysis (AO 32.A1). The fracture was treated with a LCP Distal Femur Plate using 7 locked screws and one partially threaded cancellous screw (6 screw-holes were left unoccupied over the fracture site). After 6 months, indirect bone healing with marked callus formation occurred.

Interpretation: The large working length (6 unoccupied screw-holes over the fracture site) led to a flexible construct with an axial stiffness of 0.9 kN/mm and an interfragmentary motion of 0.7 mm (Nassiri et al., 2012), promoting callus formation. Initial loads might have been small, but we do not know. The large callus may compensate for initially large in-plane movements (Plecko et al., 2012). The importance of PWL diminishes as more load is shared by the callus tissue and less by the plate over time.

4.3. Sampling of clinical *in vivo* data for implant failure

4.3.1. Reported failure cases and some possible explanations

Button et al. (2004) report 3 more cases with 1 plate breakage and 2 screw-cut-throughs and attribute this to:

1) high load, high body weight (400 pounds).

Interpretation: We would add the use of a short plate, and no empty screw holes proximally. The low PWL leads to high plate stress over a small fracture gap (MacLeod and Pankaj, 2018).

2) plate too anterior, screw-cut through cortex, using mono-cortical screws

Interpretation: Screw and plate placement can be demanding and there is room for technical improvements, especially concerning more tissue sparing techniques that still ensure correct placement.

3) no reason given

Interpretation: We might assume insufficient screw purchase proximally. With the long plate and 162mm PWL (7 empty holes) and no empty screw holes between proximal screws, there was a large force pulling at the screws.

Chen et al. (2010) contrast two clinical cases with different plate working length. The first case is a rigid fixation using a titanium plate (PWL ca. 20 mm), leading to breakage after 7 weeks while the second case is a flexible fixation using a steel plate (PWL ca. 120 mm), leading to fracture healing with obvious callus growth at 4 months.

Interpretation: Their computational analysis revealed that stress under 2.5 times body weight at the femoral head in the rigid fixation (540 MPa) could be significantly higher than that in flexible fixation (390 MPa). Fatigue analyses showed that, with the stress level in flexible fixation (i.e. with fewer screws and higher plate working length), the plate was able to endure 2000 days, and that the plate in rigid fixation could fail by fatigue fracture in 20 days. Their paper concludes that the rigid fixation method resulted in serious stress concentrations in the plate, which induced fatigue failure while the flexible fixation provided sufficient stiffness and led to fracture healing (Chen et al., 2010).

Poole et al. (2017) report 4 failures in a series of 127 distal femoral fracture fixations with locking plates. Three of those four surgical failures were seen when a plate with 12 or fewer holes was used to fix a fracture with a working length of three or four holes. In contrast, there was only one failure in the 95 fractures where a plate with 13 holes or more was used, with a 16-hole VA-Condylar plate with an unusually long working length of eight holes. Long plates also reduce the risk of a secondary fracture above them, a complication that occurred in three of the 122 patients after successful union of the primary fracture.

Interpretation: Using long plates enables to leave space between screws (well-distributed screw spacing) which has been shown to reduce bone and plate stress (MacLeod et al., 2016c). Short plate working length has been mentioned as a risk factor for plate failure or non-union (Simpson and Tsang, 2018). Some clinical studies could not show a significant influence of plate working length (bridge span) on the emergence of implant failure or non-union (Henderson et al., 2011b, Harvin et al., 2017, Parks et al., 2018), although Henderson et al. (2011b) report that healed fractures had significantly more unfilled holes adjacent to the fracture than those that did not heal. Ten of 14 (71%) non-unions in their study had zero unfilled holes adjacent to the fracture area and the remaining four non-unions had only one unfilled hole. Sometimes, plate working length was even excluded from analysis because of the difficulty in defining it when screws traversed the fracture planes (Rodriguez et al., 2016). There might be an optimal range between low and high plate working length (bridge span) that needs to be found for each individual case considering other factors such as fracture geometry and plate material (Elkins et al., 2016), as well as loading. In a series of 335 distal femur fractures, Ricci et al. (2014) found that higher BMI, and shorter overall plate length are independent predictors of proximal implant failure. When shorter plates (less than 9 holes) with shorter proximal lengths (less than 8 holes) were used,

there was a 14% failure rate compared with 1% failure with longer plates when the entire cohort was considered. Thus, the parameter set of each individual case and the resulting specific (invariant) tissue deformation has to be evaluated or a corresponding surrogate measure.

4.3.2. Unavoidable failures and revisions

Even when fixations are adapted to the patient characteristics, unwanted events may lead to failure.

For midshaft clavicular fractures, Meeuwis et al. (2017) report a high number of screw cut-outs mostly in possibly insufficient bone quality in comparably older patients and for less than 3 bi-cortical screws per fragment, as well as some plate breakages with bridging plates and rather short plate working length. Certain non-load bearing bones might not withstand screw loading and are further weakened by bone adaptation after long-term stress shielding. In those cases, more screws at other locations might be required.

Furthermore, bone might re-fracture during falling events. However, it has been shown that braced bones with a plate are stronger than the intact native bone alone.

Thapa et al. (2015) describe a case of steel plate corrosion and subsequent fatigue failure after overloading. Although the mechanical conditions play a major role for corrosion as well, material flaws may start the corrosion process at first.

Chapter 5. Employing mechano-therapy

Discussion and future perspectives of mechano-therapy for osteosynthesis

How can we improve fracture healing further?

Relevant publications:

Rendenbach, C., Steffen, C., Sellenschloh, K., Heyland, M., Morlock, M.M., Toivonen, J., Moritz, N., Smeets, R., Heiland, M., Vallittu, P.K. & Huber, G. (2018). Patient specific glass fiber reinforced composite versus titanium plate: a comparative biomechanical analysis under cyclic dynamic loading. Submitted to the Journal of the Mechanical Behavior of Biomedical Materials (In Review).

Heyland, M., Duda, G. N., Märdian, S., Schütz, M., & Windolf, M. (2017). Stahl oder Titan bei der Osteosynthese. *Der Unfallchirurg*, 120(2), 103-109.

Heyland, M., Schmoelz, W., Duda, G. N., Schaser, K.-D. & Märdian, S. (2017). Interfragmentary lag screw fixation reduces resulting shear movements in simple fracture patterns. Podium presentation. 23rd Congress of the European Society of Biomechanics (ESB 2017), July 2-5 2017, Seville. <https://esbiomech.org/conference/index.php/esb2017/seville/paper/view/1254>

Heyland, M., Duda, G. N., Urda, A. L., Cilla, Myriam & Märdian, S. (2017). Fracture risk for ipsilateral stemmed implants. Podium presentation. 23rd Congress of the European Society of Biomechanics (ESB 2017), July 2-5 2017, Sevilla. <https://esbiomech.org/conference/index.php/esb2017/seville/paper/view/1257>

Heyland, M., Duda, G. N., Urda, A. L., Cilla, Myriam & Märdian, S. (2017). Analytische Modellvorhersage des interprothetischen Fraktur-Risikos. Podium presentation. Deutscher Kongress für Orthopädie und Unfallchirurgie (DKOU 2017) October 24-27 2017, Berlin. <http://www.eqms.de/static/de/meetings/dkou2017/17dkou123.shtml>

Märdian, S., Duda, G. N., Schwabe, P., Moewis, P., Cilla, Myriam & Heyland, M. (2016). Finite element analysis for fracture risk assessment as a function of inter-prosthetic distance. Poster. 22nd Congress of the European Society of Biomechanics (ESB 2016), July 10-13 2016, Lyon. <https://esbiomech.org/conference/index.php/congress/lyon2016/paper/view/723>

Märdian, S., Schmözl, W., Schaser, K. D., Duda, G. N., & Heyland, M. (2015). Interfragmentary lag screw fixation in locking plate constructs increases stiffness in simple fracture patterns. *Clinical Biomechanics*, 30(8), 814-819.

Märdian, S., Schaser, K. D., Duda, G. N., & Heyland, M. (2015). Working length of locking plates determines interfragmentary movement in distal femur fractures under physiological loading. *Clinical biomechanics (Bristol, Avon)*, 30(4), 391-6.

Heyland, M., Duda, G. N., Haas, N. P., Trepczynski, A., Döbele, S., Höntzsch, D., Schaser, K.-D. & Märdian, S. (2015). Semi-rigid screws provide an auxiliary option to plate working length to control interfragmentary movement in locking plate fixation at the distal femur. *Injury*, 46, S24-S32.

5.1. Consequences: Guidelines for surgeons?

The optimal mechanical environment for instance after a distal femur fracture treated with locking implants remains uncertain (Henderson et al., 2011b), despite basic knowledge on optimal tissue stimulation. Empirical studies seem to fail to control the fracture healing progress in detail, but only report extreme failure cases. Prediction of healing disturbances is so far limited to a general risk assessment and not specific to mechanical loading.

5.1.1. Fracture healing progress prediction and risk assessment

Simplified assessments of scalar parameters (Harvin et al., 2017) do not correlate with clinical success rates. Implant stiffness only correlates for well-controlled studies and experiments (Parks et al., 2018, MacLeod et al., 2018a, Grant et al., 2015). To be sure, local tissue deformation has to be assessed directly and confounding factors such as implant failure have to be controlled for.

The local strain is determined by the mechanical conditions produced by interfragmentary in-plane (tangential) motion in contrast to out-of-plane (normal) motion. Epari et al. (2006b) found in a FEA study that large interfragmentary shear (tangential) movements produced comparable strain and less fluid flow and pressure than moderate axial interfragmentary movements, while combined axial and shear movements did not result in overall increases in strain and strain magnitudes were similar to those produced by axial movements alone. Only with axial movements (uniaxial), the non-distortional component of the pressure-deformation theory influenced the initial tissue predictions. This study by Epari et al. (2006b) concludes that mechanical stimuli generated by interfragmentary shear and torsion differed from those produced by axial interfragmentary movements, and the initial tissue formation as predicted by the mechano-biological theories was dominated by the deformation stimulus. So, when a complex loading situation is considered, the minimization of distortional strain, i.e. in-plane motion, should play the dominant role for improving the tissue stimulation. However, fixation stiffness should also enable a certain minimal total interfragmentary movement with an in-plane component for successful secondary fracture healing.

5.1.1.1. Tools to estimate stimulation

The goal of an analytical tool in contrast to a more complex FE model is the reduction to a comparably simple problem of elasto-statics with few discrete spatial domains and comparably few, well-defined

and comparably certain input parameters. Thus, a simple analytical model may lead to fast results with minimal effort of parameter identification at the cost of local resolution, which is mostly dispensable for the question of healing progress and failure risk. The difference to empirical models such as simple, empiric correlations (Wee et al., 2017) is that the substantially genuine process is modeled (in detail, i.e. with measurable intermediate data with physical meaning) instead of a black-box model. This approach covers the substantial aspects of the real process (variables) and enables to explore parameter studies and thus estimate the effect of medical interventions (for any intermediate data value). Such an analytical method has been suggested by MacLeod and Pankaj (2014)⁴⁹. However, there have been only rudimentary implementations for surgeons as end-users yet.

5.1.1.2. Fast-FEA with automatic model generation for planning

There has been an extensive proposition to automate patient-specific fracture care (BMW grant: KF 2016102AK2)⁵⁰ and find the best implant design or configuration⁵¹ (Wittkowske et al., 2017). Strongly automated FE-models based on CT-voxels with high numbers of DOF have found their way into scientific research⁵². However, this approach using patient-specific finite element models turned out to be cumbersome, inefficient, unproductive and unattractive for non-scientific users and especially the target group of surgeons. Even when highly automated (voxel-hex elements directly from imaging

⁴⁹ MacLeod, Alisdair Roderick 2015. Modelling and optimising the mechanical behaviour of fractures treated with locking plates. <https://www.era.lib.ed.ac.uk/handle/1842/21693>, last accessed 19th September 2018.

⁵⁰ Federal Ministry of Economics and Technology BMWi Grant for research group of Computer Aided Plastic Surgery (CAPS) of Prof. Dr. med. Laszlo Kovacs (+4 companies, 2 hospitals): Osteosynthesis Project: Method for the patient-specific fracture care in the aging society, BMWi Nr.: KF 2016102AK2, Running time: 01.06.2012 – 30.11.2014
Research institutes: Klinik für Unfall- und Wiederherstellungschirurgie, Berufsgenossenschaftliche Klinik Tübingen (Leitung: Prof. Dr. U. Stöckle), Institut für Röntgendiagnostik, Klinikum rechts der Isar, TU München (Leitung: Prof. Dr. med. Ernst Rummeny)
Companies: CADFEM GmbH, Dynardo GmbH
Application partners: SYNTHES GmbH, Innomedic GmbH
https://www.caps.me.tum.de/index.php?id=38&tx_ttnews%5Btt_news%5D=55&cHash=18972d167fc0868b4e6eced869bd3623

Also compare:

https://www.dynardo.de/fileadmin/Material_Dynardo/bibliothek/WOST10/03_WOST2013_Optimization_Schimmelpfennig_Paper.pdf

⁵¹ Prof. Duda and I visited the group of Höntzsch, Stöckle, Döbele, Freude et. al. on 2/3 April 2014 and presented our first modeling results. At the time, we were unaware of the ongoing large FEA study on locking plates of the CAPS group, which clearly took place mostly in Munich.

⁵² Large-scale micro-finite element (μ FE) analysis: Levchuk, A., Zwahlen, A., Weigt, C., Lambers, F. M., Badilatti, S. D., Schulte, F. A., Kuhn, G. & Müller, R. (2014). The clinical biomechanics award 2012—presented by the European society of biomechanics: large scale simulations of trabecular bone adaptation to loading and treatment. *Clinical biomechanics*, 29(4), 355-362.

needing supercomputing time), this approach took a foothold only in few research settings. As a result, it is likely that only models that are more accessible to the surgeons as users⁵³ could possibly sustain a permanent place in fracture fixation planning. An additional requirement would be fast computation time to allow for different options that the surgeon may consider. Carlier et al. (2015a) attribute the lack of translation of computational models from bench to bed side to a number of barriers such as the mismatch between the open clinical questions and the current modeling efforts, the scarcity of patient-specific quantitative data and the lack of adequate model validation. Simplifying the modeling approaches using well-founded assumptions and winning surgeons as the direct operators with an immediate benefit for patients and surgeons might enable us to overcome these barriers. However, alongside streamlined mechanical models, for a more comprehensive approach, revised biological modeling will also have to be part of such a surgeon-operated simulation approach (Carlier et al., 2015b).

5.1.1.3. Guidelines from the literature

Based on *in vitro* experiments and FEA, Stoffel et al. (2003) give some advice for screw placement: In simple fractures with an interfragmentary gap smaller than 2 mm, one or even two plate holes near the fracture gap should be omitted to allow fracture motion and bone contact to occur. For comminuted fractures, they recommend three screws on either side of the fragment with two screws as close as practicable to the fracture site. In plate osteosynthesis of the humerus and the forearm, where mainly torsional load predominates, three to four screws in each main fragment are recommended, as torsional rigidity depends more on the number of screws than axial stiffness (Stoffel et al., 2003).

Empirical advice for instance for plate fixation has been derived⁵⁴. The suggestion of empiric indices such as screw density index (Cronier et al., 2010, Wagner and Frigg, 2006, Gautier and Sommer, 2003,

⁵³ The FE-Net (Thematic Network, funded by the European Commission) identified in 2005 already “that the use of analysis and simulation for bio-medical purposes is increasing dramatically but is still quite immature. In contrast to other industrial sectors most analysis work is carried out by “specialists” in consultancies, universities or research establishments and industrial “practises” are in there infancy. Nevertheless the potential benefits are substantial.” <https://www.nafems.org/about/projects/past-projects/fenet/industry/bio/>, last accessed 7 December 2018.
https://www.nafems.org/downloads/FENet_Meetings/St_Julians_Malta_May_2005/fenet_malta_may2005_bio_medical.pdf, last accessed 7 December 2018.

⁵⁴ Heyland, M. (2018). *Role of Screw Location, Screw Type and Plate Working Length! Podium presentation. Basic Science Focus Forum at the 2018 Annual Meeting of the Orthopaedic Trauma Association (OTA 2018), October 17-20, 2018, Kissimmee (Orlando area), Florida.* <https://ota.org/sites/files/2018->

Rozbruch et al., 1998), plate span width (bridge span or plate working length), total screw density, proximal screw density; or scores composed of those and other values such as a rigidity score (Rodriguez et al., 2016), do not systematically address the invariant values, so they are only valid in well-defined boundaries.

Optimization of fracture fixation requires device selection and configuration based on three key variables of interest (MacLeod et al., 2016a) under the presumption that the biological capacity is preserved:

- (1) interfragmentary movement (IFM), i.e. more specifically the movement components relative to the fracture geometry or even better local strain;
This enables to estimate the mechanical stimulus (or also disruption) of healing.
- (2) strain concentrations around screws;
This enables the estimation of screw subsidence, and screw/bone failure. Using locking screws, this point can be neglected assuming a minimal bone quality (MacLeod et al., 2016c, MacLeod et al., 2016a, MacLeod et al., 2014, MacLeod et al., 2012b).
- (3) stress levels within the implants (especially plate).
This enables estimation of implant ultimate and fatigue strength relative to time point of expected healing.

Patient-specific adaptation of fixation could be performed with the help of a decision making tree as a first step towards comprehensive guidelines which do not yet exist.

[08/PRF12%20%280807%29%20OTA%20AM18%20BSFF%20ONLINE%20Pgm.pdf](https://ota.org/education/meetings-and-courses/2018-annual-meeting/ota-business-meeting/annual-meeting-session), last accessed 30 November 2018.

Although there are recommendations for surgeons, there was a question from the auditorium for an optimal plate working length at the congress of the Orthopaedic Trauma Association 2018:

Plate working length is the main factor determining interfragmentary movement (IFM) for certain locking plate fixations, but the answer for an optimal plate working length is still complex and there is no automated procedure to come up with the answer yet. I am aware that at least one large orthopaedic company is developing an algorithm that considers IFM, but as long as parameter identification (especially load and fracture geometry, i.e. necessary decomposition of IFM into in-plane and out-of-plane-components) is insufficient, I do not believe such a solution alone can establish added value.

Compare Symposium 2 in <https://ota.org/education/meetings-and-courses/2018-annual-meeting/ota-business-meeting/annual-meeting-session>, last accessed 30 November 2018.

https://ota.org/sites/files/2018-10/Wed_Symp%202_Speaker%202_Heyland.pdf, last accessed 30 November 2018.

<https://ota.org/media/299090/4-plate-biomechanics.pdf>, last accessed 30 November 2018.

MacLeod and Pankaj (2018) suggest a planning algorithm that respects the mechanical boundaries or working principles of different fixation types and configurations in relation to certain fracture configurations. For instance, working length of locking plates can only realize its working principle of plate bending if there is bone-plate offset, as with a flush application, effective working length could be reduced to fracture gap size (Chao et al., 2013).

5.1.2. Adapted mechano-therapy for mechano-biologic stimulation

Fixation stiffness has been confirmed as a determining factor for fracture healing (Epari et al., 2007, Epari et al., 2006a) in a research setting, but is also becomes apparent in a clinical setting with the summarized mechanical construct characteristics into a rigidity score predisposing to non-union (Rodriguez et al., 2016). Modification of fixation configuration (MacLeod and Pankaj, 2018, Bartnikowski et al., 2017, Bartnikowski, 2016, Krishnakanth, 2012) or simple fracture gap tissue stiffness modification (e.g. using blot clots or polymer injections, or scaffolds) may control the fracture healing process through alteration of local mechanical stimulation (given intact biological potential). Furthermore, increased fluid flow could be achieved with other means such as a closed chamber (outer membrane) of varying pressure with valves or pores for fluid exchange, or electro-magnetic, or thermo-stimulation. However, such interventions or therapies should be planned and adapted to the specific environment.

Mehboob and Chang (2018) simulated the healing process of a fractured femoral shaft with different intramedullary nail materials and found that for a transverse fracture angle there is a dependency of callus stiffness increase on fracture location but not for the consistently well-healing oblique fracture: Mid-shaft fractures healed best and transverse distal femur shaft fractures healed worst. This underlines the clinical perception that distal femur fractures represent critical fracture type and locked plating has been suggested as a treatment option rather than the otherwise favored intramedullary nailing. However, when differentiating for fracture angle, nailing might be an option for steeply oblique distal femur fractures. Oblique fracture line plate fixation has been suggested to be less effective than transverse plate fixation (Mehboob and Chang, 2014, Son and Chang, 2013, Kim et al., 2011). For intramedullary nail fixation, transverse fracture line fixation has been suggested to be less effective than moderate oblique fracture line fixation in certain locations (Mehboob and Chang, 2018, Mehboob et al., 2013). As most fracture line slopes are associated to certain fracture locations, the association of fixation type plate/nail and fracture location might explain healing issues and successes in some cases.

A more comprehensive approach that considers the interfragmentary movement in early fracture healing under locking plate fixation could show that the average mechanical stimulation and dominant cell differentiation during the early stage of healing, at near cortex and far cortex depends on fractures size, bone-plate distance, and plate working length (Miramini et al., 2015a).

Viscoelastic tissue may operate like a sponge after being compressed and regaining the initial shape, pressure gradient may suck up solution with cells, growth factors and nutrients, binding to the extracellular matrix may occur and with a further load cycle wastes and substances that cannot bind may be flushed outside, this effect may also help with the mineralization (through dehydration). The relaxation time of the tissue would directly influence the fluid flow: when the tissue quickly relaxes, the fluid in-flow can be maximized. For maximum waste flush out, the loading phase should be long with a high peak or frequently repeated at an appropriate rate with a medium peak and sufficient time of unloading. Work from the Julius Wolff institute could show that cell spreading, proliferation, and osteogenic differentiation of mesenchymal stem cells (MSCs) are all enhanced in cells cultured in gels with faster relaxation (Chaudhuri et al., 2016) and this relaxation time may also regulate bone formation in vivo (Darnell et al., 2017). Bone scaffolds can be modified to conform with the predominant loads to optimize fluid flow. Loads might be adapted to optimize the flow for a current callus tissue stiffness.

5.1.3. Adapted mechano-therapy for implant survival

Locking plate fixations shows relative fragment rotation, which affects the local tissue deformation and callus formation. Callus formation is asymmetric with on average 64% more callus at the medial cortex than at the anterior or posterior cortices (Lujan et al., 2010), and compared with stainless steel plates, titanium plates had 76%, 71%, and 56% more callus at week 6, week 12, and week 24 (Lujan et al., 2010). There might exist a paradox behavior of a locking plate fixation that may allow a stiffer plate fixation to achieve medial bony support at comparably small loads, similar to a more flexible fixation, see Figure 8 in (Döbele et al., 2010). The early plateau of cis-cortical IFM with locking screws (due to medial bony support, Figure 5-1) strongly limits the mechanical stimulation, and may also lead to higher plate stresses compared to a more compliant fixation (MacLeod and Pankaj, 2018), Figure 1 there. This effect may become even more pronounced when considering the gap tissue: the bending axis (neutral axis) is not constant, but assuming a composite beam (plate-gap tissue) and applying Steiner's principle, the position of the neutral axis changes with the moduli of elasticity and areas of the cross-sections (Gautier et al., 2000), (F 2). Thus, a comparably stiff lateral fixation would shift the

bending axis towards the lateral surface of the bone, virtually bending almost around the neutral axis of the plate. A more flexible lateral fixation adjacent to comparably stiff gap tissue (large area) would leave the bending axis closer to the center of the bone. However, during bending with equal fracture gap size, rotation around a point at the surface of the bone or even further away with an offset, stiff plate requires much smaller angles until medial contact is reached than rotation around the center of bone.

Assuming for instance a transverse gap of $g=1\text{mm}$, a bone diameter $b=30\text{mm}$ and a shift of the neutral axis of the bone z . Case 1: z_1 half bone diameter plus plate-bone distance plus half plate thickness, $z_1=20\text{mm}$ or Case 2: z_2 to be half of (half bone diameter plus plate-bone distance plus half plate thickness), $z_2=10\text{mm}$. The maximum angle or rotation around the pivot with the shift z from the bone center that is needed for medial contact to occur can be given as:

$$\sin \alpha \approx \frac{g}{\frac{b}{2} + z}$$

For the example cases 1 and 2, the resulting maximum angles would be $\alpha_1=1.64$ degree and $\alpha_2= 2.29$ degree. It could be retorted that stiffer fixation yields higher total bending stiffness of the (composite bone-plate) beam, leading to smaller rotation angles. However, the difference in angular rotation due to shifted neutral axis has to be considered here as it shows a similar magnitude as the change in total bending stiffness. When gaps are bridged under load, the importance of the fixation stiffness for stimulation of secondary fracture healing diminishes drastically (Heyland et al., 2017).

Adapting mechano-therapy includes balancing the rate of nonunion and hardware failure. The surgeons can strongly influence when medial bony support can be expected: Rodriguez et al. (2014) report inter-institutional nonunion rates and interventions done for hardware failure during distal femoral fracture treatment. The time to intervention was longest (425 days) in the institution with the lowest nonunion rate (8.5%). This institution also had the most cases operated for hardware failure, so Rodriguez et al. (2014) suggest that this hospital's management approach tends towards longer waiting times and late intervention. Conversely, the institution with the highest nonunion rate (13.1%) had a shorter mean time to intervention (285 days) with most of these interventions for reasons other than hardware failure, suggesting according to Rodriguez et al. (2014) that at this institution surgeons may tend to intervene earlier, rather than waiting for late failure of hardware to occur. We would suggest the additional possibility that surgeons may favor certain fixation types. Either such fixations lead to bony support at low loads, unloading fixation implants through load-sharing (bony contact support, Figure 5-1), but limiting the gap tissue deformation (stimulation) or alternatively, surgeons may tend to favor fixations that lead to comparably large gap tissue

deformation even for elevated loads with large callus formation without bony support strongly loading fixation implants. This might be another option to explain the disparity and balance in non-union rate and hardware failure rate. A clear delineation should be developed when bony support e.g. through tilting segment contact or a scaffold/graft (i.e. medial strut) is needed. This is only possible when the consequences of fracture healing caused by gap tissue deformation are jointly evaluated together with implant stress⁵⁵.

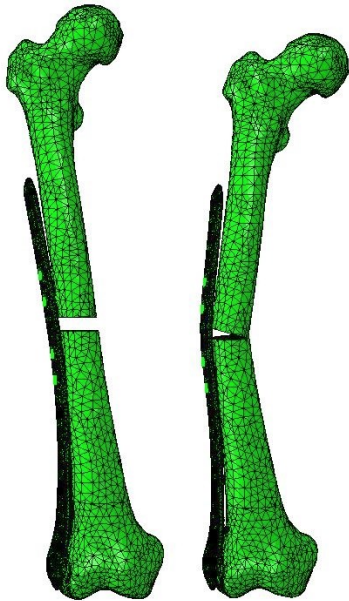


Figure 5-1: Locking plate placement laterally (left) may lead to medial bony support under load (right).

5.1.4. Recent evolution of fracture treatment concepts

In recent years, with the successful implementation of both standard compression and more and more options of locking fixation, there has been more and more confusion also leading to unclear treatment concepts using hybrid fixation. For instance Hanschen and Biberthaler (2013), Hanschen et al. (2014)

⁵⁵ The example (from 1.5.2) of plate material steel versus titanium with short-termed elevation of implant stress and increased tissue stimulation using titanium versus steel should be re-addressed here (MacLeod et al., 2015). To optimize implants in terms of (biomechanically tested) fatigue life implementing thicker, stiffer implants is unreasonable as it may impair the intended healing process and will eventually lead to failure anyhow. While experimental in vitro studies show that stiffer plates can bear more loading cycles, clinical results indicate that stiffer plate constructs tend to lead to plate failures. An explanation was suggested by MacLeod et al. (2015), MACLEOD, A. R., SIMPSON, H. & PANKAJ, P. 2015. In vitro testing of locking plate fracture fixation wrongly predicts the performance of different implant materials. *European Society of Biomechanics*. Prague, goo.gl/awmLYX. Stiffer constructs fail in the clinics, although in vitro the failure rate is lower than for more flexible plates, because in vitro there is less plate bending and lower strain for stiffer constructs. However, in the physiological setting such stiff plates maintain higher strain over a long time in later healing phases (load sharing with callus according to stiffness ratio). Additionally, there is the intensifying effect that more flexible plates lead to faster callus formation. At this point, it should be added that bony support and thus reduction of plate stress through load-sharing also has to be evaluated which has so not been done.

used lag screws for interfragmentary compression and a locking plate as a bridge plate and achieved best results with the stiffer configuration (poly-axial screw placement in stiffer NCB, Zimmer plate, versus parallel screws placement in LISS, Synthes plate). They fail to mention why this concept of absolute stability was chosen, and even worse, their description of “locking plates in distal femur fractures” suggests fixation for relative stability. They also discuss and reference “motion in the osteotomy gap” from another study.

Hybrid concepts (locking plate fixation + interfragmentary lag screw or locking fixation + non-locking plate screws or application of compression + positional screw) are very heterogeneous and need clarification and standardization in nomenclature and execution. Goswami et al. (2011) have shown that a locking screw near the fracture gap increased the axial and torsional strength of the locked plate system compared to a conventional screw. Surgeons have implemented this technique of mixing lag and locking screws in order to improve reduction and operation techniques (Wenger et al., 2017, Horn et al., 2011, Chung et al., 2016, Yang et al., 2015, Märdian et al., 2015b). However, only well-controlled experiments or clinical studies that report invariant values are still comparable, while most clinical studies are not. Mechanical conditions are not reported in sufficient detail within most clinical fracture fixation studies. As a result, despite strong interest and a clear need for improved fracture fixation, the development of “dynamic fixation” implants and fracture treatment concepts has not yielded significant improvements in recent years. Even worse, promising implant candidates that showed distinctly improved fracture healing in well-controlled animal experiments, often fail to perform superiorly in prospective human trials (Höntzsch et al., 2014, Kaspar et al., 2005). For all the known risk factors and the extensive armamentarium of surgeons, especially peri-prosthetic fractures still show a high variance in outcome.

5.1.5. Requirements for future principles of fracture fixation

As mentioned before, locking fixation may enable improved fixation strength in low to medium bone density due to its working principle. Kregor et al. (2004) found that locking screws could maintain distal femoral fixation without any loss of fixation in the distal femoral condyles in all 30 treated patients older than 65 years. This could eliminate one major factor of optimization of fracture fixation: no more need to check the screw-bone interface as long as patients or just areas with deficient bone quality are excluded. Given an initially safe implant stress, the optimization of interfragmentary movement components for fast healing might alleviate the need for dedicated implant stress evaluation. As with healing gap tissue, implant stress will continually decline sufficiently fast to avoid fatigue failure, even

if the endurance limit (plateau of the Wöhler curve after 10^6 to 10^7 load cycles) might be violated initially. Thus, for certain fracture fixations that remain to be delimited, only (initial) gap tissue deformation needs to be assessed in detail.

5.2. Outlook: Potential of osteosynthesis instrumentation

5.2.1. Adapted implant choice

New or better coordinated combinations of existing implants, such as interfragmentary lag screws, which can be used to reduce the fracture gap and maintain this reduction, in conjunction with locking plates (Chung et al., 2016) could gain more attention, as some interfragmentary displacement is allowed but restricted (Märdian et al., 2015b).

5.2.2. Adapted implant designs

Optimized mechano-biology (preserving cell-viability, creating mechanical stimulation) using optimized implants (for minimal tissue damage) and fixation strategies (for best stimulation) creates new opportunities. Plate stiffness, especially as part of a resulting construct stiffness, might be optimized already in clinical practice with less axial and more torsional/shear stiffness of the whole construct by distinct variation of plate material or PWL. Plate geometry could be adapted further to exhibit a high stiffness against twisting with pipe or tubular cross sections. Plate position (offset or more favorable inclination of plate to the axis of the bone leads to higher shear stiffness, (Krishnakanth, 2012), p. 77-8. Further options for an improved plate geometry & position together include helical plates winding around bone, which might furthermore represent an adaptation to individual (spiral) fracture lines (Krishna et al., 2008, Fernández, 2002). Combinations with lateral and helical plate (Perren et al., 2018), may improve safety of double plate fixation of comminuted or defect fractures for instance of the distal femur. Also, changes to the plate-screw interface, e.g. a permanently sliding interface in nails (Dailey et al., 2013, Dailey et al., 2012) or plates (Henschel et al., 2017, Madey et al., 2017, Bottlang et al., 2016) or even a self-dynamizable sliding screw (Mitković et al., 2017, Mitkovic et al., 2012) enables for more longitudinal relative motion of the fragments. However, for large defects or a high slope of the fracture line, we already stressed that this might be detrimental as it could be associated to elevated levels of shear. Current implants are insufficiently

characterized (3D-stiffness components, (Duda et al., 1998)), e.g. (Bottlang et al., 2016) and may function in a different manner than suggested in some physiological set-ups. Staggered screw arrangement (Denard et al., 2011) may help to minimize twisting of the plate (shear) without compromising axial interfragmentary movement.

Future adjustable or self-adjusting (modular) implants may also serve to minimize trauma through smaller surgical access and uniqueness of surgery due to automatic or controlled implant assembly or adjustment (unfolding or shaping) within the patient. According to the principle of a tiny cross-section balloon catheter could be filled within the patient to achieve an adjusted but durable fixation. There might not even be the need for additional surgery to remove/add a screw etc. for dynamization/additional clinical stabilization later on (as some the filling material might be removed through a valve at a certain time point). Therapeutic potential of magnesium ions from degrading implants has been shown (Zhang et al., 2016). This improved biological potential could potentially be employed using magnesium plate plugs that may initially serve as spacers to avoid bone-plate contact when using bridging plates and allow for free bending of the plate when loaded, then degrade, improve fracture healing, allow late plate-bone contact (at higher loads) and eventually even allow easier plate removal. Shape memory implants with a temperature-change induced change of structure have already been tried in a research setting, i.e. for an adaptable stiffness (Decker et al., 2015, Müller et al., 2015, Pfeifer et al., 2013, Determann, 2016) or creating interfragmentary compression (Tarniță et al., 2010).

5.2.3. Active implants for mechano-biologic stimulation

Other implants using sensors and potentially actuators might follow next to implants that monitor the healing process with telemetric systems (Faschingbauer et al., 2007, Seide et al., 2012, Fountain et al., 2015, Windolf et al., 2014). This would allow for an adapted tissue stimulation, and examples for this could be either a direct stimulation approach using for instance ultrasound (low-intensity pulsed ultrasound: LIPUS). Such a direct stimulation can actively deform the tissue periodically with an attachment device to the fixation; or an indirect approach could be implemented influencing the patient activities' dynamics with variable implant stiffness (for instance strain-rate dependent stiffness using a non-Newtonian fluid or changing fixation implant characteristics such as material degradation). Such novel implants may also allow for desired and adapted dynamization⁵⁶ (Wolter et al., 1999) or

⁵⁶ Dynamization in medical terms refers to a method or strategy that increases interfragmentary movement or compressive loading to promote bone healing in fractures. This can be achieved for instance by removing selected screws or changing the fixation altogether.

(after initial osteogenic differentiation in a sizable callus) inverse dynamization (decreasing movement), either actively using actuators or passively converting muscle and joint forces using the (directional) implant stiffness (components) as a control factor as suggested (Epari et al., 2007, Epari et al., 2013).

5.3. Concept: Comprehensive, coherent mechano-therapy with dynamic fixation

At this point, there is no ultimate solution to all problems of fracture fixation even with intact biological potential, as the fixation always has to be adapted to the specific conditions. We could show that those mechanical boundary conditions include fracture angle (slope and orientation) as well as fracture gap size, expected amount and quality of loading (weight bearing), bony contact support or presence of a graft (such as medial strut support) or scaffold of relevant stiffness. The different qualities of tissue deformation need to be considered in detail, i.e. cyclic volume-changing moderate movement enhances secondary fracture healing while shear should be minimized. Fortunately, the in-plane or out-of-plane components of interfragmentary movement correlate to the helpful normal strain and the harmful distortional strain of the regenerative tissue respectively. Thus, an estimation of those components opens opportunities for improving the fracture healing process further, as long as biological regenerative capacity remains sufficient.

5.3.1. Preserving the regenerative capacity

Fixation in compression for the clinical principle of absolute stability (meaning rigid fixation for direct, primary fracture healing) is a superior principle of fracture healing in simple fractures with sufficient bone quality. However, the reproducibility of compression is most certainly low in some specific cases as the amount of compression is not quantified at this point in the clinics and loss of compression may result in major complications. This kind of rigid fixation has a larger margin of error particularly if bone quality (low density, little bone mass) or regenerative biological capacity is compromised. Then interfragmentary compression is not very robust. On the other hand, the indications and correct utilization of locking plates for locations such as proximal humerus, distal radius, and distal femur and for osteoporotic bone are important to understand so locking fixation is not used inappropriately (Scolaro and Jaimo Ahn, 2011, Schmidt, 2010, Smith et al., 2008). However, the use of locking fixation may enable the protection of the living tissue with smaller access, minimal touch and preservation of cell viability. On the other hand, measures to enhance regenerative capacity from the realm of tissue

engineering and cell therapy may further improve healing, but we believe that such approaches also always require an adequate mechanical environment.

5.3.2. Stimulating the healing process

The clear delimitation of different treatable fractures has to be elaborated on. So far, too many fractures are treated in a standard fashion, a few of which would require different or additional care. Most delayed unions or non-unions can be treated successfully if there is a mechanical cause (Giannoudis et al., 2015). However, despite additional care, large defects are still associated with deficient success rates. A closer look at the fundamental mechanical boundary conditions as well as the biological potential may institute new approaches that directly address healing issues. As an example, we could show that fractures at the femur with fracture lines that run from proximal lateral anterior to distal medial posterior can be mechano-biologically optimized by screw placement, i.e. plate working length, which may thus lead to faster and robust healing results. In contrast, fractures with proximal medial posterior to distal lateral anterior fracture lines see more shear independent of load or locking plate fixation and this shear delays healing and induces a larger callus. Although this dependency of relative movement components on fracture geometry might seem trivial, and is already considered in the Pauwel's classification at the proximal femur (Wang et al., 2016, Parker and Dynan, 1998), it is not implemented for other locations than the proximal femur. Even worse, its validity might even be disputed in some cases (Parker and Dynan, 1998). For a more systematic approach to the stimulation of the fracture healing process, invariant strain, or at least interfragmentary in-plane and out-of-plane components should be evaluated and reported. The different options such as conventional and locking plate, or locking, lag, and dynamic locking screw, for fracture fixation offer a sufficiently rich tool box to surgeons that should be exploited in line with the other mechanical boundary conditions, so that the local tissue strain is optimized.

5.3.3. Avoiding implant and bone failure

When interfragmentary compression cannot be achieved reliably, i.e. that primary healing cannot be achieved safely, then in the presence of a fracture gap, adjusted mechano-therapy should occur. The risk of implant or bone failure versus the stimulation of the gap tissue needs to be balanced. The choice and placement of fracture fixation determines all those risks, but those risks also depend on fracture localization and characteristics. For instance, MacLeod and Pankaj (2018) suggest to use a lower plate

working length (bridge span) for large fracture gaps to reduce plate stress in a bone plate system where no interfragmentary contact can occur (the plate is supporting all applied loads). For a small gap, they suggest to use the load sharing resulting in lower plate stresses with larger working length. We would add here to look out for a suitable tissue stimulation (deformation with minimal shear, but moderate compression). Different variables on plate stress and tissue deformation have to be considered together including: bone-plate offset, fracture gap size and working length (MacLeod and Pankaj, 2018), Figure 8 there. In some cases of large gaps (e.g. after tumor resection) or high loads (e.g. high BMI-patients), additional fixation using grafts, scaffolds or even double plating are necessary to achieve sufficient construct strength. In those cases, stimulation can hardly be ideal, but as long as it remains tolerable, healing may still occur.

5.3.4. Achieving and verifying fracture healing results

Diagnostic markers such as groups of cells (Reinke et al., 2013), molecules (Pountos et al., 2013, Sousa et al., 2015) or genes (Dimitriou et al., 2011, Dimitriou et al., 2013) have been suggested to monitor fracture healing and healing outcome. The mechanical environment in form of adequate stimulation has been playing a neglected role, because the mechanical therapy (mechano-therapeutics) was either already sufficiently successful (such as for most fractures that heal sufficiently swift and reliably) or it was circumvented using rigid osteosynthesis (such as shear-susceptible fracture for instance at the femoral neck). Modern dynamic fixation may provide auxiliary options for further improvement, but their development has been empirical so far. Insights into the working principles of mechano-biology form the basis for target-oriented mechano-therapeutics. Known mechanical factors that influence the biological healing cascade should be reported more frequently and standardized in biological experiments to achieve more consistent results (Reifenrath et al., 2014). However, when biological results such as diagnostic markers are identified, care should be taken before they are directly applied to clinical trauma cases, because the variance in mechanical stimulation will fluctuate much more than in the research setting. Only a comprehensive approach that recognizes the connections of sub-systems such as generally described by the diamond concept (Willie et al., 2010, Giannoudis et al., 2007) can satisfactorily identify the sensitivity of diagnostic markers and therapeutic interventions. As a result, fracture healing has to be monitored using different modalities such as radiological imaging, functional assessment, clinical examination, and laboratory (marker) tests. The full picture can only be obtained if the range of parameters is at least roughly known. However, problematic issues may be identified for a few parameter thresholds or combinations of critical parameters. Thus, a prediction of

healing outcome or more accurately assessment of risk does not necessitate an overly complex approach, because the system is quite robust itself.

5.2.4. Standardization of modeling and virtual implant testing

Standardization in computational modeling studies in the bio-medical field, especially orthopedics, is still in its infancy with few, quite recent and quite general guidelines of researchers (Erdemir et al., 2012, Viceconti et al., 2005, Pankaj, 2013, Poelert et al., 2013) and regulatory bodies (<https://www.fda.gov/downloads/MedicalDevices/DeviceRegulationandGuidance/GuidanceDocuments/UCM381813.pdf>, last accessed 7 December 2018.). However, such guidance for model creation and reporting does not specifically consider the paradox behavior when healing tissue properties are considered: The healing tissue properties play a crucial role in the assessment of the final outcome as the fatigue limit of for instance locked plate constructs equaled 1.9 times body weight for an average 70-kg patient over a simulated 10-week postoperative course while distal femoral loads during gait have been estimated to be more than 2 times body weight (Granata et al., 2012). The comparison of numerical simulations with clinical case studies of healing bones under unilateral fixation suggests that the use of computational strategies shows potential in pre-clinical testing of fixation devices and configurations (Comiskey, 2010). Such software solutions could be used for risk assessment of known complications and estimation of the rate of healing. However, a comprehensive approach has to be followed considering mechano-biology, otherwise for instance thicker plates are favored for higher fatigue life (Grujicic et al., 2010) which is not needed or even counterproductive if the fracture healing progresses through proper tissue strain with slimmer plates.

Additionally, material and interaction considerations such as corrosion must be included in the safety, efficacy and longevity assessment of the fracture fixation systems (Thapa et al., 2015).

The development of further standards of computational modeling in the bio-medical field is highly needed.

Summary

While mechanical overloading caused a fracture, well-controlled mechanical loading can be an integral part of a coordinated fracture healing process. The relative movement of fracture segments affects tissue strain close to the fracture and thus controls the healing pathway. More specifically, moderate hydrostatic or volumetric strain improves osteogenic development while high distortional or deviatoric strain impairs the healing process. Strain is often not directly accessible, but fortunately in-fracture-plane and out-of-fracture-plane interfragmentary movement relative to gap volume correlate to the harmful and beneficial strain respectively. The locking plate configuration, i.e. specifically the screw location and screw type, and most importantly plate working length (bridge span) determine the interfragmentary movement as long as bony contact bridging can be neglected. With a plate-bone clearance and for large or comminuted gaps, the total amount of interfragmentary movement can be controlled. However, the components of in-plate and out-of-plane movement are coupled: Large transverse defects cannot be fixated with locking plates alone because a large plate working length leads to high shear compared to axial interfragmentary movement. Furthermore, the relative amount of shear strain to normal strain is determined by fracture configuration (gap size, comminution, slope as well as orientation of fracture lines). Small gaps up to 3mm can be fixated with locking plates reliably, but also for such small gaps, the optimal mechano-biology can only be achieved for certain orientations of the fracture lines (proximal lateral anterior to distal medial posterior). Fracture lines running proximal medial posterior to distal lateral anterior might need more adapted fixation. Furthermore, as soon as bony support occurs, e.g. with bone fragment to bone fragment contact under load or bridging with a graft or scaffold or bridging of the stiffening healing tissue, the importance of fixation stiffness diminishes dramatically.

Analyzing individual case settings could allow for pre- or intra-operative planning for a certain fracture gap size and fracture line to find an individual fixation setting, which might be derived computationally. Finite element modeling of individual cases is possible, but the degree of process automation and the need for interpretation are currently barriers for a clinical use. A faster and easier tool for surgeon users is needed. The control of total interfragmentary movement can be achieved with screw positioning: Adjusting plate working length leads to increased axial interfragmentary movement, but even more increased shear in the presence of a gap. If stimulation within the desired range cannot be achieved, there are further options such as dynamic locking screws or active plates with sliding elements. If secondary fracture healing still cannot be expected before implant failure, bony contact support under load should be considered, which is also possible with a graft or scaffold. For small gaps, reduction using a lag screw and fixation with a neutralization locking plate are currently covered topics. For large gaps, double plating and additional scaffolding are currently under investigation. There should be sufficient options to treat most fractures already, but the selection procedure depends on the estimation of implant fatigue strength versus fracture healing speed. Additional opportunities for an acceleration of fracture healing with further reduction of shear have been identified.

Zusammenfassung

Während mechanische Überlastung zu einer Fraktur führt, kann eine kontrollierte mechanische Belastung ein integraler Bestandteil eines koordinierten Frakturheilungsprozesses sein. Die Relativbewegung der Fraktursegmente beeinflusst die Gewebeerformung nahe der Fraktur und steuert somit den Heilungsprozess. Insbesondere verbessert eine moderate hydrostatische oder volumetrische Verformung die osteogene Entwicklung, während eine hohe verzerrende Verformung die Heilung verlangsamt. Die Gewebeerformung ist oft nicht direkt erfassbar, aber glücklicherweise entsprechen die interfragmentären Bewegungen tangential zur Bruchebene und normal der Bruchebene relativ zum Spaltvolumen der schädlichen bzw. vorteilhaften Verformungsstimulation. Die Konfiguration winkelstabiler Verriegelungsplatten, d. h. insbesondere die Schraubenposition und der Schraubentyp, und vor allem die Plattenschwingstrecke (Überbrückungsspanne oder freie Biegelänge) bestimmen die interfragmentäre Bewegung, solange die knöchernen Kontaktüberbrückung vernachlässigt werden kann. Mit einem Platten-Knochen-Abstand und bei großem Frakturspalt oder Trümmerbruch kann der Betrag der interfragmentären Bewegung gesteuert werden. Die Komponenten der Bewegung tangential und normal der Frakturebene sind jedoch gekoppelt: Große transverse Defekte können nicht allein mit winkelstabilen Platten fixiert werden, da eine große Arbeitslänge der Platte im Vergleich zu einer axialen interfragmentären Bewegung zu einer hohen Scherung führt. Darüber hinaus wird der relative Betrag der Scherung zur normalen Dehnung durch die Bruchkonfiguration (Spaltgröße, Spaltanzahl bei Trümmerfrakturen, Steigung sowie Orientierung der Bruchlinien) bestimmt. Kleine Spalte von bis zu 3 mm können mit winkelstabilen Verriegelungsplatten zuverlässig fixiert werden, aber auch für solche kleinen Spalte kann die optimale Mechanobiologie nur für bestimmte Orientierungen der Frakturlinien (proximal lateral anterior nach distal medial posterior) erreicht werden. Frakturlinien, die proximal medial posterior nach distal lateral anterior verlaufen, müssen möglicherweise angepasst versorgt werden. Sobald eine knöchernen Abstützung auftritt, also wenn ein Knochenfragment mit dem anderen Knochenfragment unter Belastung Kontakt aufnimmt, oder die Segmente durch Überbrückung mit einem Transplantat oder Gerüst (Scaffold) oder durch versteiftes neues Gewebes verbunden ist, nimmt der Einfluss der Fixationssteifigkeit auf den weiteren Heilungsverlauf dramatisch ab. Durch Analyse individueller Fallparameter könnte eine prä- oder intraoperative Planung für eine bestimmte Frakturspaltgröße und Frakturlinie vorgenommen werden, um eine spezifische Fixation zu finden, die rechnerisch abgeleitet werden kann. Die Finite-Elemente-Modellierung von Einzelfällen ist möglich, aber der Grad der Prozessautomatisierung und der Interpretationsbedarf sind derzeit Hindernisse für eine klinische Anwendung. Ein schnelleres und einfacheres Werkzeug für Chirurgen als direkte Nutzer ist erforderlich. Die Steuerung des Betrags der interfragmentären Bewegung kann durch Schraubenpositionierung erreicht werden: Durch das Einstellen der Arbeitslänge der Platte wird die axiale interfragmentäre Bewegung erhöht, die Scherkraft jedoch noch stärker erhöht, solange ein Spalt vorhanden bleibt. Wenn die Verformungsstimulation den gewünschten Bereich nicht erreicht, gibt es weitere Optionen wie dynamische Verriegelungsschrauben oder „aktive“ Platten mit Gleitelementen. Wenn vor dem erwarteten Implantatversagen keine sekundäre Frakturheilung zu erwarten ist, sollte eine knöchernen Abstützung unter Last in Betracht gezogen werden, die auch mit einem Transplantat oder Gerüst möglich ist. Bei kleinem Spalt werden derzeit die Reduktion mit einer Zugschraube und die Fixierung mit einer Neutralisationsplatte diskutiert. Bei großem Spalt werden derzeit Doppelplattenfixationen und zusätzliche Scaffolds untersucht. Es sollten bereits ausreichend Optionen vorhanden sein, um die meisten Frakturen zu behandeln. Das Auswahlverfahren hängt jedoch von der Einschätzung der Implantatermüdung im Verhältnis zur Heilungsgeschwindigkeit der Frakturen ab. Zusätzliche Möglichkeiten für eine Beschleunigung der Frakturheilung mit weiterer Verringerung der Scherung wurden identifiziert.

Danksagung

Mein ausgesprochener Dank für die Möglichkeiten, die sich mir eröffnet haben, geht natürlich an Georg Duda und Manfred Zehn. Für die klinische Zusammenarbeit bedanke ich mich bei Gabriele Rußow, Sven Märdian, Klaus-Dieter Schaser, Norbert Haas und Michael Schütz, und auch bei den weiteren klinischen Kollegen. Vielen Dank vor allem an Patrick Strube und Christian Kleber für deren Unterstützung. Ich möchte mich bei Gerd Diederichs bedanken für die Aufklärung der Frage nach dem CT-Phantom, dass sich als Standard-Phantom entpuppte. Vielen Dank für die Unterstützung auch an Annette Bowitz und Anne Zergiebel mit den Arbeiten im Archiv.

Eine besondere Anerkennung der Unterstützung gebührt auch meinen direkten Kollegen Adam Trepczynski, Alexey Sharenkov, Alison Agres, Philippe Moewis, Heide Boeth und allen anderen, die mich im Büro über die Zeit begleitet haben, z.B. Yanlin Zhong, Shuyang Han, Myriam Cilla, Peter Raffalt, Leonie Krahl, Sónia Alves, Maria Neutzner, Thomas Neitmann, sowie allen anderen.

Ich möchte mich bedanken bei Markus O. Heller, der mich eingestellt hat und immer noch sporadisch ein freundlicher Gesprächspartner ist, und auch bei Berry Pöpplau, die ich beide zu Anfang noch kurz kennenlernen durfte. Thank you to William R. (Bill) Taylor, who always had and still has an open ear for new ideas and keeps giving inspiration in passing. Vielen Dank richte ich auch an Hajar Razi, und Edoardo Borgiani, Sara Checa und die weiteren Kollegen und Ex-Kollegen vom Standort Campus Virchow Klinikum. Beim Zuse Institut Berlin bedanke ich mich besonders bei Moritz Ehlke und Stefan Zachow. Vielen Dank an Manav Mehta und Daniel Toben mit denen meine Zeit beim Julius Wolff Institut begonnen hat.

Ich möchte den Einsatz von Sebastian Gühring würdigen, der uns ermöglicht hat das Tübinger Pontos System in Innsbruck zu nutzen. An dieser Stelle geht auch mein Dank an Dankward Höntzsch, Sebastian Döbele, und die weiteren Kollegen der BG-Unfallklinik Tübingen für Ihren wertvollen Input zur Diskussion, und ihr PONTOS System für die Messungen in Innsbruck, aber ganz besonders schätze ich die Gastfreundschaft die uns in Tübingen zuteilwurde. Ich danke Werner Schmölz und der Unfallchirurgie der Universitätskliniken Innsbruck für die Möglichkeit Laborversuche dort durchzuführen. Ein Dankeschön geht auch an Jan-Erik Ode (ehemals Hoffmann) für die Einarbeitung in das Biomechanik-Labor des Julius Wolff Instituts und an Alexander Schill und Dag Wulsten für Rat und Tat.

My gratitude is due to Peter Varga for helping me with input for the initial modeling, especially concerning material properties in FEA and boundary conditions for validation studies.

I'd like to express my appreciation for the work of Alisdair MacLeod and thank him for the talks we had.

Daniel Andermatt, Stefan Dudé, und André Weber von DepuySynthes möchte ich für die technische Unterstützung danken.

Curriculum Vitae

A brief curriculum vitae is contained in the printed version.

Ein Kurzlebenslauf ist in der gedruckten Version enthalten.

PhD Portfolio

Publications

2013 or earlier

Mehta, M., Lienau, J., Heyland, M., Woloszyk, A., Fratzl, P., & Duda, G. (2010). Quantitative spatio-temporal callus patterning during bone defect healing using 4D monitoring. *Bone*, 47, S101-2.

Mehta, M., Checa, S., Lienau, J., Hutmacher, D., & Duda, G. N. (2012). In vivo tracking of segmental bone defect healing reveals that callus patterning is related to early mechanical stimuli. *Eur Cell Mater*, 24, 358-71. (Acknowledged M. Heyland).
<http://www.ecmjournal.org/papers/vol024/vol024a26.php>

Frisch, J. T. (2012). *Frakturheilung bei Immuninsuffizienz* (Doctoral dissertation, Freie Universität Berlin). (Acknowledged M. Heyland)

El Khassawna, M. S. T. (2013). *Cellular and molecular analysis of fracture healing in a neurofibromatosis type 1 conditional knockout mice model* (Doctoral dissertation, Humboldt-Universität zu Berlin). (Acknowledged M. Heyland)

Heyland, M., Mehta, M., Toben, D., & Duda, G. N. (2013). Microstructure and homogeneity of distribution of mineralized struts determine callus strength. *Eur Cell Mater*, 25, 366-79.

2014

Heyland, M., Duda, G. N., Trepczynski, A., Dudé, S., Weber, A., Schaser, K.-D. & Märdian, S. (2014). Winkelstabile Plattenfixation für typische Problemfrakturen des distalen Femur: in silico Analyse verschiedener Schraubenauswahl und -belegungen um die Osteosynthesesteifigkeit zu kontrollieren. Podium presentation. Deutscher Kongress für Orthopädie und Unfallchirurgie (DKOU 2014) 28.10. - 31.10.2014, Berlin. <http://www.egms.de/static/en/meetings/dkou2014/14dkou073.shtml>

Heyland, M., Duda, G. N., Trepczynski, A., Schaser, K.-D. & Märdian, S. (2014). Locking plate osteosynthesis fixation configurations for typical problem fractures of the distal femur: in silico analysis of different simulated screw selection and placement to control osteosynthesis stiffness. Poster. 7th World Congress of Biomechanics (WCB 2014), July 6-11 2014, Boston.

2015

Heyland, M., Trepczynski, A., Duda, G. N., Zehn, M., Schaser, K.-D., & Märdian, S. (2015). Selecting boundary conditions in physiological strain analysis of the femur: Balanced loads, inertia relief method and follower load. *Medical engineering & physics*, 37(12), 1180-5.

Märdian, S., Schaser, K. D., Duda, G. N., & Heyland, M. (2015). Working length of locking plates determines interfragmentary movement in distal femur fractures under physiological loading. *Clinical biomechanics* (Bristol, Avon), 30(4), 391-6.

Heyland, M., Duda, G. N., Haas, N. P., Trepczynski, A., Döbele, S., Höntzsch, D., Schaser, K.-D. & Märdian, S. (2015). Semi-rigid screws provide an auxiliary option to plate working length to control interfragmentary movement in locking plate fixation at the distal femur. *Injury*, 46, S24-S32.

Ehlke, M., Heyland, M., Märdian, S., Duda, G. N., & Zachow, S. (2015). Assessing the relative positioning of an osteosynthesis plate to the patient-specific femoral shape from plain 2D radiographs. Podium presentation. Proceedings of the 15th Annual Meeting of CAOS-International, June 17-20, 2015, Vancouver. [http://www.caos-international.org/2015/papers/CAOS%202015%20-%20Paper%20%20\(71\).pdf](http://www.caos-international.org/2015/papers/CAOS%202015%20-%20Paper%20%20(71).pdf)

Ehlke, M., Heyland, M., Märdian, S., Duda, G. N., & Zachow, S. (2015). 3D Assessment of Osteosynthesis based on 2D Radiographs. Podium presentation by Stefan Zachow. 14. Jahrestagung der Deutschen Gesellschaft für Computer- und Roboterassistierte Chirurgie (CURAC 2015), September 17-19 2015, Bremen. https://opus4.kobv.de/opus4-zib/files/5621/ZIBReport_15-47.pdf

Heyland, M., Duda, G. N., Schmoelz, W., Schaser, K.-D. & Märdian, S. (2015). Mechanical behavior of different locking plate fracture fixation options at the distal femur. Poster. 21st Congress of the European Society of Biomechanics (ESB 2015), July 5-8 2015, Prague.

2016

Heyland, M., Duda, G. N., Schaser, K.-D., Schmoelz, W. & Märdian, S. (2016). Finite element (FE) analysis of locking plate fixation is a valid method for predicting interfragmentary movement. Podium presentation. 22nd Congress of the European Society of Biomechanics (ESB 2016), July 10-13 2016, Lyon.

Heyland, M., Duda, G. N., Schwabe, P. & Märdian, S. (2016). Influence of fracture angle on interfragmentary movement. Podium presentation. 22nd Congress of the European Society of Biomechanics (ESB 2016), July 10-13 2016, Lyon.

Märdian, S., Schmoelz, W., Schaser, K.-D., Duda, G. N. & Heyland, M. (2016). Interfragmentäre Zugschrauben reduzieren insbesondere die Scherbewegung bei winkelstabiler Plattenfixierung einfacher Femurfrakturen. Podium presentation. Deutscher Kongress für Orthopädie und Unfallchirurgie (DKOU 2016) 25.10. - 28.10.2016, Berlin. <https://www.egms.de/static/en/meetings/dkou2016/16dkou481.shtml>

2017

Heyland, M., Duda, G. N., Märdian, S., Schütz, M. & Windolf, M. (2017). Stahl oder Titan bei der Osteosynthese. *Der Unfallchirurg*, 120(2), 103-109.

Märdian, S., Duda, G. N., Schwabe, P., Moewis, P., Cilla, M. & Heyland, M. (2017). [Interprosthetic zone – what is biomechanically safe?] Interprothetische Zone – Wie viel ist biomechanisch sicher genug? Podium presentation. Endoprothesenkongress 16.–18. February 2017, Berlin.

Heyland, M., Duda, G.N., Urda, A. L., Cilla, M. & Märdian, S. (2017). Fracture risk for ipsilateral stemmed implants. Podium presentation. 23rd Congress of the European Society of Biomechanics (ESB), Seville (Spain).

Heyland, M., Duda, G. N., Urda, A. L., Cilla, M. & Märdian, S. (2017). Analytische Modellvorhersage des interprothetischen Fraktur-Risikos. Podium presentation. Deutscher Kongress für Orthopädie und Unfallchirurgie (DKOU 2017) 24.10. - 27.10.2017, Berlin. <https://www.egms.de/static/de/meetings/dkou2017/17dkou123.shtml>

2018

Heyland, M. (2018). Brief Commentary on Mechano-Biological Fixation. Journal of investigative surgery: the official journal of the Academy of Surgical Research, 1-2.

*Heyland, M., Bähr, A., Duda, G. N. & Märdian, S. (2018). Femur anatomy features in structural analysis: the position of Trochanter major as a risk factor for periprosthetic femoral shaft fractures? Poster. 8th World Congress of Biomechanics (WCB 2018), July 8-12 2018, Dublin.
<https://app.oxfordabstracts.com/stages/123/programme-builder/submission/20085>*

*Heyland, M., Märdian, S. & Duda, G. N. (2018). Peri-prosthetic fracture risk assessment during sideways falling: An iterative, multi-factorial analytical approach isolating individual parameter influence. Poster. 8th World Congress of Biomechanics (WCB 2018), July 8-12 2018, Dublin.
<https://app.oxfordabstracts.com/stages/123/programme-builder/submission/20079>*

*Heyland, M. (2018). Role of Screw Location, Screw Type and Plate Working Length! Podium presentation. Basic Science Focus Forum at the 2018 Annual Meeting of the Orthopaedic Trauma Association (OTA 2018), October 17-20, 2018, Kissimmee (Orlando area), Florida.
<https://ota.org/sites/files/2018-08/PRF12%20%280807%29%20OTA%20AM18%20BSFF%20ONLINE%20Pgm.pdf>*

Heyland, M., Märdian, S. & Duda, G. N. (2018). Periprosthetisches Fraktur-Risiko beim seitlichen Sturz: Multifaktorieller, analytischer Ansatz zur Isolation des Einflusses individueller Parameter. Podium presentation. Deutscher Kongress für Orthopädie und Unfallchirurgie (DKOU 2018) 23.10. - 26.10.2018, Berlin. <https://www.eqms.de/static/en/meetings/dkou2018/18dkou252.shtml>

Heyland, M., Checa, S., Kendoff, D. & Duda, G. N. (2018). Anatomic grooved stem mitigates strain shielding compared to established total hip arthroplasty stem designs in finite-element models. Scientific Reports, [In Print].

2019

Märdian, S., Seemann, R., Schmidt-Bleek, K., Heyland, M. & Duda, G. (2019). [Biology and Biomechanics of Fracture Healing and Fracture Fixation] Biologie und Biomechanik der Frakturheilung und Osteosynthese. Orthopädie und Unfallchirurgie up2date, 2-2019, 1-21 [In Print].

Rußow, G., Heyland, M., Märdian, S., Duda, G. N. (2019). [Bone fracture healing and clinical loading stability] Knochenbruchheilung und klinische Belastungsstabilität, OP-JOURNAL 2019; 35: 1-9 [In Print].

Awards

European Society of Biomechanics Travel Award 2018

Patents

Heyland, M., Strube, P., Mehta, M. & Duda, G. (2012-11-14). Facet joint prosthesis. DE102012220808A1, WO2014076084A1.

Membership in professional societies

European Society of Biomechanics (ESB), <https://esbiomech.org/>

Deutsche Gesellschaft für Biomechanik (DGfB), <http://bio-mechanik.org>

References

- AHMAD, M., NANDA, R., BAJWA, A., CANDAL-COUTO, J., GREEN, S. & HUI, A. 2007. Biomechanical testing of the locking compression plate: when does the distance between bone and implant significantly reduce construct stability? *Injury*, 38, 358-64.
- AL-AHAIDEB, A., QUINN, A., SMITH, E., YACH, J., ELLIS, R. & PICHORA, D. 2009. Computer assisted LISS plate placement: an in vitro study. *Comput Aided Surg*, 14, 123-6.
- ALIERTA, J., PÉREZ, M. & GARCÍA-AZNAR, J. 2014. An interface finite element model can be used to predict healing outcome of bone fractures. *J Mech Behav Biomed Mater*, 29, 328-38.
- ALIERTA, J., PÉREZ, M., SERAL, B. & GARCÍA-AZNAR, J. 2016. Biomechanical assessment and clinical analysis of different intramedullary nailing systems for oblique fractures. *Comput Methods Biomech Biomed Engin*, 19, 1266-77.
- ANDERSEN, D. J., BLAIR, W. F., STEVERS JR, C. M., ADAMS, B. D., EL-KHOURI, G. Y. & BRANDSER, E. A. 1996. Classification of distal radius fractures: an analysis of interobserver reliability and intraobserver reproducibility. *J Hand Surg Am*, 21, 574-82.
- ANITHA, D., DAS DE, S., SUN, K. K., DOSHI, H. K. & LEE, T. 2015. Improving stability of locking compression plates through a design modification: a computational investigation. *Comput Methods Biomech Biomed Engin*, 18, 153-61.
- ARNONE, J. C., EL-GIZAWY, A. S., CRIST, B. D., DELLA ROCCA, G. J. & WARD, C. V. 2013. Computer-Aided Engineering Approach for Parametric Investigation of Locked Plating Systems Design. *J Med Devices* 7, 021001-8.
- ARO, H. T. & CHAO, E. Y. 1993. Bone-healing patterns affected by loading, fracture fragment stability, fracture type, and fracture site compression. *Clin Orthop Relat Res*, 293, 8-17.
- ARO, H. T., WAHNER, H. T. & CHAO, E. Y. 1991. Healing patterns of transverse and oblique osteotomies in the canine tibia under external fixation. *J Orthop Trauma*, 5, 351-64.
- AUGAT, P., BURGER, J., SCHORLEMMER, S., HENKE, T., PERAUS, M. & CLAES, L. 2003. Shear movement at the fracture site delays healing in a diaphyseal fracture model. *J Orthopaed Res*, 21, 1011-7.
- AUGAT, P., FASCHINGBAUER, M., SEIDE, K., TOBITA, K., CALLARY, S., SOLOMON, L. & HOLSTEIN, J. 2014. Biomechanical methods for the assessment of fracture repair. *Injury*, 45 Suppl 2, S32-8.
- AUGAT, P., MARGEVICIUS, K., SIMON, J., WOLF, S., SUGER, G. & CLAES, L. 1998. Local tissue properties in bone healing: influence of size and stability of the osteotomy gap. *J Orthop Res*, 16, 475-81.
- AUGAT, P., PENZKOFER, R., NOLTE, A., MAIER, M., PANZER, S., V OLDENBURG, G., PUESCHL, K., SIMON, U. & BÜHREN, V. 2008. Interfragmentary movement in diaphyseal tibia fractures fixed with locked intramedullary nails. *Journal of orthopaedic trauma*, 22, 30-36.
- AUGAT, P., SIMON, U., LIEDERT, A. & CLAES, L. 2005. Mechanics and mechano-biology of fracture healing in normal and osteoporotic bone. *Osteoporos Int*, 16 Suppl 2, S36-43.
- AUGAT, P. & VON RÜDEN, C. 2018. Evolution of fracture treatment with bone plates. *Injury*, 49, S2-S7.
- BACA, V., HORAK, Z., MIKULENKA, P. & DZUPA, V. 2008. Comparison of an inhomogeneous orthotropic and isotropic material models used for FE analyses. *Med Eng Phys*, 30, 924-30.
- BARTNIKOWSKI, N., CLAES, L. E., KOVAL, L., GLATT, V., BINDL, R., STECK, R., IGNATIUS, A., SCHUETZ, M. A. & EPARI, D. R. 2017. Modulation of fixation stiffness from flexible to stiff in a rat model of bone healing. *Acta Orthop*, 88, 217-22.
- BARTNIKOWSKI, N. J. 2016. *Modifying fixation stiffness to improve bone healing*. PhD PhD, Queensland University of Technology.
- BAYOGLU, R. & OKYAR, A. F. 2015. Implementation of boundary conditions in modeling the femur is critical for the evaluation of distal intramedullary nailing. *Med Eng Phys*, 37, 1053-60.

- BEINGESSNER, D., MOON, E., BAREI, D. & MORSHED, S. 2011. Biomechanical analysis of the less invasive stabilization system for mechanically unstable fractures of the distal femur: comparison of titanium versus stainless steel and bicortical versus unicortical fixation. *J Trauma*, 71, 620-4.
- BEKLER, H., BULUT, G., USTA, M., GOKCE, A., OKYAR, F. & BEYZADEOGLU, T. 2008. The contribution of locked screw-plate fixation with varying angle configurations to stability of osteoporotic fractures: an experimental study. *Acta Orthop Traumatol Turc*, 42, 125-9.
- BELLAPIANTA, J., DOW, K., PALLOTTA, N. A., HOSPODAR, P. P., UHL, R. L. & LEDET, E. H. 2011. Threaded screw head inserts improve locking plate biomechanical properties. *Journal of orthopaedic trauma*, 25, 65-71.
- BELTRAN, M. J., GARY, J. L. & COLLINGE, C. A. 2015. Management of distal femur fractures with modern plates and nails: state of the art. *J Orthop Trauma*, 29, 165-72.
- BERGMANN, G., BENDER, A., GRAICHEN, F., DYMKE, J., ROHLMANN, A., TREPCZYNSKI, A., HELLER, M. O. & KUTZNER, I. 2014. Standardized loads acting in knee implants. *PLoS One*, 9, e86035.
- BERGMANN, G., DEURETZBACHER, G., HELLER, M., GRAICHEN, F., ROHLMANN, A., STRAUSS, J. & DUDA, G. 2001. Hip contact forces and gait patterns from routine activities. *J Biomech*, 34, 859-71.
- BERGMANN, G., GRAICHEN, F., ROHLMANN, A., BENDER, A., HEINLEIN, B., DUDA, G., HELLER, M. & MORLOCK, M. 2010. Realistic loads for testing hip implants. *Biomed Mater Eng*, 20, 65-75.
- BETTS, D. C. & MÜLLER, R. 2014. Mechanical regulation of bone regeneration: theories, models, and experiments. *Front Endocrinol (Lausanne)*, 5, 211.
- BHANDARI, M., FONG, K., SPRAGUE, S., WILLIAMS, D. & PETRISOR, B. 2012. Variability in the definition and perceived causes of delayed unions and nonunions: a cross-sectional, multinational survey of orthopaedic surgeons. *J Bone Joint Surg Am*, 94, e1091-6.
- BIELER, F. H. 2011. *Angiogenic Potential of Mesenchymal Cells and T Lymphocytes Induced by Mechanical Stimuli that Improve Bone Healing - An In Vitro 2D and 3D Bioreactor Study*. Dr.-Ing. Doctoral Thesis, Technische Universität Berlin.
- BORGIANI, E., DUDA, G., WILLIE, B. & CHECA, S. 2015. Bone healing in mice: Does it follow generic mechano-regulation rules? *Facta Universitatis, Series: Mechanical Engineering*, 13, 217-27.
- BOTTLANG, M., DOORNINK, J., LUJAN, T. J., FITZPATRICK, D. C., MARSH, J. L., AUGAT, P., VON RECHENBERG, B., LESSER, M. & MADEY, S. M. 2010. Effects of construct stiffness on healing of fractures stabilized with locking plates. *J Bone Joint Surg Am*, 92 Suppl 2, 12-22.
- BOTTLANG, M. & FEIST, F. 2011. Biomechanics of far cortical locking. *J Orthop Trauma*, 25 Suppl 1, S21-8.
- BOTTLANG, M., TSAI, S., BLIVEN, E. K., VON RECHENBERG, B., KLEIN, K., AUGAT, P., HENSCHER, J., FITZPATRICK, D. C. & MADEY, S. M. 2016. Dynamic stabilization with active locking plates delivers faster, stronger, and more symmetric fracture-healing. *J Bone Joint Surg Am*, 98, 466-74.
- BOYER, K. A., ANDRIACCHI, T. P. & BEAUPRE, G. S. 2012. The role of physical activity in changes in walking mechanics with age. *Gait Posture*, 36, 149-53.
- BRAUN, B. J., BUSHUVEN, E., HELL, R., VEITH, N. T., BUSCHBAUM, J., HOLSTEIN, J. H. & POHLEMANN, T. 2016. A novel tool for continuous fracture aftercare—Clinical feasibility and first results of a new telemetric gait analysis insole. *Injury*, 47, 490-4.
- BUTTON, G., WOLINSKY, P. & HAK, D. 2004. Failure of less invasive stabilization system plates in the distal femur: a report of four cases. *J Orthop Trauma*, 18, 565-70.
- BYRNE, D. P., LACROIX, D. & PRENDERGAST, P. J. 2011. Simulation of fracture healing in the tibia: mechanoregulation of cell activity using a lattice modeling approach. *J Orthop Res*, 29, 1496-503.
- CALORI, G., COLOMBO, M., MAZZA, E., MAZZOLA, S., MALAGOLI, E., MARELLI, N. & CORRADI, A. 2014. Validation of the Non-Union Scoring System in 300 long bone non-unions. *Injury*, 45 Suppl 6, S93-7.

- CALORI, G. M., PHILLIPS, M., JEETLE, S., TAGLIABUE, L. & GIANNOUDIS, P. 2008. Classification of non-union: need for a new scoring system? *Injury*, 39 Suppl 2, S59-63.
- CARLIER, A., GERIS, L., LAMMENS, J. & VAN OOSTERWYCK, H. 2015a. Bringing computational models of bone regeneration to the clinic. *Wiley Interdiscip Rev Syst Biol Med*, 7, 183-94.
- CARLIER, A., LAMMENS, J., OOSTERWYCK, H. & GERIS, L. 2015b. Computational modeling of bone fracture non-unions: four clinically relevant case studies. *In Silico Cell Tissue Sci*, 2, 1.
- CHAO, E., INOUE, N., KOO, T. K. K. & KIM, Y. H. 2004. Biomechanical considerations of fracture treatment and bone quality maintenance in elderly patients and patients with osteoporosis. *Clin Orthop Relat Res*, 425, 12-25.
- CHAO, P., CONRAD, B. P., LEWIS, D. D., HORODYSKI, M. & POZZI, A. 2013. Effect of plate working length on plate stiffness and cyclic fatigue life in a cadaveric femoral fracture gap model stabilized with a 12-hole 2.4 mm locking compression plate. *BMC Vet Res*, 9, 125.
- CHAUDHURI, O., GU, L., KLUMPERS, D., DARNELL, M., BENCHERIF, S. A., WEAVER, J. C., HUEBSCH, N., LEE, H. P., LIPPENS, E., DUDA, G. N. & MOONEY, D. J. 2016. Hydrogels with tunable stress relaxation regulate stem cell fate and activity. *Nat Mater*, 15, 326-34.
- CHECA, S., PRENDERGAST, P. J. & DUDA, G. N. 2011. Inter-species investigation of the mechano-regulation of bone healing: comparison of secondary bone healing in sheep and rat. *J Biomech*, 44, 1237-45.
- CHEN, G., SCHMUTZ, B., WULLSCHLEGER, M., PEARCY, M. & SCHUETZ, M. 2010. Computational investigations of mechanical failures of internal plate fixation. *Proceedings of the Institution of Mechanical Engineers, Part H: Journal of Engineering in Medicine*, 224, 119-126.
- CHEN, G., WU, F. Y., ZHANG, J. Q., ZHONG, G. Q. & LIU, F. 2015. Sensitivities of biomechanical assessment methods for fracture healing of long bones. *Med Eng Phys*, 37, 650-6.
- CHEN, X., HE, K. & CHEN, Z. 2017. A novel computer-aided approach for parametric investigation of custom design of fracture fixation plates. *Comput Math Methods Med*, 2017, 7372496.
- CHUNG, J. Y., CHO, J. H., KWEON, H. J. & SONG, H. K. 2016. The use of interfragmentary positional screw in minimally invasive plate osteosynthesis for simple distal femur fractures in elderly patients: A retrospective, single-centre pilot study. *Injury*, 47, 2795-9.
- CLAES, L. 2006. Biologie und Biomechanik der Osteosynthese und Frakturheilung. *Orthopädie und Unfallchirurgie up2date*, 1, 329-341.
- CLAES, L. 2011. Biomechanical principles and mechanobiologic aspects of flexible and locked plating. *J Orthop Trauma*, 25 Suppl 1, S4-7.
- CLAES, L. 2017a. Mechanobiologie der Frakturheilung Teil 1. *Der Unfallchirurg*, 120, 14-22.
- CLAES, L. 2017b. Mechanobiologie der Frakturheilung Teil 2. *Der Unfallchirurg*, 120, 23-31.
- CLAES, L. 2018. [Dynamization of fracture fixation : Timing and methods]. *Unfallchirurg*, 121, 3-9.
- CLAES, L., AUGAT, P., SUGER, G. & WILKE, H.-J. 1997. Influence of size and stability of the osteotomy gap on the success of fracture healing. *J Orthop Res*, 15, 577-84.
- CLAES, L., BLAKYTTY, R., GÖCKELMANN, M., SCHOEN, M., IGNATIUS, A. & WILLIE, B. 2009. Early dynamization by reduced fixation stiffness does not improve fracture healing in a rat femoral osteotomy model. *J Orthop Res*, 27, 22-7.
- CLAES, L., ECKERT-HÜBNER, K. & AUGAT, P. 2002. The effect of mechanical stability on local vascularization and tissue differentiation in callus healing. *J Orthop Res*, 20, 1099-105.
- CLAES, L., ECKERT-HÜBNER, K. & AUGAT, P. 2003. The fracture gap size influences the local vascularization and tissue differentiation in callus healing. *Langenbecks Arch Surg*, 388, 316-22.
- CLAES, L., RECKNAGEL, S. & IGNATIUS, A. 2012. Fracture healing under healthy and inflammatory conditions. *Nat Rev Rheumatol*, 8, 133-43.
- CLAES, L., WILKE, H., AUGAT, P., RÜBENACKER, S. & MARGEVICIUS, K. 1995. Effect of dynamization on gap healing of diaphyseal fractures under external fixation. *Clin Biomech (Bristol, Avon)*, 10, 227-34.
- CLAES, L. E. & HEIGELE, C. A. 1999. Magnitudes of local stress and strain along bony surfaces predict the course and type of fracture healing. *J Biomech*, 32, 255-66.

- CLAES, L. E., HEIGELE, C. A., NEIDLINGER-WILKE, C., KASPAR, D., SEIDL, W., MARGEVICIUS, K. J. & AUGAT, P. 1998. Effects of mechanical factors on the fracture healing process. *Clin Orthop Relat Res*, 355 Suppl, S132-47.
- COLLINGE, C. A., GARDNER, M. J. & CRIST, B. D. 2011. Pitfalls in the application of distal femur plates for fractures. *J Orthop Trauma*, 25, 695-706.
- COMISKEY, D. 2010. *Predictive modelling of the form and development of bone fracture healing*. PhD, Dublin City University.
- COMISKEY, D., MACDONALD, B., MCCARTNEY, W., SYNNOTT, K. & O'BYRNE, J. 2012. Predicting the external formation of a bone fracture callus: an optimisation approach. *Comput Methods Biomech Biomed Engin*, 15, 779-85.
- COMISKEY, D., MACDONALD, B., MCCARTNEY, W., SYNNOTT, K. & O'BYRNE, J. 2010. The role of interfragmentary strain on the rate of bone healing—A new interpretation and mathematical model. *J Biomech*, 43, 2830-4.
- COMISKEY, D., MACDONALD, B., MCCARTNEY, W., SYNNOTT, K. & O'BYRNE, J. 2013. Predicting the external formation of callus tissues in oblique bone fractures: idealised and clinical case studies. *Biomech Model Mechanobiol*, 12, 1277-82.
- CORRALES, L. A., MORSHED, S., BHANDARI, M. & MICLAU, T. 2008. Variability in the assessment of fracture-healing in orthopaedic trauma studies. *J Bone Joint Surg Am*, 90, 1862-8.
- COURT-BROWN, C. M. & CAESAR, B. 2006. Epidemiology of adult fractures: A review. *Injury*, 37, 691-7.
- COWIN, S. C. & MEHRABADI, M. M. 1989. Identification of the elastic symmetry of bone and other materials. *J Biomech*, 22, 503-15.
- CRISTOFOLINI, L., SCHILEO, E., JUSZCZYK, M., TADDEI, F., MARTELLI, S. & VICECONTI, M. 2010. Mechanical testing of bones: the positive synergy of finite–element models and in vitro experiments. *Philos Trans A Math Phys Eng Sci*, 368, 2725-63.
- CRONIER, P., PIETU, G., DUJARDIN, C., BIGORRE, N., DUCELLIER, F. & GERARD, R. 2010. The concept of locking plates. *Orthop Traumatol Surg Res*, 96, S17-S36.
- CUADRADO, A., YÁNEZ, A., CARTA, J. A. & GARCÉS, G. 2013. Suitability of DCPs with Screw Locking Elements to allow sufficient interfragmentary motion to promote secondary bone healing of osteoporotic fractures. *Med Eng Phys*, 35, 852-9.
- CUI, S., BLEDSOE, J. G., ISRAEL, H., WATSON, J. T. & CANNADA, L. K. 2014. Locked plating of comminuted distal femur fractures: does unlocked screw placement affect stability and failure? *J Orthop Trauma*, 28, 90-6.
- CURREY, J. D. 2002. *Bones: structure and mechanics*, Princeton, New Jersey., Princeton University Press.
- D'LIMA, D. D., FREGLY, B. J., PATIL, S., STEKLOV, N. & COLWELL, C. W., JR. 2012. Knee joint forces: prediction, measurement, and significance. *Proc Inst Mech Eng H*, 226, 95-102.
- DAILEY, H. L., DALY, C. J., GALBRAITH, J. G., CRONIN, M. & HARTY, J. A. 2012. A novel intramedullary nail for micromotion stimulation of tibial fractures. *Clin Biomech (Bristol, Avon)*, 27, 182-8.
- DAILEY, H. L., DALY, C. J., GALBRAITH, J. G., CRONIN, M. & HARTY, J. A. 2013. The Flexible Axial Stimulation (FAST) intramedullary nail provides interfragmentary micromotion and enhanced torsional stability. *Clin Biomech (Bristol, Avon)*, 28, 579-85.
- DALSTROM, D. J., NELLES, D. B., PATEL, V., GOSWAMI, T., MARKERT, R. J. & PRAYSON, M. J. 2012. The protective effect of locking screw placement on nonlocking screw extraction torque in an osteoporotic supracondylar femur fracture model. *J Orthop Trauma*, 26, 523-7.
- DAMM, P., SCHWACHMEYER, V., DYMKE, J., BENDER, A. & BERGMANN, G. 2013. In vivo hip joint loads during three methods of walking with forearm crutches. *Clin Biomech (Bristol, Avon)*, 28, 530-5.
- DARNELL, M., YOUNG, S., GU, L., SHAH, N., LIPPENS, E., WEAVER, J., DUDA, G. & MOONEY, D. 2017. Substrate Stress-Relaxation Regulates Scaffold Remodeling and Bone Formation In Vivo. *Adv Healthc Mater*, 6, 1601185.

- DECKER, S., KRÄMER, M., MARTEN, A.-K., PFEIFER, R., WESLING, V., NEUNABER, C., HURSCHLER, C., KRETTEK, C. & MÜLLER, C. W. 2015. A nickel-titanium shape memory alloy plate for contactless inverse dynamization after internal fixation in a sheep tibia fracture model: A pilot study. *Technol Health Care*, 23, 463-74.
- DENARD, P. J., DOORNINK, J., PHELAN, D., MADEY, S. M., FITZPATRICK, D. C. & BOTTLANG, M. 2011. Biplanar fixation of a locking plate in the diaphysis improves construct strength. *Clin Biomech (Bristol, Avon)*, 26, 484-90.
- DETERMANN, I. 2016. *Beeinflussung der Knochenheilung durch Implantate mit variabler Steifigkeit auf Basis von Formgedächtnislegierungen: Untersuchung der Steifigkeitsänderung und deren Auswirkung auf die Frakturheilung durch kontaktfreie elektromagnetische Induktion im Schafmodell*. Dr. med. vet., Hannover, Tierärztliche Hochsch., Diss., 2016.
- DIMITRIOU, R., CARR, I. M., WEST, R. M., MARKHAM, A. F. & GIANNOUDIS, P. V. 2011. Genetic predisposition to fracture non-union: a case control study of a preliminary single nucleotide polymorphisms analysis of the BMP pathway. *BMC Musculoskelet Disord*, 12, 44.
- DIMITRIOU, R., KANAKARIS, N., SOUCACOS, P. & GIANNOUDIS, P. 2013. Genetic predisposition to non-union: evidence today. *Injury*, 44 Suppl 1, S50-3.
- DÖBELE, S., GARDNER, M., SCHRÖTER, S., HÖNTZSCH, D., STÖCKLE, U. & FREUDE, T. 2014. DLS 5.0-the biomechanical effects of dynamic locking screws. *PLoS One*, 9, e91933.
- DÖBELE, S., HORN, C., EICHHORN, S., BUCHHOLTZ, A., LENICH, A., BURGKART, R., NÜSSLER, A. K., LUCKE, M., ANDERMATT, D. & KOCH, R. 2010. The dynamic locking screw (DLS) can increase interfragmentary motion on the near cortex of locked plating constructs by reducing the axial stiffness. *Langenbecks Arch Surg*, 395, 421-8.
- DÖBELE, S., SCHRÖTER, S., HÖNTZSCH, D., STÖCKLE, U. & FREUDE, T. 2012a. Dynamic Locking Screw-DLS. *Op-Journal*, 28, 174-7.
- DÖBELE, S., SIEBENLIST, S., VESTER, H., WOLF, P., HAGN, U., SCHREIBER, U., STÖCKLE, U. & LUCKE, M. 2012b. New method for detection of complex 3D fracture motion-Verification of an optical motion analysis system for biomechanical studies. *BMC Musculoskelet Disord*, 13, 33.
- DOBLARÉ, M., GARCÍA, J. & GÓMEZ, M. 2004. Modelling bone tissue fracture and healing: a review. *Eng Fract Mech*, 71, 1809-40.
- DOCUMENTATION ABAQUS 6.8 2008. 11.1 Inertia relief. *Abaqus Analysis User's Manual 6.8*.
- DONALDSON, L. J., COOK, A. & THOMSON, R. G. 1990. Incidence of fractures in a geographically defined population. *J Epidemiol Community Health*, 44, 241-5.
- DOORNINK, J., FITZPATRICK, D. C., BOLDHAUS, S., MADEY, S. M. & BOTTLANG, M. 2010. Effects of hybrid plating with locked and nonlocked screws on the strength of locked plating constructs in the osteoporotic diaphysis. *J Trauma*, 69, 411-7.
- DOORNINK, J., FITZPATRICK, D. C., MADEY, S. M. & BOTTLANG, M. 2011. Far cortical locking enables flexible fixation with periarticular locking plates. *J Orthop Trauma*, 25 Suppl 1, S29-34.
- DROSOS, G., BISHAY, M., KARNEZIS, I. & ALEGAKIS, A. 2006. Factors affecting fracture healing after intramedullary nailing of the tibial diaphysis for closed and grade I open fractures. *J Bone Joint Surg Br*, 88, 227-31.
- DUDA, G. N., BARTMEYER, B., SPORRER, S., TAYLOR, W. R., RASCHKE, M. & HAAS, N. P. 2003a. Does partial weight bearing unload a healing bone in external ring fixation? *Langenbecks Arch Surg*, 388, 298-304.
- DUDA, G. N., KIRCHNER, H., WILKE, H. J. & CLAES, L. 1998. A method to determine the 3-D stiffness of fracture fixation devices and its application to predict inter-fragmentary movement. *J Biomech*, 31, 247-52.
- DUDA, G. N., MALDONADO, Z. M., KLEIN, P., HELLER, M. O., BURNS, J. & BAIL, H. 2005. On the influence of mechanical conditions in osteochondral defect healing. *J Biomech*, 38, 843-51.
- DUDA, G. N., MANDRUZZATO, F., HELLER, M., GOLDHAHN, J., MOSER, R., HEHLI, M., CLAES, L. & HAAS, N. P. 2001. Mechanical boundary conditions of fracture healing: borderline indications in the treatment of unreamed tibial nailing. *J Biomech*, 34, 639-50.

- DUDA, G. N., MANDRUZZATO, F., HELLER, M., KASSI, J. P., KHODADADYAN, C. & HAAS, N. P. 2002. Mechanical conditions in the internal stabilization of proximal tibial defects. *Clin Biomech (Bristol, Avon)*, 17, 64-72.
- DUDA, G. N., SPORRER, S., SOLLMANN, M., HOFFMANN, J. E., KASSI, J.-P., KHODADADYAN, C. & RASCHKE, M. 2003b. Interfragmentary movements in the early phase of healing in distraction and correction osteotomies stabilized with ring fixators. *Langenbecks Arch Surg*, 387, 433-40.
- DUFFY, P., TRASK, K., HENNIGAR, A., BARRON, L., LEIGHTON, R. K. & DUNBAR, M. J. 2006. Assessment of fragment micromotion in distal femur fracture fixation with RSA. *Clin Orthop Relat Res*, 448, 105-13.
- EBERLE, S., GABEL, J., HUNGERER, S., HOFFMANN, S., PÄTZOLD, R., AUGAT, P. & BÜHREN, V. 2012. Auxiliary locking plate improves fracture stability and healing in intertrochanteric fractures fixated by intramedullary nail. *Clin Biomech (Bristol, Avon)*, 27, 1006-10.
- EBERT, J. R., ACKLAND, T. R., LLOYD, D. G. & WOOD, D. J. 2008. Accuracy of partial weight bearing after autologous chondrocyte implantation. *Arch Phys Med Rehabil*, 89, 1528-34.
- EGOL, K. A., KUBIAK, E. N., FULKERSON, E., KUMMER, F. J. & KOVAL, K. J. 2004. Biomechanics of locked plates and screws. *J Orthop Trauma*, 18, 488-93.
- EHLINGER, M., DUCROT, G., ADAM, P. & BONNOMET, F. 2013. Distal femur fractures. Surgical techniques and a review of the literature. *Orthop Traumatol Surg Res*, 99, 353-60.
- EHLKE, M., HEYLAND, M., MÄRDIAN, S., DUDA, G. N. & ZACHOW, S. 2015. Assessing the Relative Positioning of an Osteosynthesis Plate to the Patient-Specific Femoral Shape from Plain 2D Radiographs. *ZIB-Report* [Online]. Available: <https://opus4.kobv.de/opus4-zib/frontdoor/index/index/docId/5426>.
- EINHORN, T. A. 1995. Enhancement of fracture-healing. *J Bone Joint Surg Am*, 77, 940-56.
- EINHORN, T. A. 1998. The cell and molecular biology of fracture healing. *Clin Orthop Relat Res*, 357, 7-21.
- ELKINS, J., MARSH, J. L., LUJAN, T., PEINDL, R., KELLAM, J., ANDERSON, D. D. & LACK, W. 2016. Motion Predicts Clinical Callus Formation: Construct-Specific Finite Element Analysis of Supracondylar Femoral Fractures. *J Bone Joint Surg Am*, 98, 276-84.
- ELLIOTT, D., NEWMAN, K., FORWARD, D., HAHN, D., OLLIVERE, B., KOJIMA, K., HANDLEY, R., ROSSITER, N., WIXTED, J., SMITH, R. & MORAN, C. 2016. A unified theory of bone healing and nonunion: BHN theory. *Bone Joint J*, 98-B, 884-91.
- EPARI, D., WEHNER, T., IGNATIUS, A., SCHUETZ, M. & CLAES, L. 2013. A case for optimising fracture healing through inverse dynamization. *Med Hypotheses*, 81, 225-7.
- EPARI, D. R., KASSI, J. P., SCHELL, H. & DUDA, G. N. 2007. Timely fracture-healing requires optimization of axial fixation stability. *J Bone Joint Surg Am*, 89, 1575-85.
- EPARI, D. R., SCHELL, H., BAIL, H. J. & DUDA, G. N. 2006a. Instability prolongs the chondral phase during bone healing in sheep. *Bone*, 38, 864-70.
- EPARI, D. R., TAYLOR, W. R., HELLER, M. O. & DUDA, G. N. 2006b. Mechanical conditions in the initial phase of bone healing. *Clin Biomech (Bristol, Avon)*, 21, 646-55.
- ERDEMIR, A., GUESS, T. M., HALLORAN, J., TADEPALLI, S. C. & MORRISON, T. M. 2012. Considerations for reporting finite element analysis studies in biomechanics. *J Biomech*, 45, 625-33.
- ETCHELS, L. W. 2014. *Optimisation Of Fixation Methods For Vancouver Type B2 And B3 Periprosthetic Femoral Fracture Treatment*. PhD, University of Leeds.
- FASCHINGBAUER, M., SEIDE, K., WEINRICH, N., WACKENHUT, F., WURM, M., GILLE, J., JÜRGENS, C. & MÜLLER, J. 2007. Fixateur interne mit Telemetriesystem. *Trauma Berufskr*, 9, 88-97.
- FELSENBERG, D. 2001. Struktur und Funktion des Knochens: Stützwerk aus Kollagen und Hydroxylapatit. *Pharm in uns Zeit*, 30, 488-94.
- FERGUSON, S., WYSS, U. & PICHORA, D. 1996. Finite element stress analysis of a hybrid fracture fixation plate. *Med Eng Phys*, 18, 241-50.
- FERNÁNDEZ, D. O. A. 2002. The principle of helical implants. Unusual ideas worth considering. *Injury*, 33, SA1.

- FIROOZABADI, R., MCDONALD, E., NGUYEN, T., BUCKLEY, J. & KANDEMIR, U. 2012. Does plugging unused combination screw holes improve the fatigue life of fixation with locking plates in comminuted supracondylar fractures of the femur? *J Bone Joint Surg Br*, 94, 241-8.
- FITZPATRICK, D. C., DOORNINK, J., MADEY, S. M. & BOTTLANG, M. 2009. Relative stability of conventional and locked plating fixation in a model of the osteoporotic femoral diaphysis. *Clin Biomech (Bristol, Avon)*, 24, 203-9.
- FOUNTAIN, S., WINDOLF, M., HENKEL, J., TAVAKOLI, A., SCHUETZ, M. A., HUTMACHER, D. W. & EPARI, D. R. 2015. Monitoring Healing Progression and Characterizing the Mechanical Environment in Preclinical Models for Bone Tissue Engineering. *Tissue Eng Part B Rev*, 22, 47-57.
- FRATZL, P. & GUPTA, H. S. 2007. Nanoscale mechanisms of bone deformation and fracture. In: BÄUERLEIN, E. (ed.) *Handbook of Biomineralization: Biological Aspects and Structure Formation*. Weinheim: Wiley-VCH.
- FRATZL, P. & WEINKAMER, R. 2007. Nature's hierarchical materials. *Prog Mater Sci*, 52, 1263-1334.
- FREEMAN, A. L., TORNETTA III, P., SCHMIDT, A., BECHTOLD, J., RICCI, W. & FLEMING, M. 2010. How much do locked screws add to the fixation of "hybrid" plate constructs in osteoporotic bone? *J Orthop Trauma*, 24, 163-9.
- FREGELY, B. J., BESIER, T. F., LLOYD, D. G., DELP, S. L., BANKS, S. A., PANDY, M. G. & D'LIMA, D. D. 2012. Grand challenge competition to predict in vivo knee loads. *J Orthop Res*, 30, 503-13.
- FREUDE, T., SCHRÖTER, S., GONSER, C. E., STÖCKLE, U., ACKLIN, Y. P., HÖNTZSCH, D. & DÖBELE, S. 2014. Controlled dynamic stability as the next step in "biologic plate osteosynthesis" - a pilot prospective observational cohort study in 34 patients with distal tibia fractures. *Patient Saf Surg*, 8, 3.
- FREUDE, T., SCHRÖTER, S., KRAUS, T., HÖNTZSCH, D., STÖCKLE, U. & DÖBELE, S. 2013. [Dynamic locking screw 5.0-first clinical experience]. *Z Orthop Unfall*, 151, 284-90.
- FRIGG, R. 2001. Locking Compression Plate (LCP). An osteosynthesis plate based on the Dynamic Compression Plate and the Point Contact Fixator (PC-Fix). *Injury*, 32 Suppl 2, 63-6.
- FRIGG, R. 2003. Development of the locking compression plate. *Injury*, 34 Suppl 2, B6-10.
- FRIGG, R., APPENZELLER, A., CHRISTENSEN, R., FRENK, A., GILBERT, S. & SCHAVAN, R. 2001. The development of the distal femur Less Invasive Stabilization System (LISS). *Injury*, 32 Suppl 3, SC24-31.
- FULKERSON, E., EGOL, K. A., KUBIAK, E. N., LIPORACE, F., KUMMER, F. J. & KOVAL, K. J. 2006. Fixation of diaphyseal fractures with a segmental defect: a biomechanical comparison of locked and conventional plating techniques. *J Trauma*, 60, 830-5.
- GANSE, B., YANG, P.-F., GARDLO, J., GAUGER, P., KRIECHBAUMER, A., PAPE, H.-C., KOY, T., MÜLLER, L.-P. & RITTEWEGER, J. 2016. Partial weight bearing of the tibia. *Injury*, 47, 1777-82.
- GARCÍA-AZNAR, J. M., KUIPER, J. H., GÓMEZ-BENITO, M. J., DOBLARÉ, M. & RICHARDSON, J. B. 2007. Computational simulation of fracture healing: Influence of interfragmentary movement on the callus growth. *J Biomech*, 40, 1467-76.
- GARDNER, M. J., NORK, S. E., HUBER, P. & KRIEG, J. C. 2009. Stiffness modulation of locking plate constructs using near cortical slotted holes: a preliminary study. *J Orthop Trauma*, 23, 281-7.
- GARDNER, M. J., NORK, S. E., HUBER, P. & KRIEG, J. C. 2010. Less rigid stable fracture fixation in osteoporotic bone using locked plates with near cortical slots. *Injury*, 41, 652-6.
- GAUTIER, E., PERREN, S. & CORDEY, J. 2000. Effect of plate position relative to bending direction on the rigidity of a plate osteosynthesis. A theoretical analysis. *Injury*, 31 Suppl 3, C14-20.
- GAUTIER, E. & SOMMER, C. 2003. Guidelines for the clinical application of the LCP. *Injury*, 34 Suppl 2, B63-76.
- GERIS, L., REED, A. A., VANDER SLOTEN, J., SIMPSON, A. H. R. & VAN OOSTERWYCK, H. 2010a. Occurrence and treatment of bone atrophic non-unions investigated by an integrative approach. *PLoS Comput Biol*, 6, e1000915.

- GERIS, L., SLOTEN, J. V. & VAN OOSTERWYCK, H. 2010b. Connecting biology and mechanics in fracture healing: an integrated mathematical modeling framework for the study of nonunions. *Biomech Model Mechanobiol*, 9, 713-24.
- GERIS, L., VANDAMME, K., NAERT, I., SLOTEN, J. V., VAN OOSTERWYCK, H. & DUYCK, J. 2010c. Mechanical loading affects angiogenesis and osteogenesis in an in vivo bone chamber: a modeling study. *Tissue Eng Part A*, 16, 3353-61.
- GIANNOUDIS, P. V., EINHORN, T. A. & MARSH, D. 2007. Fracture healing: the diamond concept. *Injury*, 38 Suppl 4, S3-6.
- GIANNOUDIS, P. V. & GIANNOUDIS, V. P. 2017. Far cortical locking and active plating concepts: New revolutions of fracture fixation in the waiting? *Injury*, 48, 2615-8.
- GIANNOUDIS, P. V., GUDIPATI, S., HARWOOD, P. & KANAKARIS, N. K. 2015. Long bone non-unions treated with the diamond concept: a case series of 64 patients. *Injury*, 46 Suppl 8, S48-54.
- GÓMEZ-BENITO, M. J., GARCÍA-AZNAR, J. M., KUIPER, J. H. & DOBLARÉ, M. 2005. Influence of fracture gap size on the pattern of long bone healing: a computational study. *J Theor Biol*, 235, 105-19.
- GOODSHIP, A. & KENWRIGHT, J. 1985. The influence of induced micromovement upon the healing of experimental tibial fractures. *J Bone Joint Surg Br*, 67, 650-5.
- GOODSHIP, A. E., CUNNINGHAM, J. L. & KENWRIGHT, J. 1998. Strain rate and timing of stimulation in mechanical modulation of fracture healing. *Clin Orthop Relat Res*, 355 Suppl, S105-15.
- GOSWAMI, T., PATEL, V., DALSTROM, D. J. & PRAYSON, M. J. 2011. Mechanical evaluation of fourth-generation composite femur hybrid locking plate constructs. *J Mater Sci Mater Med*, 22, 2139-46.
- GRANATA, J. D., LITSKY, A. S., LUSTENBERGER, D. P., PROBE, R. A. & ELLIS, T. J. 2012. Immediate weight bearing of comminuted supracondylar femur fractures using locked plate fixation. *Orthopedics*, 35, e1210-3.
- GRANT, C. 2012. *Mechanical testing and modelling of a bone-implant construct*. PhD QUT Thesis (PhD) Queensland University of Technology.
- GRANT, C. A., SCHUETZ, M. & EPARI, D. 2015. Mechanical testing of internal fixation devices: A theoretical and practical examination of current methods. *J Biomech*, 48, 3989-94.
- GREENBAUM, M. & KANAT, I. 1993. Current concepts in bone healing. Review of the literature. *J Am Podiatr Med Assoc*, 83, 123-9.
- GRUJICIC, M., ARAKERE, G., XIE, X., LABERGE, M., GRUJICIC, A., WAGNER, D. & VALLEJO, A. 2010. Design-optimization and material selection for a femoral-fracture fixation-plate implant. *Materials & Design*, 31, 3463-3473.
- GUPTA, H. S., SETO, J., WAGERMAIER, W., ZASLANSKY, P., BOESECKE, P. & FRATZL, P. 2006. Cooperative deformation of mineral and collagen in bone at the nanoscale. *Proc Natl Acad Sci USA*, 103, 17741-6.
- HAIDUKEWYCH, G. J. 2004. Innovations in locking plate technology. *J Am Acad Orthop Surg*, 12, 205-12.
- HAK, D. J., ALTHAUSEN, P. & HAZELWOOD, S. J. 2010a. Locked plate fixation of osteoporotic humeral shaft fractures: are two locking screws per segment enough? *J Orthop Trauma*, 24, 207-11.
- HAK, D. J., TOKER, S., CHENGLA, Y. I. & TORESON, J. 2010b. The influence of fracture fixation biomechanics on fracture healing. *Orthopedics*, 33, 752-5.
- HANKENSON, K., ZIMMERMAN, G. & MARCUCIO, R. 2014. Biological perspectives of delayed fracture healing. *Injury*, 45 Suppl 2, S8-S15.
- HANSCHEN, M., ASCHENBRENNER, I. M., FEHSKE, K., KIRCHHOFF, S., KEIL, L., HOLZAPFEL, B. M., WINKLER, S., FUECHTMEIER, B., NEUGEBAUER, R., LUEHRS, S., LIENER, U. & BIBERTHALER, P. 2014. Mono-versus polyaxial locking plates in distal femur fractures: a prospective randomized multicentre clinical trial. *Int Orthop*, 38, 857-63.
- HANSCHEN, M. & BIBERTHALER, P. 2013. Mono- vs. polyaxiale winkelstabile Plattensysteme [Mono-versus polyaxial locking plates]. *Unfallchirurg*, 116, 733-41; quiz 742-3.

- HARRISON, L., CUNNINGHAM, J., STRÖMBERG, L. & GOODSHIP, A. 2003. Controlled induction of a pseudarthrosis: a study using a rodent model. *J Orthop Trauma*, 17, 11-21.
- HARTKOPP, A., MURPHY, R. J., MOHR, T., KJAER, M. & BIERING-SORENSEN, F. 1998. Bone fracture during electrical stimulation of the quadriceps in a spinal cord injured subject. *Arch Phys Med Rehabil*, 79, 1133-6.
- HARVIN, W. H., OLADEJI, L. O., DELLA ROCCA, G. J., MURTHA, Y. M., VOLGAS, D. A., STANNARD, J. P. & CRIST, B. D. 2017. Working length and proximal screw constructs in plate osteosynthesis of distal femur fractures. *Injury*, 48, 2597-601.
- HEINLEIN, B., KUTZNER, I., GRAICHEN, F., BENDER, A., ROHLMANN, A., HALDER, A. M., BEIER, A. & BERGMANN, G. 2009. ESB clinical biomechanics award 2008: Complete data of total knee replacement loading for level walking and stair climbing measured *in vivo* with a follow-up of 6–10 months. *Clin Biomech (Bristol, Avon)*, 24, 315-26.
- HELGASON, B., PERILLI, E., SCHILEO, E., TADDEI, F., BRYNJÓLFSSON, S. & VICECONTI, M. 2008. Mathematical relationships between bone density and mechanical properties: a literature review. *Clin Biomech (Bristol, Avon)*, 23, 135-46.
- HELLER, M., BERGMANN, G., KASSI, J.-P., CLAES, L., HAAS, N. & DUDA, G. 2005a. Determination of muscle loading at the hip joint for use in pre-clinical testing. *J Biomech*, 38, 1155-63.
- HELLER, M. O., BERGMANN, G., DEURETZBACHER, G., CLAES, L., HAAS, N. P. & DUDA, G. N. 2001a. Influence of femoral anteversion on proximal femoral loading: measurement and simulation in four patients. *Clin Biomech (Bristol, Avon)*, 16, 644-9.
- HELLER, M. O., BERGMANN, G., DEURETZBACHER, G., DÜRSELEN, L., POHL, M., CLAES, L., HAAS, N. P. & DUDA, G. N. 2001b. Musculo-skeletal loading conditions at the hip during walking and stair climbing. *J Biomech*, 34, 883-93.
- HELLER, M. O., BERGMANN, G., KASSI, J. P., CLAES, L., HAAS, N. P. & DUDA, G. N. 2005b. Determination of muscle loading at the hip joint for use in pre-clinical testing. *J Biomech*, 38, 1155-63.
- HENDERSON, C. E., KUHL, L. L., FITZPATRICK, D. C. & MARSH, J. L. 2011a. Locking plates for distal femur fractures: is there a problem with fracture healing? *J Orthop Trauma*, 25 Suppl 1, S8-14.
- HENDERSON, C. E., LUJAN, T. J., KUHL, L. L., BOTTLANG, M., FITZPATRICK, D. C. & MARSH, J. L. 2011b. 2010 mid-America Orthopaedic Association Physician in Training Award: healing complications are common after locked plating for distal femur fractures. *Clin Orthop Relat Res*, 469, 1757-65.
- HENSCHEL, J., TSAI, S., FITZPATRICK, D. C., MARSH, J. L., MADEY, S. M. & BOTTLANG, M. 2017. Comparison of 4 methods for dynamization of locking plates: differences in the amount and type of fracture motion. *J Orthop Trauma*, 31, 531-7.
- HENTE, R., CORDEY, J. & PERREN, S. M. 2003. In vivo measurement of bending stiffness in fracture healing. *Biomed Eng Online*, 2, 8.
- HERNANDEZ, R. K., DO, T. P., CRITCHLOW, C. W., DENT, R. E. & JICK, S. S. 2012. Patient-related risk factors for fracture-healing complications in the United Kingdom General Practice Research Database. *Acta Orthop*, 83, 653-60.
- HEYLAND, M., DUDA, G., MÄRDIAN, S., SCHÜTZ, M. & WINDOLF, M. 2017. Stahl oder Titan bei der Osteosynthese. *Der Unfallchirurg*, 120, 103-109.
- HEYLAND, M., DUDA, G. N., HAAS, N. P., TREPCZYNSKI, A., DÖBELE, S., HÖNTZSCH, D., SCHASER, K.-D. & MÄRDIAN, S. 2015a. Semi-rigid screws provide an auxiliary option to plate working length to control interfragmentary movement in locking plate fixation at the distal femur. *Injury*, 46 Suppl 4, S24-32.
- HEYLAND, M., TREPCZYNSKI, A., DUDA, G. N., ZEHN, M., SCHASER, K. D. & MÄRDIAN, S. 2015b. Selecting boundary conditions in physiological strain analysis of the femur: Balanced loads, inertia relief method and follower load. *Med Eng Phys*, 37, 1180-5.
- HOEGEL, F. W., HOFFMANN, S., WENINGER, P., BUHREN, V. & AUGAT, P. 2012. Biomechanical comparison of locked plate osteosynthesis, reamed and unreamed nailing in conventional

- interlocking technique, and unreamed angle stable nailing in distal tibia fractures. *J Trauma Acute Care Surg*, 73, 933-8.
- HOFFMEIER, K. L., HOFMANN, G. O. & MÜCKLEY, T. 2011. Choosing a proper working length can improve the lifespan of locked plates:: A biomechanical study. *Clin Biomech (Bristol, Avon)*, 26, 405-9.
- HÖLZER, A., SCHRÖDER, C., WOICZINSKI, M., SADOGLI, P., SCHARPF, A., HEIMKES, B. & JANSSON, V. 2012. Subject-specific finite element simulation of the human femur considering inhomogeneous material properties: A straightforward method and convergence study. *Comput Methods Programs Biomed*, 110, 82-8.
- HOLZMAN, M. A., HANUS, B. D., MUNZ, J. W., O'CONNOR, D. P. & BRINKER, M. R. 2016. Addition of a Medial Locking Plate to an In Situ Lateral Locking Plate Results in Healing of Distal Femoral Nonunions. *Clin Orthop Relat Res*, 474, 1498-505.
- HÖNTZSCH, D., SCHASER, K.-D., HOFMANN, G. O., POHLEMANN, T., HEM, E. S., ROTHENBACH, E., KRETTEK, C. & ATTAL, R. 2014. Evaluation of the effectiveness of the angular stable locking system in patients with distal tibial fractures treated with intramedullary nailing: a multicenter randomized controlled trial. *J Bone Joint Surg Am*, 96, 1889-97.
- HÖRDEMANN, M. 2010. *Biomechanischer In-vitro-Vergleich der LC-DCP-und LCP-Osteosynthese am Os femoris neugeborener Kälber*. PhD, Ludwig-Maximilians-Universität München.
- HORN, C., DÖBELE, S., VESTER, H., SCHÄFFLER, A., LUCKE, M. & STÖCKLE, U. 2011. Combination of interfragmentary screws and locking plates in distal meta-diaphyseal fractures of the tibia: A retrospective, single-centre pilot study. *Injury*, 42, 1031-7.
- HSU, C.-C., LEE, C.-H. & HSU, S.-M. 2018. An optimization study of screw position and number of screws for the fixation stability of a distal femoral locking compression plate using genetic algorithms. Proceedings of the Genetic and Evolutionary Computation Conference Companion, 2018a Kyoto, Japan. New York, NY, USA: ACM, 282-3.
- HSU, H.-W., BASHKUEV, M., PUMBERGER, M. & SCHMIDT, H. 2018b. Differences in 3D vs. 2D analysis in lumbar spinal fusion simulations. *J Biomech*.
- HURKMANS, H. L., BUSSMANN, J. B., SELLES, R. W., BENDA, E., STAM, H. J. & VERHAAR, J. A. 2007. The difference between actual and prescribed weight bearing of total hip patients with a trochanteric osteotomy: long-term vertical force measurements inside and outside the hospital. *Arch Phys Med Rehabil*, 88, 200-6.
- HWANG, J. H., OH, J. K., OH, C. W., YOON, Y. C. & CHOI, H. W. 2012. Mismatch of anatomically pre-shaped locking plate on asian femurs could lead to malalignment in the minimally invasive plating of distal femoral fractures: a cadaveric study. *Arch Orthop Trauma Surg*, 132, 51-6.
- IBRAHIM, S. 2010. *Application of an optimisation algorithm to configure an internal fixation device*. Master of Engineering Master, Queensland University of Technology.
- ISAKSSON, H. 2012. Recent advances in mechanobiological modeling of bone regeneration. *Mech Res Commun*, 42, 22-31.
- ISAKSSON, H., WILSON, W., VAN DONKELAAR, C. C., HUISKES, R. & ITO, K. 2006. Comparison of biophysical stimuli for mechano-regulation of tissue differentiation during fracture healing. *J Biomech*, 39, 1507-16.
- ISAKSSON, H. H. 2007. *Mechanical and mechanobiological influences on bone fracture repair: identifying important cellular characteristics*. PhD Doctoral thesis, Technische Universiteit Eindhoven.
- JAZRAWI, L., KUMMER, F., SIMON, J., BAI, B., HUNT, S., EGOL, K. & KOVAL, K. 2000. New technique for treatment of unstable distal femur fractures by locked double-plating: case report and biomechanical evaluation. *J Trauma*, 48, 87-92.
- JIAMTON, C. & APIVATTHAKAKUL, T. 2015. The safety and feasibility of minimally invasive plate osteosynthesis (MIPO) on the medial side of the femur: a cadaveric injection study. *Injury*, 46, 2170-6.
- JUSZCZYK, M., SCHILEO, E., MARTELLI, S., CRISTOFOLINI, L. & VICECONTI, M. 2010. A Method to Improve Experimental Validation of Finite-Element Models of Long Bones. *Strain*, 46, 242-51.

- KÄÄB, M., FRENK, A., SCHMELING, A., SCHASER, K., SCHUETZ, M. & HAAS, N. 2004. Locked internal fixator: sensitivity of screw/plate stability to the correct insertion angle of the screw. *J Orthop Trauma*, 18, 483-7.
- KÄÄB, M., STÖCKLE, U., SCHÜTZ, M., STEFANSKY, J., PERKA, C. & HAAS, N. 2006. Stabilisation of periprosthetic fractures with angular stable internal fixation: a report of 13 cases. *Archives of orthopaedic and trauma surgery*, 126, 105-110.
- KAMMERLANDER, C., RIEDMÜLLER, P., GOSCH, M., ZEGG, M., KAMMERLANDER-KNAUER, U., SCHMID, R. & ROTH, T. 2012. Functional outcome and mortality in geriatric distal femoral fractures. *Injury*, 43, 1096-101.
- KANAKARIS, N. K. & GIANNOUDIS, P. V. 2010. Locking plate systems and their inherent hitches. *Injury*, 41, 1213-9.
- KASPAR, K., SCHELL, H., SEEBECK, P., THOMPSON, M. S., SCHÜTZ, M., HAAS, N. P. & DUDA, G. N. 2005. Angle stable locking reduces interfragmentary movements and promotes healing after unreamed nailing. Study of a displaced osteotomy model in sheep tibiae. *J Bone Joint Surg Am*, 87, 2028-37.
- KASSI, J.-P., HOFFMANN, J.-E., HELLER, M., RASCHKE, M. & DUDA, G. 2001. Bewertung der Stabilität von Frakturfixationssystemen: Mechanische Vorrichtung zur Untersuchung der 3-D-Steifigkeit in vitro-Assessment of the Stability of Fracture Fixation Systems: Mechanical Device to Investigate the 3-D Stiffness in vitro. *Biomedizinische Technik/Biomedical Engineering*, 46, 247-252.
- KENWRIGHT, J. & GOODSHIP, A. E. 1989. Controlled mechanical stimulation in the treatment of tibial fractures. *Clin Orthop Relat Res*, 36-47.
- KENWRIGHT, J., RICHARDSON, J., CUNNINGHAM, J., WHITE, S., GOODSHIP, A., ADAMS, M., MAGNUSSEN, P. & NEWMAN, J. 1991. Axial movement and tibial fractures. A controlled randomised trial of treatment. *J Bone Joint Surg Br*, 73, 654-9.
- KHALAFI, A., CURTISS, S., HAZELWOOD, S. & WOLINSKY, P. 2006. The effect of plate rotation on the stiffness of femoral LISS: a mechanical study. *J Orthop Trauma*, 20, 542-6.
- KIM, H.-J., CHANG, S.-H. & JUNG, H.-J. 2012. The simulation of tissue differentiation at a fracture gap using a mechano-regulation theory dealing with deviatoric strains in the presence of a composite bone plate. *Compos Part B-Eng*, 43, 978-87.
- KIM, H.-J., KIM, S.-H. & CHANG, S.-H. 2011. Bio-mechanical analysis of a fractured tibia with composite bone plates according to the diaphyseal oblique fracture angle. *Composites Part B: Engineering*, 42, 666-674.
- KIM, J. J., OH, H. K., BAE, J.-Y. & KIM, J. W. 2014. Radiological assessment of the safe zone for medial minimally invasive plate osteosynthesis in the distal femur with computed tomography angiography. *Injury*, 45, 1964-9.
- KIM, T., AYTURK, U. M., HASKELL, A., MICLAU, T. & PUTTLITZ, C. M. 2007. Fixation of osteoporotic distal fibula fractures: a biomechanical comparison of locking versus conventional plates. *J Foot Ankle Surg*, 46, 2-6.
- KLEIN, P., SCHELL, H., STREITPARTH, F., HELLER, M., KASSI, J.-P., KANDZIORA, F., BRAGULLA, H., HAAS, N. P. & DUDA, G. N. 2003. The initial phase of fracture healing is specifically sensitive to mechanical conditions. *J Orthop Res*, 21, 662-9.
- KLOEN, P. 2009. Supercutaneous plating: use of a locking compression plate as an external fixator. *J Orthop Trauma*, 23, 72-5.
- KOLB, W., GUHLMANN, H., WINDISCH, C., MARX, F., KOLB, K. & KOLLER, H. 2008. Fixation of distal femoral fractures with the Less Invasive Stabilization System: a minimally invasive treatment with locked fixed-angle screws. *J Trauma*, 65, 1425-34.
- KRANZ, H.-W., WOLTER, D., FUCHS, S. & REIMERS, N. 1999. Therapie von Pseudarthrosen, Fehlstellungen und Frakturen im Unterschenkelschaftbereich mit einem Titanfixateur interne. *Trauma Berufschr*, 1, 356-60.

- KREGOR, P. J., STANNARD, J. A., ZLOWODZKI, M. & COLE, P. A. 2004. Treatment of distal femur fractures using the less invasive stabilization system: surgical experience and early clinical results in 103 fractures. *J Orthop Trauma*, 18, 509-20.
- KRISCHAK, G., BECK, A., WACHTER, N., JAKOB, R., KINZL, L. & SUGER, G. 2003. Relevance of primary reduction for the clinical outcome of femoral neck fractures treated with cancellous screws. *Arch Orthop Trauma Surg*, 123, 404-9.
- KRISHNA, K. R., SRIDHAR, I. & GHISTA, D. N. 2008. Analysis of the helical plate for bone fracture fixation. *Injury*, 39, 1421-1436.
- KRISHNAKANTH, P. 2012. *Mechanical considerations in fracture fixation*. Doctor of Philosophy, Queensland University of Technology.
- KUBIAK, E. N., FULKERSON, E., STRAUSS, E. & EGOL, K. A. 2006. The evolution of locked plates. *J Bone Joint Surg Am*, 88 Suppl 4, 189-200.
- KUTZNER, I., TREPCZYNSKI, A., HELLER, M. O. & BERGMANN, G. 2013. Knee adduction moment and medial contact force--facts about their correlation during gait. *Plos One*, 8, e81036.
- LACROIX, D. & PRENDERGAST, P. 2002. A mechano-regulation model for tissue differentiation during fracture healing: analysis of gap size and loading. *J Biomech*, 35, 1163-71.
- LEE, C.-H., SHIH, K.-S., HSU, C.-C. & CHO, T. 2014. Simulation-based particle swarm optimization and mechanical validation of screw position and number for the fixation stability of a femoral locking compression plate. *Med Eng Phys*, 36, 57-64.
- LENZ, M., STOFFEL, K., GUEORGUIEV, B., KLOS, K., KIELSTEIN, H. & HOFMANN, G. O. 2016. Enhancing fixation strength in periprosthetic femur fractures by orthogonal plating—A biomechanical study. *J Orthop Res*, 34, 591-596.
- LEONG, P. & MORGAN, E. 2008. Measurement of fracture callus material properties via nanoindentation. *Acta Biomater*, 4, 1569-75.
- LIENAU, J., SCHELL, H., DUDA, G. N., SEEBECK, P., MUCHOW, S. & BAIL, H. J. 2005. Initial vascularization and tissue differentiation are influenced by fixation stability. *J Orthop Res*, 23, 639-45.
- LIM, H.-S., KIM, C.-K., PARK, Y.-S., MOON, Y.-W., LIM, S.-J. & KIM, S.-M. 2016. Factors associated with increased healing time in complete femoral fractures after long-term bisphosphonate therapy. *J Bone Joint Surg Am*, 98, 1978-1987.
- LUJAN, T. J., HENDERSON, C. E., MADEY, S. M., FITZPATRICK, D. C., MARSH, J. L. & BOTTLANG, M. 2010. Locked plating of distal femur fractures leads to inconsistent and asymmetric callus formation. *J Orthop Trauma*, 24, 156-62.
- MACLEOD, A., PANKAJ, P. & SIMPSON, H. 2012a. The effect of varying screw configuration on the mechanical response of locking plate fixators. *Journal of Biomechanics*, 45, S218-S218.
- MACLEOD, A., SIMPSON, A. & PANKAJ, P. 2018a. Experimental and numerical investigation into the influence of loading conditions in biomechanical testing of locking plate fracture fixation devices. *Bone Joint Res*, 7, 111-120.
- MACLEOD, A., SIMPSON, A. H. R. W. & PANKAJ, P. 2018b. Experimental and numerical investigation into the influence of loading conditions in biomechanical testing of locking plate fracture fixation devices. *Bone Joint Res*, 7, 111-20.
- MACLEOD, A., SIMPSON, H. & PANKAJ, P. 2016a. How patient-optimised device configuration can provide fracture site stimulation and reduce age-related screw loosening risk in locked plating. *J Orthop Trans*, 7, 83.
- MACLEOD, A. R. & PANKAJ, P. A simple analytical tool to optimise locking plate configuration 7th World Congress of Biomechanics, 2014 Boston.
- MACLEOD, A. R. & PANKAJ, P. 2018. Pre-operative planning for fracture fixation using locking plates: device configuration and other considerations. *Injury*, 49 Suppl 1, S12-S18.
- MACLEOD, A. R., PANKAJ, P. & SIMPSON, A. 2012b. Does screw-bone interface modelling matter in finite element analyses? *J Biomech*, 45, 1712-6.
- MACLEOD, A. R., ROSE, H. & GILL, H. S. 2016b. A Validated Open-Source Multisolver Fourth-Generation Composite Femur Model. *J Biomech Eng*, 138.

- MACLEOD, A. R., SIMPSON, A. & PANKAJ, P. 2016c. Age-related optimisation of screw placement for reduced loosening risk in locked plating. *J Orthop Res*, 34, 1856-64.
- MACLEOD, A. R., SIMPSON, A. H. & PANKAJ, P. 2014. Reasons why dynamic compression plates are inferior to locking plates in osteoporotic bone: a finite element explanation. *Comput Methods Biomech Biomed Engin*, 18, 1818-25.
- MACLEOD, A. R., SIMPSON, H. & PANKAJ, P. 2015. In vitro testing of locking plate fracture fixation wrongly predicts the performance of different implant materials. *European Society of Biomechanics*. Prague, goo.gl/awmLYX.
- MADEY, S., TSAI, S., FITZPATRICK, D., EARLEY, K., LUTSCH, M. & BOTTLANG, M. 2017. Dynamic Fixation of Humeral Shaft Fractures Using Active Locking Plates: A Prospective Observational Study. *The Iowa orthopaedic journal*, 37, 1.
- MÄRDIAN, S., SCHASER, K.-D., DUDA, G. N. & HEYLAND, M. 2015a. Working length of locking plates determines interfragmentary movement in distal femur fractures under physiological loading. *Clin Biomech (Bristol, Avon)*, 30, 391-6.
- MÄRDIAN, S., SCHMÖLZ, W., SCHASER, K.-D., DUDA, G. N. & HEYLAND, M. 2015b. Interfragmentary lag screw fixation in locking plate constructs increases stiffness in simple fracture patterns. *Clin Biomech (Bristol, Avon)*, 30, 814-9.
- MARKEL, M. & BOGDANSKE, J. 1994. The effect of increasing gap width on localized densitometric changes within tibial ostectomies in a canine model. *Calcified Tissue Int*, 54, 155-9.
- MARSELL, R. & EINHORN, T. A. 2011. The biology of fracture healing. *Injury*, 42, 551-5.
- MARSH, D. R. & LI, G. 1999. The biology of fracture healing: optimising outcome. *Br Med Bull*, 55, 856-69.
- MARTI, A., FANKHAUSER, C., FRENK, A., CORDEY, J. & GASSER, B. 2001. Biomechanical evaluation of the less invasive stabilization system for the internal fixation of distal femur fractures. *J Orthop Trauma*, 15, 482-7.
- MARTI, R. K., SCHULLER, H. M. & RAAYMAKERS, E. L. 1989. Intertrochanteric osteotomy for non-union of the femoral neck. *J Bone Joint Surg Br*, 71, 782-7.
- MARTIN, R. B., BURR, D. B. & SHARKEY, N. A. 1998. *Skeletal tissue mechanics*, New York., Springer.
- MATTHEWS, S. J. E., NIKOLAOU, V. S. & GIANNOUDIS, P. V. 2008. Innovations in osteosynthesis and fracture care. *Injury*, 39, 827-38.
- MCKIBBIN, B. 1978. The biology of fracture healing in long bones. *J Bone Joint Surg Br*, 60-B, 150-62.
- MCLACHLIN, S., KREDER, H., NG, M., JENKINSON, R., WHYNE, C. & LAROUCHE, J. 2017. Proximal Screw Configuration Alters Peak Plate Strain Without Changing Construct Stiffness in Comminuted Supracondylar Femur Fractures. *J Orthop Trauma*, 31, e418-e424.
- MEEUWIS, M. A., TER GUNNE, A. P., VERHOFSTAD, M. & VAN DER HEIJDEN, F. 2017. Construct failure after open reduction and plate fixation of displaced midshaft clavicular fractures. *Injury*, 48, 715-9.
- MEHBOOB, A. & CHANG, S.-H. 2018. Biomechanical simulation of healing process of fractured femoral shaft applied by composite intramedullary nails according to fracture configuration. *Composite Structures*, 185, 81-93.
- MEHBOOB, H. & CHANG, S.-H. 2014. Application of composites to orthopedic prostheses for effective bone healing: A review. *Compos Struct*, 118, 328-41.
- MEHBOOB, H. & CHANG, S.-H. 2015. Effect of structural stiffness of composite bone plate-scaffold assembly on tibial fracture with large fracture gap. *Compos Struct*, 124, 327-36.
- MEHBOOB, H., SON, D.-S. & CHANG, S.-H. 2013. Finite element analysis of tissue differentiation process of a tibia with various fracture configurations when a composite intramedullary rod was applied. *Compos Sci Technol*, 80, 55-65.
- MEHLING, I., HOEHLE, P., STERNSTEIN, W., BLUM, J. & ROMMENS, P. 2013. Nailing versus plating for comminuted fractures of the distal femur: a comparative biomechanical in vitro study of three implants. *Eur J Trauma Emerg Surg*, 39, 139-46.

- MEHTA, M., CHECA, S., LIENAU, J., HUTMACHER, D. & DUDA, G. N. 2012. In vivo tracking of segmental bone defect healing reveals that callus patterning is related to early mechanical stimuli. *Eur Cell Mater*, 24, 358-71.
- MEHTA, M., HEYLAND, M., TOBEN, D. & DUDA, G. N. 2013. Microstructure and homogeneity of distribution of mineralised struts determine callus strength. *Eur Cell Mater*, 25, 366-79.
- MEHTA, M., STRUBE, P., PETERS, A., PERKA, C., HUTMACHER, D., FRATZL, P. & DUDA, G. N. 2010. Influences of age and mechanical stability on volume, microstructure, and mineralization of the fracture callus during bone healing: Is osteoclast activity the key to age-related impaired healing? *Bone*, 47, 219-28.
- MELTON III, L. J., CROWSON, C. & O'FALLON, W. 1999. Fracture incidence in Olmsted County, Minnesota: comparison of urban with rural rates and changes in urban rates over time. *Osteoporos Int*, 9, 29-37.
- MILLER, D. L. & GOSWAMI, T. 2007. A review of locking compression plate biomechanics and their advantages as internal fixators in fracture healing. *Clin Biomech (Bristol, Avon)*, 22, 1049-62.
- MIRAMINI, S., ZHANG, L., RICHARDSON, M., MENDIS, P. & EBELING, P. R. 2016. Influence of fracture geometry on bone healing under locking plate fixations: A comparison between oblique and transverse tibial fractures. *Med Eng Phys*, 38, 1100-8.
- MIRAMINI, S., ZHANG, L., RICHARDSON, M., MENDIS, P., OLOYEDE, A. & EBELING, P. 2015a. The relationship between interfragmentary movement and cell differentiation in early fracture healing under locking plate fixation. *Australasian Physical & Engineering Sciences in Medicine*, 1-11.
- MIRAMINI, S., ZHANG, L., RICHARDSON, M., PIRPIRIS, M., MENDIS, P., OLOYEDE, K. & EDWARDS, G. 2015b. Computational simulation of the early stage of bone healing under different configurations of locking compression plates. *Comput Methods Biomech Biomed Engin*, 18, 900-13.
- MITCHELL, P. M., LEE, A. K., COLLINGE, C. A., ZIRAN, B. H., HARTLEY, K. G. & JAHANGIR, A. A. 2018. Early Comparative Outcomes of Carbon Fiber-Reinforced Polymer Plate in the Fixation of Distal Femur Fractures. *J Orthop Trauma*, 32, 386-390.
- MITKOVIC, M., MILENKOVIC, S., MICIC, I. & MLADENOVIC, D. 2012. Results of the femur fractures treated with the new selfdynamisable internal fixator (SIF). *Eur J Trauma Emerg Surg*, 38, 191-200.
- MITKOVIĆ, M. M., MILENKOVIĆ, S. S., MICIĆ, I. D., KOSTIĆ, I. M., STOJILJKOVIĆ, P. M. & MITKOVIĆ, M. B. 2017. Operation time and intraoperative fluoroscopy time in different internal fixation methods for subtrochanteric fractures treatment. *Srp Arh Celok Lek*, 42-42.
- MOAZEN, M., JONES, A. C., LEONIDOU, A., JIN, Z., WILCOX, R. K. & TSIRIDIS, E. 2011. Rigid versus flexible plate fixation for periprosthetic femoral fracture - Computer modelling of a clinical case. *Med Eng Phys*, 34, 1041-8.
- MOAZEN, M., MAK, J. H., JONES, A. C., JIN, Z., WILCOX, R. K. & TSIRIDIS, E. 2013. Evaluation of a new approach for modelling the screw-bone interface in a locking plate fixation: A corroboration study. *Proc Inst Mech Eng H*, 227, 746-56.
- MOEWIS, P., WOLTERBEEK, N., DIEDERICHS, G., VALSTAR, E., HELLER, M. O. & TAYLOR, W. R. 2012. The quality of bone surfaces may govern the use of model based fluoroscopy in the determination of joint laxity. *Medical Engineering & Physics*, 34, 1427-1432.
- MORGAN, E. F., BAYRAKTAR, H. H. & KEAVENY, T. M. 2003. Trabecular bone modulus-density relationships depend on anatomic site. *J Biomech*, 36, 897-904.
- MÜLLER, C. W., PFEIFER, R., MEIER, K., DECKER, S., REIFENRATH, J., GÖSLING, T., WESLING, V., KRETTEK, C., HURSCHLER, C. & KRÄMER, M. 2015. A Novel Shape Memory Plate Osteosynthesis for Noninvasive Modulation of Fixation Stiffness in a Rabbit Tibia Osteotomy Model. *Biomed Res Int*, 2015, 652940.
- NANAVATI, N. & WALKER, M. 2014. Current concepts to reduce mechanical stiffness in locked plating systems: a review article. *Orthop Res Rev*, 6, 91-5.

- NASR, S., HUNT, S. & DUNCAN, N. A. 2013. Effect of screw position on bone tissue differentiation within a fixed femoral fracture. *J Biomed Science Eng*, 6, 71-83
- NASSIRI, M., MACDONALD, B. & O'BYRNE, J. 2013. Computational modelling of long bone fractures fixed with locking plates—How can the risk of implant failure be reduced? *J Orthop*, 10, 29-37.
- NASSIRI, M., MACDONALD, B. & O'BYRNE, J. 2012. Locking compression plate breakage and fracture non-union: a finite element study of three patient-specific cases. *Eur J Orthop Surg Tr*, 22, 275-81.
- NIINOMI, M. 1998. Mechanical properties of biomedical titanium alloys. *Mat Sci Eng a-Struct*, 243, 231-236.
- NOURISA, J. & ROUHI, G. 2016. Biomechanical evaluation of intramedullary nail and bone plate for the fixation of distal metaphyseal fractures. *J Mech Behav Biomed Mater*, 56, 34-44.
- NYQUIST, F., BERGLUND, M., NILSSON, B. E. & OBRANT, K. J. 1997. Nature and healing of tibial shaft fractures in alcohol abusers. *Alcohol Alcohol*, 32, 91-5.
- O'HALLORAN, K., COALE, M., COSTALES, T., ZERHUSEN JR, T., CASTILLO, R. C., NASCONE, J. W. & O'TOOLE, R. V. 2016. Will My Tibial Fracture Heal? Predicting Nonunion at the Time of Definitive Fixation Based on Commonly Available Variables. *Clin Orthop Relat Res*, 474, 1385-95.
- OH, J. K., HWANG, J. H., LEE, S. J. & KIM, J. I. 2011. Dynamization of locked plating on distal femur fracture. *Arch Orthop Trauma Surg*, 131, 535-9.
- OH, J. K., SAHU, D., AHN, Y. H., LEE, S. J., TSUTSUMI, S., HWANG, J. H., JUNG, D. Y., PERREN, S. M. & OH, C. W. 2010. Effect of fracture gap on stability of compression plate fixation: a finite element study. *J Orthop Res*, 28, 462-7.
- ONNERFALT, R. 1978. Fracture of the tibial shaft treated by primary operation and early weight-bearing. *Acta Orthop Scand Suppl*, 171, 1-63.
- OTTO, R. J., MOED, B. R. & BLEDSOE, J. G. 2009. Biomechanical comparison of polyaxial-type locking plates and a fixed-angle locking plate for internal fixation of distal femur fractures. *J Orthop Trauma*, 23, 645-52.
- PANKAJ, P. 2013. Patient-specific modelling of bone and bone-implant systems: the challenges. *Int J Numer Method Biomed Eng*, 29, 233-49.
- PARK, S.-H., O'CONNOR, K., MCKELLOP, H. & SARMIENTO, A. 1998. The influence of active shear or compressive motion on fracture-healing. *J Bone Joint Surg Am*, 80, 868-78.
- PARKER, M. J. & DYNAN, Y. 1998. Is Pauwels classification still valid? *Injury*, 29, 521-523.
- PARKS, C., MCANDREW, C. M., SPRAGGS-HUGHES, A., RICCI, W. M., SILVA, M. J. & GARDNER, M. J. 2018. In-vivo stiffness assessment of distal femur fracture locked plating constructs. *Clin Biomech (Bristol, Avon)*, 56, 46-51.
- PATEL, V. 2008. *Biomechanical Evaluation Of Locked And Non-locked Constructs Under Axial And Torsion Loading*. Master of Science in Engineering Master of Science in Engineering (MSEgr), Wright State University.
- PATERNO, M. V. & ARCHDEACON, M. T. 2009. Is there a standard rehabilitation protocol after femoral intramedullary nailing? *J Orthop Trauma*, 23, S39-46.
- PÄTZOLD, R., FRIEDERICHS, J., VON RÜDEN, C., PANZER, S., BÜHREN, V. & AUGAT, P. 2017. The pivotal role of the coronal fracture line for a new three-dimensional CT-based fracture classification of bicondylar proximal tibial fractures. *Injury*, 48, 2214-20.
- PAUWELS, F. 1935. *Der Schenkelhalsbruch: Ein mechanisches Problem. Grundlagen des Heilungsvorganges, Prognose und Kausale Therapie*, Stuttgart, Ferdinand Enke Verlag.
- PEKMEZCI, M., MCDONALD, E., BUCKLEY, J. & KANDEMIR, U. 2014. Retrograde intramedullary nails with distal screws locked to the nail have higher fatigue strength than locking plates in the treatment of supracondylar femoral fractures - A cadaver-based laboratory investigation. *Bone Joint J*, 96-B, 114-21.
- PERREN, S. 1979. Physical and biological aspects of fracture healing with special reference to internal fixation. *Clin Orthop Relat Res*, 175-96.

- PERREN, S. 2015. Fracture healing: fracture healing understood as the result of a fascinating cascade of physical and biological interactions. Part II. *Acta Chir Orthop Traumatol Cech*, 82, 13-21.
- PERREN, S., REGAZZONI, P., LENZ, M. & FERNÁNDEZ, A. 2018. Double locking plate, surgical trauma and construct stiffness improved by the helical plate.
- PERREN, S. M. 2002. Evolution of the internal fixation of long bone fractures: the scientific basis of biological internal fixation: choosing a new balance between stability and biology. *J Bone Joint Surg Br*, 84B, 1093-110.
- PERREN, S. M. & BUCHANAN, J. S. 1995. Basic concepts relevant to the design and development of the point contact fixator (PC-Fix). *Injury*, 26, B1-B4.
- PERREN, S. M., CORDEY, J., RAHN, B. A., GAUTIER, E. & SCHNEIDER, E. 1988. Early Temporary Porosis of Bone Induced by Internal Fixation Implants A Reaction to Necrosis, Not to Stress Protection? *Clin Orthop Relat Res*, 139-51.
- PFEIFER, R., MÜLLER, C. W., HURSCHLER, C., KAIERLE, S., WESLING, V. & HAFERKAMP, H. 2013. Adaptable Orthopedic Shape Memory Implants. *Procedia CIRP*, 5, 253-8.
- PHIEFFER, L. S. & GOULET, J. A. 2006. Delayed unions of the tibia. *J Bone Joint Surg Am*, 88, 205-16.
- PHILLIPS, A. 2009. The femur as a musculo-skeletal construct: a free boundary condition modelling approach. *Med Eng Phys*, 31, 673-80.
- PHILLIPS, A., PANKAJ, P., HOWIE, C., USMANI, A. & SIMPSON, A. 2007. Finite element modelling of the pelvis: inclusion of muscular and ligamentous boundary conditions. *Med Eng Phys*, 29, 739-48.
- PLECKO, M., LAGERPUSCH, N., PEGEL, B., ANDERMATT, D., FRIGG, R., KOCH, R., SIDLER, M., KRONEN, P., KLEIN, K., NUSS, K., GEDET, P., BÜRKI, A., FERGUSON, S. J., STOECKLE, U., AUER, J. A. & VON RECHENBERG, B. 2012. The influence of different osteosynthesis configurations with locking compression plates (LCP) on stability and fracture healing after an oblique 45 degrees angle osteotomy. *Injury*, 43, 1041-51.
- POELERT, S., VALSTAR, E., WEINANS, H. & ZADPOOR, A. A. 2013. Patient-specific finite element modeling of bones. *Proc Inst Mech Eng H*, 227, 464-78.
- POLGAR, K., GILL, H., VICECONTI, M., MURRAY, D. & O'CONNOR, J. 2003. Strain distribution within the human femur due to physiological and simplified loading: finite element analysis using the muscle standardized femur model. *Proc Inst Mech Eng H*, 217, 173-89.
- POLGAR, K., VICECONTI, M. & CONNOR, J. 2001. A comparison between automatically generated linear and parabolic tetrahedra when used to mesh a human femur. *Proc Inst Mech Eng H*, 215, 85-94.
- POOLE, W., WILSON, D., GUTHRIE, H., BELLRINGER, S., FREEMAN, R., GURYEL, E. & NICOL, S. 2017. 'Modern' distal femoral locking plates allow safe, early weight-bearing with a high rate of union and low rate of failure: five-year experience from a United Kingdom major trauma centre. *Bone Joint J*, 99-B, 951-957.
- POTTER, B. K. 2016. From Bench to Bedside: How Stiff is Too Stiff? Far-cortical Locking or Dynamic Locked Plating May Obviate the Question. *Clin Orthop Relat R*, 474, 1571-3.
- POUNTOS, I., GEORGOULI, T., BLOKHUIS, T. J., PAPE, H. C. & GIANNOUDIS, P. V. 2008. Pharmacological agents and impairment of fracture healing: what is the evidence? *Injury*, 39, 384-94.
- POUNTOS, I., GEORGOULI, T., PNEUMATICOS, S. & GIANNOUDIS, P. V. 2013. Fracture non-union: Can biomarkers predict outcome? *Injury*, 44, 1725-32.
- PRENDERGAST, P., HUISKES, R. & SØBALLE, K. 1997. Biophysical stimuli on cells during tissue differentiation at implant interfaces. *J Biomech*, 30, 539-48.
- PUNO, R. M., TEYNOR, J. T., NAGANO, J. & GUSTILO, R. B. 1986. Critical analysis of results of treatment of 201 tibial shaft fractures. *Clin Orthop Relat Res*, 212, 113-21.
- RAMOS, A. & SIMOES, J. 2006. Tetrahedral versus hexahedral finite elements in numerical modelling of the proximal femur. *Med Eng Phys*, 28, 916-24.

- REIFENRATH, J., ANGRISANI, N., LALK, M. & BESDO, S. 2014. Replacement, refinement, and reduction: Necessity of standardization and computational models for long bone fracture repair in animals. *J Biomed Mater Res A*, 102, 2884-900.
- REILLY, D. T. & BURSTEIN, A. H. 1975. The elastic and ultimate properties of compact bone tissue. *Journal of biomechanics*, 8, 393-405.
- REINA-ROMO, E., GIRÁLDEZ-SÁNCHEZ, M., MORA-MACÍAS, J., CANO-LUIS, P. & DOMÍNGUEZ, J. 2014. Biomechanical design of Less Invasive Stabilization System femoral plates: Computational evaluation of the fracture environment. *Proc Inst Mech Eng H*, 228, 1043-52.
- REINKE, S., GEISLER, S., TAYLOR, W. R., SCHMIDT-BLEEK, K., JUELKE, K., SCHWACHMEYER, V., DAHNE, M., HARTWIG, T., AKYUZ, L., MEISEL, C., UNTERWALDER, N., SINGH, N. B., REINKE, P., HAAS, N. P., VOLK, H.-D. & DUDA, G. N. 2013. Terminally differentiated CD8(+) T cells negatively affect bone regeneration in humans. *Sci Transl Med*, 5, 177ra36.
- RICCI, W. M., STREUBEL, P. N., MORSHED, S., COLLINGE, C. A., NORK, S. E. & GARDNER, M. J. 2014. Risk factors for failure of locked plate fixation of distal femur fractures: an analysis of 335 cases. *J Orthop Trauma*, 28, 83-9.
- RODRIGUEZ-MERCHAN, E. C. & FORRIOL, F. 2004. Nonunion: general principles and experimental data. *Clin Orthop Relat Res*, 419, 4-12.
- RODRIGUEZ, E. K., BOULTON, C., WEAVER, M. J., HERDER, L. M., MORGAN, J. H., CHACKO, A. T., APPLETON, P. T., ZURAKOWSKI, D. & VRAHAS, M. S. 2014. Predictive factors of distal femoral fracture nonunion after lateral locked plating: a retrospective multicenter case-control study of 283 fractures. *Injury*, 45, 554-9.
- RODRIGUEZ, E. K., ZURAKOWSKI, D., HERDER, L., HALL, A., WALLEY, K. C., WEAVER, M. J., APPLETON, P. T. & VRAHAS, M. 2016. Mechanical Construct Characteristics Predisposing To Non-Union After Locked Lateral Plating Of Distal Femur Fractures. *J Orthop Trauma*, 30, 403-8.
- ROZBRUCH, R. S., MÜLLER, U., GAUTIER, E. & GANZ, R. 1998. The evolution of femoral shaft plating technique. *Clin Orthop Relat Res*, 354, 195-208.
- RUFFONI, D., WIRTH, A. J., STEINER, J. A., PARKINSON, I. H., MULLER, R. & VAN LENTHE, G. H. 2012. The different contributions of cortical and trabecular bone to implant anchorage in a human vertebra. *Bone*, 50, 733-8.
- SAHLIN, Y. 1990. Occurrence of fractures in a defined population: a 1-year study. *Injury*, 21, 158-60.
- SAN ANTONIO, T., CIACCIA, M., MÜLLER-KARGER, C. & CASANOVA, E. 2012. Orientation of orthotropic material properties in a femur FE model: A method based on the principal stresses directions. *Med Eng Phys*, 34, 914-9.
- SANTOLINI, E., GOUMENOS, S. D., GIANNOUDI, M., SANGUINETI, F., STELLA, M. & GIANNOUDIS, P. V. 2014. Femoral and tibial blood supply: A trigger for non-union? *Injury*, 45, 1665-73.
- SANTOLINI, E., WEST, R. & GIANNOUDIS, P. V. 2015. Risk factors for long bone fracture non-union: a stratification approach based on the level of the existing scientific evidence. *Injury*, 46 Suppl 8, S8-S19.
- SARMIENTO, A., MCKELLOP, H. A., LLINAS, A., PARK, S. H., LU, B., STETSON, W. & RAO, R. 1996. Effect of loading and fracture motions on diaphyseal tibial fractures. *J Orthop Res*, 14, 80-4.
- SCHANDELMAIER, P., PARTENHEIMER, A., KOENEMANN, B., GRÜN, O. & KRETTEK, C. 2001. Distal femoral fractures and LISS stabilization. *Injury*, 32 Suppl 3, 55-63.
- SHELL, H., EPARI, D. R., KASSI, J. P., BRAGULLA, H., BAIL, H. J. & DUDA, G. N. 2005. The course of bone healing is influenced by the initial shear fixation stability. *J Orthop Res*, 23, 1022-8.
- SCHEMITSCH, E., KOWALSKI, M., SWIONTKOWSKI, M. & SENFT, D. 1994. Cortical bone blood flow in reamed and unreamed locked intramedullary nailing: a fractured tibia model in sheep. *Journal of orthopaedic trauma*, 8, 373-382.
- SCHILEO, E., DALL'ARA, E., TADDEI, F., MALANDRINO, A., SCHOTKAMP, T., BALEANI, M. & VICECONTI, M. 2008. An accurate estimation of bone density improves the accuracy of subject-specific finite element models. *J Biomech*, 41, 2483-91.

- SCHILEO, E., TADDEI, F., MALANDRINO, A., CRISTOFOLINI, L. & VICECONTI, M. 2007. Subject-specific finite element models can accurately predict strain levels in long bones. *J Biomech*, 40, 2982-9.
- SCHINDELER, A., MCDONALD, M. M., BOKKO, P. & LITTLE, D. G. 2008. Bone remodeling during fracture repair: the cellular picture. *Semin Cell Dev Biol*, 19, 459-66.
- SCHMAL, H., STROHM, P. C., JAEGER, M. & SÜDKAMP, N. P. 2011. Flexible Fixation and Fracture Healing: Do Locked Plating 'Internal Fixators' Resemble External Fixators? *J Orthop Trauma*, 25 Suppl 1, S15-20.
- SCHMIDT, A. H. Locking Plates: Shouldn't Everyone Get One? Geriatric Orthopaedic Fracture Conference 2010, December 2-3, 2010 St. Paul, MN. 13.
- SCHMIDT, U., PENZKOFER, R., BACHMAIER, S. & AUGAT, P. 2013. Implant material and design alter construct stiffness in distal femur locking plate fixation: a pilot study. *Clin Orthop Relat Res*, 471, 2808-14.
- SCOLARO, J. & JAIMO AHN, M. D. 2011. Locked Plating in Practice: Indications and Current Concepts. *University of Pennsylvania Orthopedic Journal*, 21, 18-22.
- SEIDE, K., ALJUDAIBI, M., WEINRICH, N., KOWALD, B., JÜRGENS, C., MÜLLER, J. & FASCHINGBAUER, M. 2012. Telemetric assessment of bone healing with an instrumented internal fixator A preliminary study. *J Bone Joint Surg Br*, 94, 398-404.
- SEIDE, K., MORLOCK, M. M., SCHÜMANN, U. & WOLTER, D. 1999. Wirkprinzipien der winkelstabilen Platten-Schrauben-Verbindung bei Fixateur-interne-Osteosynthesen. *Trauma Berufskr*, 1, 320-5.
- SEIDE, K., ZIEROLD, W., WOLTER, D. & KORTMANN, H. R. 1990. [The effect of an angle-stable plate-screw connection and various screw diameters on the stability of plate osteosynthesis. An FE model study]. *Unfallchirurg*, 93, 552-8.
- SELLEI, R. M., GARRISON, R. L., KOBBE, P., LICHTER, P., KNOBE, M. & PAPE, H. C. 2011. Effects of near cortical slotted holes in locking plate constructs. *J Orthop Trauma*, 25 Suppl 1, S35-40.
- SIMPSON, A. & TSANG, S. T. J. 2018. Non-union after plate fixation. *Injury*, 49 Suppl 1, S78-S82.
- SINGER, B., MCLAUCHLAN, G., ROBINSON, C. & CHRISTIE, J. 1998. Epidemiology of fractures in 15 000 adults the influence of age and gender. *J Bone Joint Surg Br*, 80, 243-8.
- SMITH, T., HEDGES, C., MACNAIR, R. & SCHANKAT, K. 2009. Early rehabilitation following less invasive surgical stabilisation plate fixation for distal femoral fractures. *Physiotherapy*, 95, 61-75.
- SMITH, W. R., ZIRAN, B. H., ANGLIN, J. O. & STAHEL, P. F. 2008. Locking plates: tips and tricks. *Instr Course Lect*, 57, 25-36.
- SON, D.-S. & CHANG, S.-H. 2013. The simulation of bone healing process of fractured tibia applied with composite bone plates according to the diaphyseal oblique angle and plate modulus. *Compos Part B-Eng*, 45, 1325-35.
- SON, D.-S., MEHBOOB, H. & CHANG, S.-H. 2014a. Simulation of the bone healing process of fractured long bones applied with a composite bone plate with consideration of the blood vessel growth. *Compos Part B-Eng*, 58, 443-50.
- SON, D.-S., MEHBOOB, H., JUNG, H.-J. & CHANG, S.-H. 2014b. The finite element analysis for endochondral ossification process of a fractured tibia applied with a composite IM-rod based on a mechano-regulation theory using a deviatoric strain. *Compos Part B-Eng*, 56, 189-96.
- SONDEREGGER, J., GROB, K. R. & KUSTER, M. S. 2010. Dynamic plate osteosynthesis for fracture stabilization: how to do it. *Orthop Rev (Pavia)*, 2, e4.
- SONG, H. K., NOH, J. W., LEE, J. H. & YANG, K. H. 2012. Avoiding rotational mismatch of locking distal tibia plates depends on proper plate position. *J Orthop Trauma*, 27, e147-51.
- SOUSA, C. P., DIAS, I. R., LOPEZ-PEÑA, M., CAMASSA, J. A., LOURENÇO, P. J., JUDAS, F. M., GOMES, M. E. & REIS, R. L. 2015. Bone turnover markers for early detection of fracture healing disturbances: A review of the scientific literature. *An Acad Bras Cienc*, 87, 1049-61.
- SPEIRS, A. D., HELLER, M. O., DUDA, G. N. & TAYLOR, W. R. 2007. Physiologically based boundary conditions in finite element modelling. *J Biomech*, 40, 2318-23.

- SQUYER, E. R., DIKOS, G. D., KAEHR, D. M., MAAR, D. C. & CRICHLLOW, R. J. 2016. Early prediction of tibial and femoral fracture healing: Are we reliable? *Injury*, 47, 2805–8
- STEINER, J. A., CHRISTEN, P., AFFENTRANGER, R., FERGUSON, S. J. & VAN LENTHE, G. H. 2017. A novel in silico method to quantify primary stability of screws in trabecular bone. *Journal of Orthopaedic Research*.
- STEINER, J. A., FERGUSON, S. J. & VAN LENTHE, G. H. 2015. Computational analysis of primary implant stability in trabecular bone. *J Biomech*, 48, 807-15.
- STEINER, J. A., FERGUSON, S. J. & VAN LENTHE, G. H. 2016. Screw insertion in trabecular bone causes peri-implant bone damage. *Med Eng Phys*, 38, 417-22.
- STEINER, M., CLAES, L., IGNATIUS, A., NIEMEYER, F., SIMON, U. & WEHNER, T. 2013. Prediction of fracture healing under axial loading, shear loading and bending is possible using distortional and dilatational strains as determining mechanical stimuli. *J R Soc Interface*, 10, 20130389.
- STEINER, M., CLAES, L., IGNATIUS, A., SIMON, U. & WEHNER, T. 2014. Numerical simulation of callus healing for optimization of fracture fixation stiffness. *PLoS one*, 9, e101370.
- STOFFEL, K., DIETER, U., STACHOWIAK, G., GÄCHTER, A. & KUSTER, M. S. 2003. Biomechanical testing of the LCP--how can stability in locked internal fixators be controlled? *Injury*, 34 Suppl 2, B11-9.
- STRAUSS, E. J., SCHWARZKOPF, R., KUMMER, F. & EGOL, K. A. 2008. The current status of locked plating: the good, the bad, and the ugly. *J Orthop Trauma*, 22, 479-86.
- SUÁREZ, D. R. 2015. Theories of mechanically induced tissue differentiation and adaptation in the musculoskeletal system. *Ingeniería y Universidad*, 20, 21-40.
- SUN, J., ABEL, E. & ROWLEY, D. 1998. Mechanical performance of an axially mobile plate for fracture fixation. *J Trauma*, 44, 368-71.
- SUZUKI, T., SMITH, W. R., STAHEL, P. F., MORGAN, S. J., BARON, A. J. & HAK, D. J. 2010. Technical problems and complications in the removal of the less invasive stabilization system. *J Orthop Trauma*, 24, 369-73.
- SZWEDOWSKI, T. D., TAYLOR, W. R., HELLER, M. O., PERKA, C., MÜLLER, M. & DUDA, G. N. 2012. Generic rules of mechano-regulation combined with subject specific loading conditions can explain bone adaptation after THA. *PLoS One*, 7, e36231.
- TADDEI, F., CRISTOFOLINI, L., MARTELLI, S., GILL, H. & VICECONTI, M. 2006a. Subject-specific finite element models of long bones: an in vitro evaluation of the overall accuracy. *J Biomech*, 39, 2457-67.
- TADDEI, F., MARTELLI, S., REGGIANI, B., CRISTOFOLINI, L. & VICECONTI, M. 2006b. Finite-element modeling of bones from CT data: sensitivity to geometry and material uncertainties. *IEEE Trans Biomed Eng*, 53, 2194-200.
- TADDEI, F., SCHILEO, E., HELGASON, B., CRISTOFOLINI, L. & VICECONTI, M. 2007. The material mapping strategy influences the accuracy of CT-based finite element models of bones: an evaluation against experimental measurements. *Med Eng Phys*, 29, 973-9.
- TAN, S. & BALOGH, Z. J. 2009. Indications and limitations of locked plating. *Injury*, 40, 683-91.
- TARNIȚĂ, D., TARNIȚĂ, D., HACMAN, L., COPILUȘ, C. & BERCEANU, C. 2010. In vitro experiment of the modular orthopedic plate based on Nitinol, used for human radius bone fractures. *Rom J Morphol Embryol*, 51, 315-20.
- TAYLOR, W. R., HELLER, M. O., BERGMANN, G. & DUDA, G. N. 2004. Tibio-femoral loading during human gait and stair climbing. *J Orthop Res*, 22, 625-32.
- TEJWANI, N. C. & GUERADO, E. 2011. Improving fixation of the osteoporotic fracture: the role of locked plating. *J Orthop Trauma*, 25 Suppl 2, S56-60.
- THAPA, N., PRAYSON, M. & GOSWAMI, T. 2015. A failure study of a locking compression plate implant. *Case Stud Eng Fail Anal*, 3, 68-72.
- THEVENDRAN, G., WANG, C., PINNEY, S. J., PENNER, M. J., WING, K. J. & YOUNGER, A. S. 2015. Nonunion risk assessment in foot and ankle surgery: proposing a predictive risk assessment model. *Foot & ankle international*, 36, 901-907.

- THEWLIS, D., CALLARY, S. A., FRAYSSE, F. & SOLOMON, L. B. 2015. Peak loading during walking is not associated with fracture migration following tibial plateau fracture: A preliminary case series. *J Orthop Res*, 33, 1398-406.
- TOBEN, D., SCHROEDER, I., EL KHASSAWNA, T., MEHTA, M., HOFFMANN, J. E., FRISCH, J. T., SCHELL, H., LIENAU, J., SERRA, A., RADBRUCH, A. & DUDA, G. N. 2011. Fracture Healing Is Accelerated in the Absence of the Adaptive Immune System. *Journal of Bone and Mineral Research*, 26, 113-124.
- TOMPKINS, M., PALLER, D. J., MOORE, D. C., CRISCO, J. J. & TEREK, R. M. 2013. Locking buttons increase fatigue life of locking plates in a segmental bone defect model. *Clin Orthop Relat Res*, 471, 1039-44.
- TRABELSI, N. & YOSIBASH, Z. 2011. Patient-specific finite-element analyses of the proximal femur with orthotropic material properties validated by experiments. *J Biomech Eng*, 133, 061001.
- TREPCZYNSKI, A., KUTZNER, I., BERGMANN, G., TAYLOR, W. R. & HELLER, M. O. 2014. Modulation of the relationship between external knee adduction moments and medial joint contact forces across subjects and activities. *Arthritis Rheumatol*, 66, 1218-27.
- TREPCZYNSKI, A., KUTZNER, I., KORNAPOULOS, E., TAYLOR, W. R., DUDA, G. N., BERGMANN, G. & HELLER, M. O. 2012. Patellofemoral joint contact forces during activities with high knee flexion. *J Orthop Res*, 30, 408-15.
- TZIOUPIS, C. & GIANNOUDIS, P. V. 2007. Prevalence of long-bone non-unions. *Injury*, 38 Suppl 2, S3-9.
- UHL, J. M., SEGUIN, B., KAPATKIN, A. S., SCHULZ, K. S., GARCIA, T. C. & STOVER, S. M. 2008. Mechanical comparison of 3.5 mm broad dynamic compression plate, broad limited-contact dynamic compression plate, and narrow locking compression plate systems using interfragmentary gap models. *Vet Surg*, 37, 663-73.
- UHTHOFF, H. K., POITRAS, P. & BACKMAN, D. S. 2006. Internal plate fixation of fractures: short history and recent developments. *J Orthop Sci*, 11, 118-26.
- VASARHELYI, A., BAUMERT, T., FRITSCH, C., HOPFENMÜLLER, W., GRADL, G. & MITTLMEIER, T. 2006. Partial weight bearing after surgery for fractures of the lower extremity—is it achievable? *Gait posture*, 23, 99-105.
- VETTER, A., WITT, F., SANDER, O., DUDA, G. & WEINKAMER, R. 2011. The spatio-temporal arrangement of different tissues during bone healing as a result of simple mechanobiological rules. *Biomech Model Mechanobiol*, 11, 147-60.
- VICECONTI, M., OLSEN, S., NOLTE, L. P. & BURTON, A. K. 2005. Extracting clinically relevant data from finite element simulations. *Clin Biomech (Bristol, Avon)*, 20, 451-4.
- WAGNER, M. 2010. [Advantages and disadvantages of locked plating]. *Orthopade*, 39, 149-59.
- WAGNER, M. & FRIGG, R. 2006. *AO manual of fracture management: internal fixators: concepts and cases using LCP/LISS*, Stuttgart, New York., Thieme.
- WÄHNERT, D., GRÜNEWELLER, N., GEHWEILER, D., BRUNN, B., RASCHKE, M. J. & STANGE, R. 2017. Double plating in Vancouver type B1 periprosthetic proximal femur fractures: A biomechanical study. *J Orthop Res*, 35, 234-239.
- WÄHNERT, D., WINDOLF, M., BRIANZA, S., ROTHSTOCK, S., RADTKE, R., BRIGHENTI, V. & SCHWIEGER, K. 2011. A comparison of parallel and diverging screw angles in the stability of locked plate constructs. *J Bone Joint Surg Br*, 93, 1259-64.
- WALCHER, M. G., GIESINGER, K., DU SART, R., DAY, R. E. & KUSTER, M. S. 2016. Plate Positioning in Periprosthetic or Interprosthetic Femur Fractures With Stable Implants—A Biomechanical Study. *The Journal of arthroplasty*, 31, 2894-2899.
- WANG, C., CHEN, H., SHEN, M., ZHAO, S. & RUI, Y.-F. 2016. An update on the Pauwels classification. *Journal of orthopaedic surgery and research*, 11, 161.
- WEE, H., REID, J. S., CHINCHILLI, V. M. & LEWIS, G. S. 2017. Finite Element-Derived Surrogate Models of Locked Plate Fracture Fixation Biomechanics. *Ann Biomed Eng*, 45, 668-680.
- WEHNER, T., PENZKOFER, R., AUGAT, P., CLAES, L. & SIMON, U. 2011. Improvement of the shear fixation stability of intramedullary nailing. *Clin Biomech (Bristol, Avon)*, 26, 147-51.

- WEHNER, T., STEINER, M., IGNATIUS, A. & CLAES, L. 2014. Prediction of the time course of callus stiffness as a function of mechanical parameters in experimental rat fracture healing studies—a numerical study. *PLoS One*, 9, e115695.
- WEINER, S. & WAGNER, H. D. 1998. The material bone: structure-mechanical function relations. *Annu Rev Mater Sci*, 28, 271-98.
- WENGER, D. & ANDERSSON, S. 2018. Low risk of nonunion with lateral locked plating of distal femoral fractures—A retrospective study of 191 consecutive patients. *Injury*.
- WENGER, R., OEHME, F., WINKLER, J., PERREN, S., BABST, R. & BEERES, F. 2017. Absolute or relative stability in minimal invasive plate osteosynthesis of simple distal meta or diaphyseal tibia fractures? *Injury*, 48, 1217-1223.
- WIEDING, J., SOUFFRANT, R., FRITSCH, A., MITTELMEIER, W. & BADER, R. 2012. Finite element analysis of osteosynthesis screw fixation in the bone stock: an appropriate method for automatic screw modelling. *PLoS One*, 7, e33776.
- WILLENEGGER, H., PERREN, S. & SCHENK, R. 1971. [Primary and secondary healing of bone fractures]. *Chirurg*, 42, 241-52.
- WILLIE, B. M., BLAKYTNY, R., GLÖCKELMANN, M., IGNATIUS, A. & CLAES, L. 2011. Temporal variation in fixation stiffness affects healing by differential cartilage formation in a rat osteotomy model. *Clin Orthop Relat Res*, 469, 3094-101.
- WILLIE, B. M., PETERSEN, A., SCHMIDT-BLEEK, K., CIPITRIA, A., MEHTA, M., STRUBE, P., LIENAU, J., WILDEMANN, B., FRATZL, P. & DUDA, G. 2010. Designing biomimetic scaffolds for bone regeneration: why aim for a copy of mature tissue properties if nature uses a different approach? *Soft Matter*, 6, 4976-87.
- WILSON, C. J., SCHUETZ, M. A. & EPARI, D. R. 2015. Effects of strain artefacts arising from a pre-defined callus domain in models of bone healing mechanobiology. *Biomech Model Mechanobiol*, 14, 1129-41.
- WINDOLF, M., ERNST, M., SCHWYN, R., PERREN, S., MATHIS, H., WILKE, M. & RICHARDS, R. A. Biofeedback System for Continuous Monitoring of Bone Healing. BIODEVICES International Conference on Biomedical Electronics and Devices, 2014. 243-48.
- WINDOLF, M., KLOS, K., WÄHNERT, D., VAN DER POL, B., RADTKE, R., SCHWIEGER, K. & JAKOB, R. P. 2010. Biomechanical investigation of an alternative concept to angular stable plating using conventional fixation hardware. *BMC Musculoskelet Disord*, 11, 95.
- WITTKOWSKA, C., RAITH, S., EDER, M., VOLF, A., KIRSCHKE, J. S., KÖNIG, B., IHLE, C., MACHENS, H.-G., DÖBELE, S. & KOVACS, L. 2017. Computer assisted evaluation of plate osteosynthesis of diaphyseal femur fracture considering interfragmentary movement: a finite element study. *Biomed Tech (Berl)*, 62, 245-55.
- WOLF, S., JANOUSEK, A., PFEIL, J., VEITH, W., HAAS, F., DUDA, G. & CLAES, L. 1998. The effects of external mechanical stimulation on the healing of diaphyseal osteotomies fixed by flexible external fixation. *Clin Biomech (Bristol, Avon)*, 13, 359-64.
- WOLTER, D. & JÜRGENS, C. 2006. Winkelstabile Verbindungen bei Osteosyntheseimplantaten. *Trauma Berufskrankh*, 8, 206-11.
- WOLTER, D., SCHÜMANN, U. & SEIDE, K. 1999. Universeller Titanfixateur interne. *Trauma Berufskr*, 1, 307-19.
- WOOD, G. C. A., NAUDIE, D. R., MCAULEY, J. & MCCALDEN, R. W. 2011. Locking compression plates for the treatment of periprosthetic femoral fractures around well-fixed total hip and knee implants. *J Arthroplasty*, 26, 886-92.
- YÁNEZ, A., CARTA, J. & GARCÉS, G. 2010. Biomechanical evaluation of a new system to improve screw fixation in osteoporotic bones. *Med Eng Phys*, 32, 532-41.
- YÁNEZ, A., CUADRADO, A., CARTA, J. & GARCÉS, G. 2012. Screw locking elements: A means to modify the flexibility of osteoporotic fracture fixation with DCPs without compromising system strength or stability. *Med Eng Phys*, 34, 717-24.

- YANG, H. S., MA, X. & GUO, T. T. 2010. Some factors that affect the comparison between isotropic and orthotropic inhomogeneous finite element material models of femur. *Med Eng Phys*, 32, 553-60.
- YANG, K.-H., WON, Y., KANG, D.-H., OH, J.-C. & KIM, S.-J. 2015. Role of appositional screw fixation in minimally invasive plate osteosynthesis for distal tibial fracture. *J Orthop Trauma*, 29, e331-5.
- YOSIBASH, Z., PADAN, R., JOSKOWICZ, L. & MILGROM, C. 2007. A CT-based high-order finite element analysis of the human proximal femur compared to in-vitro experiments. *J Biomech Eng*, 129, 297-309.
- ZEHNDER, S., BLEDSOE, J. G. & PURYEAR, A. 2009. The effects of screw orientation in severely osteoporotic bone: a comparison with locked plating. *Clin Biomech (Bristol, Avon)*, 24, 589-94.
- ZHANG, Y., XU, J., RUAN, Y. C., YU, M. K., O'LAUGHLIN, M., WISE, H., CHEN, D., TIAN, L., SHI, D., WANG, J., CHEN, S., FENG, J. Q., CHOW, D. H., XIE, X., ZHENG, L., HUANG, L., HUANG, S., LEUNG, K., LU, N., ZHAO, L., LI, H., ZHAO, D., GUO, X., CHAN, K., WITTE, F., CHAN, H. C., ZHENG, Y. & QIN, L. 2016. Implant-derived magnesium induces local neuronal production of CGRP to improve bone-fracture healing in rats. *Nat Med*, 22, 1160-9.
- ZURA, R., BRAID-FORBES, M. J., JERAY, K., MEHTA, S., EINHORN, T. A., WATSON, J. T., DELLA ROCCA, G. J., FORBES, K. & STEEN, R. G. 2017a. Bone fracture nonunion rate decreases with increasing age: A prospective inception cohort study. *Bone*, 95, 26-32.
- ZURA, R., WATSON, J. T., EINHORN, T., MEHTA, S., DELLA ROCCA, G. J., XIONG, Z., WANG, Z., JONES, J. & STEEN, R. G. 2017b. An inception cohort analysis to predict nonunion in tibia and 17 other fracture locations. *Injury*, 48, 1194-1203.